Report No. R72-33

M.I.T. TEST SECTION INSTRUMENTATION MASSACHUSETTS BAY TRANSPORTATION AUTHORITY HAYMARKET-NORTH EXTENSION PROJECT MASS -MTD-2

Prepared by

SOIL MECHANICS DIVISION
DEPARTMENT OF CIVIL ENGINEERING
MASSACHUSETTS INSTITUTE OF TECHNOLOGY
and
CONSTRUCTION DEPARTMENT
MASSACHUSETTS BAY TRANSPORTATION AUTHORITY

MARCH 1972

FINAL PROJECT REPORT

Prepared for

DEPARTMENT OF TRANSPORTATION
URBAN MASS TRANSPORTATION ADMINISTRATION
WASHINGTON, D.C. 20590

M.I.T. TEST SECTION INSTRUMENTATION
MASSACHUSETTS BAY TRANSPORTATION AUTHORITY
HAYMARKET - NORTH EXTENSION
PROJECT MASS - MTD-2

PROJECT REPORT

Prepared by

SOIL MECHANICS DIVISION
DEPARTMENT OF CIVIL ENGINEERING
MASSACHUSETTS INSTITUTE OF TECHNOLOGY

and

CONSTRUCTION DEPARTMENT
MASSACHUSETTS BAY TRANSPORTATION AUTHORITY

March, 1972

The contents of this report reflect the views of the Massachusetts Bay Transportation Authority which is responsible for the facts and accuracy of the data presented herein. The contents do not necessarily reflect the official views or policy of the Department of Transportation. This report does not constitute a standard, specification, or regulation.

This report has been partially funded by a grant awarded by the U. S. Department of Transportation, Urban Mass. Transportation Act of 1964, as amended.

ABSTRACT

During the period 1966-1970 the Massachusetts Bay Transportation Authority constructed a "cut and cover" section of subway from Haymarket Square to Charlestown which required a deep braced excavation. Prompted by the many uncertainties associated with engineering a braced excavation the MBTA and the MIT Department of Civil Engineering initiated a research project prior to construction. The general research objective has been to develop means to reduce the costs and risks and improve engineering design and control of underground construction. The heart of this research effort has been two thoroughly instrumented portions of the subway extension.

This final project report has the following objectives:

1. Describe the field instrumentation scheme

2. Describe the data management system

3. Report the measured performance of the two instrumented sections of the braced excavation

4. Compare measured performance with performance predicted by several analytical methods. In particular, analytical results obtained from a finite element program developed during the research effort are described.

TABLE OF CONTENTS

	Page No.
GENERAL PROJECT SUMMARY	1
DESCRIPTION OF PROJECT REPORT	21
ACKNOWLEDGMENTS	23
PART I - ANALYSIS	
LIST OF TABLES	26
LIST OF FIGURES	27
CHAPTER ONE - INTRODUCTION	
1.1 Introduction	33
1.2 Report Objectives	33
1.3 Report Scope	34
CHAPTER TWO - FINITE ELEMENT SIMULATION OF BRACED EXCAVATIONS	
2.1 Introduction	35
2.2 Finite Element Analysis of Braced Excavations	35
2.3 Method of Excavation	38
2.4 Sequence of Strut Installation	44
CHAPTER THREE - EXAMPLE STUDIES OF BRACED EXCAVATIONS USING LINEARLY ELASTIC STRESS-STRAIN RELATIONS	
3.1 Introduction	47
3.2 Influence of Depths of Excavation on Movements of Open Excavations	47
3.3 Influence of Unstrutted Sheeting on Behavior of Excavations	48
3.4 Influence of Wall Stiffness on Behavior of Braced Excavations in Normally Consolidated Clays with Linearly Increasing Modulus with Depth	49

TABLE OF CONTENTS (Continued)

		Page No.
3.5	Influence of Overconsolidation Ratio on Behavior of Braced Excavations in Clays	52
3.6	Influence of Modulus Variation with Depth of Clay on Behavior of Braced Excavations	54
3.7	Braced Cuts in Clays with Some OCR but Different Moduli	57
CHAPTER FOUR - EXAMPLE STUDIES OF BRACED EXCAVATIONS USING BILINEARLY AND ANISOTROPIC, NONLINEARLY ELASTIC STRESS-STRAIN RELATIONS		
4.1	Introduction	59
4.2	Bilinear and Nonlinear Approximations of Stress-Strain Relations in Soils	60
4.3	Example Studies of Braced Excavations Using Bilinearly Elastic Stress-Strain Relations	61
4.4	Example Studies of Braced Excavations Using Anisotropic, Nonlinearly Elastic Stress-Strain Relations	67
CHAPTER FIVE - PREDICTED PERFORMANCES OF TEST SECTIONS A AND B, NORTH STATION, BOSTON		
5.1	Introduction	71
5.2	Pore Pressures Near Excavations	71
5.3	Horizontal Stresses and Strut Loads	74
5.4	Wall Movements	77
5.5	Ground Settlements	78
5.6	Comparisons Between Predicted Performance and Measured Performance	80
CHAPTER SIX - CONCLUSIONS		
6.1	Development of New Method	83
6.2	Summary of Insights Gained from Example Studies	83
6.3	Comparison Between Predicted and Measured Performances	85

TABLE OF CONTENTS (Continued)

	Page No.
REFERENCES	87
LIST OF SYMBOLS	93
TABLES	
FIGURES	
APPENDIX I-A - USER'S MANUAL FOR FINITE ELEMENT COMPUTER PROGRAM BRACE	215
APPENDIX I-B - DETAILS OF ONE-DIMENSIONAL BAR ELEMENTS USED FOR THE SIMULATION OF WALL	233
APPENDIX I-C - ESTIMATION OF SOIL PARAMETERS USED FOR THE PREDICTION OF THE PERFORMANCE OF TEST SECTIONS A AND B MADE BY BRACE	239
PART II - EXPERIMENTAL WORK	
LIST OF FIGURES	244
Measured Performance of Test Sections A and B	
1. Introduction	247
2. Soil Profile	248
3. Layout of Field Instruments	249
4. Construction Procedure	250
5. Pore Pressure Near Excavations	251
6. Horizontal Stresses and Strut Loads	252
7. Movements Near Excavations	253
APPENDIX II-A - INSTRUMENT DETAILS AND SUMMARY OF DATA	279
APPENDIX II-B - DATA ACQUISITION AND MANAGEMENT	333
- Enclosure I	343

GENERAL PROJECT SUMMARY

Introduction

Excavations in soil are commonplace. Road construction, foundations for buildings, canals, tunnels, etc. all involve soil excavations. We can classify excavations into three types: 1) unretained (unsupported) earth slopes, 2) braced (supported) excavations, and 3) tunnels. Fig. 1 gives simple examples of the three types of excavations. An unretained earth slope is the most common excavation method and is used extensively in highway construction. Open pit mining is an example of a very deep excavation employing unretained earth slopes. Often times, especially in urban areas, the sides of an excavation cannot be sloped because of adjacent property lines or adjacent structures. In this case, a vertical cut is made and bracing is used, if necessary, to hold the excavation open. Tunneling in soil is done either by hand or with a tunneling machine and usually requires a permanent liner for support.

During the period 1966-1970 the Massachusetts Bay Transportation Authority (MBTA) constructed a section of subway from Haymarket Square to Charlestown. The construction scheme was to excavate a deep trench in the ground using a braced excavation, construct the subway structure at the bottom of the excavated trench, and then cover the structure. This construction method is generally referred to as "cut and cover."

The soil engineer had to answer the following questions when designing this braced excavation:

1. What are the loads applied to the steel sheeting by the soil and water retained by the sheeting?

2. How are these loads transferred to the bracing system, i.e., what are the strut loads?

3. How much will the sides of the excavation and the adjacent ground move?

4. What will be the changes in ground water hydrology due to construction?

5. Will the ground movements due to the excavation cause damage to adjacent structures?

6. Is underpinning of adjacent structures required?

7. What field measurements need to be made to control construction?

Insight into the answers to these questions can be found by studying the measured performance of past braced excavations. Unfortunately, the number of braced excavations where performance has been measured is very small due to the large costs of obtaining such data. Therefore, these questions could not be answered with any certainty prior to construction. In order to provide answers to these questions during construction, so that the original design could be altered as necessary, field measurements of the performance of the braced excavations were essential. Moreover, the need for an additional documented case study of the performance of a braced excavation was clear.

A research group headed by Professor T. William Lambe in the Soil Mechanics Division of the Department of Civil Engineering at Massachusetts Institute of Technology was already actively engaged in a program of field research to document the performance of buildings on the M.I.T. campus. This group was ideally suited to carry out the installation of field measuring devices, collect data, and analyze the results of the measured performance of the MBTA braced excavation.

Therefore, prior to the start of construction the MBTA and M. I. T. initiated a research project which was aided by federal funds.

Research Objectives and Tasks

The general research objective has been to develop means to reduce the costs and risks and improve engineering design and control for underground construction. The heart of this research effort has been two thoroughly instrumented portions of the subway extension along Accolon Way near Haymarket Square.

Four major steps were followed to achieve the research objective:

1. Carefully and thoroughly measure and document the performance of the MBTA braced excavation.
2. Compare the measured field performance to predicted performance. Evaluate prediction methods based on this comparison.
3. Develop improved analytical methods if necessary.
4. Report research findings to the engineering profession.

In addition, many particular activities have combined to produce the results of the research:

Instrumentation design and installation
Soil sampling
Soil testing
Instrument readings and portrayal
Development of data acquisition and management systems
Construction activity observations
Analysis of field data
Computer programming
Analysis of bracing systems

Development of construction control procedures

Coordination and transmittal of results to constructors.

A bar chart showing the schedule of research activities is shown in Fig. 2. The original planning was established in 1966 based on the Contractor's CPM schedule. Major modifications were made to the research schedule in February 1969 to adjust to delays and other scheduling changes by the Contractor.

Fig. 3 is a plan view of the subway extension. Two thoroughly instrumented portions of the subway, called Test Sections A and B, are the heart of the research effort. Figs. 4 and 5 show the soil profiles at Test Sections A and B. Test Section B was instrumented and constructed prior to Test Section A. The instrumentation was designed to give the following information:

1. Horizontal Movements. The engineer is interested in the horizontal movement of the walls of the braced excavation as well as the movement of adjacent ground toward the excavation. These measurements can be related to damage of adjacent structures and also give warning before collapse of the braced excavation. An inclinometer (slope indicator) is used to obtain these data.

2. Vertical Movements. The vertical movement of the ground near the excavation and the vertical movement of adjacent structures is measured to monitor the effects of making the excavation. These data allow the engineer to evaluate his design during construction and redesign if it appears adjacent structures are likely to be damaged.

3. Strut Loads. By measuring the loads in the struts which hold the excavation open the engineer can compare measured and predicted strut loads and evaluate his design methods. Geonor vibrating wire strain gauges were used to measure the strain in the strut. The stress and load are then deduced from the measured load.

4. Pressure on Sheeting. Design methods make assumptions about the soil and water pressure on the sheeting. Total stress cells were installed to measure the pressure from the soil and water on the sheeting.

5. Water Pressure in the Ground. A knowledge of pressure in the water that fills the voids of a soil is extremely important in understanding how soil behaves. Piezometers are used to measure pore water pressure.

The progress of construction, notes on the construction procedure, description of soil as excavated, and numerous other observations complement the five particular aspects of performance that were measured. Figs. 6 and 7 are plan views of Test Sections A and B showing the layout of field instrumentation.

Results of the Research Project

A giant step forward has been made toward achieving the general research objective of developing means to reduce the costs and risks and improve engineering design and control for underground construction. In particular, this research effort has resulted in: 1) a thorough evaluation of the state-of-art for predicting behavior of braced excavations; 2) an approach to engineering a large and important excavation; 3) an important addition to the meager list of braced excavations where field behavior has been measured; and 4) development of analytical

tools. The following paragraphs give a summary of the four major results.

State-of-Art of Braced Excavations. In general, the state-of-art for predicting the behavior of braced excavations is far from good. The engineer cannot at the present time predict with confidence the strut loads and movement of soil outside an open excavation. This unfortunate fact is caused by the difficulty in selecting the proper soil parameters and field boundary conditions and in predicting the details of construction. This finding seriously limits the designer and specification writer who attempt to specify the details of braced, underground construction before construction starts without providing for a sensitive control system and decision-making apparatus concurrent with construction to make needed changes.

The engineer can expect improvements for both design and construction control as intensive research in underground construction continues. The most fruitful line of study will be a two-pronged attack consisting of:

1. Parametric studies based on finite element methods employing soil parameters obtained by stress path tests and field tests.
2. The evaluation of the actual performance of thoroughly instrumented field cases. The complexities of braced excavations require many field instrumented cases.

Engineering an Excavation. Engineering an excavation is fraught with unknowns and uncertainties and thus is an ideal candidate for the Observational Method (Peck, 1969) and for the ICEP Approach (Lambe, 1970). Full engineering, ranging from planning and investigation through design and construction supervision, is justified on a large and

important excavation. The logical steps in the engineering of an excavation are:

1. Explore and test subsoil
2. Select dimensions of excavation
3. Survey adjacent structures and utilities
4. Establish permissible movements
5. Select bracing (if needed) and construction scheme
6. Predict movements caused by excavation and dewatering
7. Compare predicted with permissible movements
8. Alter bracing and construction scheme (if needed)
9. Instrument and monitor construction and alter bracing and construction as needed.

MBTA Case History. The case history reported herein thoroughly documents the measured and predicted performance of two different sections of subway construction. It is the example of necessary research that permits the engineering approach outlined above. Many procedures, techniques, and hardware needed to accomplish the nine engineering engineering tasks outlined have been developed and improved on this project. A few examples are:

1. BRACE computer program for predicting movements.
2. Automated inclinometer system to rapidly measure field movements.
3. Data handling computer programs to quickly compute, plot and record measured data for use by decision makers.
4. Methods to modify bracing and excavation procedures based on field measured performance to limit movements and damage to adjacent structures.

Analytical Tools. The major analytical innovation of the research was the development of the BRACE computer program. Making use of the finite element method, BRACE has the capability of predicting movements, stresses and strut loads in a rational manner taking into account bending stiffness of the retaining wall and the nonlinear aspects of soil behavior. In addition, the user can simulate the sequence of excavation and strut installation employed in the field. Comparisons of measured and predicted performance at the two instrumented sections showed good agreement. However, the limitations of BRACE must be clearly understood.

One obvious criteria for acceptance of any computer program is that it can analyze correctly the wide range of problems it was designed to analyze. The effort necessary to check that the program is working properly increases rapidly with the complexity of the program. We are continually evaluating our programs at M.I.T. Our most recent evaluation of the uses and limitations of the BRACE program as well as an updated listing of BRACE is enclosed as an addendum to this project report.

The next criteria for the acceptance of BRACE as an engineering tool is that it must be able to predict the measured performance of actual braced excavations. Even though the prediction by BRACE agrees well with the measured performance of the two MBTA subway sections, it is not possible to evaluate the usefulness of BRACE until more field cases have been analyzed.

Benefits of this Research Project

Benefits to MBTA. The field data obtained provided major assistance in construction control of the Accolon Way portion of the subway. For example, the research data have given:

1. The actual locations of the sheet piles as driven near Section B, showing the amount of encroachment on the subway walls;

2. The ground movements caused by the excavation and construction operations;

3. The variation of ground water pressure with tides and construction operations;

4. The movements of buildings near the construction;

5. Data necessary for the design and evaluation of the ground water recharge system;

6. Data for the determination of movement (if any) of the central artery footings;

7. Needed modifications for construction procedures at Test Section A to minimize damage to the adjacent tall buildings.

In addition, the data obtained had a constructive influence on other subway projects, notably the MBTA South Cove Project in Boston and the Washington, D.C. system.

National Benefits. Published papers and conferences of the American Society of Civil Engineers are major benefits of the research on a national level since they reach the design engineers responsible for designing braced excavations. The main publications that have presented results to the profession are:

1. "Measured Performance of a Braced Excavation," by Lambe, Wolfskill and Wong, published in the ASCE Proceedings in 1970 and giving the evaluated data on one section of the Accolon Way Subway.

2. "Predicted Performance of Braced Excavation," by Golder, Gould, Lambe, Tschebotarioff and Wilson, published in the ASCE Proceedings in 1970 and giving the predictions by four of the Profession's experts on braced cuts for the Accolon Way Subway performance.

3. "Braced Excavations," by Lambe, published and presented at the ASCE 1970 Specialty Conference: Lateral Stresses in the Ground and Design of Earth Retaining Structures. This paper summarizes the state-of-art on engineering for braced excavations and is primarily based on the MBTA-MIT engineering and research on subway excavations.

4. "The Integrated Civil Engineering Project," by Lambe the 1970 Terzaghi Lecture to the ASCE National Meeting in New York City, presenting the engineering approach to complex construction projects like subways.

5. "Effects of Foundation Construction on Nearby Structures," by D'Appolonia (MIT), the state-of-art paper presented to the 1971 Panamerican Conference on Soil Mechanics and Foundation Engineering held in San Juan, Puerto Rico. A major portion of the paper deals with effects of subway construction on nearby structures and is based in part on the MBTA-MIT experiences.

The interpreted data and analysis of the MBTA subway sections presented in these papers are all presented in this comprehensive technical project report. In addition, the project report contains much additional important interpreted data and analytical results that could not be included in the profession papers due to space limitations.

Financial Summary of the Research Project

Fig. 8 summarizes the cost of the research project and gives a breakdown of cost for the major activities.

Proposed Further Research

The following areas of continued research are recommended as the most effective method of further advancing our understanding of

the performance of braced excavations:

1. Perform additional parametric studies using the finite element program BRACE. This is an effective and relatively inexpensive method of gaining insight into the behavior of braced excavations. These studies would have the additional benefit of further developing the BRACE program.

2. Document the measured performance of more braced excavations with the perspective and objectives of relating the results of the case study to the advancement of design and construction practice.

3. Improve instrumentation to increase performance and cut costs. In particular, the development of new and improved field methods of measuring in situ stresses and soil deformability and strength is needed.

4. Improve data handling systems. One important improvement would be having the resident engineer get the field data directly rather than first going to the research group and then the engineering group.

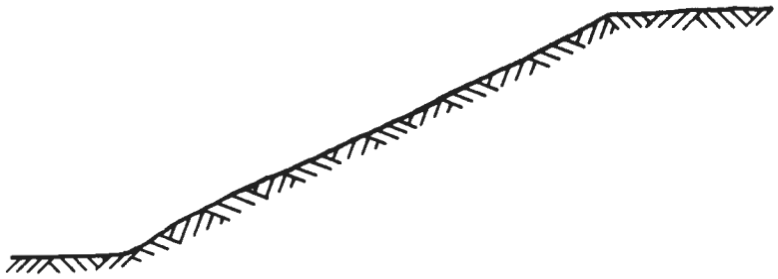

a. Unretained Earth Slope

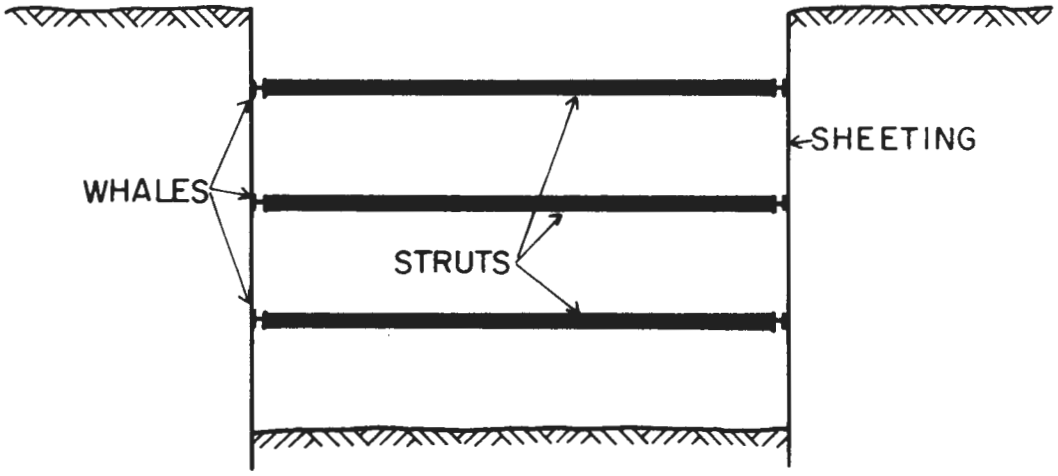

b. Braced Excavation

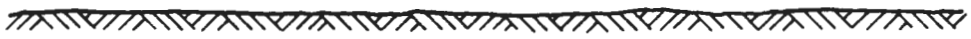

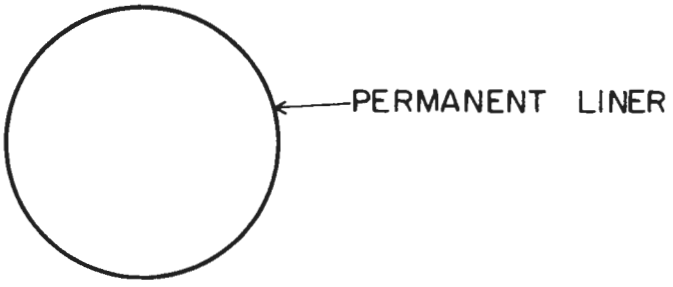

c. Tunnel

FIGURE 1 TYPES OF EXCAVATIONS

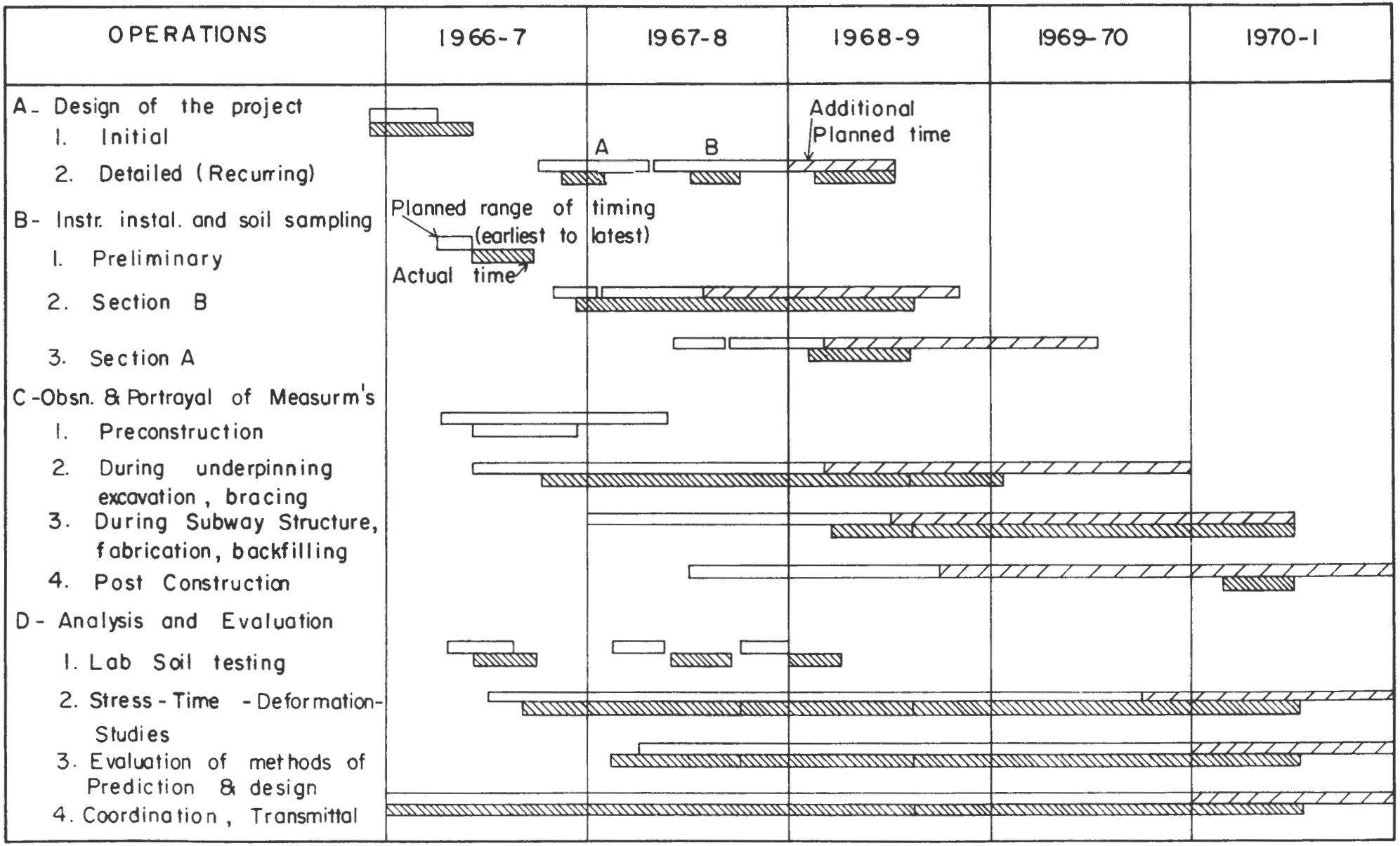

FIGURE 2 PROJECT WORK SCHEDULE (Revised Feb. 1969)

MBTA - MIT SOIL INSTRUMENTATION HAYMARKET SQ. -CHARLESTOWN

Based on CPM Construction Plan, Perini Corp., Sep. 1966

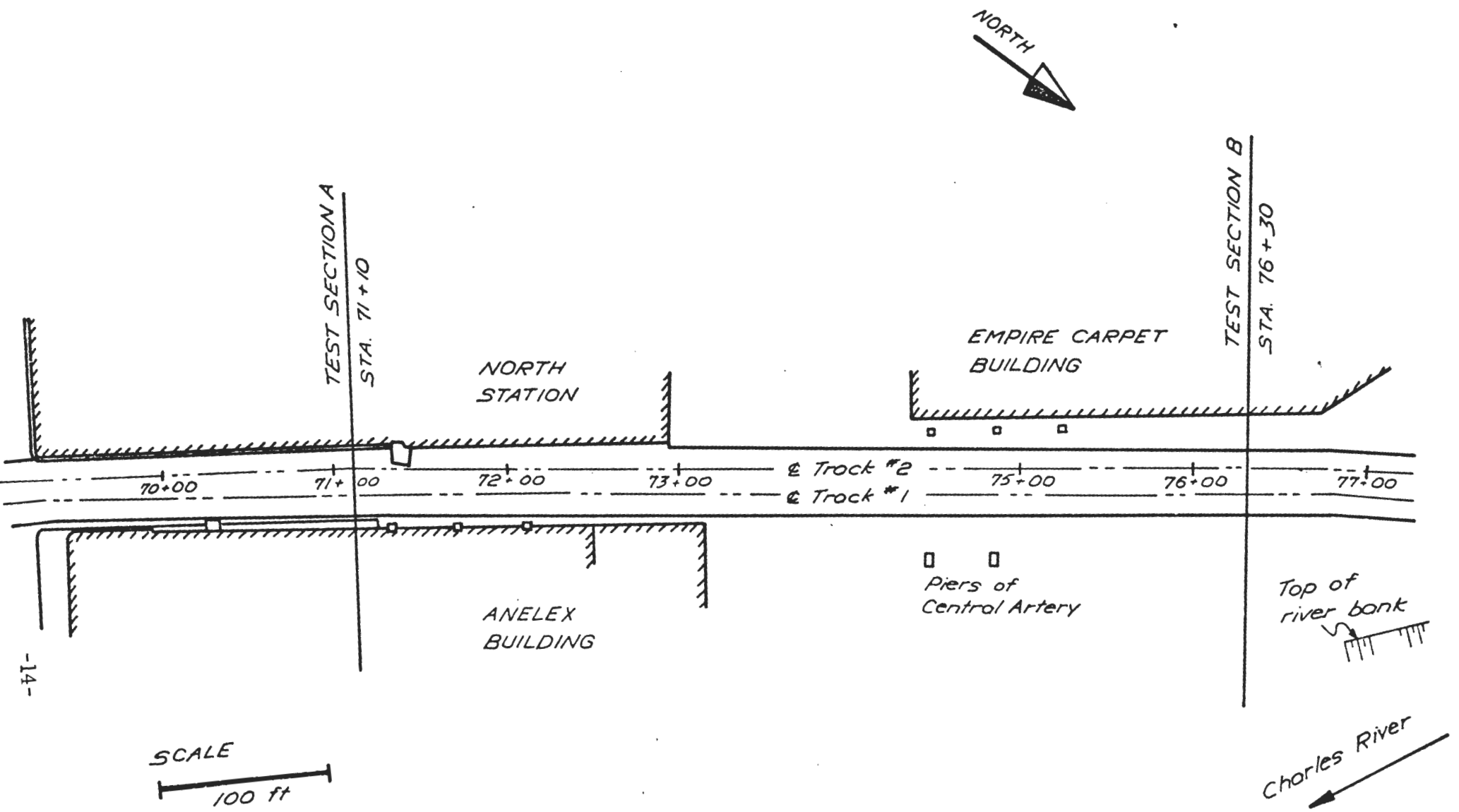

FIGURE 3 PLAN VIEW OF SUBWAY EXTENSION

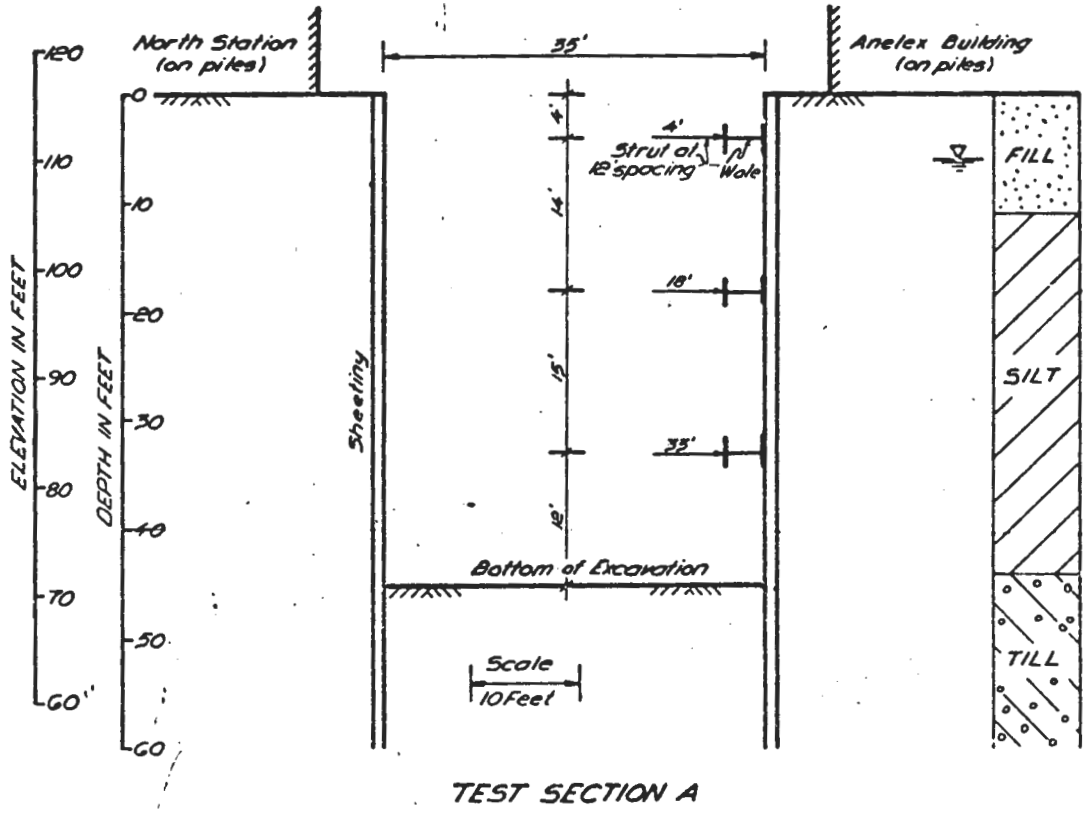

TEST SECTION A

FIGURE 4 CROSS SECTION AT TEST SECTION A

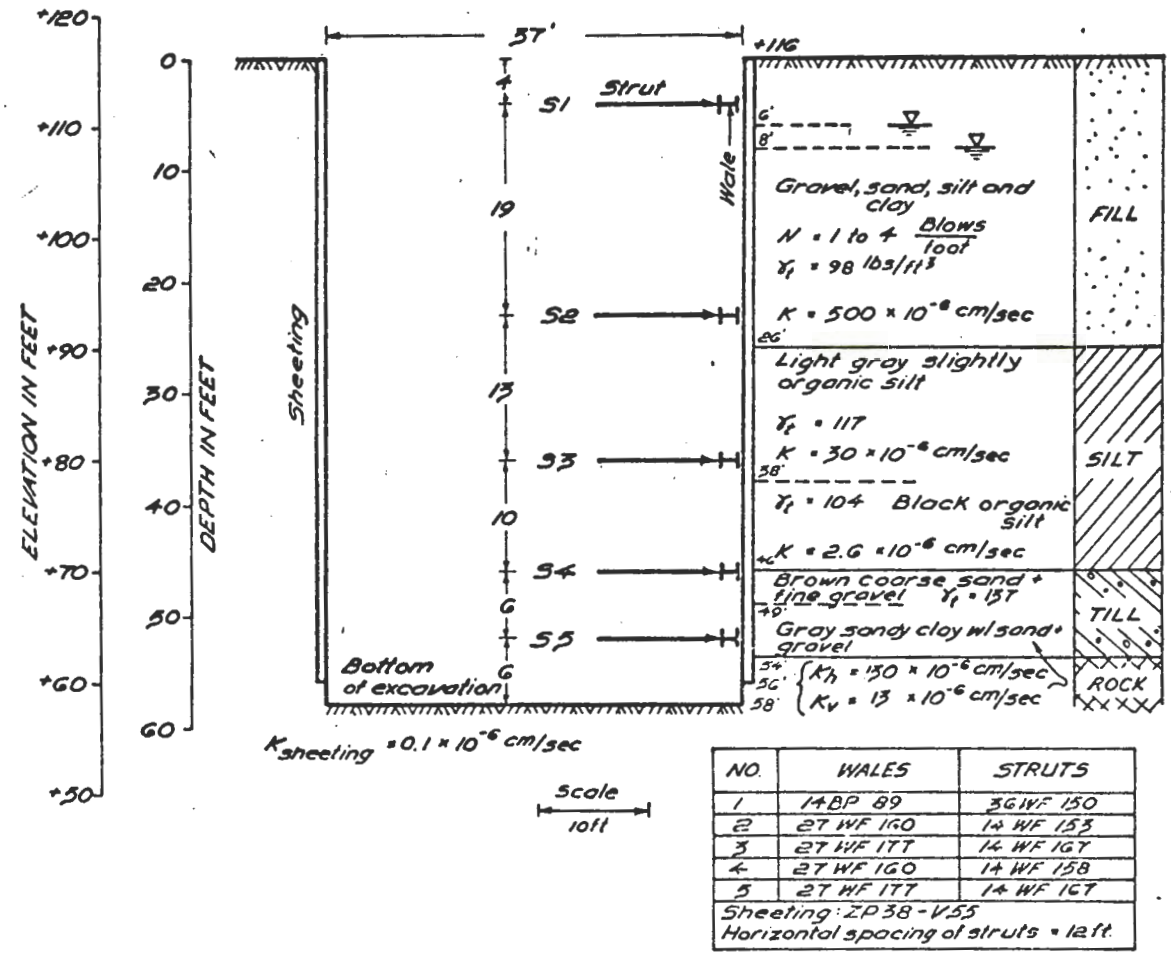

NO.	WALES	STRUTS
1	14BP 89	36WF 150
2	27 WF 160	14 WF 158
3	27 WF 177	14 WF 167
4	27 WF 160	14 WF 158
5	27 WF 177	14 WF 167

Sheeting: ZP 38 - V 55
Horizontal spacing of struts = 12 ft.

FIGURE 5 CROSS SECTION AT TEST SECTION B

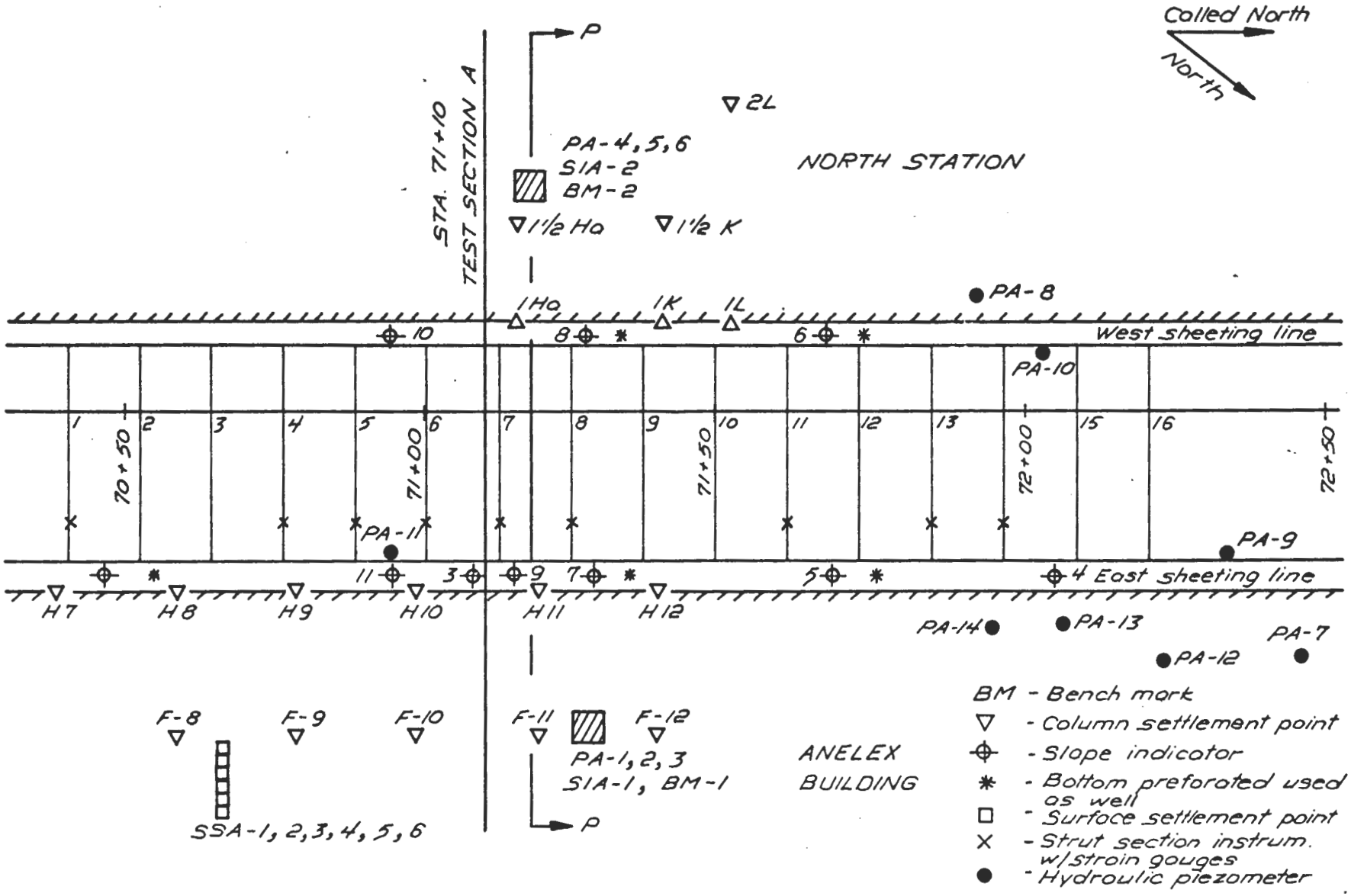

FIGURE 6 PLAN VIEW OF TEST SECTION A

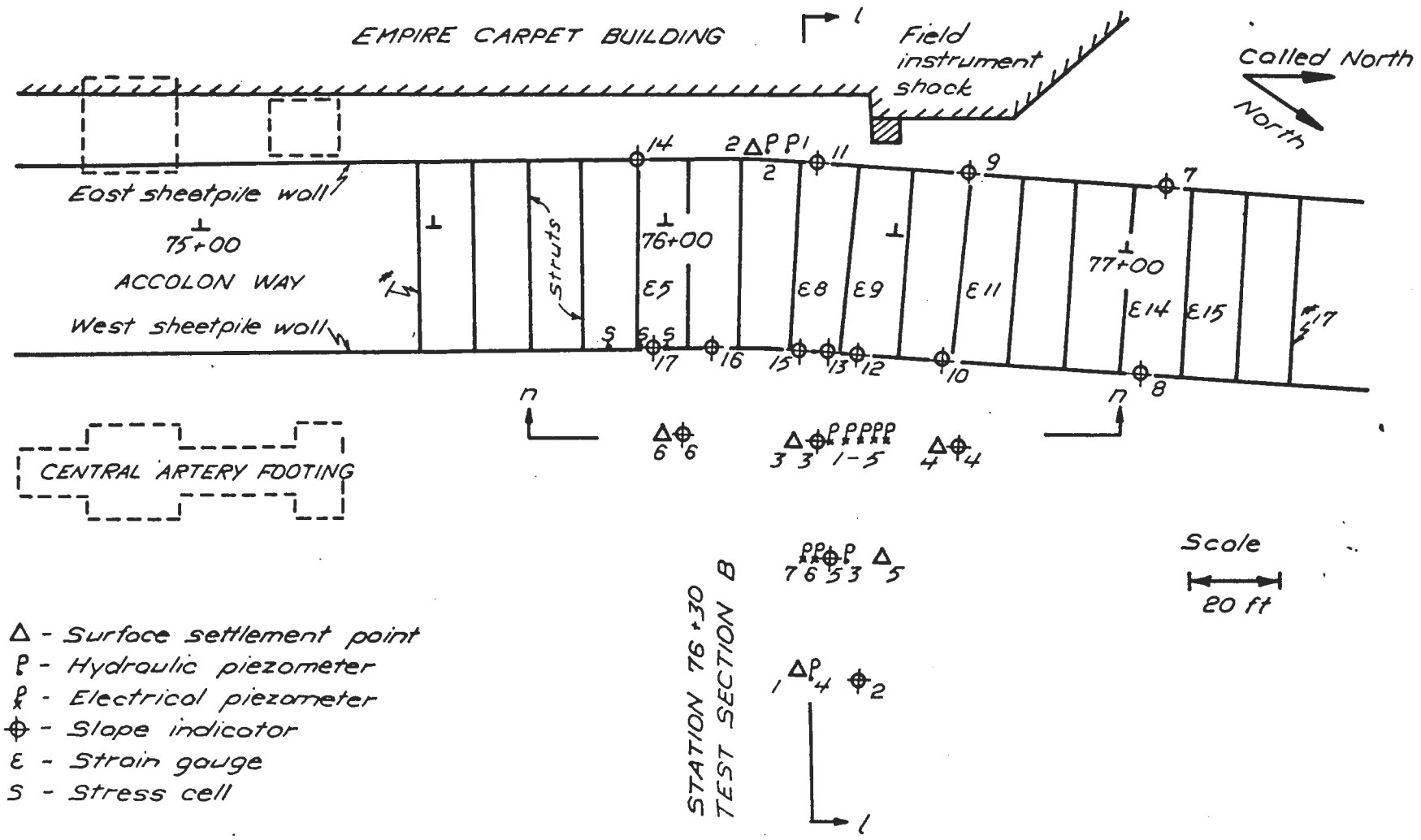

FIGURE 7 PLAN VIEW OF TEST SECTION B

ITEM	FY '67	FY '68	FY '69	FY '70	FY '71	TOTAL
Planned MIT Budget*	67,259	109,580	134,000	119,000	26,000	455,839
1. Salaries and Wages incl. O/H and Employee Benefits						
a. Analysis	27,537	38,854	46,386	85,925	32,668	219,451
b. Experimental	13,770	19,426	23,193	42,962	16,667	111,000
2. Travel	79	800	500	99	400	1,878
3. Materials, Services and Computer	616	2,500	3,000	4,000	2,000	12,116
4. Instrumentation, Repairs	25,257	48,000	17,500	2,500	1,200	94,457
M.I.T. TOTALS	67,259	109,580	90,579	135,486	52,935	455,839
MBTA TOTAL : To cover overhead and report preparations costs						65,383
					FINAL TOTAL	$ 521,222

* Based on amended contract dated 10 July 1969.

FIGURE 8 FINANCIAL SUMMARY OF RESEARCH PROJECT

DESCRIPTION OF PROJECT REPORT

The project report is presented in two parts. Part I, Analysis, has three objectives:

1. To develop a method for analyzing braced excavations based on the principles of soil mechanics and on the finite element technique;
2. To provide insight into the undrained behavior of a braced excavation in clay;
3. To predict the performance of two instrumented sections of a braced excavation and compare the measured performance with the predicted performance.

The major innovation of the analytical studies was the development of a finite element program, BRACE, which provides a rational means of predicting the performance of braced excavations. This analytical tool has the capability for predicting: 1) movements of the soil mass adjacent to an excavation; 2) movements of the retaining wall; 3) stresses on the retaining wall; and 4) loads in the struts.

The measured performances of the sections of braced excavation instrumented during the research project were compared with the performances predicted by BRACE; generally the comparison was good. However, it must be clearly understood that many more such comparisons must be made before any definitive statement about the reliability of BRACE can be made.

A listing of the most recent versions of BRACE as well as our present evaluation of its use and limitations is enclosed as an addendum to the project report.

Part II, Experimental Work, presents the measured performance of the two instrumented sections of the MBTA braced excavation. This part of the report describes the soil profile, layout and description of field instrumentation, construction procedure, pore pressures near excavations, horizontal stresses and strut loads, and movements near the excavation. In this presentation, considerable work has been done in summarizing and presenting in readily usable form the raw data from the field instrumentation. Appendix II-A describes the details of the instruments at Test Sections A and B and presents uninterpreted plots of the measurements obtained.

Appendix II-B describes the data acquisition and management system that was developed to handle the enormous amount of data generated in this research project.

ACKNOWLEDGMENTS

The MBTA deserves appreciation for their progressive attitude and assistance towards the field research project. James D. Fitzgerald formerly Director of New Construction, and Warren J. Higgins, formerly Executive Director of Planning and Construction, have been particularly helpful. The MBTA project staff - J. A. Carey, F. M. Keville, S. J. Murdock and J. McCall cooperated very closely.

The Contractor, the Perini Corporation, and especially its Chief Structural Engineer, Harold V. McKittrick, cooperated fully with the research.

This report was written by I. H. Wong and R. C. Kirby and reviewed by T. W. Lambe and L. A. Wolfskill. The bulk of the analysis presented herein was taken from a doctoral thesis by I. H. Wong. W. E. Jaworski updated the BRACE users manual and evaluated the present uses and limitations of BRACE.

The MIT ICEP staff, headed by Professor T. W. Lambe and managed by L. A. Wolfskill, are due credit for the mass of reliable data collected and analyzed. ICEP staff who participated on the project include: L. G. Bromwell, D. J. D'Appolonia, C. C. Ladd, J. T. Christian, W. R. Beckett, N. F. Braathen, E. J. Cardoza, I. Wong, H. McPherson, R. C. Kirby, J. Bromwell, M. X Haley, P. Saulnier and L. Bombardier.

PART I - ANALYSIS

PART I

LIST OF TABLES

Table No.	Title
1.3.1	Analysis of Braced Excavations
3.1.1	Summary of Input Variables Linearly Elastic Analyses
3.4.1	Properties of Wall
4.3.1	Summary of Input Variables Bilinearly Elastic Analyses
4.3.2	Dimensionless Number N for Excavations in Soil With Properties of Boston Blue Clay
4.3.3	Factor of Safety Against Base Failure for Excavations in Soil With Properties of Boston Blue Clay
4.4.1	Summary of Input Variables Nonlinearly Elastic Analyses
5.5.1	Soil Properties for Consolidation Settlement Calculation

PART I

LIST OF FIGURES

Figure No.	Title
2.2.1	Typical Finite Element Grid of A Plain Strain Excavation Problem
2.3.1	Sequence of Excavation and Strut Installation in Example Study
2.3.2	Simulation of Excavation Process
2.3.3	Sign Convention of Positive Stresses in Finite Element Analysis
2.3.4	Two Finite Element Grids
2.3.5	Influence of Number of Lifts of Excavation on Vertical Movements of Open Cut
2.3.6	Influence of Number of Lifts of Excavation on Horizontal Movements of Open Cut
2.3.7	Movement of Vertical Face of Open Cut - No Averaging
2.3.8	Movement of Vertical Face of Open Cut - Averaging
2.3.9	Horizontal Movements of Open Cut with Different Methods of Stress Release
2.3.10	Vertical Movements of Open Cut with Different Methods of Stress Release
2.3.11	Vertical Stress on Vertical Face of Open Cut
2.3.12	Horizontal Stress on Vertical Face of Open Cut
2.3.13	Shear Stress on Vertical Face of Open Cut
2.3.14	Shear Stress on Vertical Face of Open Cut with Different Methods of Stress Release
2.3.15	Horizontal Stress on Vertical Face of Open Cut with no Averaging
2.3.16	Horizontal Stress on Vertical Face of Open Cut with Different Methods of Stress Release
2.3.17	Comparison of Stresses in 3-Lift and 1-Lift Terraced Cuts
2.3.18	Comparison of Stresses in 3-Lift and 1-Lift Vertical Cuts

2.3.19 Comparison of Movements in 3-Lift and 1-Lift Terraced Cuts

2.3.20 Comparison of Movements in 3-Lift and 1-Lift Vertical Cuts

2.3.21 Stress Distributions for Row of Elements for Excavation to 20 feet

2.3.22 Location of Two Rows of Elements Below Bottom of Excavation

2.3.23 Horizontal Movements of Open Cuts Stress Release by Extrapolation

2.3.24 Vertical Movements of Open Cuts Stress Release by Extrapolation

2.3.25 Horizontal Stress Acting on Vertical Face of Open Cuts Stress Release by Extrapolation

3.2.1 Vertical Movement of Open Cuts with Depth of Instantaneous Excavation

3.2.2 Horizontal Movement of Open Cuts with Depth of Instantaneous Excavation

3.2.3 Bottom Heave of Open Cuts with Depth of Instantaneous Excavation

3.3.1 Movements of Line AA with and without Sheeting

3.3.2 Horizontal Stresses on Vertical Face with and without Sheeting

3.4.1 Deformed Soil Mass Linearly Elastic Analysis

3.4.2 Wall Movements Toward Excavation Linearly Elastic Analysis

3.4.3 Horizontal Stress on Wall

3.4.4. Horizontal Stress Behind Sheeting Linearly Elastic Analysis

3.4.5 Horizontal Stress in Front of Sheeting Linearly Elastic Analysis

3.4.6 Stresses in Soil Mass Linearly Elastic Analysis

3.4.7 Stresses in Soil Mass Linearly Elastic Analysis

3.4.8 Strut Loads with Different Walls

3.4.9 Bending Moment in Sheeting Linearly Elastic Analysis

3.4.10 Shear Force in Sheeting Linearly Elastic Analysis

3.5.1 K_o vs. Overconsolidation Ratio for Boston Blue Clay

3.5.2	Movements at Different OCR's
3.5.3	Stresses on Sheeting at Different OCR's
3.5.4	Geostatic Horizontal Stresses in Dry Soils
3.5.5	Orientation of Total Principal Stresses Linearly Elastic Analysis OCR = 2
3.5.6	Orientation of Total Principal Stresses Linearly Elastic Analysis OCR = 5
3.6.1	Modulus Variations for Linearly Elastic Analysis
3.6.2	Sheeting Movement with Different Modulus Variations
3.6.3	Ground Settlement with Different Modulus Variations
3.6.4	Bottom Heave with Different Modulus Variations
3.6.5	Horizontal Stress on Walls Elastic Analysis
3.6.6	Strut Loads with Different Modulus Variations
3.7.1	Influence of Soil Stiffness on Movements near Excavation
3.7.2	Strut Loads with Different Moduli
4.2.1	Time Independent Idealizations of Stress-Strain Behavior of Soils
4.2.2	Comparison of Hyperbolic Prediction Equation and Measured Response for Various Conditions
4.2.3	Comparison of Hyperbolic Prediction Equation and Measured Response for Various Conditions
4.2.4	Polynomial Approximations of Stress-Strain Behavior OCR = 1
4.2.5	Polynomial Approximations of Stress-Strain Behavior OCR = 2
4.3.1	Soil Properties Used in Bilinearly Elastic Analysis
4.3.2	Development of Yielded Zones During Excavation OCR = 1 with Sheeting
4.3.3	Development of Yielded Zones During Excavation OCR = 2 with Sheeting
4.3.4	Development of Yielded Zones During Excavation OCR = 5 with Sheeting
4.3.5	Development of Yielded Zones During Excavation OCR = 25 with Sheeting

4.3.6	Development of Yielded Zones in Thick Layer During Excavation OCR = 1
4.3.7	Development of Yielded Zones During Excavation OCR = 1 with Slurry Wall
4.3.8	Development of Yielded Zones During Excavation OCR = 1 with Stiff Crust and Sheeting
4.3.9	Wall Movements Linear and Bilinear Analysis OCR = 1
4.3.10	Wall Movements from Bilinear Analyses
4.3.11	Ground Settlements from Linear and Bilinear Analysis OCR = 1
4.3.12	Deformed Soil Mass Linear and Bilinear Analysis
4.3.13	Horizontal Stresses on Sheeting Bilinearly Elastic Analysis OCR = 1 with Sheeting
4.3.14	Horizontal Stresses on Sheeting Bilinear Analysis OCR = 2 with Sheeting
4.3.15	Strut Loads in Linearly and Bilinearly Elastic Analysis
4.3.16	Maximum Stresses due to Bending in Retaining Wall
4.4.1	Ground Settlement Anisotropic Nonlinear Analysis
4.4.2	Ground Settlement in Linearly Bilinearly Anisotropic Nonlinearly Elastic Analysis
4.4.3	Sheeting Movement Anisotropic Nonlinearly Elastic Analysis
4.4.4	Deformed Soil Mass Anisotripic, Nonlinearly Elastic Analysis
4.4.5	Orientation of Total Principal Stresses Anisotropic Nonlinearly Elastic Analysis
4.4.6	Contours of Maximum Shear Stress Anisotropic Nonlinearly Elastic Analysis
4.4.7	Strut Loads from Anisotropic Nonlinearly Elastic Analysis
4.4.8	Strut Loads from Three Analyses
5.2.1	Permeabilities of Subsoils North Station Test Sections A and B
5.2.2	Finite Element Grid for Seepage Analysis Test Section B
5.2.3	Pore Pressures on Sheeting with Different Sheeting Permeabilities Test Section B

5.2.4 Pore Pressure on Sheeting Test Section B

5.2.5 Predicted Contours of Total Head Test Section B

5.2.6 Predicted Total Head 20 feet from Wall Test Section B

5.2.7 Pore Pressures on Wall Test Section A

5.3.1 Stress in Soil Near Excavation

5.3.2 Test Section B Analyzed by Terzaghi - Peck Method

5.3.3 Test Section A Analyzed by Terzaghi - Peck Method

5.3.4 Horizontal Stresses on Wall Predicted by Stress Ratio Method Test Section B

5.3.5 Horizontal Stresses on Wall Predicted by Stress Ratio Method Test Section A

5.3.6 Strut Loads at Full Excavation Test Section B

5.3.7 Strut Loads at Full Excavation Test Section A

5.3.8 Strut Loads During Excavation Test Section B

5.3.9 Strut Loads During Excavation Test Section A

5.3.10 Soil Properties Used in Bilinearly Elastic Analysis Test Sections A and B by BRACE

5.4.1 Predicted Wall Movement - Elastic Beam with Springs Test Section B

5.4.2 Predicted Wall Movement - Elastic Beam with Springs Test Section A

5.4.3 Predicted Wall Movements Finite Element Program BRACE Test Section B

5.4.4 Predicted Wall Movements Finite Element Program BRACE Test Section A

5.5.1 Predicted Movements at Test Section B

5.6.1 Maximum Strut Loads Test Section B

5.6.2 Maximum Strut Loads Test Section A

5.6.3 Measured and Predicted Wall Movements - Maximum Values

5.6.4 Measured and Predicted Wall Movements at Final Excavation

CHAPTER ONE

INTRODUCTION

1.1 INTRODUCTION

When designing the support system for a braced excavation, an engineer must ensure that the following two criteria are satisfied:

(1) The loads acting on or in the support system do not become so large that failure occurs and the excavation collapses;

(2) The movements of the soil adjacent to the excavation do not become so large that adjacent structures are damaged.

Methods for predicting loads and movements associated with braced excavations are highly empirical and in many ways unsatisfactory. Owing to the indeterminate nature of the soil-support system the methods of analysis currently used by the engineering profession either are semi-empirical or involve greatly simplified approximations. The state-of-the-art for predicting the performance of braced excavations is indicated by Golder et al. (1970), where four authorities on lateral stresses made predictions of the stresses and movements for a section[1] of braced excavation in Boston. Their methods ranged from the use of semiempirical rules to an exercise of engineering judgment.

1.2 REPORT OBJECTIVES

This report has three objectives. They are:

---

[1]This test section is known as Test Section B and will be analyzed in this report.

(1) To develop a method for analyzing braced excavations based on the principles of soil mechanics and on the finite element technique.

(2) To provide insight into the undrained behavior of braced excavations in clay.

(3) To predict the performance of two instrumented sections of a braced excavation. The predictions are made using currently available methods, as well as the finite element method developed. The predicted performance is compared with the measured performance.

1.3 REPORT SCOPE

The finite element method of analysis developed has the capability of handling the bending stiffness of the retaining wall and the nonlinear aspect of soil behavior. It also has the capability of simulating sequentially the process of excavation and strut installation employed in the field.

Insights into the factors controlling the undrained behavior of braced excavations are obtained through example studies. The key factors investigated in these example studies are: (1) bending stiffness of the retaining wall; (2) overconsolidation ratio of the soil; (3) modulus variation with depth of the soil; and (4) linearly, bilinearly and nonlinearly elastic stress-strain behavior of soil.

The aspects of the performance of the two test sections predicted are: (1) pore pressures; (2) strut loads; (3) wall movements; and (4) ground surface settlements. The finite element program BRACE is used to predict the strut loads, wall movements and the initial settlements of the ground surface. Table 1.3.1 summarizes all the methods of prediction used, together with the aspects of performance predicted.

CHAPTER TWO

FINITE ELEMENT SIMULATION OF BRACED EXCAVATIONS

2.1 INTRODUCTION

This chapter presents the development of a finite element computer program for analyzing braced excavations. The program has the capability of:

(1) Handling the bending stiffness of the retaining wall;

(2) Simulating sequentially the process of excavation and strut installation;

(3) Modeling the nonlinear aspects of soil behavior.

In the next section the fundamental concepts of the finite element method are briefly discussed, and the simulation of the retaining wall by one-dimensional bar elements is described. The last two sections outline the simulation of excavation and strut installation. The modeling of the nonlinear aspects of soil behavior is presented in Chapter Four. In Appendix A the user's manual for the computer program developed is presented. The name of this program is BRACE.

2.2 FINITE ELEMENT METHOD

The finite element method involves the idealization of a continuous structure by a system of discrete components of elements that are one, two or three dimensional. The three main components of the finite element method of analysis of a continuum are: (1) structural idealization; (2) evaluation of the element stiffness; and (3) structural analysis of the element assemblage. These components are explained in the following subsections.

2.2.1 Structural Idealization

Figure 2.2.1 illustrates a typical structural idealization of a

braced excavation problem. Only half of the profile is shown as the excavation is symmetrical about the center line. The wall is simulated by one-dimensional bar elements and the soil continuum is simulated by two-dimensional quadrilateral elements composed of four constant strain triangles (Wilson, 1965).

In Fig. 2.2.1 the compressible soil layer rests on rigid rock. This soil-rock interface is represented by a "rough" base along which the nodes remained fixed. The nodes on the right-hand and the left-hand boundaries are on vertical rollers, i.e., they can move vertically but not horizontally. The right-hand boundary is far away so that the boundary condition is not important. For convenience vertical rollers are used.

The structural idealization that is chosen depends on the geometry of excavation, the support system and the soil profile. As the stresses and strains in each element are assumed to be constant, the grid is constructed in such a way that the elements are small in regions where stress gradients are largest.

2.2.2 Evaluation of the Element Stiffness

The material properties of the elements represent the properties of the soil, and therefore the material properties assigned to the elements should resemble those of the soil as closely as possible.

In the analyses conducted in this report, the soil is regarded to be piecewise linearly elastic, i.e., linearly elastic within each increment of loading. Over the entire range of loading three types of elastic behavior are simulated: linear, bilinear, and anisotropically nonlinear. The sheeting is linearly elastic throughout.

Once the stress-strain properties of the elements are specified the soil element stiffness matrix [K], (Clough 1965, Wilson 1965 and Zienkiewicz and Cheung 1967) and wall element stiffness matrix [S], (Martin 1966, and Przemieniecki 1968) can be obtained.

2.2.3 Structural Analysis of the Element Assemblage

Solution for the displacements and stresses of the element assemblage requires that equilibrium, compatibility and force displacement relationships are satisfied simultaneously at all the nodes.

Although the forces acting at each node are in equilibrium, the stresses acting on the boundaries between elements are not. The stress discontinuity is a result of the assumption of constant strain in each element. This stress discontinuity influences the simulation of excavation which is discussed in a later section of this chapter.

Displacement compatibility is maintained on interelement boundaries for soil elements, but displacement compatibility is not maintained on the boundaries between one-dimensional wall elements and two-dimensional soil elements. The wall elements have three degrees of freedom per node, two translational and one rotational. Thus the wall elements are curved in the deformed state. Quadrilateral soil elements have only two degrees of freedom. In the deformed state their boundaries remain straight.

The wall element stiffness matrix [S] is a 6 x 6 matrix, as there are two nodes per wall element and three degrees of freedom per node. The total stiffness matrix for m wall elements is

$$[SH] = \sum_{1}^{m} [S]$$

where [SH] is a 3 (m + 1) x 3 (m + 1) matrix. Christian (1970) reduces [SH] by static condensation of a 2 (m + 1) x 2 (m + 1) matrix. In this way, the unknowns corresponding to the rotations of the sheeting nodes are separated out of [SH]. A full description of the wall elements and static condensation is given in Appendix B.

The stiffness matrix [T] for the complete system of n soil elements and m wall elements is given by the summation of element stiffness:

$$[T] = \sum_{1}^{n} [K] + [SH]$$

The equation for the relationship between the applied nodal forces (q) and the nodal point displacements (u) is

$$(q) = [T] \cdot (u) \qquad 2.2.3.1$$

The finite element method can handle any boundary conditions specified as either forces or displacements at the nodes. Solution of the system of equations represented by Eq. 2.2.3.1 yields the unknown nodal displacements. The strains and the stress changes in the elements are then determined from the nodal displacements.

2.3 METHOD OF EXCAVATION

The numerical procedures used to simulate excavation and strut installation are illustrated in Fig. 2.3.1 with the aid of an example. In this example five stages of excavation are performed and four levels of struts are installed sequentially, simulating the construction sequence of actual braced excavations.

2.3.1 Simulation of Excavation

When the ground surface is horizontal and external surface loads are absent, the initial stress distribution in the ground is geostatic. This means the principal stresses act in the vertical and horizontal directions and shear stresses are absent on the horizontal and vertical planes.

Excavation in a soil having geostatic initial stresses is represented in Fig. 2.3.2a. Initially, the principal stresses are normal to the surface to be exposed. After excavation the surface is stress-free. This is achieved by applying, on the newly exposed surface, tractions equal in magnitude but opposite in direction to the stresses present on the surface before excavation takes place. Figure 2.3.2b shows the stress releases corresponding to the second stage of excavation. The stresses to be released are the sum of the original

in situ stresses and the stress changes induced by the first stage of excavation. In this case, both normal and shear stresses contribute to the tractions to be applied in simulating excavation.

The sign convention used in the finite element analysis is shown in Fig. 2.3.3. Tensile normal stresses are taken to be positive.

2.3.2 Methods of Stress Release

In the finite element method of analysis stresses and stress changes are computed at the centroids of the elements. As the surface of excavation occurs along interelement boundaries, a problem arises in estimating stresses along the boundaries.

Estimation of the stresses acting on horizontal interelement boundaries is straightforward. The average of the stresses in the two elements immediately across, i.e., above and below the boundary is computed, and this average stress is released. For estimating the stresses acting on a vertical boundary the following three alternatives are possible:

(1) Averaging the stresses in the two elements immediately across the boundary of excavation.

(2) No averaging, but using the stresses in the element immediately adjacent to the vertical boundary in the mass to be removed.

(3) Extrapolating the stresses at the vertical boundary by considering the stress distribution in a horizontal band of elements to be removed. Extrapolation is performed by first fitting a polynomial of up to the tenth degree through the stresses in these elements and then evaluating the polynomial at the vertical boundary.

In the following sections the movements and stress changes obtained using the first two procedures are examined for uniqueness

of solution. Arguments are then put forward for using the method of extrapolation. In this discussion the soil is homogeneous, isotropic and linearly elastic. Initially, the stresses are geostatic and there are no pore pressures so that total and effective stresses are equal. The excavation is open.[1]

2.3.3 Uniqueness of Solution

Brown and Goodman (1963) and Goodman and Brown (1963) demonstrate mathematically for a built-up body such as an embankment, that the state of stress in the body would be different depending on whether the embankment is constructed in many lifts or in one single lift, even if the material is linearly elastic. Clough and Woodward (1967) show that displacements are also different depending on the number of lifts used.

For an excavation the same is not true. Brown and King (1966) state that if the material is linearly elastic the stresses and strains at the final stage of excavation are independent of the number and shape of the excavation steps used. This statement has been recently proven by Ishihara (1970) for an arbitrary initial state of equilibrium stresses.

2.3.4 Influence of Methods of Stress Release on Movements of Open Cuts

In this section the influence of stress release on the movements of open cuts is studied. The final excavation is 80 feet deep and 40 feet wide using a finite element grid shown in Fig. 2.3.4a. The soil properties are:

$$\text{Young's Modulus } E = 100 \text{ kips/ft}^2$$

$$\mu = 1/3$$

$$K_o = 1/2$$

$$\gamma = 0.12 \text{ kips/ft}^3$$

---

[1] In this report an open excavation is one which is completely unsupported.

Figures 2.3.5 and 2.3.6 summarize the movements of two points as a function of the number of lifts used when no averaging is performed across a vertical boundary (Method 2). The two points used for comparison are Point B and Point C. Point B is located at the center line of the final bottom of the excavation, Point C is located at the corner between the vertical face of the excavation and the ground surface.

Figure 2.3.5 shows that greatly different vertical movements occur at Point C when different numbers of lifts are used to achieve the same final depth of excavation. When only 1 lift is used, Point C moves down 0.4 ft.; when 8 lifts are used, Point C moves up 0.8 ft. On the other hand, the vertical movements of Point B are insensitive to the number of lifts used. Figure 2.3.6 further demonstrates that both the horizontal movement of Point C and the maximum horizontal movement of the vertical face of the cut are very sensitive to the number of lifts.

To test whether the lack of uniqueness described in the last paragraph is due to the coarseness of the grid used, a finer grid with 363 elements (Fig. 2.3.4b) is also used to study the influence of the number of lifts of excavation on movements. The soil properties are the same as before. Figures 2.3.7 (Method 2) and 2.3.8 (Method 1) show that the vertical and horizontal movements of points along the vertical face are greatly influenced by the number of lifts used. Figures 2.3.9 and 2.3.10 compare the movements obtained when Methods 1 and 2 are used to estimate the stresses at the boundary. When Method 1 is used the movements are even more sensitive to the number of lifts than when Method 2 is used. Again, the vertical movement of Point B is insensitive to the number of lifts used.

2.3.5 Influence of Methods of Stress Release on Stresses in Open Cuts

Figures 2.3.11, 2.3.12, and 2.3.13 show the vertical, horizontal and shear stresses acting on both sides of a plane coinciding with the vertical face of the cut, when Method 1 is used for releasing the stresses

on the vertical boundary. The horizontal and shear stresses acting on the vertical face of the cut are different depending on the number of lifts. For 1 lift the vertical face of the cut is, for a large part, almost free of horizontal and shear stresses, except near the bottom of the cut. When several lifts are used, residual stresses remain on the vertical fact of the cut and the stress distribution becomes oscillatory. The oscillations are more intense as the number of lifts is increased, i.e., fewer rows of elements are removed per lift. Finally, when 16 lifts are used, with one row of elements per lift, the horizontal and shear stress distributions on the vertical face of the cut become almost linear with depth (Figs. 2.3.14 and 2.3.15). In Fig. 2.3.16 a comparison is made of the distributions of horizontal stresses for a 4-lift excavation made with Methods 1 and 2.

2.3.6 Residual Stresses

Figures 2.3.12 through 2.3.15 show that there is a severe stress concentration at the bottom corner of the excavation. They also show the presence of residual stresses acting on the vertical face of the open cut. This boundary should be stress-free. It is therefore postulated that both the method of averaging and the method of no averaging do not give the true stresses on the vertical boundary of excavation.

If the cut is not along a straight face, but rather occurs in a terraced manner, single-step and multi-step excavations will give very close results (Figs. 2.3.17 and 2.3.19). Duncan and Dunlop (1970) also show, for a terraced cut, that the final values of the stresses calculated using 1 step and 3 steps are nearly identical. On the other hand, single-step and multi-step excavations along a straight vertical face produce movements very different from one another (Figs. 2.3.18 and 2.3.20). The grids and soil properties used for the analyses of the terraced cuts and of the vertical cuts are identical. The reason why terraced cuts are not sensitive to the number of steps of excavation while cuts along a straight face are sensitive is that terracing a cut

avoids the necessity of releasing the stresses in corners where the stress concentration is very high.

2.3.7 Method for Estimating Stresses on Vertical Face by Extrapolation

Figure 2.3.21 shows the stress distributions in two horizontal rows of elements beneath the cut. For the row of elements immediately below the bottom of the cut, the rapid increase in both the horizontal and shear stresses near the bottom corner of the cut is very conspicuous. See Fig. 2.3.22 for the locations of the two horizontal rows of elements.

By polynomial least square curve fitting a polynomial of up to the tenth degree can be fitted through the values of the stresses in the horizontal band of elements. The polynomial is then evaluated at the vertical boundary of excavation to obtain the stresses to be released. In Fig. 2.3.21 the horizontal and shear stresses extrapolated in this way are indicated by the ringed dot ⊙. The polynomial used for the extrapolation shown in Fig. 2.3.21 is of the sixth degree. The polynomial least square fitting procedure requires at least two more data points than the degree of the specified polynomial. Figure 2.3.22 shows that there are 8 elements in each horizontal row to be excavated. This means the polynomial specified should not be greater than 6. As illustrated in Fig. 2.3.22, the elements in each horizontal row to be excavated must be either square or rectangles.

The subject of polynomial least square curve fitting is well discussed in standard texts (Hamming 1962, Ralston 1965, and Liebelt 1967). The computer program is available in the Scientific Subroutine Package (IBM 1968).

Figures 2.3.23 and 2.3.24 show that the movements obtained using these extrapolated stresses at the vertical boundary of cut are virtually independent of the number of lifts of excavation. Figure 2.3.25 further shows that the net residual horizontal stresses on the vertical face of the open cut are nearly zero, using the method of extrapolation. There is

still oscillation about the zero line, but the algebraic sum is zero. The solutions obtained using the method of extrapolation therefore satisfy the condition of uniqueness better than those obtained using the other two methods.

It is concluded that for excavation with a straight vertical boundary, the method of extrapolation is the best way of estimating the stresses to be released along the vertical boundary. This method is especially applicable to braced excavations where the presence of the wall renders averaging across the vertical boundary impossible.

2.4 SEQUENCE OF STRUT INSTALLATION

The numerical procedures used to simulate strut installation are illustrated in Fig. 2.3.1 with the aid of an example. As excavation proceeds, struts are installed to reduce further movements.

Depending on the details of the wedging procedure used by the contractor, the movement of the wall at the strut level after the strut has been installed may or may not be appreciable. If the wedges placed between the wale and the wall are rigid, no further wall movement at the strut level will occur. This situation is simulated by fixing the node at which the strut is installed. On the other hand, if the wedges are soft a large movement may continue to occur at the strut level after the strut is installed. This situation is simulated by specifying a further wall movement at the strut level as a percentage of the wall movement that occurs before the strut is installed. This percentage will be based on the judgment of the person performing the analysis. Elastic behavior of struts is not simulated because in general the elastic shortening of struts is very small.[2] Prestressing of struts is frequently employed

---

[2] For example, the largest average load recorded at Test Section B is 296 kips (Fig. 5.6.1). Using an area of cross section of the strut of 0.336 ft^2, a half length of 18 ft and a Young's Modulus of 4.17×10^6 $kips/ft^2$, the elastic shortening calculated is only about 0.004 ft.

in the field. Prestressing can be simulated in the computer program by applying a force equal to the preload acting at the node where a strut is installed.

The user's manual contained in Appendix II-A explains in detail the working of the finite element computer program BRACE.

CHAPTER THREE

EXAMPLE STUDIES OF BRACED EXCAVATIONS USING LINEARLY ELASTIC STRESS-STRAIN RELATIONS

3.1 INTRODUCTION

This chapter presents the results of example studies of braced excavations using the finite element program BRACE. The influence of the following factors on the behavior of braced excavations are studied:

(a) Depth of excavation
(b) Presence of unstrutted sheeting
(c) Wall stiffness
(d) Overconsolidation ratio of soil
(e) Modulus variation with depth of soil
(f) Modulus of soil.

Table 3.1.1 shows the computer runs made and summarizes the input variables used in the example studies. The stress-strain relations of the soil are isotropic and linearly elastic. Initially the stresses in the soil are geostatic. In Runs L1 through L3 pore pressures are not present in the soil so that total and effective stresses are equal. In Runs L4 through L11 the soil is fully saturated with the water table at the ground level. The soil parameters for Runs L4 through L11 are based on results of laboratory tests on Boston blue clay reported by D'Appolonia and Lambe (1970) and Kinner (1970).

3.2 INFLUENCE OF DEPTH OF EXCAVATION ON MOVEMENTS OF OPEN EXCAVATIONS

This section presents results of an investigation into the influence of the depth of excavation on the movements of the soil adjacent to an open excavation. The excavation is 40 feet wide. The finite element grid is shown in Fig. 2.3.2a and the soil properties used are summarized under Run No. L1 in Table 3.1.1.

Two points are used to summarize the movements of the excavation. Point B is located at the center line of the bottom of the excavation. Point C is located at the corner between the vertical face of the excavation and the ground surface.

Figure 3.2.1 shows the vertical movements of Point C as the depth of excavation increases. At shallow depths of excavation Point C moves upward. As the depth of excavation increases, the upward movement at Point C decreases and when the depth of excavation reaches 80 feet, Point C experiences a net downward movement of 0.43 feet. Two factors contribute to vertical movement at Point C: the vertical forces pulling up at the bottom of the excavation and the horizontal forces pulling away from the vertical face of the excavation. At shallow depths of excavation the upward pull dominates and Point C moves up. At greater depths of excavation the horizontal pull dominates and Point C moves down.

Figure 3.2.2 shows that both the horizontal movement at Point C as well as the maximum horizontal movement of the vertical face of the open excavation increase greatly as the depth of excavation increases. Figure 3.2.3 shows that the upward movement of the bottom of the excavation at first increases and then decreases with increasing depth of excavation. These trends have also been reported by DiBiagio (1966).

3.3 INFLUENCE OF UNSTRUTTED SHEETING ON BEHAVIOR OF EXCAVATIONS

This section presents results of an investigation into the influence of an unstrutted sheeting on the movements of, and the horizontal stresses acting on, the vertical face of an excavation. Two cases are compared. One case involves an open excavation. The other case involves an excavation retained by Bethlehem ZP38 sheeting. In both cases the sides of the excavation are not supported by struts. The finite element grid is shown in Fig. 2.3.4b and the soil properties are

summarized under Runs L2 and L3 in Table 3.1.1. The soil layer is 80 feet thick. The excavation is 40 feet deep and the sheeting is 70 feet long.

Figure 3.3.1 shows that the unstrutted sheeting does not significantly reduce the inward horizontal movement of the vertical face for the two cases analyzed. It does, however, alter the deflected shape of line AA along the vertical face of the excavation. With no sheeting there is a discontinuity in the deflected shape near the bottom corner of the excavation. When the sheeting is present its rigidity helps to smooth out this discontinuity.

Figure 3.3.2 compares the horizontal stresses acting on the vertical face of the excavation with and without sheeting. For the open excavation, the vertical face is almost free of horizontal stresses except near the bottom corner of the excavation where there is a large stress concentration. The rigidity of the sheeting causes a redistribution of the horizontal stresses acting on the vertical face and also causes tensile stresses to develop near the top of the cut. Further down large horizontal stresses are present, but there is no concentration of stresses near the bottom corner of the excavation.

3.4 INFLUENCE OF WALL STIFFNESS ON BEHAVIOR OF BRACED EXCAVATIONS IN NORMALLY CONSOLIDATED CLAYS WITH LINEARLY INCREASING MODULUS WITH DEPTH

This section presents results of an investigation into the influence of wall stiffness on the behavior of braced excavations. Four walls are studied: (1) ZP38 sheeting, (2) a 3 foot thick slurry wall, (3) imaginary wall with zero stiffness and (4) an open excavation. The aspects of behavior studied are: (1) movements, (2) stresses acting on wall, (3) stresses in soil, (4) strut loads, and (5) bending moments and shear forces in wall.

The finite element grid and the sequence of excavation and strut installation are shown in Fig. 2.3.1. The soil properties are summarized

under Runs L4 through L7 in Table 3.1.1. The final depth of excavation is 50 feet. The width of the excavation is 40 feet. The soil layer is 70 feet thick. The walls are 60 feet long. Excavations are made under undrained conditions. The slurry wall[1] is simulated by one-dimensional bar elements. Table 3.4.1 summarizes the properties of the walls.

After each strut is installed, further movement of the sheeting at that strut level is prevented. Five stages of excavation are performed and four levels of struts are installed sequentially. The struts are not prestressed.

3.4.1 Movements

Figure 3.4.1 shows the deformed states of the soil mass corresponding to the final stage of excavation for four cases of wall supports. The strutted wall greatly reduces both the horizontal movements of the vertical face of the excavation as well as the vertical settlement of the ground. Moreover, as expected, the stiffer the wall, the smaller are the movements. On the other hand, the heave of the bottom of the excavation is virtually independent of the stiffness of the wall.

Figure 3.4.2 shows the horizontal movements of the three walls through the five stages of excavation, as well as the horizontal movements of the vertical face of the open excavation. For zero wall stiffness, strutting the sides reduces the maximum horizontal movement of the vertical face by half. With the ZP38 sheeting the maximum horizontal movement is 0.21 feet, while with the slurry wall it is 0.16 feet.

3.4.2 Stresses Acting on Wall

Figure 3.4.3 shows the horizontal stresses acting on the slurry

---

[1] The term "slurry wall" is used in this report to mean a concrete retaining wall built in a mechanically excavated trench which is supported by bentonite slurry.

wall and the ZP38 sheeting. As expected, the stresses acting on the slurry wall are greater than those acting on the sheeting. The slurry wall, being stiffer, moves less and therefore the stresses acting on the slurry wall depart from the geostatic stress state less than the stresses acting on the sheeting.

Figure 3.4.4 shows the horizontal stresses acting on the ZP38 sheeting during the various stages of excavation. When soil is removed from the front face of the wall, the horizontal stresses acting on the back face of the wall generally decrease. However, if a strut is present and soil is removed from below that strut level, the stresses acting on the back face of the wall immediately above that strut level generally increase. The reason for this increase is the rotation of the wall into the soil as a consequence of the fact that the wall behaves as a continuous beam.

The horizontal stresses acting on the front face of the ZP38 sheeting below the bottom of various stages of excavation are shown in Fig. 3.4.5. At each stage of excavation there is a large stress concentration near the corner of the excavation. Except near the bottom corner of the excavation the stresses are smaller than the original geostatic horizontal stresses for the case analyzed. The soil immediately in front of the sheeting experiences both vertical unloading and horizontal loading. Figure 3.4.5 suggests that except near the bottom corner of the excavation where stress concentration is high, the effect of vertical loading on the horizontal stress distribution is greater than the effect of horizontal loading.

3.4.3 Stresses in Soil

Figure 3.4.6 shows the stresses in the soil after the second stage of excavation. The stress changes from the initial condition are smaller when a slurry wall is used than when ZP38 sheeting is used.

Figure 3.4.7 shows the stresses in the soil mass after the fifth

stage of excavation. In general, the softer the retaining wall, the greater the stress changes from the initial condition and the greater the zone over which these stress changes occur. In fact, if an infinitely stiff slurry wall is socketed in bedrock and is strutted at the top before any excavation is made then the stress changes and the strains in the soil mass will be zero. Beyond a distance from the vertical face of the cut of about twice the depth of the cut, the stress changes in the soil are very small for both walls.

3.4.4 Strut Loads

Figure 3.4.8 summarizes the strut loads during excavation. The strut loads are greater when the slurry wall is used than when the ZP38 sheeting is used. This is expected as the horizontal stresses acting on the slurry wall are greater than those acting on the sheeting. After the bottom strut is installed and further excavation is made below the bottom strut, the load in the strut immediately above the bottom strut generally decreases.

3.4.5 Bending Moments and Shear Forces in Sheeting

Figure 3.4.9 shows the bending moments and Fig. 3.4.10 shows the shear forces in the ZP38 sheeting at various stages of excavation. Positive bending moments are plotted at the side of the sheeting where tensile fiber stresses are developed. Note that Stage 2 excavation, where only one strut has been installed, corresponds qualitatively to an anchored bulkhead. Comparison of bending moment and shear force diagrams show that, as expected, maxima of the bending moment diagrams occur where the shear forces are zero. For the case represented by Fig. 3.4.9, the largest bending moment at each stage of excavation occurs below the current bottom strut.

3.5 INFLUENCE OF OVERCONSOLIDATION RATIO ON BEHAVIOR OF BRACED EXCAVATIONS IN CLAYS

This section presents results of an investigation into the influence

of overconsolidation ratio (OCR) on the behavior of braced excavations in clays. As the lateral stress ratio K_o of a soil with a given plasticity index is related to the overconsolidation ratio (Brooker and Ireland, 1965), the results of the investigation also show the influence of K_o on the behavior of braced excavations. The overconsolidation ratios studied are 1, 2 and 5, corresponding to K_o of 0.5, 0.7 and 1. These values of K_o are obtained from a relationship between K_o and OCR for Boston blue clay reported by D'Appolonia and Lambe (1970) and shown in Fig. 3.5.1.

The finite element grid and the sequence of excavation and strut installation are shown in Fig. 2.3.1. The excavation is retained by ZP38 sheeting and supported by 4 level of struts. The final depth of excavation is 50 feet. The width of excavation is 40 feet. The sheeting is 60 feet long. The soil properties are summarized under Runs L4, L8 and L9 in Table 3.1.1.

Excavations are made under undrained conditions. After each strut is installed, further movement of the sheeting at the strut level is prevented. The struts are not prestressed.

3.5.1 Movements

Figure 3.5.2 compares maximum movements for soils with different K_o. For the cases analyzed, the maximum sheeting movement, maximum bottom heave, and maximum ground settlement are relatively insensitive to the lateral stress ratio. DiBiagio (1966) shows that for open cuts in dry soil, while the bottom heave is insensitive to K_o, the maximum horizontal movement of the vertical face is almost directly proportional to K_o.

The relative insensitivity of the sheeting movements in braced cuts in saturated elastic soils to K_o is due to (a) the presence of pore

pressures which decreases the influence of K_o on σ_h, i.e., K_o with respect to total stress does not vary much, (b) the presence of the sheeting and bracing system.

3.5.2 Stress Distributions on Sheeting

Figure 3.5.3 shows the initial total lateral stessses before excavation, as well as the final total lateral stresses, for three overconsolidation ratios. The final lateral stresses depend on the initial states of stress. The higher the K_o the larger the final lateral stresses acting on the sheeting. For comparison Fig. 3.5.4 shows the initial lateral stresses for the three OCR's when the soils are completely dry and pore pressures are zero everywhere. The influence of K_o on the initial lateral stress distributions is much greater when the pore pressures are zero. The same argument can be applied to the final lateral stresses.

3.5.3 Stress Reorientations in Soils

Figures 3.5.5 and 3.5.6 show the reorientations of the total principal stresses caused by excavations in soils with OCR equal to 2 and 5 respectively. Immediately below the center line of the excavation there is almost a 90^o change in the orientation of the principal stresses. Whereas initially the major principal stress acts in the vertical direction, after excavation it acts in the horizontal direction. Immediately behind the sheeting there is also significant stress reorientation. The stress concentration near the bottom corner of the excavation is very conspicuous. The crosses show the relative magnitude of the major and the minor principal stresses and the directions in which these stresses act.

3.6 INFLUENCE OF MODULUS VARIATIONS WITH DEPTH OF CLAY ON BEHAVIOR OF BRACED EXCAVATIONS

This section presents results of an investigation into the influence of two modulus variations with depth of clay on the behavior of braced

excavations. The modulus variations with depth are:

(1) Modulus increasing linearly with depth from zero at ground surface. ($E/\bar{\sigma}_{vo} = 80$)

(2) Modulus constant with depth. ($E = 175$ kips/ft^2).

The average value of the modulus is the same for the two variations. Figure 3.6.1 illustrates these two modulus variations with depth. Movements, stresses acting on the sheeting, and strut loads are compared in Subsections 3.6.1 through 3.6.3 for excavations in clays with these two modulus variations. Note that the comparisons and discussions are relevant only to the two cases analyzed, and their particular geometry and soil properties. One important factor is the fact that the average value of the modulus is the same for the two variations.

The finite element grid and the sequence of excavation and strut installations are shown in Fig. 2.3.1. The excavation is retained by ZP38 sheeting and supported by 4 levels of struts. The final depth of excavation is 50 feet. The width of the excavation is 40 feet. The sheeting is 60 feet long. The soil properties are summarized under Run L4 and Run L10 in Table 3.1.1.

Excavations are made under undrained conditions. After each strut is installed further movement of the sheeting at that strut level is prevented. The struts are not prestressed.

3.6.1 Movements

Figure 3.6.2 compares the horizontal sheeting movements during excavation in soils with linear and with constant modulus with depth. The average modulus is the same for the two variations. During the initial stages of excavation the maximum horizontal sheeting movements are smaller in the soil with constant modulus than in the soil with linear

modulus. At the final stage of excavation the reverse is true.

Figure 3.6.3 compares the ground settlements outside the excavation for the two modulus variations. As expected, initially the settlements of the soil with linear modulus are much larger than those of the soil with constant modulus. At the final stage of excavation the maximum settlements of the two soils are almost identical.

Figure 3.6.4 compares the bottom heaves caused by excavation in soils with the two modulus variations. Initially, the soil with linear modulus heaves more than that with constant modulus. The reverse is true during the later stages of excavation. This trend is expected because elastic heave is governed by the average modulus below the bottom of the excavation.

3.6.2 Stress Distributions on Sheeting

Figure 3.6.5 compares the final horizontal stress distributions along the sheeting. It shows that the stresses near the top strut are much larger when the modulus is constant with depth than when it is linear with depth. When the modulus is constant with depth the soil near the ground surface is much stiffer than when the modulus is linear with depth. After the first strut has been installed and further excavation has proceeded below it, the sheeting rotates into the soil around the first strut, and therefore the pressures increase near the first strut. This phenomenon is more marked when the modulus is constant with depth because the soil is stiffer near the ground and softer further below than when the modulus is linear with depth. In natural soil deposits where a stiff crust usually overlies softer layers below, this phenomenon is of practical importance and is probably the basis for the trapezoidal shape of the design earth pressure diagrams suggested by Terzaghi and Peck (1967).

3.6.3 Strut Loads

Figure 3.6.6 compares the strut loads for the two modulus variations. The total strut loads as well as the loads in the top two struts are larger when the modulus is constant with depth. At the final stage of excavation, the loads in the third and the fourth struts are nearly equal for the two modulus variations. This can be explained by the fact that near the third and the fourth struts, the moduli of the two soils are nearly equal.

3.7 BRACED CUTS IN CLAYS WITH SAME OCR BUT DIFFERENT MODULI

If a material is homogeneous, isotropic and linearly elastic the deformations resulting from a given applied load will be inversely proportional to the Young's modulus, other factors being constant. In braced excavations the soil-support system constitutes a nonhomogeneous assembly. The deformations and stress changes will be influenced not only by the stiffness of the soil but also by that of the wall. In Section 3.4 the influence of the stiffness of the wall on the performance of braced excavations was investigated. In this section the influence of changing the stiffness of the soil is studied. The stiffness of the wall is kept constant.

The finite element grid and the sequence of excavation and strut installation are shown in Fig. 2.3.1. The excavation is retained by ZP38 sheeting and is supported by 4 levels of struts. The final depth of excavation is 50 feet and the width of excavation is 40 feet. The sheeting is 60 feet long. Excavations are made under undrained conditions. After each strut is installed, further movement of the sheeting at that strut level is prevented. The struts are not prestressed.

Two computer runs were made by using modulus ratio ($E/\bar{\sigma}_{vo}$) of 80 and 300. The input variables for these two runs are summarized

under Run L4 and Run L11 in Table 3.1.1.

Figure 3.7.1 compares the maximum movements resulting from identical excavations. When $E/\bar{\sigma}_{vo}$ is 80 the maximum settlement and sheeting movement are 0.1166 and 0.2156 feet, respectively. However, the maximum settlement and sheeting movement obtained from Case II by inverse proportionality are 0.1292 and 0.2388 feet, an increase of about 10%. The reason for this increase is that in a soil with a high modulus, the relative role played by a given sheeting is smaller than in a soil with a smaller modulus.

Figure 3.7.2 compares the strut loads resulting from excavation in soils with $E/\bar{\sigma}_{vo}$ = 80 and 300. When $E/\bar{\sigma}_{vo}$ is 80 the total strut loads are greater than when $E/\bar{\sigma}_{vo}$ = 300. The reason for this difference is that in the former case the sheeting behaves as a relatively stiffer wall than in the latter case and hence carries a bigger load.

CHAPTER FOUR

EXAMPLE STUDIES OF BRACED EXCAVATIONS USING BILINEARLY AND ANISOTROPIC, NONLINEARLY ELASTIC STRESS-STRAIN RELATIONS

4.1 INTRODUCTION

In the analyses presented in the preceding chapter the soils were assumed to be linearly elastic. In reality, the stress-strain behavior of soils is not linearly elastic except for small stress changes. In has been shown (D'Appolonia, 1968) that for model footing loadings on normally consolidated Boston blue clay, extensive yielded zones may be present in the soil even at factors of safety as high as 3.

Classical earth pressure theories of Rankine, Coulomb, Brinch Hansen (1953) and others assume that the soil is in a state of limiting equilibrium. The concept of limiting equilibrium provides only estimates of the stress conditions at failure, but not estimates of the stresses and strains prior to failure.

Figure 4.2.1 shows different time-independent stress-strain relations that can be used to simulate the behavior of soil. In this chapter only the bilinear and the nonlinear stress-strain relations will be considered.

Two approaches are possible. The first one is to develop fundamental relationships based on plasticity theory. An M.I.T. report (1968) describes a method based on the finite element technique for analyzing undrained loading on elasto-plastic soil. Hagmann (1971), using the finite element method, analyzes loading of strip footings on elasto-plastic and elasto-plastic-strain hardening soil. Hagmann's method can handle at the present time only drained loading on soils.

The second approach is to approximate the actual stress-strain relation of soils with either two straight lines or with a curve. The loading is applied in increments. Within each increment the stress-strain relation is linearly elastic, but over the whole range of loading it is not. This approach is used in the analyses described in this chapter.

4.2 BILINEAR AND NONLINEAR APPROXIMATIONS OF STRESS-STRAIN RELATIONS OF SOILS

The bilinear approximation consists of fitting two straight lines over the actual stress-strain curve determined in the laboratory. An example of this approximation is shown in Part C of Fig. 4.2.1. D'Appolonia and Lambe (1970), Dunlop and Duncan (1970) and Kinner (1970) have reported results of finite element analyses of strip footings and excavated slopes using bilinear stress-strain relations.

The nonlinear approximation involves fitting a curve over the actual stress-strain curve. Kondner (1963), Kondner and Zelasko (1963) suggest a hyperbolic approximation. Duncan and Chang (1970) and Chang and Duncan (1970) have used this hyperbolic approximation in finite element analyses.

However, while the hyperbola provides a good fit for some stress-strain curves, it may not do so for other curves. As there is no physical basis to show why the stress-strain curves should be hyperbolic, the use of a hyperbolic approximation is restrictive. Figures 4.2.2 and 4.2.3 from Kondner (1963) illustrate this point.

A better approximation in theory is a polynomial. The fit can be made as close to the actual curve as desired by increasing the degree of the polynomial. The fit is performed using a polynomial least square method (Hamming 1962, Ralston 1965, and Liebelt 1967). The computer program is available in the Scientific Subroutine Package (IBM 1968).

Figures 4.2.4 and 4.2.5 show four plane strain tests on resedimented Boston blue clay reported by Bovee (1970). Also shown in the figures are the polynomial approximations. The fit is very close. Beyond a certain strain a straight line with a small positive slope supplements the polynomial. For the first load increment an initial modulus of $E/\bar{\sigma}_{vo} = 450$ is used.

In both the bilinear and nonlinear analyses the bulk modulus remains unchanged throughout the entire range of loading.

4.3 EXAMPLE STUDIES OF BRACED EXCAVATIONS USING BILINEAR ELASTIC STRESS-STRAIN RELATIONS

4.3.1 Introduction

This section presents the results of example studies of braced excavations using BRACE and bilinear elastic stress-strain relations for clays.

The finite element grid and the sequence of excavation and strut installation are shown in Fig. 2.3.1. The excavation is supported by 4 levels of struts. The final depth of excavation is 50 feet. The width of excavation is 40 feet. The wall is 60 feet long. Excavations are made under undrained conditions. After each strut is installed further movement of the wall at that strut level is prevented. The struts are not prestressed.

The soil properties used in these analyses are summarized in Fig. 4.3.1. They are based on results of laboratory tests on Boston blue clay reported by D'Appolonia and Lambe (1970) and Kinner (1970). Table 4.3.1 shows the computer runs made and summarizes the input variables.

The aspects of behavior of braced excavations investigated are (a) development of yielded zones in soil, (b) stability factor in braced

excavations, (c) movements, and (d) stresses and strut loads. The following subsections describe these aspects of behavior in detail.

4.3.2 Development of Yielded Zones

The yield criterion adopted in the analyses using bilinearly elastic stress-strain relations is Tresca's criterion. According to this criterion, an element in a soil mass has yielded when the maximum shear stress in the element equals the undrained shear strength.

Figures 4.3.2 through 4.3.5 show the development of yielded zones during excavation in clays of various OCR's. For the normally consolidated clay Fig. 4.3.2 shows that even at shallow excavations of 10 and 22.5 feet extensive yielding has occurred. At the final depth of 50 feet the yielded zones in front of, and behind the sheeting have merged, forming a single continuous zone.

Figures 4.3.3 through 4.3.5 show that for overconsolidated clays with OCR ≥ 2 very little yielding occurs throughout the process of excavation. For the case when OCR = 25, the $Su/\bar{\sigma}_{vo}$ used is only 1.4 rather than the full 1.85. This reduction of 25% is to account for some loss of undrained strength with time for unloading of an overconsolidated clay. Despite this reduction very little yielding occurs.

Figure 4.3.6 shows the yielded zones when the thickness of the clay layer is 100 feet for OCR = 1. The yielded zones are quite similar to those in Fig. 4.3.2. For sheeting not driven into bedrock or other stiffer layers, the presence of a 10 foot gap (Fig. 4.3.2) between the sheeting and the bedrock allows as much development of the yielded zones as the presence of a 40 foot gap (Fig. 4.3.6).

Figure 4.3.7 shows the yielded zones when the excavation is retained by a 3-foot thick slurry wall. It shows that the use of the slurry wall does not reduce the development of the yielded zones when compared with the use of the ZP38 sheeting.

Figure 4.3.8 shows the yielded zones when the top 30 feet of the clay has an OCR = 2 and a constant Su = 0.535 kip/ft^2, and the bottom 40 feet of the clay has an OCR = 1 and $Su/\bar{\sigma}_{vo}$ = 0.342. This strength profile simulates the overconsolidation due to desiccation near the ground surface found in many soil deposits. While little yielding has occurred in the top stronger layer, large yielded zones have formed in the softer layer below when the excavation has reached into that layer.

4.3.3 Stability Factor in Braced Excavations

Bjerrum and Eide (1956) suggest that the factor of safety of excavations against failure by bottom heave can be estimated by

$$F = \frac{Su\ Nc}{\gamma D} \qquad (4.3.3.1)$$

When γ is the total unit weight, D is the depth of cut, Su is the undrained shear strength and Nc is a number depending on the geometry of the cut.

Bjerrum and Eide (1956), Terzaghi and Peck (1967) and Peck (1969) recommend that the dimensionless number N be used as an index of approaching bottom failure where

$$N = \frac{\gamma D}{Su} \qquad (4.3.3.2)$$

Combining these two equations one gets

$$F = \frac{Nc}{N} \qquad (4.3.3.3)$$

Table 4.3.2 shows the N values for braced excavation in a soil with the properties of Boston blue clay, and with OCR = 1, 2, 5 and 25. Reference to Figs. 4.3.2 and 4.3.6 for OCR = 1 shows that at N = 7.1 and D $\geq$ 42.5 feet, the yielded zones in front of and behind the sheeting have merged.

Table 4.3.3 shows the factors of safety of the braced cuts

calculated from Eq. 4.3.3.3. The Nc values were estimated from charts developed by Janbu et al (1956). It confirms that for a soil with the properties of normally consolidated Boston blue clay, when the two yielded zones have merged, the factor of safety is indeed less than 1 and that very large movements have occurred.

For overconsolidated clays whose strength increases with depth, very little yielding will occur despite a relatively high N value. Table 4.3.2 shows that for OCR = 2 the N value is 5 when the excavation depth is 50 feet. This implies that in theory an excavation can be made to any depth without danger of base failure when the $Su/\overline{\sigma}_{vo}$ ratio is constant with depth and when the OCR for the entire clay layer is equal to or greater than 2. This of course may not be true in actual field cases because the OCR for most soil deposits generally decreases with depth. The normally consolidated clays below will limit the depth to which an excavation can safely proceed (Fig. 4.3.8). Moreover, the loss with time of the undrained shear strength of overconsolidated clays may result in additional yielding.

4.3.4 Movements

Figure 4.3.9 compares the horizontal movements of the sheeting obtained in analyses using linearly and bilinearly elastic stress-strain relations. In the analysis using bilinearly elastic stress-strain relations, a large movement of the bottom of the sheeting towards the excavation has taken place during the fifth stage of excavation. Reference to Fig. 4.3.2 shows that during the fifth stage of excavation, the yielded zones in front of and behind the sheeting have merged, representing a total failure condition.

Figure 4.3.10 compares the sheeting movements obtained in four analyses using bilinearly elastic stress-strain relations. It shows

that in three excavations a large movement of the bottom of the retaining wall towards the excavation has taken place during the final stage of excavation. Reference to Figs. 4.3.2, 4.3.7 and 4.3.8 shows that total failure conditions have been reached. Bilinearly elastic analysis of excavation in a clay with OCR = 2 retained by the ZP38 sheeting shows a maximum sheeting movement of 0.08 ft. compared with 0.44 ft. obtained in bilinearly elastic analysis of excavation in a clay with OCR = 1. Reference to Fig. 4.3.5 shows that very little yielding occurs in the clay with OCR = 2.

Figure 4.3.11 compares the settlements of the ground surface outside the excavation obtained in bilinearly and linearly elastic analyses of a clay with OCR = 1 retained by the ZP38 sheeting. At the fifth stage of excavation the maximum settlement obtained in the linearly elastic analysis is 0.035 feet, compared with 1.01 feet obtained in the bilinearly elastic analysis.

Figure 4.3.12 shows the deformed soil mass at the second and fifth stage of excavation obtained in three analyses. It shows again that when yielding is allowed, as in the bilinearly elastic analyses, the movements are much bigger than when it is not allowed, as in the linearly elastic analysis. When an overconsolidated layer overlies a normally consolidated layer, bilinearly elastic analyses show that the ground settlements are much less than when the whole deposit is entirely normally consolidated. At the later stages of excavation, when the bottom of the excavation has reached the softer layer below, the bottom heaves are the same whether the overconsolidated layer is or is not present at the top.

4.3.5 Stresses and Strut Loads

Figures 4.3.13 and 4.3.14 show the horizontal stresses acting on the ZP38 sheeting when the depth of excavation is 50 feet. The

OCR's of the clay are 1 and 2. Also shown in the figure are the original geostatic stresses, and the distributions given by $\sigma_h = \gamma Z - 2$ Su, where Su varies linearly with depth.

Figure 4.3.15 shows the strut loads obtained in the bilinearly and linearly elastic analyses of a clay with OCR = 1. In the bilinearly elastic analysis of the final state of excavation the bottom strut experiences a very high load, while the third strut experiences a sharp reduction in load. This is expected as Fig. 4.3.2 shows that the yielded zones in front of and behind the sheeting have merged. The dimensionless number N at this stage is 8.32. However, the total load in all the struts is not much larger than that obtained in the analysis using linearly elastic stress-strain relations.

On the basis of the measurements from excavations in Oslo and Mexico City, Peck (1969) suggests that when N exceeds 6 a reduction factor m be applied to the Su when calculating the apparent pressure diagram. The value of m recommended is 0.4. In Fig. 4.3.13 the Terzaghi-Peck pressure diagrams for soft clay corresponding to m = 1.0 and 0.4 are shown. When m = 0.4 is used, the pressure near the upper struts is much larger than that obtained in the bilinearly elastic analysis. When a large movement of the sheeting towards the excavation has taken place below the bottom strut, the high load experienced by that strut calls for the extra margin of safety provided by the use of m = 0.4.

Figure 4.3.14 shows that for cuts in a clay with OCR = 2, the expression $\sigma_h = \gamma Z - 2$ Su gives lower values of the horizontal stresses than the values predicted by BRACE using bilinearly elastic stress-strain relations. This is expected because Fig. 4.3.3 shows that very little yielding has occurred, and that the soil mass is still essentially elastic, and therefore classical earth pressure theories based on

limiting equilibrium may not be applicable. On the other hand, the pressure distribution predicted by BRACE agrees well with the Terzaghi-Peck pressure diagram for stiff clay.

Figure 4.3.16 shows the maximum stresses due to bending experienced by the wall at the final stage of excavation when a large movement of the bottom of the wall towards the excavation has taken place. The stresses developed exceed the yield stress of the steel only in the case when the entire clay layer is completely normally consolidated. Even then the overstressing is very small.

4.4 EXAMPLE STUDIES OF BRACED EXCAVATIONS USING ANISOTROPIC: NONLINEARLY ELASTIC STRESS-STRAIN RELATIONS

4.4.1 Introduction

This section presents the results of example studies of braced excavations using BRACE and anisotropic, nonlinearly elastic stress-strain relation for clays.

The finite element grid and the sequence of excavation and strut installation are shown in Fig. 2.3.1. The excavation is retained by ZP38 sheeting and supported by 4 levels of struts. The final depth of excavation is 50 feet. The width of excavation is 40 feet. The sheeting is 60 feet long. Excavations are made under undrained conditions. After each strut is installed further movement of the wall at that strut level is prevented. The struts are not prestressed. The computer runs made and the input variables are summarized in Table 4.4.1. The stress-strain curves used in the example studies are shown in Figs. 4.2.4 and 4.2.5.

The soils are assumed to be piecewise linearly elastic. Within each load increment the undrained Young's modulus under plane strain conditions is computed as follows:

$$E = \frac{0.75\left[(\sigma_1 - \sigma_3)_i - (\sigma_1 - \sigma_3)_{i-1}\right]}{(\epsilon_{axial})_1 - (\epsilon_{axial})_{i-1}}$$

$$= \frac{1.5\left[(\sigma_1 - \sigma_3)_i - (\sigma_1 - \sigma_3)_{i-1}\right]}{(\gamma_{max})_i - (\gamma_{max})_{i-1}}$$

where γ_{max} is the maximum undrained shear strain, and i denotes the values at the end of the current increment, and (1 - 1) denotes the values at the end of the previous increment. In any increment, γ_{max} for each element at the end of that increment is put equal to $(\gamma_{max})_{i-1} + (\Delta\gamma_{max})_{i-1}$, where $(\Delta\gamma_{max})_{i-1}$ is the change in the maximum undrained shear strain for that element computed in the previous increment. $(\sigma_1 - \sigma_3)_i$ corresponding to $(\gamma_{max})_i$ is then obtained from the stress-strain curves. The modulus calculated for each element in this way approximates an increment secant modulus.

4.4.2 Influence of Stress Reorientation on Modulus

Ladd (1964) shows that the undrained modulus of a clay depends on the stress system. Triaxial extension and compression tests result in different stress-strain curves. The same is true of plane strain tests (Bovee, 1970).

Figures 3.5.5 and 3.5.6 show that during excavation there is reorientation of the total principal stress directions. Studies conducted by Duncan and Dunlop (1969) of the simple shear tests have shown the importance of the influence of stress reorientation on the stress-strain behavior of the soil. After considering cross-anisotropy theoretically, Christian (1970) suggests the following approximate relation to account for the effect of this reorientation:

$$E_\theta = E_H - (E_H - E_V)\cos^4\theta \qquad (4.4.2.1)$$

where E_V and E_H are the incremental secant moduli from active and passive tests, respectively, and θ is the orientation from the vertical of the direction of the major (compression positive) principal stress changes. E_θ is then the modulus to be used. In this way, the anisotropy of both strength and modulus of the clay is accounted for.

4.4.3 Movements

Figure 4.4.1 compares the ground surface settlements caused by excavation in clays with OCR = 1 and 2. Anistropic, nonlinearly elastic stress-strain relations are employed. The maximum settlement for OCR = 1 is 0.17 feet compared with 0.11 feet for OCR = 2.

Figure 4.4.2 compares the maximum settlements of the ground surface when linearly, bilinearly and anisotropic, nonlinearly elastic stress-strain relations are employed. The bilinearly elastic stress-strain relation gives the largest settlement.

Figure 4.4.3 shows the horizontal sheeting movements for OCR = 1 and 2 when anisotropic, nonlinearly elastic stress-strain relations are used. Comparison with Fig. 4.3.10 shows that the nonlinearly elastic analysis results in larger sheeting movements. The exception occurs during the final stage of excavation in the bilinearly elastic analysis when a large movement of the bottom of the sheeting towards the excavation has taken place. Bilinearly elastic analysis shows relatively small movements of the toe of the sheeting at shallow depths of excavation. The analysis using anisotropic, nonlinearly elastic stress-strain relations shows that appreciable toe movements have occurred even at shallow depths of excavation, the reasons being that in this analysis the stiffness of the soil is continuously changing.

Figure 4.4.4 shows the deformed soil mass at D = 22.5 and 50 feet for OCR = 1 and 2.

4.4.4 Stresses and Strut Loads

Figure 4.4.5 shows orientation of the total principal stresses in the clays at D = 22.5 and 50 feet.

Figure 4.4.6 shows the contours of maximum shear stresses in the clays at D = 22.5 and 50 feet.

Figure 4.4.7 shows the strut loads obtained in analyses of excavations in clays with OCR equal to 1 and 2 using anisotropic, nonlinearly elastic stress-strain relations. Figure 4.4.8 compares the strut loads obtained in three analyses of an excavation in normally consolidated clay using linearly, bilinearly and anisotropic, nonlinearly elastic stress-strain relations for the clay. The total strut loads obtained in the three analyses are nearly the same. At the final stage of excavation, the load in the bottom strut obtained using anisotropic, nonlinearly elastic stress-strain relations is much smaller than that obtained using bilinearly elastic stress-strain relations. The reason for this difference is that in the nonlinear case there is no large movement of the bottom of the sheeting at the final stage of excavation whereas in the bilinear case there is a large movement.

CHAPTER FIVE

PREDICTED PERFORMANCES OF TEST SECTIONS A AND B NORTH STATION, BOSTON

5.1 INTRODUCTION

In this chapter the predicted performances of Test Sections A and B are presented. The aspects of the performances predicted were pore pressures, horizontal stresses and strut loads, wall movements, and ground settlements. The measured performances of Test Sections A and B are presented in Part II of this report.

The pore pressures were predicted first, as they were needed for the predictions of the other aspects of the performances. For predicting horizontal stresses and strut loads, wall movements, and ground settlements, currently available techniques as well as the finite element program BRACE were employed.

5.2 PORE PRESSURES NEAR EXCAVATIONS

Pore pressure considerations are important in braced excavations in the following ways:

(1) Pore pressures can constitute a large portion of the stress acting on the sheeting.

(2) Decrease in pore pressures can result in settlements of nearby soils.

(3) Piping or blowup may occur in an excavation.

Section 5 in Part II of this report lists the causes for pore pressure changes at Test Sections A and B. In general, it can be expected that the pore pressures outside an excavation will not be static. For soils of high permeability steady-state seepage is quickly reached.

For soils of low permeability such as clays, transient conditions are more probable in view of the relatively short time during which an excavation is open. For clays, the excess pore pressure caused by total stress changes may also be important.

5.2.1 Steady-State Seepage Analysis

Given the hydraulic boundary conditions the following methods can be used to analyze seepage:

1. Analytical solutions, including conformal mapping and the hydograph method.
2. Graphical flow nets
3. Electrical analogues
4. The flow tanks
5. Hele-Shaw models
6. Numerical analyses - finite element or finite difference.

Analytical solutions exist for a few simple cases only. Naturally occurring soils are generally inhomogeneous and anisotropic and, therefore, the methods 2, 3, 4, and 5 are very laborious to use. On the other hand, numerical analyses, particularly the finite element analysis, are very suitable as they can handle any boundary conditions and soil inhomogeneity and anisotropy. This method will be used to analyze the seepage at Test Sections B and A.

5.2.2 Finite Element Analysis of Seepage at Test Sections B and A

The permeabilities used in the analysis are shown in Fig. 5.2.1. The permeabilities of the silts and the fill were obtained from field sensitivity tests on piezometers and observation wells. The permeability of the till was obtained from values listed in publications relating

permeabilities with soil types and particle sizes (Land and Washburn, 1946, Terzaghi and Peck, 1967).

The sheeting had holes and ruptured joints and was not water-tight (See Part II, Figs. 4.2 and 4.3). A range of values of the equvilent permeability of a sheeting of gross thickness (perpendicular to the axis of the excavation) of one foot was employed in the analyses. Figure 5.2.2 compares the pore pressures acting on the wall at Test Section B corresponding to a range of permeabilities for the sheeting. Finally, the equivalent permeability of 0.1×10^{-6} cm/sec was chosen, based on the assumption that when the excavation was about 38 feet deep, roughly equal amounts of water flowed through the sheeting as under the sheeting. This equivalent permeability of 0.1×10^{-6} cm/sec was used for all the seepage analyses to be described later in this section.

Figure 5.2.3 shows the finite element grid used for the analysis of Test Section B. The computer program called FEDAR was used (Taylor and Brown 1967).

Figure 5.2.4 compares the measured with the predicted pore pressures near the sheeting at the final stage of excavation. Figure 5.2.5 shows the contours of the total head when the excavation was 48 feet deep. It is interesting to compare it with Fig. 5.2 of Part II which shows the measured contours.

Figure 5.2.6 shows the predicted total head 20 feet from the sheeting at various stages of excavation at Test Section B. The measured values are shown in Fig. 5.1 of Part II.

A similar analysis was also performed for Test Section A. Owing to the intense recharging, the pore pressure distribution based on steady-state seepage, which did not consider recharging, was not

used. Instead, a "best estimate" distribution intermediate between the static and the steady-state seepage distributions was preferred. This "best estimate" was based on the guess that the total head in the till would be nearer the steady-state seepage condition while the total head in the fill would be nearer the static condition. Figure 5.2.7 shows the static, the steady-state seepage, the "best estimate," and the measured distributions on and near the sheeting at Test Section A. Section 5.6 contains the conclusions.

5.3 HORIZONTAL STRESSES AND STRUT LOADS

Three classes of methods will be used in this section for estimating horizontal stresses on the wall and the loads in the struts in braced excavations. They are:

(1) Semiempirical Methods

(2) Stress Ratio Methods (horizontal stresses) and Elastic Beam Analyses (Strut Loads)

(3) Finite Element Program BRACE.

In all these methods the lateral stresses can be treated as total stresses, or separately, as pore pressures and effective stresses.

Figure 5.3.1 from Lambe (1970) shows how considerations of pore pressures can sometimes be more important than those of effective stresses. For a normally consolidated soil the range of pore pressures between static steady-state seepage conditions is much greater than the range of horizontal effective stresses between at-rest and active conditions.

5.3.1 Semiempirical Methods

There are three commonly used semiempirical methods for estimating lateral stresses on a retaining wall. They are:

(1) Terzaghi-Peck (Terzaghi and Peck 1967, Peck 1969).

(2) Tschebotarioff (Tschebotarioff, 1962).

(3) Navdock (Navdock DM7, 1962).

As the last two methods are variations of the old version of the Terzaghi-Peck method and as the Terzaghi-Peck method was revised in 1967, only it will be employed as a vehicle to illustrate the use of this class of methods. Tschebotarioff's method for sand and Navdock's method for clay were also used to obtain the strut loads shown in Figs. 5.3.6 and 5.3.7. The strut loads based on these semiemperical methods are maximum loads to be used for design only.

As the Terzaghi-Peck method does not contain recommendations for handling subsoil profiles which depart from the simple cases of homogeneous "clay" or "sand," the pressure diagrams in Figs. 5.3.2 and 5.3.3 correspond to those for an undrained clay, a drained sand and a sand submerged in static water. The soil properties used for these "equivalent" sand and clay were average values of the fill, silt and till. After the horizontal stresses were obtained the load in each strut was computed by summing the stresses acting on the segment of wall halfway to each adjacent strut in the vertical direction. The strut loads computed are shown in Figs. 5.3.6 and 5.3.7.

5.3.2 Stress Ratio Methods

This method is an extension of the stress path concept (Lambe 1964 and 1967). Even though stress path tests on "average samples" were not run, the concept of stress path was used to guide the estimation of the horizontal stresses. If the deformation was likely to be large, the horizontal stress distribution based on K_a was used, whereas if the deformation was likely to be very small, the distribution based on K_o was used. K_a corresponded to the active condition and K_o corresponded to the at-rest condition. For lack of a

better name, this method is called "Stress Ratio Method."

Figures 5.3.4 and 5.3.5 show the predicted horizontal stresses acting on the sheeting at Test Sections B and A. Owing to the relatively small horizontal movements expected near the top strut, and owing to possible arching, the effective lateral stress ratio, K, was expected to be equal to or greater than K_o in the fill. At Test Section B, $K = K_o = 0.43$ was used. At Test Section A, $K = 0.6$ was used because the fill layer was relatively thin and any rotation of the top of the sheeting into the fill might cause the stress ratio to exceed K_o. For both test sections, $K = K_a$ was used for the silt as the movement of the sheeting was expected to be large enough for the active state to be developed. As the till was overconsolidated a lateral stress ratio halfway between K_o and K_a was used.

After the horizontal stresses were obtained the strut loads were estimated by two methods. The first method assumed the sheeting to consist of independent vertical segments, as in the Terzaghi-Peck method. The strut loads obtained in this way are shown in Figs. 5.3.6 and 5.3.7 under "Stress Ratio." The second method is to be explained in Section 5.4.1. It made use of a computer program to analyze beams on elastic springs.

5.3.3 Finite Element Program BRACE

The basis for this method has been explained in Chapter Two. Only the results for the two test sections will be presented here.

In this method the full process of excavation was simulated. Simulating excavation and strut installation sequentially, the strut loads during the various stages of excavation were computed. Analyses using bilinearly elastic stress-strain relations wer performed for both sections. The pore pressures used were obtained in Section 5.2.2.

At Test Section B a surcharge of 500 psf over a distance of 85 ft. was imposed on the ground surface prior to the driving of the sheeting. The surcharge represented the building load due to the Empire Carpet Building. The soil properties used in the predictions made by BRACE are summarized in Fig. 5.3.10. Appendix I-C explains how these soil properties were obtained.

The strut loads calculated are shown in Figs. 5.3.6 through 5.3.9. The movement of the sheeting at each strut level was prevented after the strut had been installed at that level. In the same analysis movements of the sheeting as well as initial settlements of the ground surface were also obtained. (See Sections 5.4.2 and 5.5.1).

5.4 WALL MOVEMENTS

Two methods were used. They were the method of elastic beams on springs and the finite element program BRACE.

5.4.1 Method of Elastic Beams on Springs

By estimating the stresses acting on the sheeting at each stage of excavation, and by using standard theories of elastic analysis of beams, the strut loads and wall movements could be obtained. In this way, the sequence of construction could be roughly simulated.

The computer program STRUDL (M.I.T. 1969) was used. In this program the soil below the bottom of excavation and inside the sheeting was simulated by springs. The spring constant KSP for each spring was $\frac{AE}{L}$, where L was the half width of the excavation, E was the Young's modulus of the soil, and A was the length halfway to each adjacent spring in the vertical direction (see Fig. 5.4.1). Linear elasticity was assumed. The struts remained fixed after installation. The Young's moduli and Poisson's ratios of the soils used were the same as those used for BRACE (Fig. 5.3.10).

Figures 5.4.1 and 5.4.2 show the wall movements as well as the strut loads obtained for Test Sections B and A. The strut loads are also shown in Figs. 5.3.6 and 5.3.9.

5.4.2 Finite Element Program BRACE

The basis of this method has been explained in Chapter Two. Only the results are shown here.

In this analysis two approaches were made regarding the movements of the sheeting after the strut installation. The first approach was that no further sheeting movement at the strut level occurred after the strut has been installed. The second approach was that after the strut had been installed a further sheeting movement at the strut level, equal to 50% of the sheeting movement prior to the strut installation, occurred. The soil properties used are shown in Fig. 5.3.10. As explained in Section 5.3.3, the analyses performed made use of the bilinearly elastic stress-strain relations of the soils.

Figs. 5.4.3 and 5.4.4 show the predicted wall movements at Test Sections B and A, respectively, during excavation. In each figure two sets of movements are shown corresponding to the assumptions of zero sheeting movement after strut installation. At Test Section B the prediction shows that (Fig. 5.4.3b) when an extra 50% movement of the sheeting at the strut level was allowed after a strut had been installed, the bottom of the sheeting would kick in when the final stage of excavation was reached. (The penetration of sheeting below the final bottom of the excavation was only 2 feet at Test Section B.)

5.5 GROUND SETTLEMENTS

There are two factors which cause settlements of the ground near an excavation. The first factor is the removal of the soil mass.

The second factor is the changes in pore pressures. Settlement due to the first factor is the initial settlement. Settlement due to the second factor is the consolidation settlement.

5.5.1 Initial Settlements

The finite element program BRACE was used to predict the initial settlements of the ground at Test Section B.

The basis of this method has been explained in Chapter Two. The soil properties used are shown in Fig. 5.3.10. As explained in Section 5.3.3 the analyses performed made use of the bilinearly elastic stress-strain relations of the soils.

Figure 5.5.1 shows the predicted initial settlements of the ground surface as well as those of the top of the silt layer at Test Section B, corresponding to the two cases when the sheeting did and did not move after strut installation. The predicted initial settlements shown correspond to the end of the fifth stage of excavation because total shear failure occurred during the sixth stage of excavation in the case when the strut was allowed to move. In the case when the strut was fixed very little further predicted settlements occurred during the sixth stage of excavation. Note that the predicted initial settlements of the top of the silt layer were much greater than those of the ground surface.

5.5.2 Consolidation Settlements

It has been shown in Chapter Five that excavation activities caused the total head in the surrounding soils at Test Sections B and A to drop. In Section 5.2 the drops in total head at Test Sections B and A were predicted.

Based on these predicted head drops, and assuming one-dimensional consolidation of the silt, the consolidation settlement

at Test Section B were predicted.

The soil parameters used in the prediction of the consolidation settlements are listed in Table 5.5.1. The predicted consolidation settlements were added to the predicted initial settlements to give the predicted total settlements of the ground surface. Figure 5.5.1 shows the predicted total settlements, in addition to the predicted initial settlements, of the ground surface.

5.6 COMPARISONS BETWEEN PREDICTED PERFORMANCE AND MEASURED PERFORMANCE

5.6.1 Pore Pressures

Figure 5.2.7 shows the predicted and the measured pore pressures on and near the wall at Test Section A. At Test Section A the seepage condition was complicated by the recharging activities. In spite of the recharging, the pore pressures near the wall were far below the static distribution, and were close to the predicted steady seepage distribution. The conclusion to be derived is that for braced excavations in sands and silts the pore pressures outside the excavations will be less than static. Figure 5.2.4 shows the predicted and the measured pore pressures on the wall at Test Section B. The agreement for Test Section B is good.

5.6.2 Strut Loads

Figures 5.3.6 and 5.3.7 show the predicted and the measured strut loads at Test Sections B and A at full excavation, while Figs. 5.3.8 and 5.3.9 show the predicted and measured strut loads during the various stages of excavation. The strut loads predicted by the finite element program BRACE (bilinearly elastic) agree quite well with the measured strut loads, and this agreement is encouraging. While it is not possible to say which method of prediction is the best,

just on the basis of comparison with measurements from only two test sections, the finite element method BRACE clearly is very attractive.

The semiempirical methods were evolved to provide maximum strut loads for design. Therefore, the strut loads predicted by these methods must be compared only with the maximum strut loads predicted by other methods or the maximum strut loads measured (Figs. 5.6.1 and 5.6.2). A comparison between the predicted and the measured loads show that the Terzaghi-Peck method for dry sand grossly underestimated the maximum strut loads, while the Terzaghi-Peck and the Navdock methods for clay grossly overestimated the loads in the top three struts at Test Section B and in all the struts at Test Section A. The reason for the disagreement was the fact that the soils at the two test sections were neither dry sands nor saturated undrained clays. Quite good agreement was obtained by the Terzaghi-Peck and the Tschebotarioff methods modified for sands submerged in static water. However, this agreement was probably fortuitous as the actual pore pressures were far from static.

5.6.3 Wall Movements

Figures 5.4.3 and 5.4.4 show the wall movements at the two test sections predicted by the finite element program BRACE. Figures 7.1 and 7.4 of Part II show the measured wall movements at the two test sections. Figure 5.6.3 summarizes the measured and the predicted maximum wall movements. The agreement obtained for Test Section B is considered good. For Test Section A the maximum predicted wall movements were less than the measured movements. For both sections the predicted shapes of the deflected wall agreed very well with the measured shapes.

Figures 5.4.1 and 5.4.2 show the wall movements predicted

by the method of elastic beams with springs. The movements predicted were less than measured because the struts were assumed fixed after installation, and because the bottom of the walls was assumed hinged.

5.6.4 Ground Settlements

Figure 5.5.1 shows the predicted ground surface settlements at Test Section B. Figure 7.1 of Part II shows the measured settlements. Both the predicted initial and the predicted total settlements of the ground surface are shown in Fig. 5.5.1. The maximum predicted total settlement was 0.6 feet and it consisted mostly of consolidation settlement. The maximum measured total settlements were 0.83 and 0.41 feet west and east of the excavation, respectively (Fig. 7.1 of Part II). The overall agreement between the maximum predicted total and the maximum measured total settlements is good.

CHAPTER SIX

SUMMARY AND CONCLUSIONS

6.1 DEVELOPMENT OF NEW METHOD

This research has developed a method based on the finite element technique for predicting: (1) movements of the soil mass adjacent to an excavation; (2) movements of the retaining wall; (3) stresses on the retaining wall; and (4) loads in the struts. This method has the capability of handling the bending stiffmess of the retaining wall and the nonlinear aspects of soil behavior. By removing soil elements and specifying the boundary conditions at the nodes where struts are installed, the user of the method can simulate the sequence of excavation and strut installation employed in the field. The computer program based on this method is called BRACE.

6.2 SUMMARY OF INSIGHTS GAINED FROM EXAMPLE STUDIES

Solution of idealized examples obtained by BRACE using soil parameters measured in laboratory tests on Boston blue clay provides insights into the undrained behavior of braced excavations. The following is a summary of the more important insights.

The stiffness of the wall has a great influence on movements and on strut loads. The lateral stress ratio, K_o, influences both the final lateral stresses acting on the wall and the movements of the wall and of the soil, but this influence on the movements is small when the soil is behaving as a linearly elastic material. The modulus variations with depth also influence the stresses and the movements even when the average modulus at the center line of the soil layer is the same. As the soil-support system is inhomogeneous, the movements

that occur are not dependent on the Young's modulus of the soil alone, and therefore these movements cannot be normalized with respective to the Young's modulus of the soil.

Excavations in normally consolidated Boston blue clay result in extensive yielding of the clay. The use of the Terzaghi-Peck dimensionless number N provides a good indication of the approach of base failure. For normally consolidated Boston blue clay when N is greater than 7, the yielded masses behind and in front of the wall have begun to merge. When N is greater than 8 a large movement of the bottom of the wall towards the excavation has taken place, accompanied by large ground settlements and by a very large load in the bottom strut. The same happens when the excavation is retained by a slurry wall instead of ZP38 sheeting. A 10-foot gap between the bottom of the wall and the bedrock gives rise to as much yielding of the clay as a 40-foot gap for the same length of sheeting. When a stiff crust overlies a layer of normally consolidated Boston blue clay, extensive yielding occurs when the excavation has reached the normally consolidated layer. In all cases, when the yielded zones around the bottom of the wall have merged the bottom strut experiences a sharp increase in load. When this happens, the strut immediately above the bottom strut experiences a corresponding reduction in load.

Excavations in overconsolidated Boston blue clay show that when the OCR is greater than or equal to 2, and when $Su/\bar{\sigma}_{vo}$ is constant with depth, very little yielding occurs. When the OCR is greater than or equal to 2, classical earth pressure theories based on limiting equilibrium would underestimate the earth pressures on the wall because the soil mass is still essentially elastic.

The nonlinear stress-strain relations of clays can be approximated by a least square polynomial curve fitting procedure. In the

analysis using a nonlinearly elastic stress-strain relation the modulus of the clay changes continuously with new stress levels and, therefore, the influence of shear strength is automatically accounted for. By using an approximate correlation between the modulus and the orientation of the principal stress changes, the anisotropy of the modulus and shear strength of the clays can be simulated. For a normally consolidated soil an analysis using anisotropic, nonlinearly elastic stress-strain relations shows larger movements of the bottom of the sheeting at shallower depth than what an analysis using bilinearly elastic stress-strain relations shows. During the final stage of excavation the load in the bottom strut obtained using nonlinearly elastic stress-strain relations is much less than that obtained using bilinearly elastic stress-strain relations.

6.3 COMPARISON BETWEEN PREDICTED AND MEASURED PERFORMANCES

In this report it has been demonstrated how the performance of two instrumented test sections could be predicted. The methods of prediction used are shown in Table 1.3.1, together with the aspects of the performance predicted. The predictions of the strut loads, the wall movements and the ground surface settlements were made using currently available methods as well as the finite element program BRACE. Bilinearly elastic stress-strain relations of the soils were used in the predictions made by BRACE.

The strut loads and wall movements predicted by BRACE agree well with those measured. The sum of the initial settlement of the ground surface predicted by BRACE and the consolidation settlement predicted by one-dimensional theory of consolidation agrees well with the total measured settlement. These agreements are encouraging.

Even though the performance predicted by the finite element program agrees well with the measured performance, it is not possible to say purely on the basis of a comparison of the predictions made by the various methods, which method of prediction is the best. More field cases will have to be analyzed before this can be ascertained. However, in view of its ability to handle the bending stiffness of the wall and the linearly, bilinearly or nonlinearly elastic stress-strain relations of the soil, and in view of its ability to simulate the excavation sequence in the field, the finite element program BRACE is clearly a very powerful method of predicting the performance of braced excavations.

REFERENCES

Bjerrum, L., Unpublished Lectures on Observed Versus Computed Settlements of Structures on Clay and Sand: given at the Massachusetts Institute of Technology, 1964.

Bjerrum, L. and Eide, I., "Stability of Strutted Excavations in Clays," Geotechnique, Vol. 6, pp. 32-47, 1956.

Bjerrum, L., Kenney, T. C. and Kjaernski, B., "Measuring Instruments for Strutted Excavations," Journal of the Soil Mechanics and Foundations Division, ASCE, Vol. 91, No. SM1, pp. 111-141, 1965.

Bovee, B. B., "Analysis of Undrained Plane Strain Shear of Boston Blud Clay," S.M. Thesis, Massachusetts Institute of Technology, 1970.

Brinch, Hansen, J., "Earth Pressure Calculations," Danish Technical Press, Copenhagen, 1953.

Brooker, E. W. and Ireland, H. O., "Earth Pressures at Rest Related to Stress History," Canadian Geotechnical Journal, 2, pp. 1-15, 1965.

Brown, C. B. and Goodman, L. E., "Gravitational Stresses in Accreted Bodies," Proceedings of the Royal Society, Series A, Vol. 276, pp. 571-576, 1963.

Brown, C. B. and King, I. P., "Automatic Embankment Analysis: Equilibrium and Instability Conditions," Geotechnique, Vol. 16, No. 3, pp. 209-219, 1966

Casagrande, A., "Soil Mechanics in the Design and Construction of the Logan Airport," Journal Boston Society of Civil Engineers, Vol. 36, No. 2. pp. 192-221, 1949

Chang, C-Y and Duncan, J. M., "Analysis of Soil Movements Around Deep Excavation," Journal of the Soil Mechanics and Foundations Division, ASCE, Vol. 96, No. SM5, Proc. Paper 7512, pp. 1655-1691, 1970.

Christian, J. T., Private Communication, 1970.

Clough, G. W., "Finite Element Analysis of Soil Structure Interaction in U-Frame Locks," Ph.D. Thesis, University of California, Berkeley,

Clough, R. W., "The Finite Element Method in Structural Mechanics," Chapter 7 in Stress Analysis, edited by O. C. Zienkiewicz and G. S. Hollister, John Wiley and Sons, London, 1965.

Clough, R. W. and Woodward, R. J., III, "Analysis of Embankment Stresses and Deformations," Journal of the Soil Mechanics and Foundations Division, ASCE, Vol. 93, No. SM4, Proc. Paper 5329, pp. 529-549, 1967.

D'Appolonia, D. J., "Prediction of Stress and Deformation for Undrained Loading Conditions," Ph. D. Thesis, Massachusetts Institute of Technology, 1968.

D'Appolonia, D. J. and Lambe, T. W., "Method for Predicting Initial Settlement," Journal of the Soil Mechanics and Foundations Division, ASCE, Vol. 96, No. SM2, Proc. Paper 7167, pp. 523-544, 1970.

DiBiagio, E. L., "Stresses and Displacements Around an Unbraced Rectangular Excavation in an Elastic Medium," Ph. D. Thesis, University of Illinois, Urbana, 1966.

Duncan, J. M. and Chang, C-Y., "Nonlinear Analysis of Stress and Strain in Soils," Journal of the Soil Mechanics and Foundations Division, ASCE, No. SM5, Vol. 96, Proc. Paper 7513, pp. 1629-1653, 1970.

Duncan, J. M. and Dunlop, P., "Behavior of Soils in Simple Shear," Proceedings of the 7th International Conference on Soil Mechanics and Foundations, pp. 101-108, 1969.

Dunlop, J. M. and Dunlop, P., Closure to "Slopes in Stiff Fissured Clays and Shales," Journal of the Soil Mechanics and Foundation Division, ASCE, Vol. 96, No. SM5, pp. 1795-1799, 1970.

Dunlop, P. and Duncan, J. M., "Development of Failure Around Excavated Slopes," Journal of the Soil Mechanics and Foundations Division, ASCE, Vol. 96, No. SM2, Proc. Paper 7162, pp. 471-494, 1970.

Golder, H. Q., Gould, J. P., Lambe, T. W., Tschebotarioff, G. P. and Wilson, S. D., "Predicted Performance of a Braced Excavation," Journal of the Soil Mechanics and Foundation Division, ASCE, Vol. 96, No. SM3, Proc. Paper 7292, pp. 801-815, 1970.

Goodman, L. E. and Brown, C. B., "Dead Load Stresses and the Instability of Slopes," Journal of the Soil Mechanics and Foundation Division, ASCE, Vol. 89, No. SM3, Proc. Paper 3514, pp. 103-134, 1963.

Hagmann, A. J., "Prediction of Stress and Strain Under Drained Loading Conditions," Sc.D. Thesis, Massachusetts Institute of Technology, 1971.

Haliburton, A. T., "Numerical Analysis of Flexible Retaining Structures," Journal of the Soil Mechanics and Foundations Division, ASCE, Vol. 94, No. SM6, Proc. Paper 6221, pp. 1233-1251, 1968.

Hamming, R. W., Numerical Methods for Scientists and Engineers, McGraw Hill, New York, 1962.

I.B.M., "System/360 Scientific Subrouting Package," February, 1969.

Ishihara, K., "Relations Between Process of Cutting and Uniqueness of Solution," Soils and Foundations, Vol. 10, No. 3, pp. 50-65, 1970.

Janbu, N., Bjerrum, L. and Kjaernski, B., "Veiledning ved Losning and Fundamentering Soppgaver," Norwegian Geotechnical Institute, Publication No. 16, 1956.

Kinner, E. B., "Load-Deformation Behavior of Saturated Clays During Undrained Shear," Sc.D. Thesis, Massachusetts Institute of Technology, 1970.

Kondner, R. L., "Hyperbolic Stress-Strain Response: Cohesive Soils," Journal of the Soil Mechanics and Foundations Division, ASCE, Vol. 89, No. SM1, Proc. Paper 3429, pp. 115-143, 1963.

Kondner, R. L. and Zelasko, J. S., "A Hyperbolic Stress-Strain Formulation for Sands," Proceedings 2nd Pan-American Conference on Soil Mechanics and Foundations Engineering, Brazil, Vol. 1, pp. 289-324, 1963.

Ladd, C. C., "Stress-Strain Modulus of Clay in Undrained Shear," Journal of the Soil Mechanics and Foundations Division, ASCE, Vol. 90, No. SM5, Proc. Paper 4039, pp. 103-132, 1964.

Lambe, T. W., "Methods of Estimating Settlement," Journal of the Soil Mechanics and Foundations Division, ASCE, Vol. 90, No. SM5, Proc. Paper 4060, pp. 43-67, 1964.

Lambe, T. W., "Stress Path Method," Journal of the Soil Mechanics and Foundations Division, ASCE, Vol. 93, No. SM6, Proc. Paper 5613, pp. 309-331, 1967.

Lambe, T. W., "Braced Excavations," Preprint for ASCE Specialty Conference on Lateral Stresses and Design of Earth Retaining Structures, pp. 149-218, 1970.

Lambe, T. W., Wolfskill, L. A. and Wong, I. H., "Measured Performance of a Braced Excavation," Journal of the Soil Mechanics and Foundation Division, ASCE, Vol. 96, No. SM3, Proc. Paper 7307, pp. 817-836, 1970.

Lambe, T. W. and Whitman, R. V., Soil Mechanics, John Wiley, New York, 1969.

Lane, K. S. and Washburn, D. E., "Capillarity Tests by Capillaimeter and by Soil Filled Tubes," Proceedings of the Highway Research Board, 1946.

Liebelt, P. B., An Introduction to Optimal Estimation, Addison-Wesley, Reading, Mass., 1967.

Martin, H. C., Introduction to Matrix Methods of Structural Analysis, McGraw-Hill, New York, 1966.

Massachusetts Institute of Technology, "Prediction of the Deformation of a Levee on a Soft Foundation," Department of Civil Engineering, Report No. R69-18, 1968.

Massachusetts Institute of Technology, "ICES-STRUDL - II," Department of Civil Engineering, Report No. R68-91, 1969.

Morgenstern, N. R. and Eisenstein, Z., "Methods of Estimating Lateral Loads and Deformations," Preprint for ASCE Specialty Conference on Lateral Stresses and Design of Earth Retaining Structures, pp. 51-102, 1970.

Navdocks DM-7, "Design Manual, Soil Mechanics, Foundations and Earth Structures," Department of the Navy, Bureau of Yards and Docks, Washington, D.C., 1962.

Peck, R. B., "Deep Excavations and Tunneling in Soft Ground," Proc. 7th International Conference on Soil Mechanics and Foundation Engineering, State-of-the-Art, pp. 225-290, 1969.

Peck, R. B., Hanson, W. E. and Thornburn, T. H., Foundation Engineering, John Wiley, New York, 1953.

Przemieniecki, J. S., Theory of Matrix Structural Analysis, McGraw-Hill, New York, 1968.

Ralston, A., A First Course in Numerican Analysis, McGraw-Hill, New York, 1965.

Simons, N. E., "Settlement Studies on Two Structures in Norway," Proc. 4th International Conference on Soil Mechanics and Foundation Engineering, Vol. 1, pp. 431-436, 1957.

Sowers, G. B. and Sowers, B. F., Introductory Soil Mechanics and Foundations, MacMillan, New York, 1951.

Taylor, R. L. and Brown, C. B., "Darcy Flow Solutions with Free Surface," Journal of the Hydraulics Division, ASCE, Vol. 93, No. HY2, pp. 25-33, 1967.

Teng, W. C., Foundation Design, Prentice-Hall, Englewood Cliffs, New Jersey, 1962.

Terzaghi, K. and Peck, R. B., Soil Mechanics in Engineering Practice, 2nd Edition, John Wiley, New York, 1967.

Tschebotarioff, G. P., "Retaining Structures," Chapter 5 in Foundation Engineering, Edited by G. Leonards, McGraw-Hill, New York, 1962.

Wilson, E. H., "Structural Analysis of Axisymetric Solids," AIAA Journal, No. 12, Vol. 3, pp. 1-32, 1965.

Wilson, S. D. and Hancock, C. W., Jr., "Horizontal Displacements of Clay Foundations," Proceedings 1st Pan-American Conference on Soil Mechanics and Foundation Engineering, Mexico, Vol. 1, pp. 41-64, 1960.

Zienkiewicz, O. C. and Cheung, Y. K., The Finite Element Method in Structural and Continuum Mechanics, McGraw-Hill Publishing Co. Ltd., London, 1967.

LIST OF SYMBOLS

Symbol	Represents
a	Henkel's pore pressure parameter
A	Area halfway to each adjacent spring in the vertical direction in STRUDL analysis
B	Width of excavation
$\overline{c}$	Cohesion intercept based on effective stresses
C_c	Compression index
C_s	Swell index
c_v	Coefficient of consolidation
D	Depth of excavation
e_o	Initial void ratio
E	Young's modulus
E^o	Yielded Young's modulus
E_o	Initial Young's modulus in nonlinear elastic analysis
E_H	Young's modulus from plane strain active test
E_V	Young's modulus from plane strain passive test
F	Factor of safety
G_s	Specific gravity of solids
H	Thickness of soil layer
k	Permeability
K	Lateral stress ratio
K_a	Active stress ratio

Symbol	Represents
K_h	Permeability in the horizontal direction
K_o	Lateral stress ratio at rest
K_p	Passive stress ratio
K_v	Permeability in the vertical direction
I	Moment of inertia
L	Half width of excavation in STRUDL analysis
N	Standard penetration resistance
N	Terzaghi-Peck dimensionless number
N_c	Bearing capacity coefficient
OCR	Overconsolidation ratio
PI	Plasticity index
r	Ratio of undrained shear strength to vertical effective stress
S_u	Undrained shear strength
S_t	Sensitivity
u, U	Pore pressure
u_s	Static pore pressure
U_s	Static pore pressure
U_{ss}	Pore pressure under steady state seepage conditions
w_ℓ	Liquid limit
w_p	Plastic limit
Z	Depth below ground surface

Symbol	Represents
[K]	Soil element stiffness matrix
[q]	Nodal force vector
[S]	Sheeting element stiffness matrix
[SH]	Total stiffness matrix for all elements
[T]	Global stiffness
[u]	Nodal displacement vector
$E/\bar{\sigma}_{vo}$	Ratio of Young's modulus to initial vertical effective stress
$Su/\bar{\sigma}_{vo}$	Ratio of undrained shear strength to initial vertical effective stress
KSP	Spring constant in STRUDL analysis
γ	Shear strain
γ, γ_t	Total unit weight
γ_b	Bouyant unit weight
γ_{max}	Maximum shear strain
Δ	Symbol indicating finite increment
ϵ	Axial strain
$\dot{\epsilon}$	Axial strain rate
θ	Angle
μ	Poisson's ratio
ρ	Settlement
ρ_i	Initial settlement
ρ_t	Total settlement

Symbol	Represent
σ	Normal stress
$\bar{\sigma}$	Effective normal stress
$\bar{\sigma}_c$	Consolidation stress
σ_{ha}	Active effective horizontal stress
$\sigma_h, \bar{\sigma}_h, \sigma_x, \bar{\sigma}_x$	Horizontal normal stress
σ_{ho}	Initial total horizontal stress
$\bar{\sigma}_{ho}$	Initial effective horizontal stress
$\sigma_v, \bar{\sigma}_v, \sigma_z, \bar{\sigma}_z$	Vertical normal stress
$\bar{\sigma}_{vm}$	Maximum past vertical consolidation stress
σ_{vo}	Initial total vertical stress
$\bar{\sigma}_{vo}$	Initial effective vertical stress
$\sigma_1, \sigma_2, \sigma_3$	Principle total stresses
$\bar{\sigma}_1, \bar{\sigma}_2, \bar{\sigma}_3$	Principal effective stresses
σ_{oct}	Octahedral normal stress
τ_{xy}, τ_{yx}	Shear stress
τ_{oct}	Octahedral shear stress
ϕ	Friction angle
$\bar{\phi}$	Friction angle based on effective stress

TYPE OF ANALYSIS		METHOD OF ANALYSIS	NEEDED INPUT	ASPECT OF BEHAVIOR DETERMINED					
				Pore pressure, u	Eff. hor. stress $\bar{\sigma}_h$	Tot. hor. stress σ_h	Strut load	Horizont. Movem.	Vertical movem.
SOIL MECHANICS	SEMI-EMPIRICAL	TERZAGHI-PECK	γ_t, S_u, $\bar{\Phi}$			x	x		
		TSCHEBOTARIOFF	γ_t, S_u, $\bar{\Phi}$			x	x		
		NAVDOCK	γ_t, S_u, $\bar{\Phi}$			x	x		
	ANALYTICAL	STRESS RATIO	γ_t, $\bar{\Phi}$, OCR (K_o)		x	x	x		
		1-D CONSOLID.		x[1]					x[2]
STRUCTURAL		ELASTIC BEAMS WITH SPRINGS	KSP, σ_h, E.I. of wall				x	x	
FINITE ELEMENT		FEDAR	K_h, K_v	x					
		BRACE	E, μ, γ_t, K_o, E.I. of wall				x	x	x

1. GIVES VARIATION OF u WITH TIME
2. GIVES CONSOLIDATION COMPONENT ONLY

TABLE 1.3.1 ANALYSIS OF BRACED EXCAVATIONS

RUN NUMBER	GRID USED	TYPE OF EXCAVATION	[1] INITIAL PORE PRESSURE CONDITION	TYPE OF WALL	UNIT WEIGHT kips/ft^3	YOUNG'S MODULUS		μ	K_o	OCR	DIMENSIONS IN FEET			
						Constant with depth E kips/ft^3	[2] Linear with depth $E/\bar{\sigma}_{vo}$				Width of excavation	Final depth of excavation	Thickness of soil layer	Length of wall
L 1	Fig. 2.3.4a	Open	Zero	None	0.12	100		0.33	0.5	1	40	80	100	
L 2	Fig. 2.3.4b	Open	Zero	None	0.12	100		0.33	0.5	1	40	40	80	
L 3	Fig. 2.3.4b	Open	Zero	Unstrutted ZP 38 Sheeting	0.12	100		0.33	0.5	1	40	40	80	70
L 4	Fig. 2.3.1	Braced	Hydro-static	ZP 38 Sheeting	0.125		80	0.49	0.5	1	40	50	70	60
L 5	Fig. 2.3.1	Braced	Hydro-static	3 ft slurry wall	0.125		80	0.49	0.5	1	40	50	70	60
L 6	Fig. 2.3.1	Braced	Hydro-static	Wall with zero stiffness, strutted	0.125		80	0.49	0.5	1	40	50	70	60
L 7	Fig. 2.3.1	Open	Hydro-static	None	0.125		80	0.49	0.5	1	40	50	70	
L 8	Fig. 2.3.1	Braced	Hydro-static	ZP 38 Sheeting	0.125		80	0.49	0.7	2	40	50	70	60
L 9	Fig. 2.3.1	Braced	Hydro-static	ZP 38 Sheeting	0.125		80	0.49	1.0	5	40	50	70	60
L 10	Fig. 2.3.1	Braced	Hydro-static	ZP 38 Sheeting	0.125	175		0.49	0.5	1	40	50	70	60
L 11	Fig. 2.3.1	Braced	Hydro-static	ZP 38 Sheeting	0.125		300	0.49	0.5	1	40	50	70	60

1. When initial pore pressures are hydrostatic, water table is at ground surface
2. Young's modulus zero at ground surface

TABLE 3.1.1 SUMMARY OF INPUT VARIABLES LINEARLY ELASTIC ANALYSES

TYPE OF WALL	AREA OF CROSS SECTION PER LINEAR FOOT ft^2	MOMENT OF INERTIA PER LINEAR FOOT ft^4	YOUNG'S MODULUS $kips/ft^2$
Bethlehem ZP 38 Sheeting	7.74×10^{-2}	1.35×10^{-2}	4.17×10^{6}
3- foot thick concrete wall	3.0	2.25	2.8×10^{5}

TABLE 3.4.1 PROPERTIES OF WALL

RUN NUMBER	TYPE OF WALL	OCR		K_o	Undrained strength		Thickness of layer ft
					Constant with depth Su kips/ft^2	[1] Linear with depth $S_u/\bar{\sigma}_{vo}$	
B 1	ZP 38 Sheeting	1		0.5		0.342	70
B 2	ZP 38 Sheeting	2		0.7		0.57	70
B 3	ZP 38 Sheeting	5		1.0		0.9	70
B 4	ZP 38 Sheeting	25		2.0		1.4	70
B 5	ZP 38 Sheeting	1		0.5		0.342	100
B 6	3 feet slurry wall	1		0.5		0.342	70
B 7	ZP 38 Sheeting	Top 30 ft	2	0.7	0.535		70
		Bot 40 ft	1	0.5		0.342	

For all runs :
Grid used is shown in Figure 2.3.1
Excavation supported by 4 levels of struts.
Initial pore pressures hydrostatic with water table at ground surface
γ_f = 0.125 kips/ft^3, μ = 0.49
$E/\bar{\sigma}_{vo}$ = 300 with zero modulus at ground level
Yielded modulus $E^o/\bar{\sigma}_{vo}$ = 0.3
Width of excavation = 40 ft. Final depth of excavation = 50 ft
Length of wall = 60 ft
[1] Except in run B 7, S_u = 0 at ground surface

TABLE 4.3.1 SUMMARY OF INPUT VARIABLES BILINEARLY ELASTIC ANALYSES

OCR	1	2	5	25
K_o	0.5	0.7	1	2
$r = S_u/\bar{\sigma}_{vo}$	0.342	0.57	0.9	1.4
D in ft	STABILITY FACTOR N			
10	1.67	1.0	0.63	0.41
22.5	3.75	2.25	1.42	0.92
32.5	5.42	3.25	2.05	1.32
42.5	7.10	4.25	2.68	1.73
50	8.32	5.0	3.16	2.03

$$N = \frac{\gamma D}{S_u}$$

γ = Unit weight of soil = 0.125 kips/ft^3
D = Depth of cut
S_u = Undrained shear strength

TABLE 4.3.2 DIMENSIONLESS NUMBER N FOR EXCAVATIONS IN SOIL WITH PROPERTIES OF BOSTON BLUE CLAY

OCR	1	2	5	25	
K_o	0.5	0.7	1	2	
$r = S_u/\bar{\sigma}_{vo}$	0.342	0.57	0.9	1.4	

DEPTH OF CUT D in ft	FACTOR OF SAFETY			$F = \frac{N_c}{N}$	D/B	N_c
10	3.30	5.50	8.70	13.40	0.25	5.5
22.5	1.57	2.62	4.15	6.40	0.56	5.9
32.5	1.14	1.91	3.02	4.7	0.81	6.2
42.5	0.90	1.51	2.39	3.73	1.05	6.4
50	0.78	1.30	2.08	3.20	1.25	6.5

B = width of cut = 40 feet

TABLE 4.3.3 FACTORS OF SAFETY AGAINST BASE FAILURE FOR EXCAVATIONS IN SOIL WITH PROPERTIES OF BOSTON BLUE CLAY

RUN NUMBER	OCR	K_o	STRESS-STRAIN CURVES USED
N 1	1	0.5	Fig. 4.2.4
N2	2	0.7	Fig. 4.2.5

For both runs :
Grid used is shown in figure 2.3.1
Excavation supported by 4 levels of struts
Initial pore pressures hydrostatic with water table at ground surface
γ_t = 0.125 kips/ft^3, μ = 0.49
Initial modulus $E_o/\bar{\sigma}_{vo}$ = 450
Width of excavation = 40 ft
Final depth of excavation = 50 ft
Length of wall = 60 ft
Young's modulus normalized with respect to $\bar{\sigma}_{vo}$

TABLE 4.4.1 SUMMARY OF INPUT VARIABLES NONLINEARLY ELASTIC ANALYSES

	SLIGHTLY ORGANIC SILT	ORGANIC SILT
c_v CM/S	157×10^{-4}	20×10^{-4}
C_s		0.12
C_c	0.152	1.07
e_o	0.8836	1.944
OCR	1	1.2
$\bar{\sigma}_{vm}$ PSF		2460

	TEST SECTION B		TEST SECTION A
COMPRESSIBLE LAYER	SLIGHTLY ORGANIC SILT	ORGANIC SILT	SLIGHTLY ORGANIC SILT
U_s AT ℄ PSF	1630	2180	1340
$\bar{\sigma}_{vo}$ PSF	1540	2060	1610
THICKNESS OF COMPRESSIBLE LAYER IN FT, H	12	6	33.5

TABLE 5.5.1 SOIL PROPERTIES FOR CONSOLIDATION SETTLEMENT CALCULATION

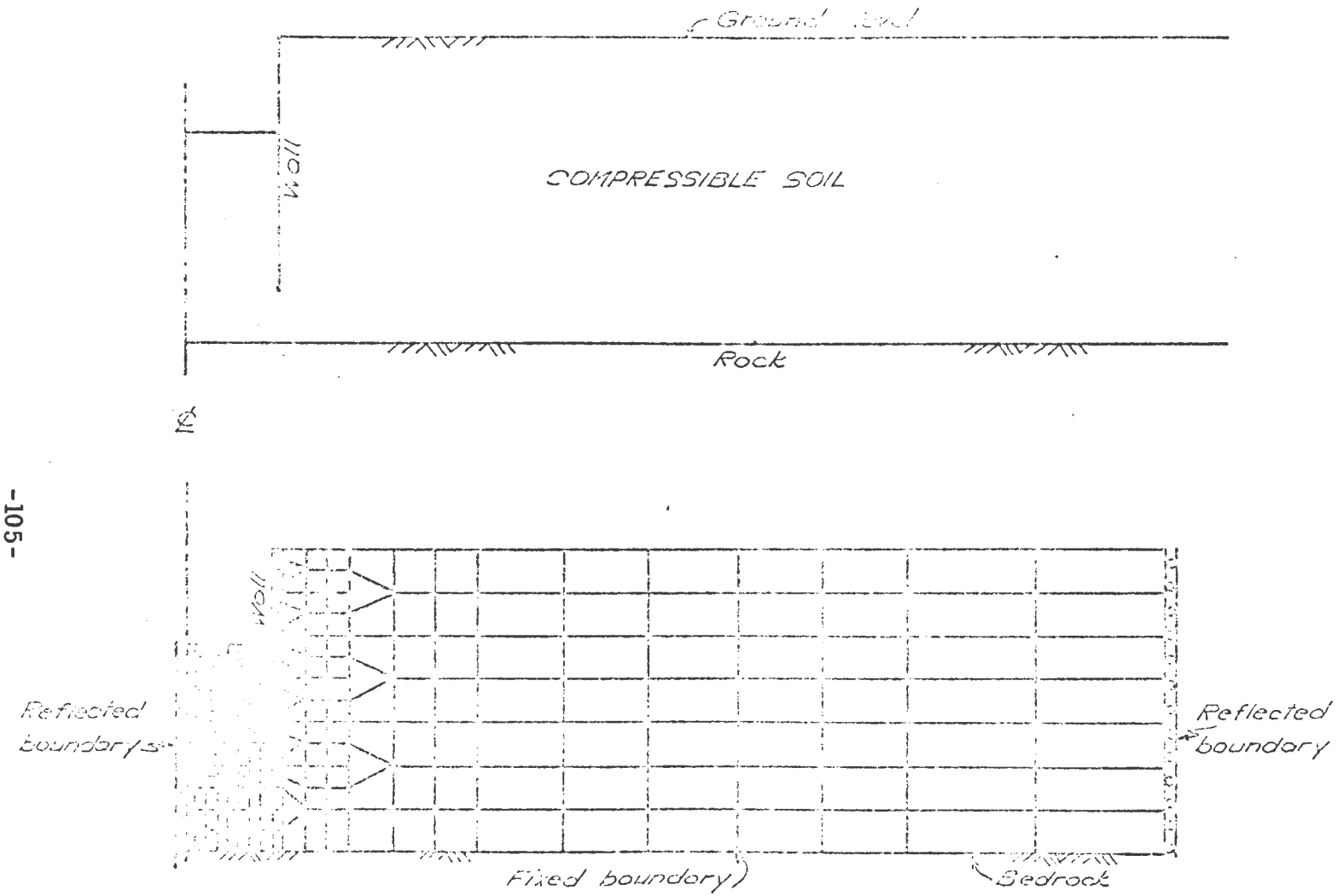

FIGURE 2.2.1 TYPICAL FINITE ELEMENT GRID OF A PLANE STRAIN EXCAVATION PROBLEM

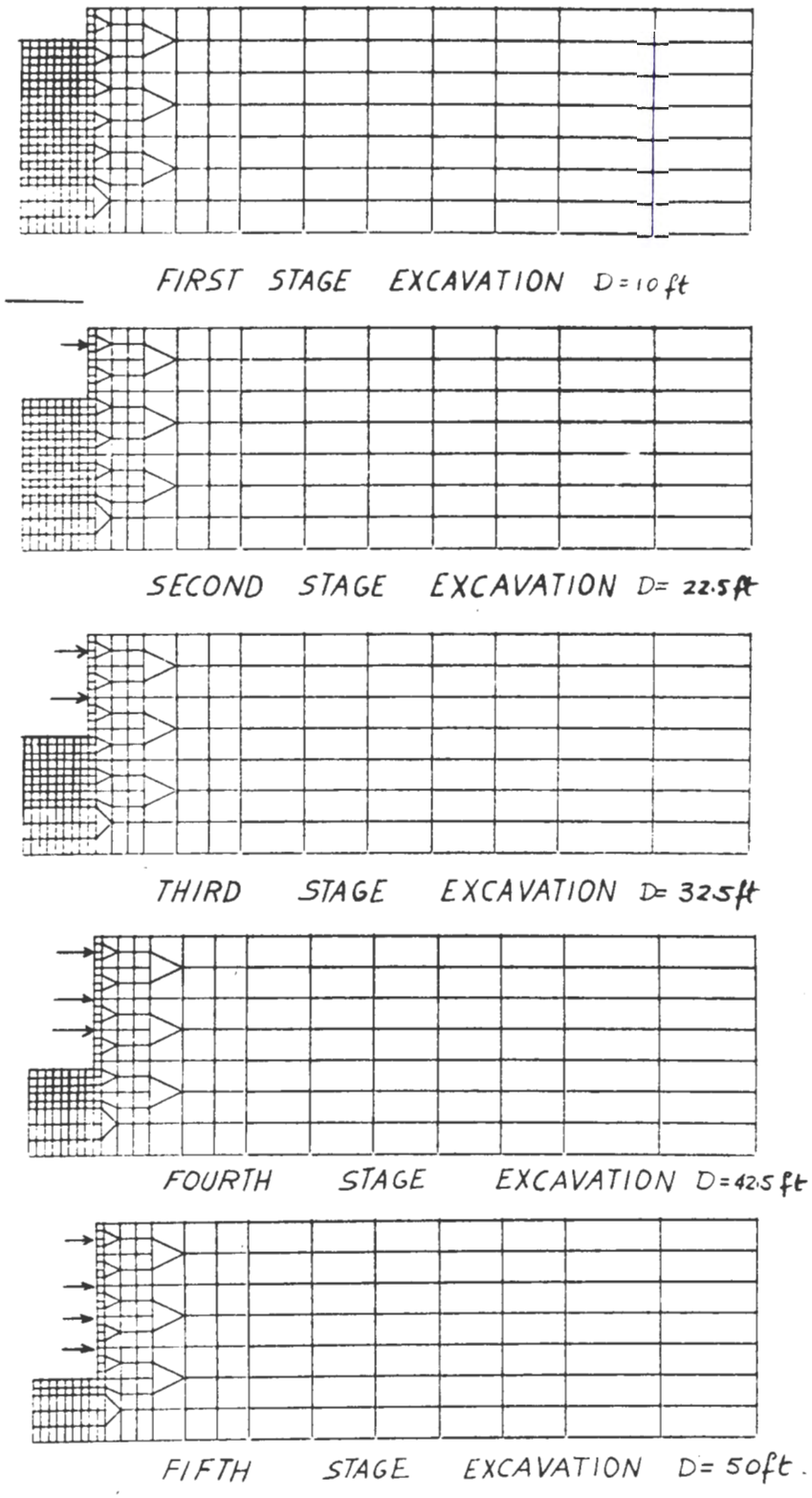

FIGURE 2.3.1 SEQUENCE OF EXCAVATION AND STRUT INSTALLATION IN EXAMPLE STUDY

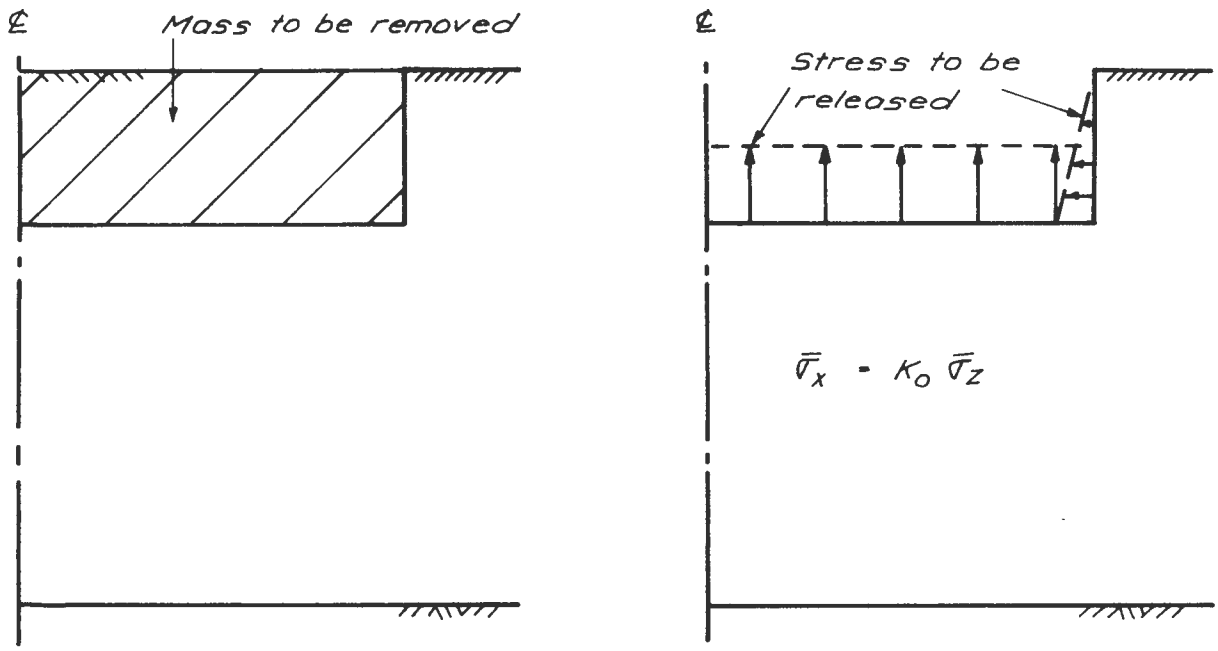

a) FIRST STAGE

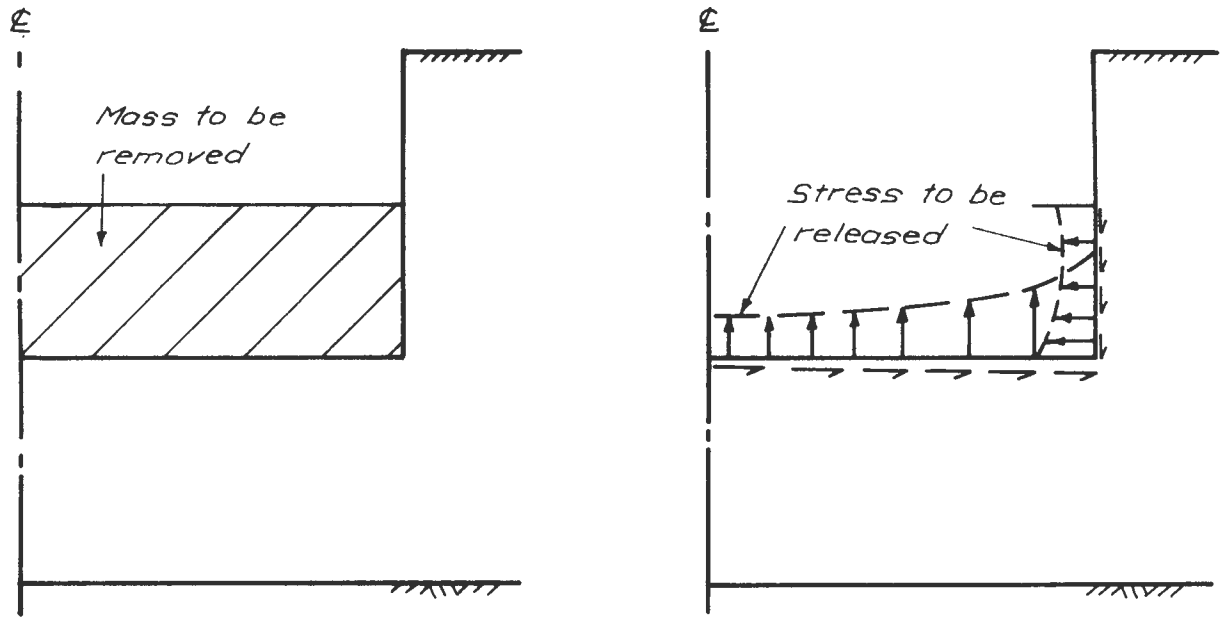

b) SECOND STAGE

FIGURE 2.3.2 SIMULATION OF EXCAVATION PROCESS

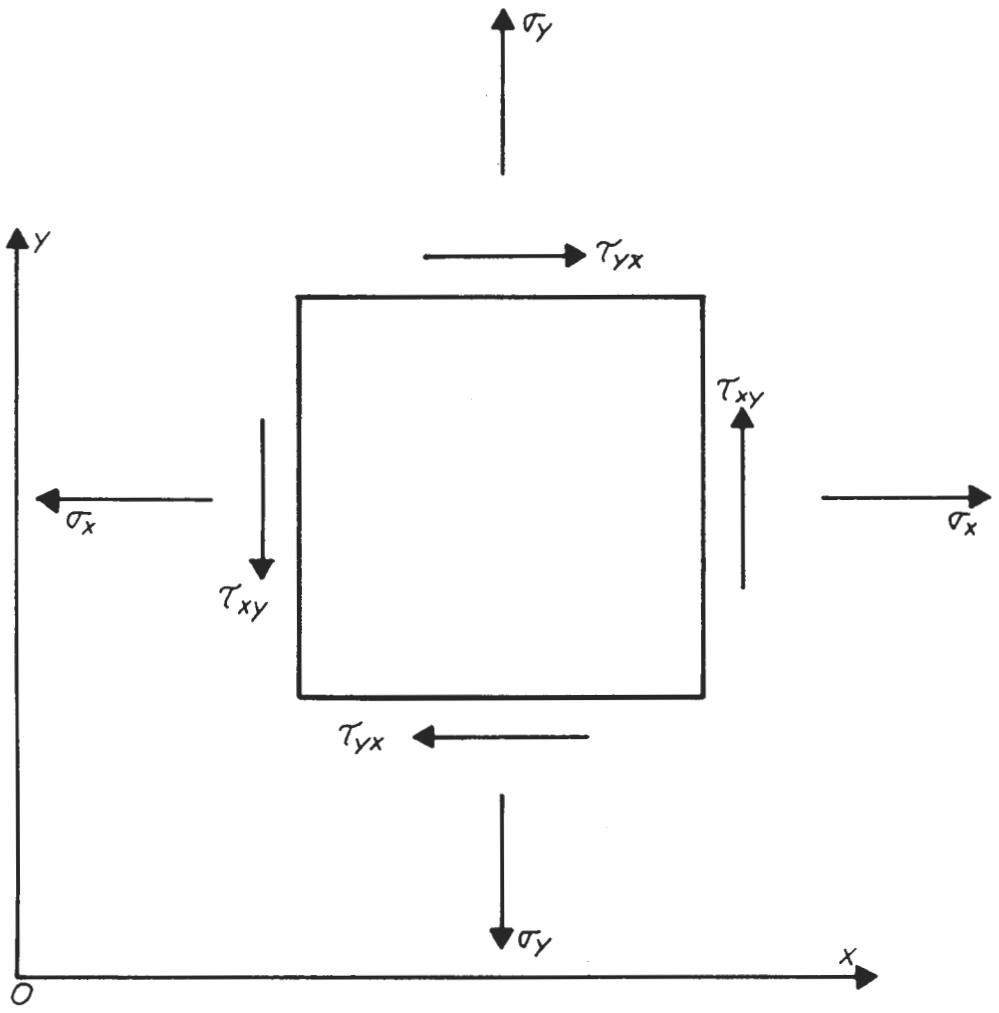

FIGURE 2.3.3 SIGN CONVENTION FOR POSITIVE STRESSES IN FINITE ELEMENT ANALYSIS

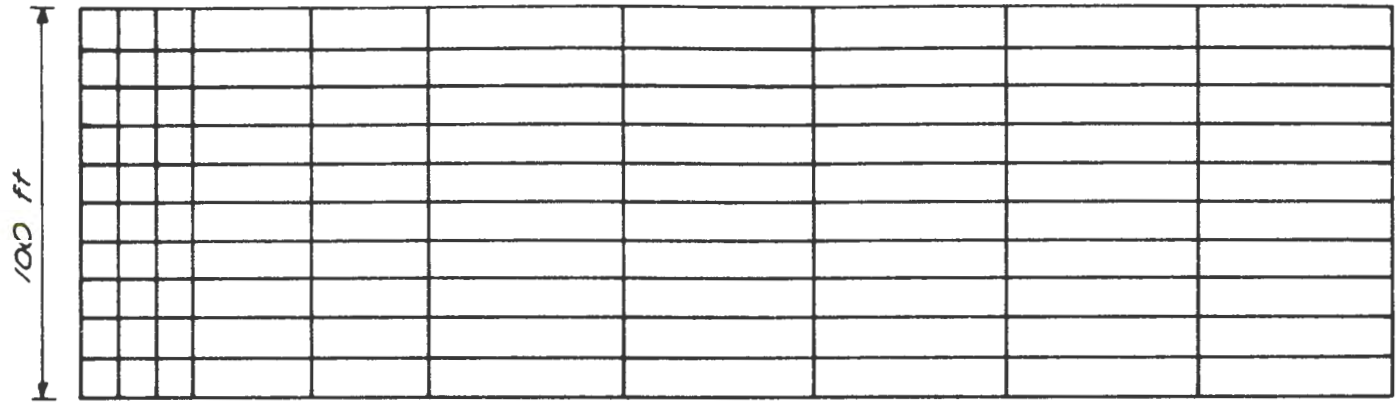

(a) Grid A 100 Elements

For both grids
$E = 100\ kips/ft^2$
$K_o = 1/2$
$\mu = 1/3$
$\gamma = 0.12\ kips/ft^3$

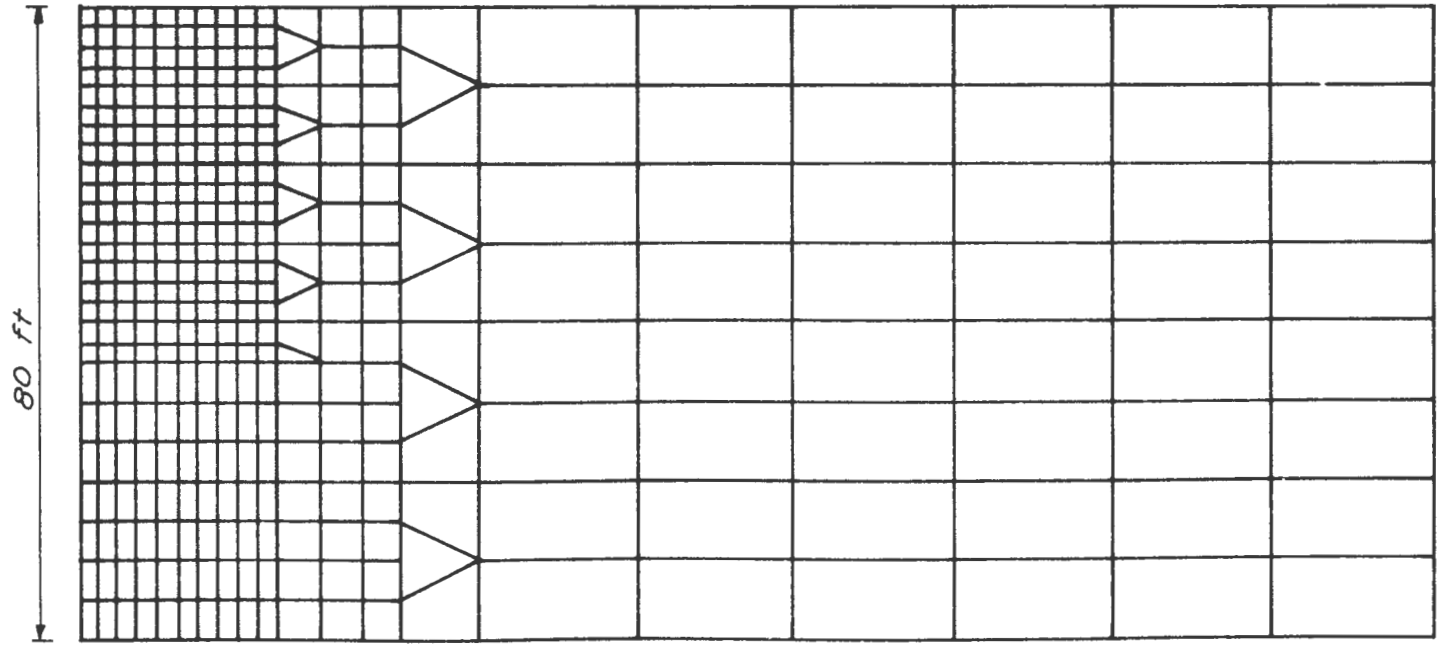

(b) Grid B 363 Elements

FIGURE 2.3.4 TWO FINITE ELEMENT GRIDS

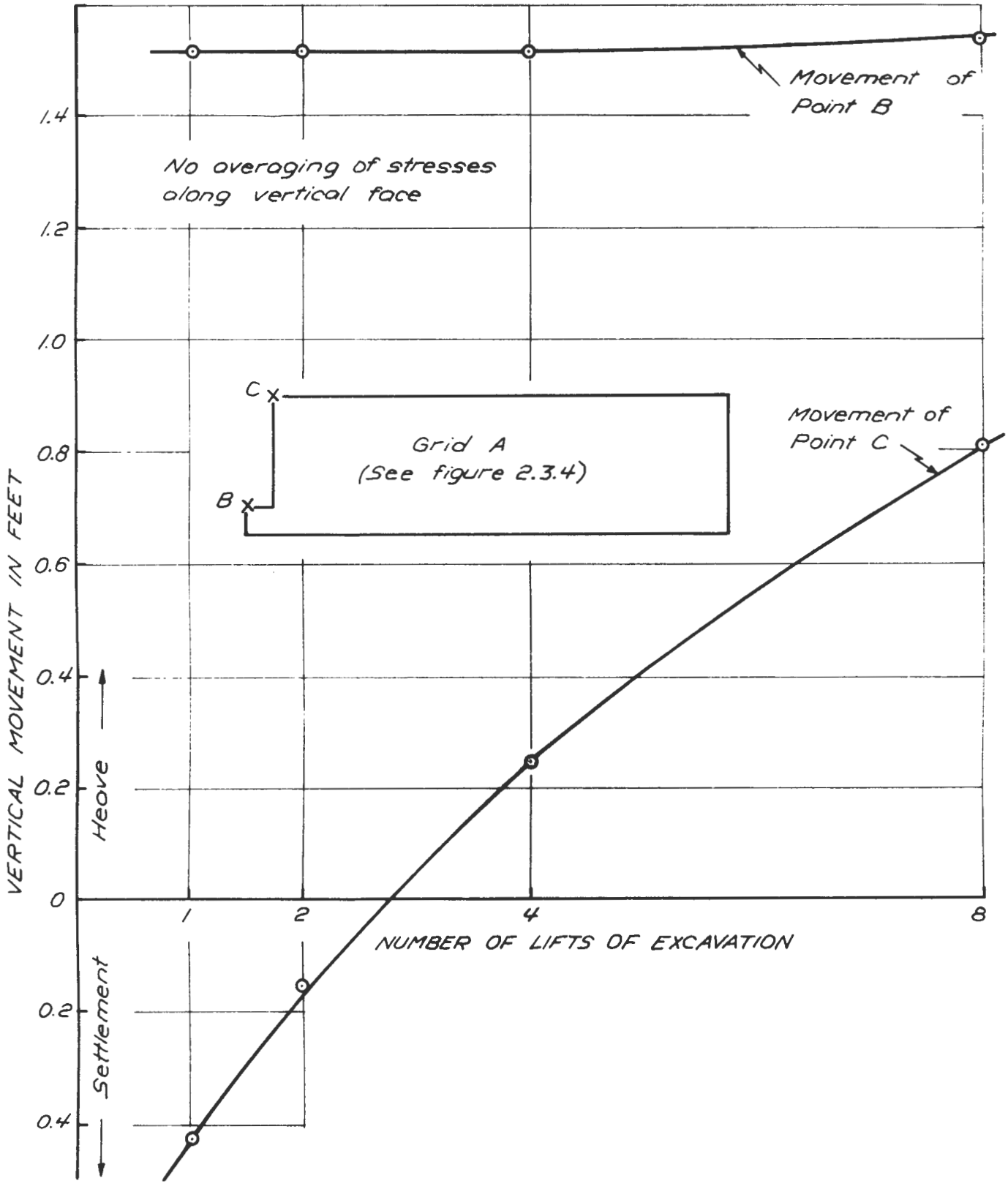

FIGURE 2.3.5 INFLUENCE OF NUMBER OF LIFTS OF EXCAVATION ON VERTICAL MOVEMENTS OF OPEN CUT

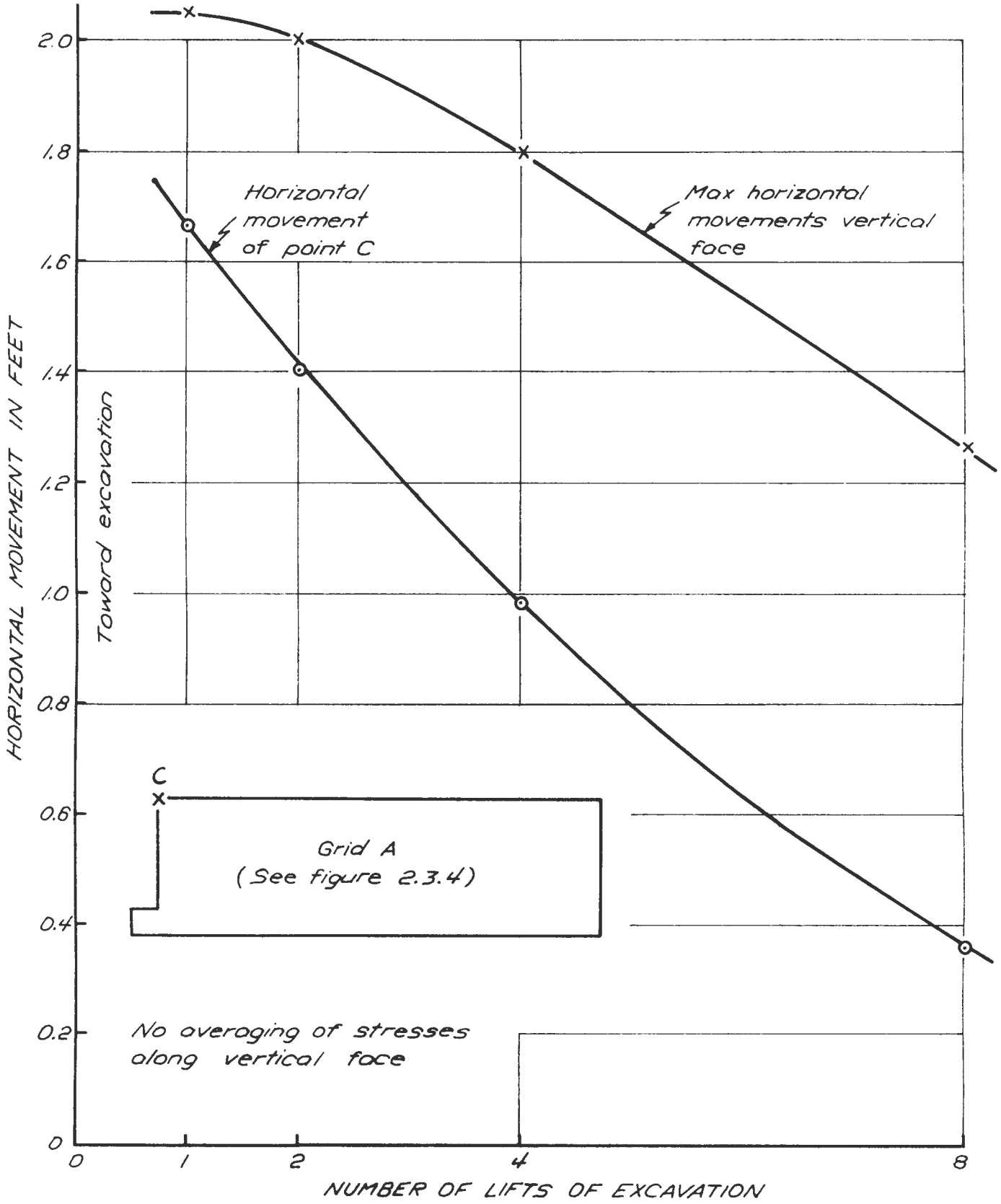

FIGURE 2.3.6 INFLUENCE OF NUMBER OF LIFTS OF EXCAVATION ON HORIZONTAL MOVEMENTS OF OPEN CUT

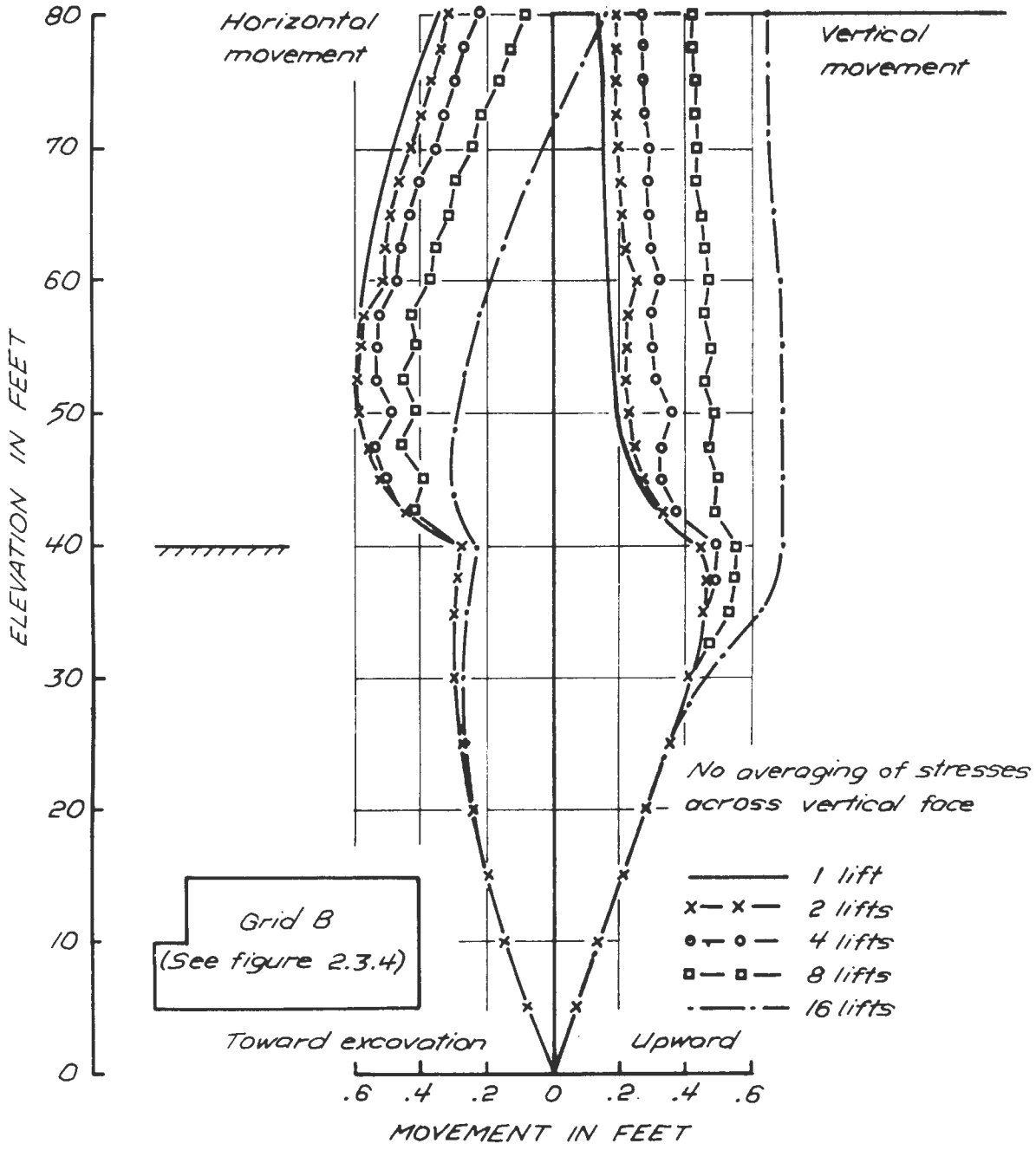

FIGURE 2.3.7 MOVEMENT OF VERTICAL FACE OF OPEN CUT NO AVERAGING

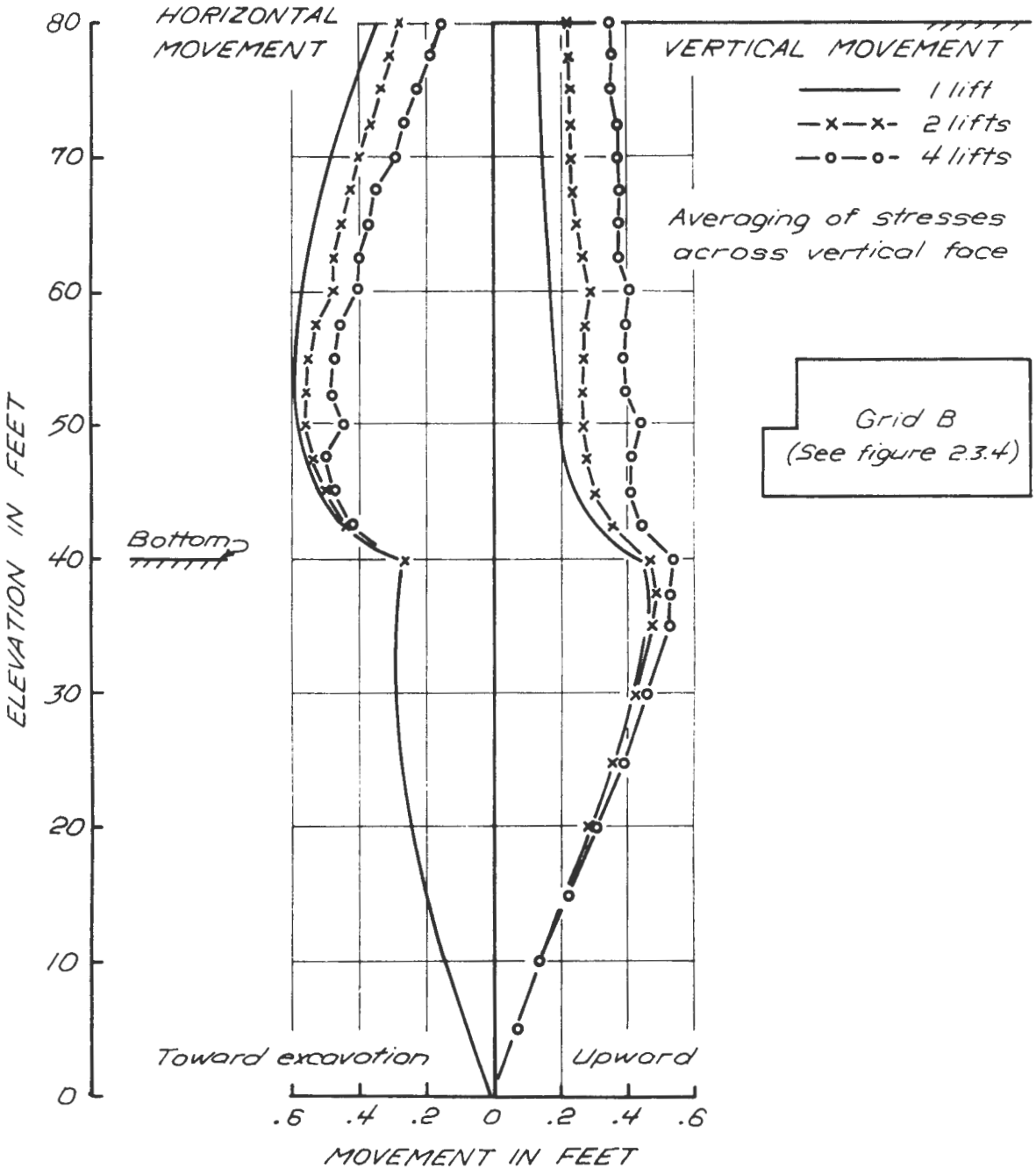

FIGURE 2.3.8 MOVEMENT OF VERTICAL FACE OF OPEN CUT - AVERAGING

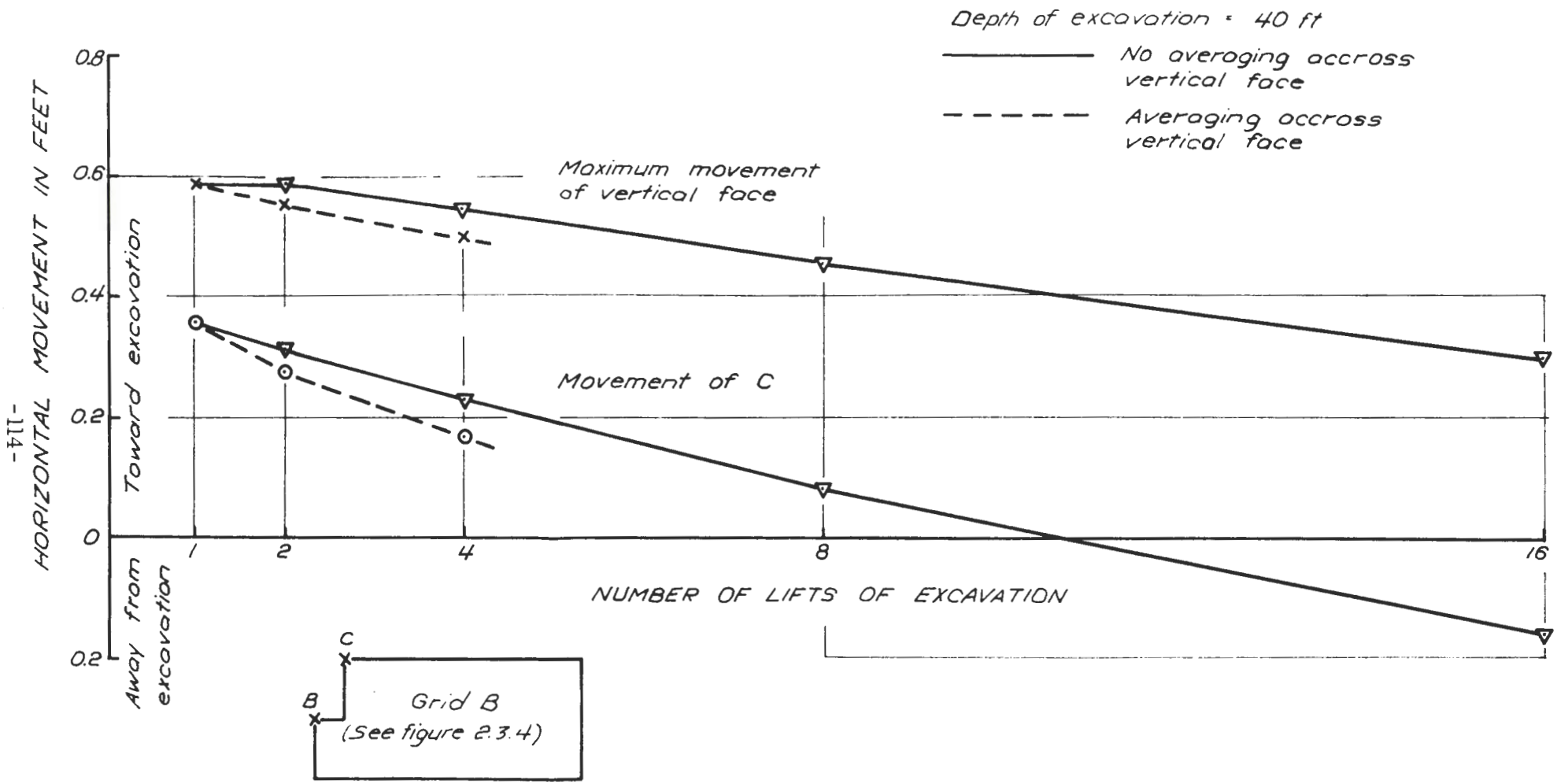

FIGURE 2.3.9 HORIZONTAL MOVEMENTS OF OPEN CUT WITH DIFFERENT METHODS OF STRESS RELEASE

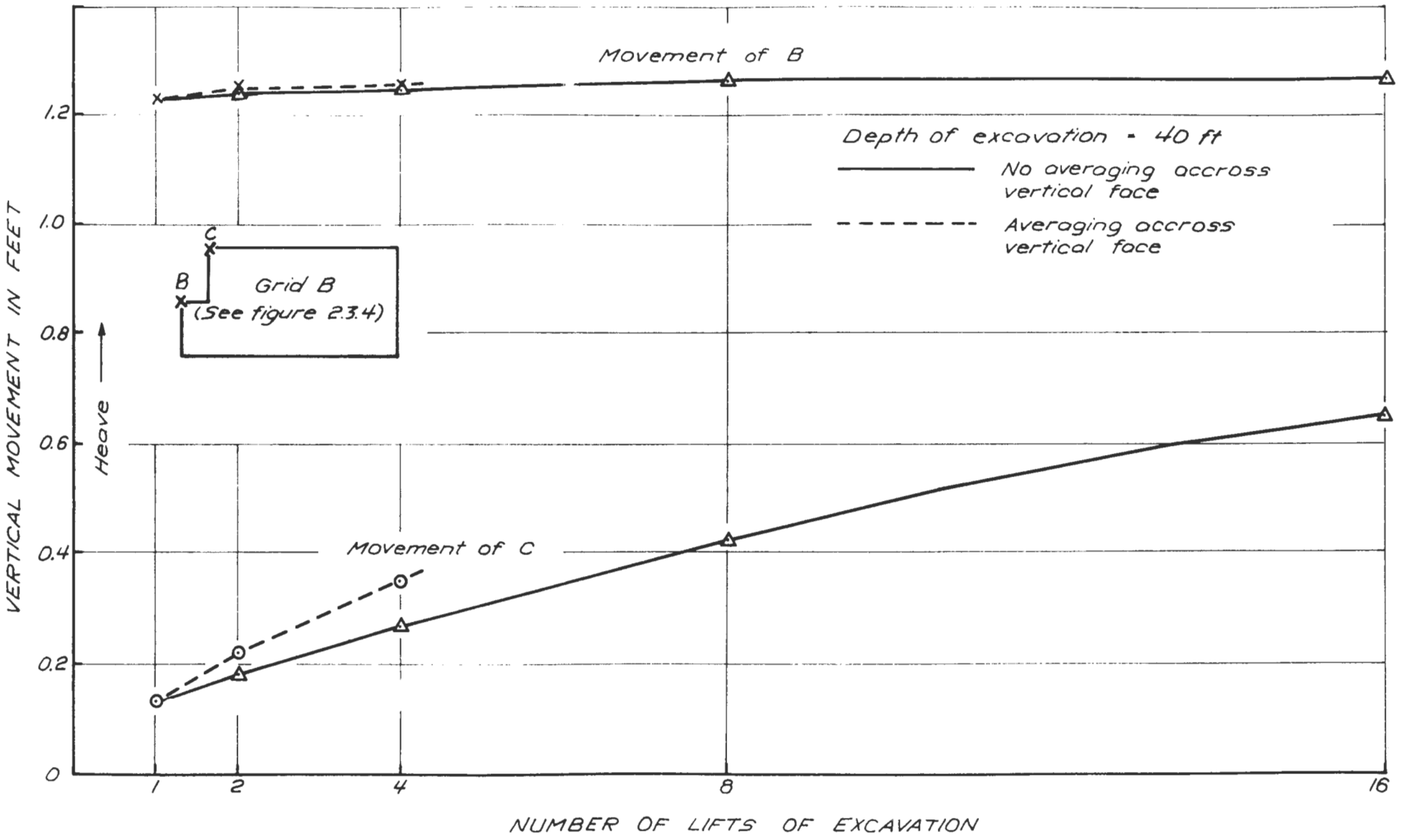

FIGURE 2.3.10 VERTICAL MOVEMENTS OF OPEN CUT WITH DIFFERENT METHODS OF STRESS RELEASE

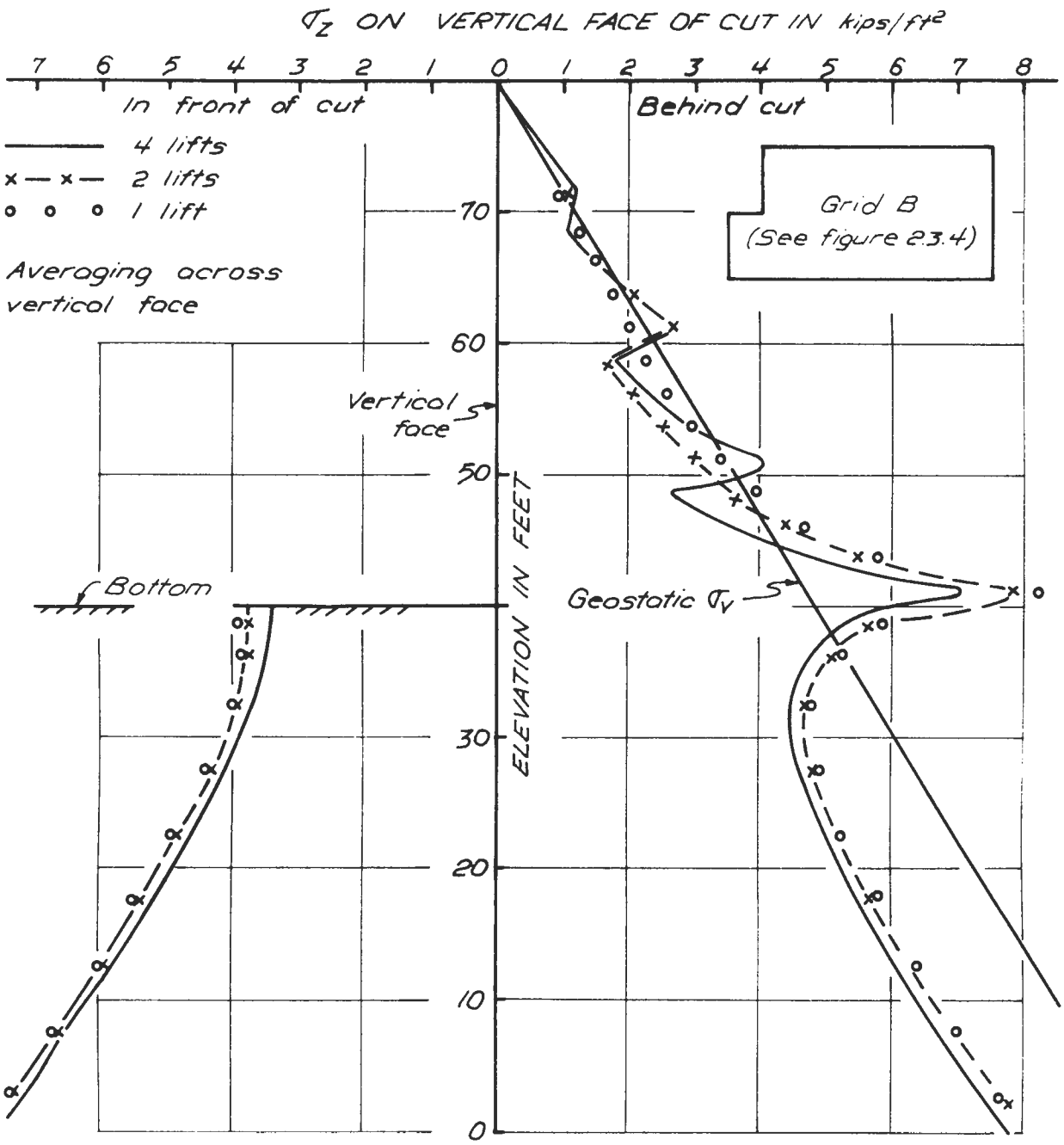

FIGURE 2.3.11 VERTICAL STRESS ON VERTICAL FACE OF OPEN CUT

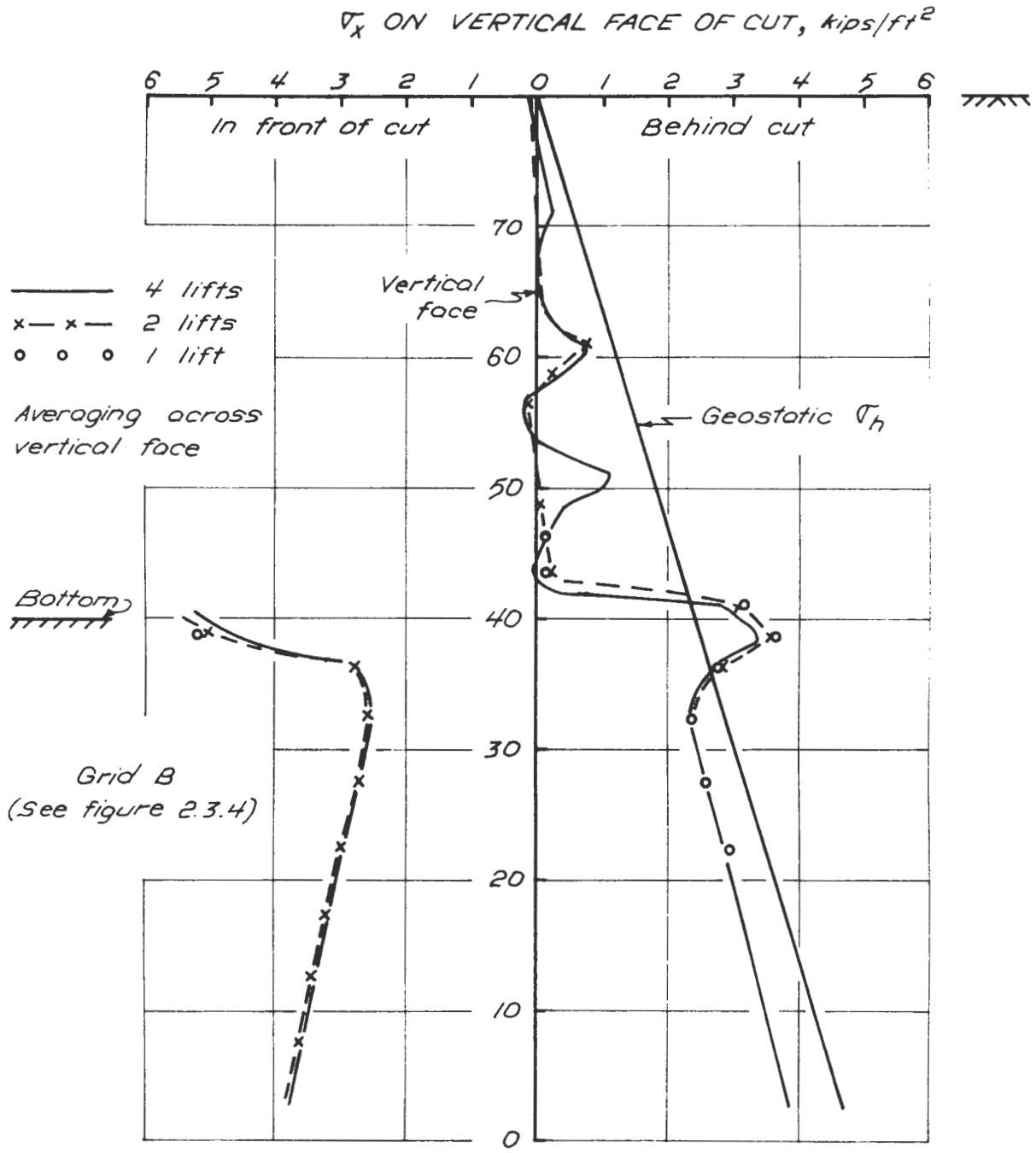

FIGURE 2.3.12 HORIZONTAL STRESS ON VERTICAL FACE OF OPEN CUT

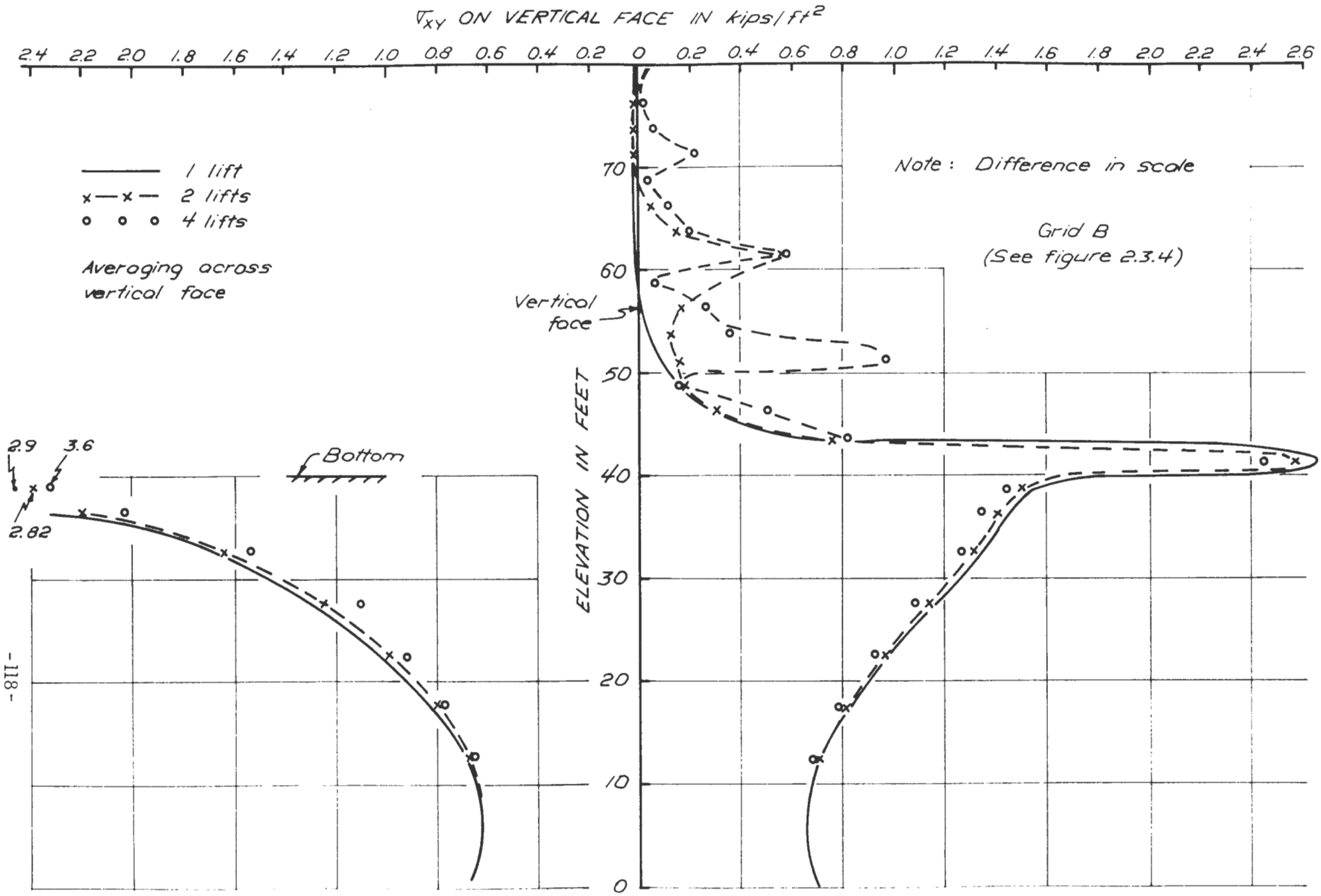

FIGURE 2.3.13 SHEAR STRESS ON VERTICAL FACE OF OPEN CUT

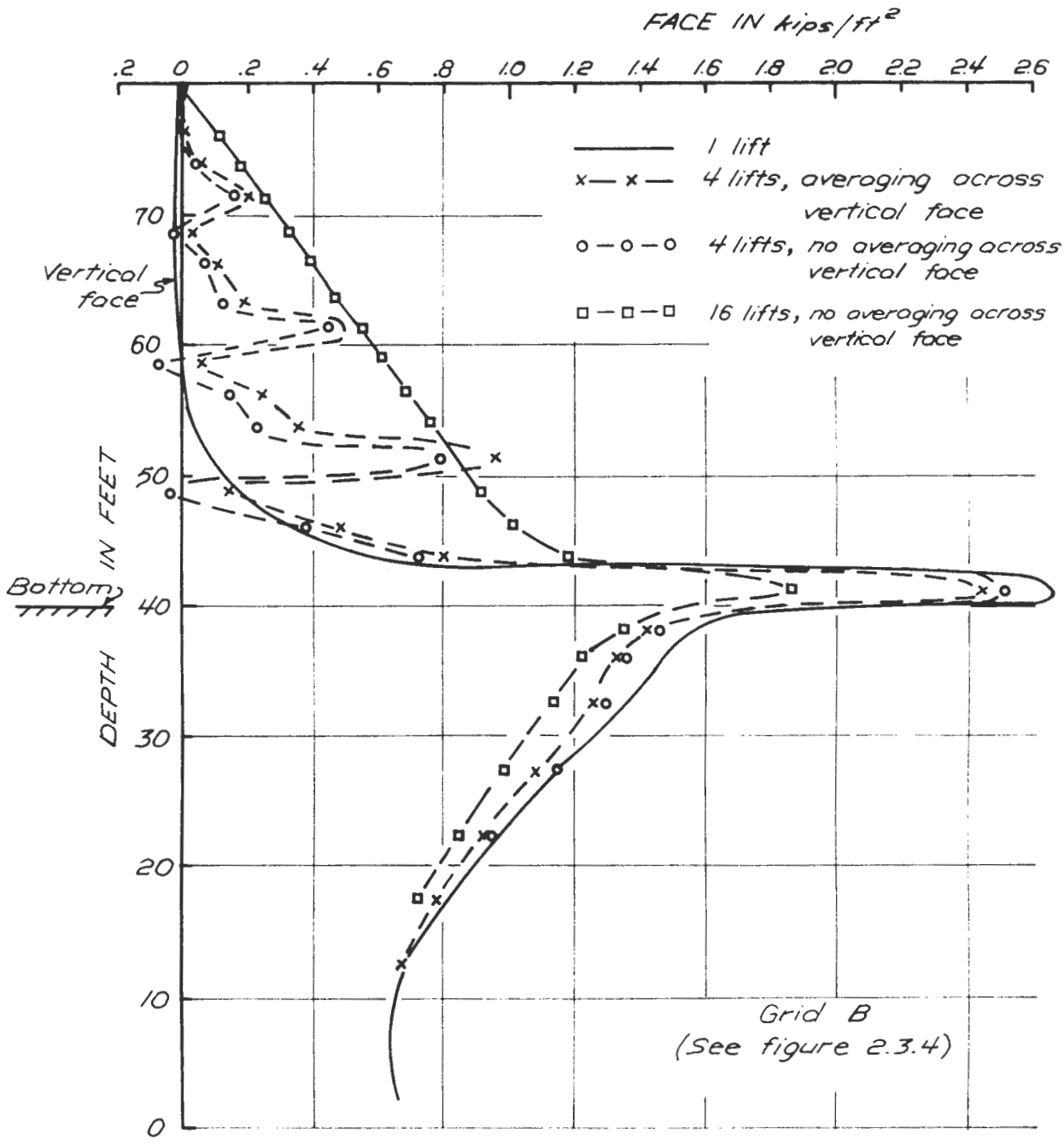

FIGURE 2.3.14 SHEAR STRESS ON VERTICAL FACE OF OPEN CUT WITH DIFFERENT OF METHODS OF STRESS RELEASE

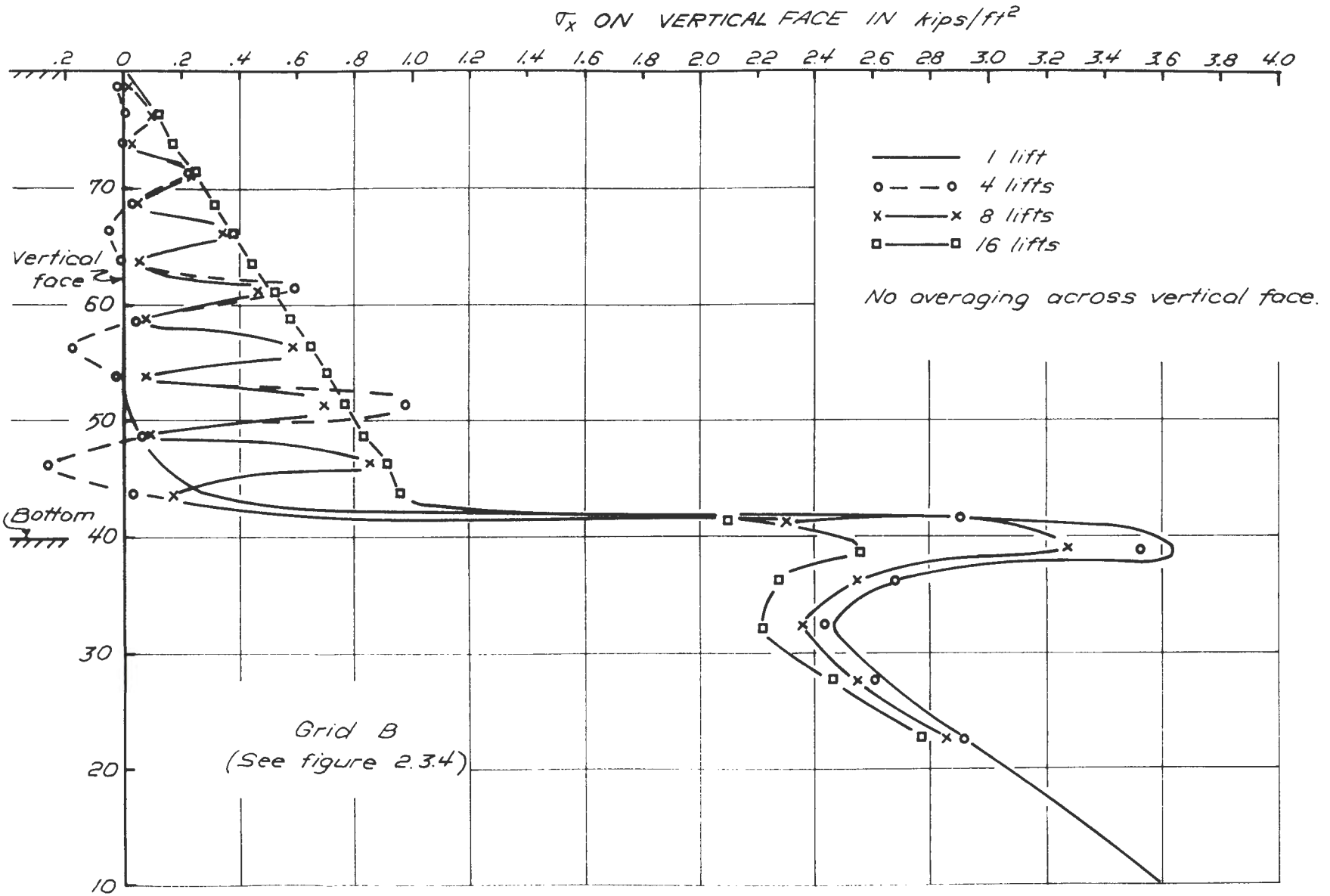

FIGURE 2.3.15 HORIZONTAL STRESS ON VERTICAL FACE OF OPEN CUT WITH NO AVERAGING

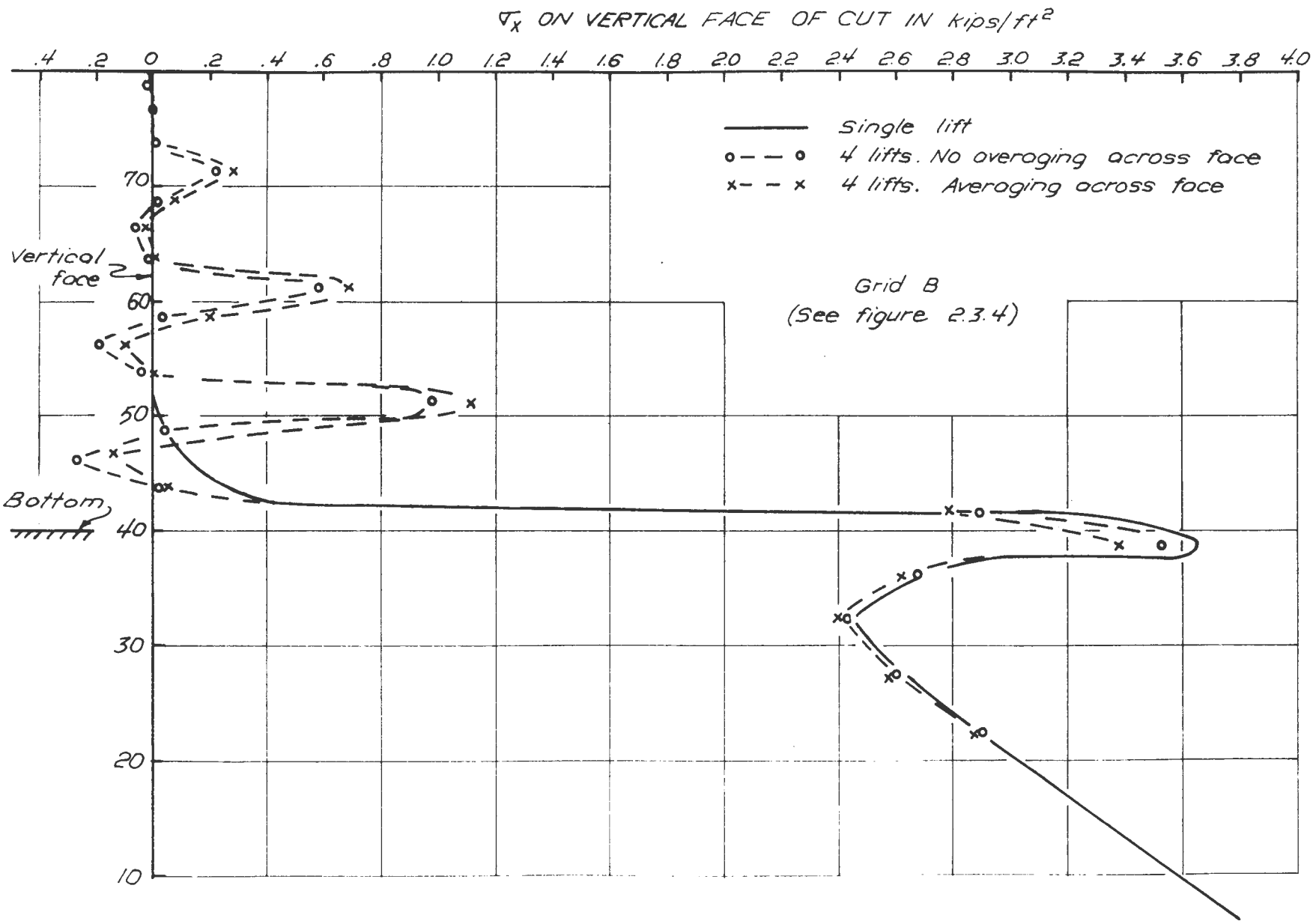

FIGURE 2.3.16 HORIZONTAL STRESS ALONG FACE OF OPEN CUT WITH DIFFERENT METHODS OF STRESS RELEASE

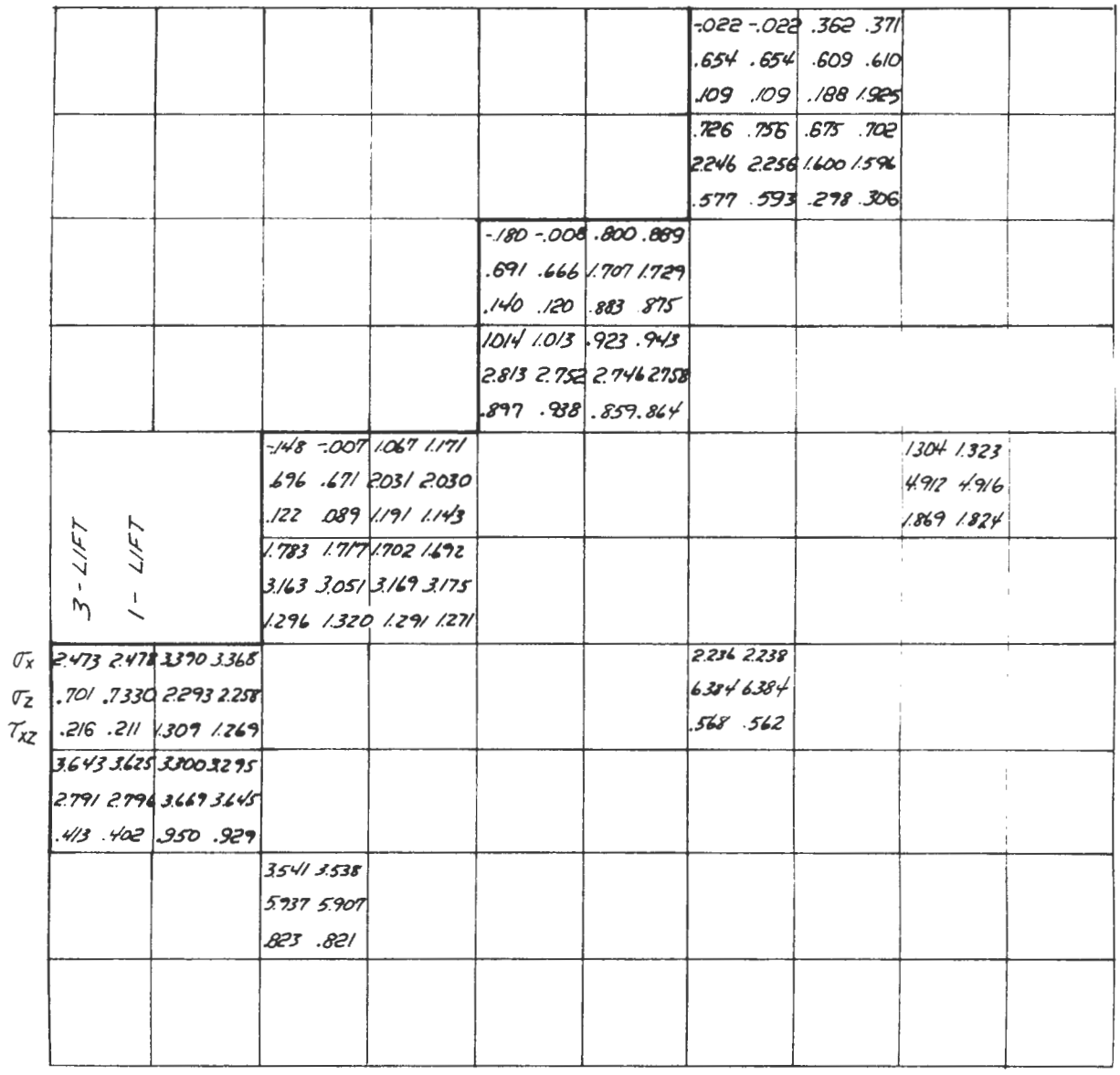

Note: Stresses in kips/ft^2

FIGURE 2.3.17 COMPARISON OF STRESSES IN 3-LIFT AND 1-LIFT TERRACED CUTS

							-.046 -.104	.210 -.143	.338	.408
							.640 .597	.603 .593	.572	.586
							.083 0	.126 -.025	.063	.020
							.451 .002	.348 -.017	.427	.452
							2.908 1.759	1.665 1.795	1.720	1.717
							.353 .057	.190 -.054	.131	.043
							.123 .014	.517 .107	.540	.585
							2.626 2.900	2.938 3.036	2.802	2.822
							.236 .039	.264 -.003	.164	.059
							.763 .091	.571 .273	.750	.783
							4.863 4.139	3.800 4.288	3.900	3.879
							.791 .055	.393 .182	.283	.077
							.239 .114	.961 .723	1.022	.067
							4.355 5.618	5.081 5.557	4.870	4.909
							.460 .362	.550 .581	.309	.045
	3-LIFT						1.604 1.983	1.410 1.684	1.445	1.424
	1-LIFT						6.636 7.900	5.607 6.105	5.838	5.895
							1.625 1.586	6.783 .675	.342	.100
σ_x	1.084 1.129	1.063 1.101	1.038 1.064	1.093 1.165	1.351 1.413	2.724 2.714	2.115 2.247	1.996 2.832	1.816	1.864
σ_z	.571 .585	.571 .588	.570 .574	.652 .682	.645 .674	3.388 3.734	5.865 6.494	6.499 7.068	.734	6.903
τ_{xz}	-.016 -.017	-.045 -.049	.057 -.065	0 -.014	.286 .289	1.856 2.032	1.080 1.071	.530 .401	.293	.089
	1.722 1.778	1.796 1.856	1.963 2.035	2.232 2.331	2.671 2.818	2.415 2.526	2.259 2.359	2.314 2.453	2.379	2.427
	1.750 1.761	1.767 1.782	1.847 1.870	2.058 2.103	2.938 3.077	4.639 4.962	6.424 6.948	7.324 7.832	2.935	7.916
	0 -.0	.012 .009	.083 .081	.305 .321	.907 .781	1.436 1.553	1.036 1.075	.569 .520	.290	.094
	2.216 2.271	2.324 2.390	2.534 2.620	.2821 .2.933	2.980 3.104	2.985 3.103	2.923 3.052	3.020 3.161	3.158	3.242
	2.999 3.021	3.053 3.256	3.220 3.256	3.673 3.756	4.567 4.743	5.903 6.213	7.229 7.651	8.170 8.636	8.682	8.901
	.049 .051	.163 .171	.334 .356	.626 .672	.983 1.060	1.183 1.269	1.021 1.072	.688 .690	.383	.123
	2.467 2.582	2.649 2.796	2.720 2.778	2.966 3.047	3.263 3.372	3.553 3.684	3.843 4.000	4.107 4.287	4.313	4.421
	4.357 4.377	4.440 4.472	4.680 4.736	5.177 5.253	6.014 6.207	7.106 7.404	8.204 8.591	9.050 9.483	9.570	9.803
	.100 .107	.316 .340	.580 .623	.878 .947	3.092 1.234	1.260 1.348	1.146 1.212	.868 .901	.524	.174

Note: Stresses in kips/ft^2

FIGURE 2.3.18 COMPARISON OF STRESSES IN 3-LIFT AND 1-LIFT VERTICAL CUTS

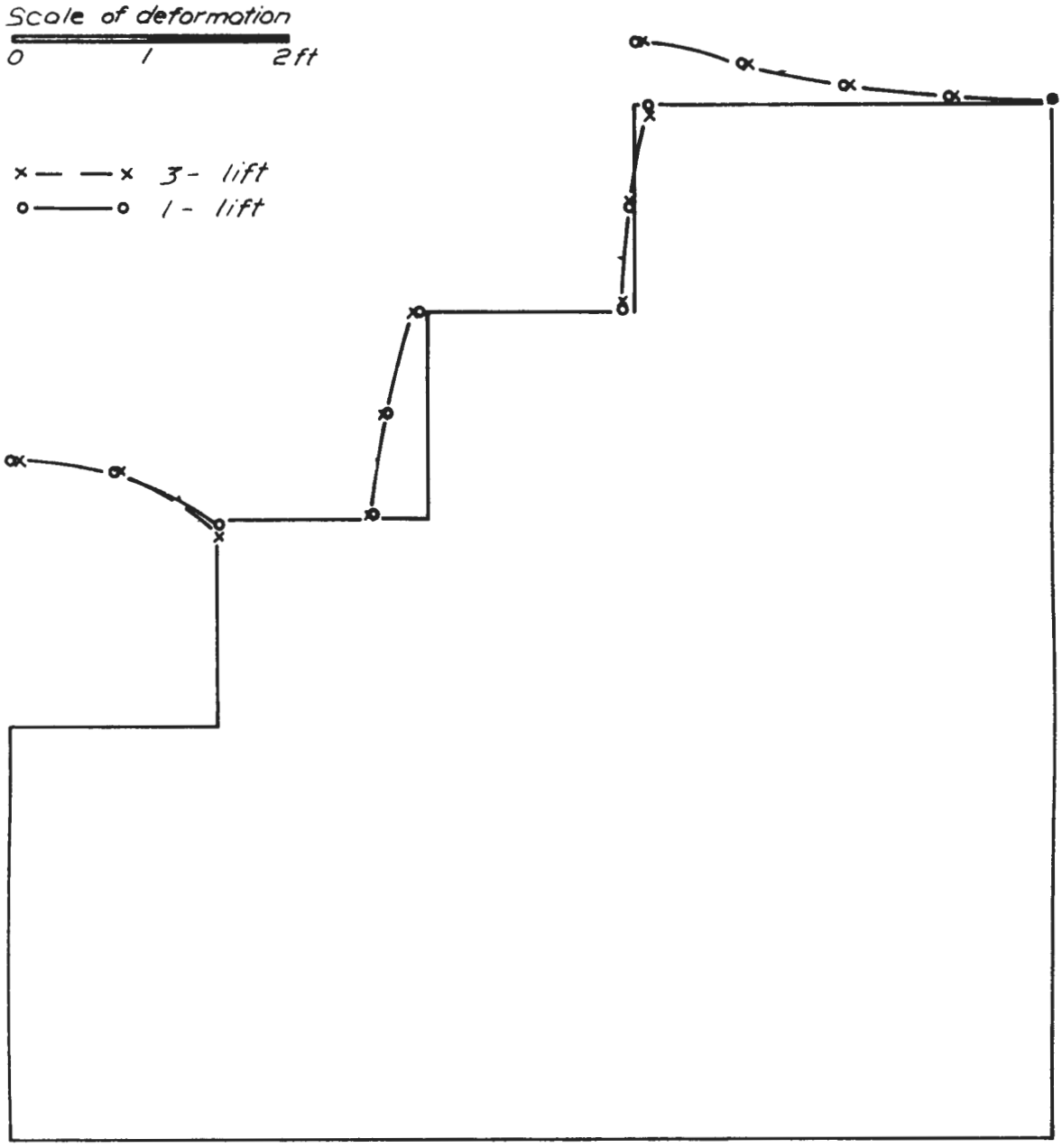

FIGURE 2.3.19 COMPARISON OF MOVEMENTS IN 3-LIFT AND 1-LIFT TERRACED CUTS

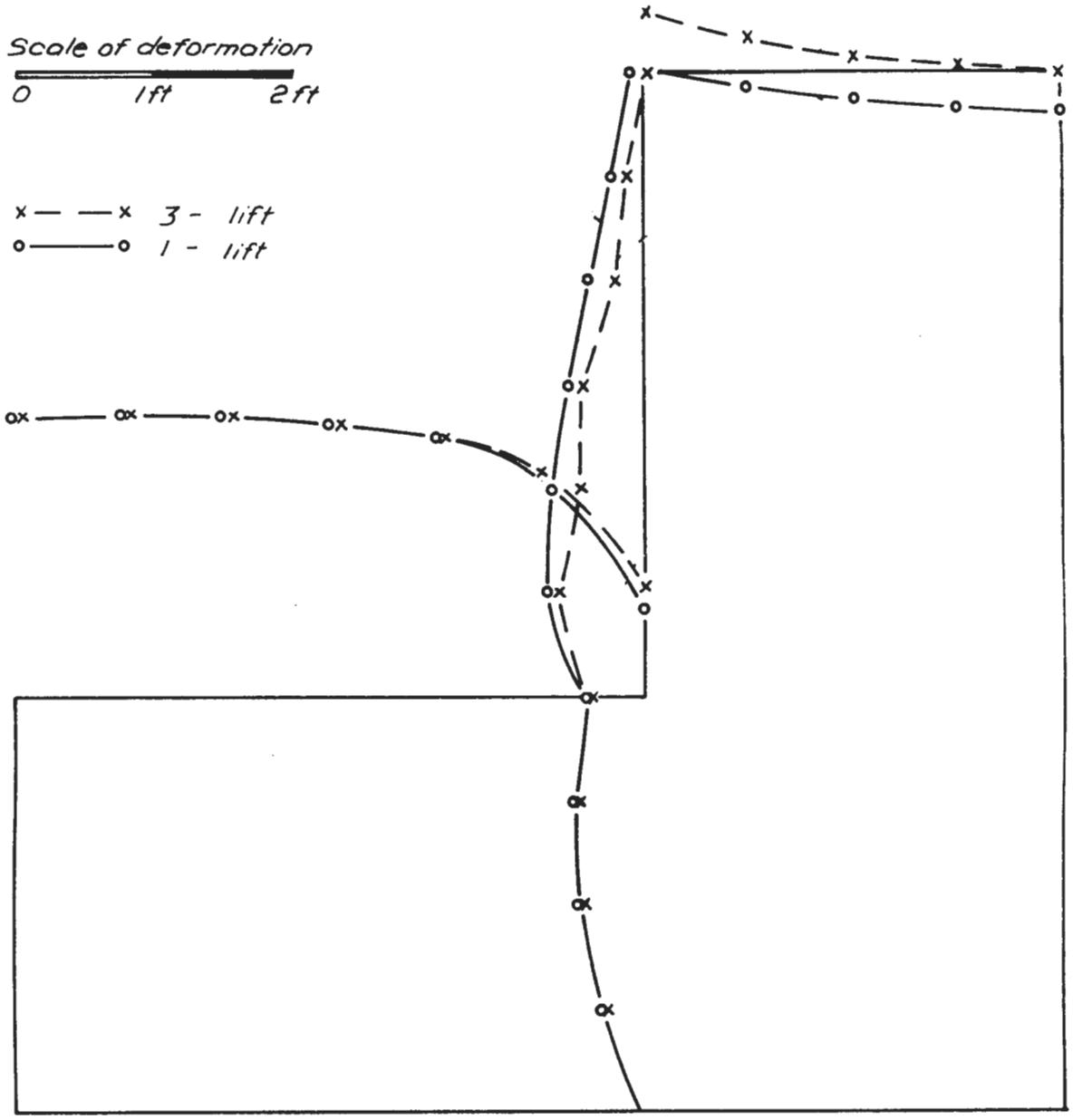

FIGURE 2.3.20 COMPARISON OF MOVEMENTS IN 3-LIFT AND 1-LIFT VERTICAL CUTS

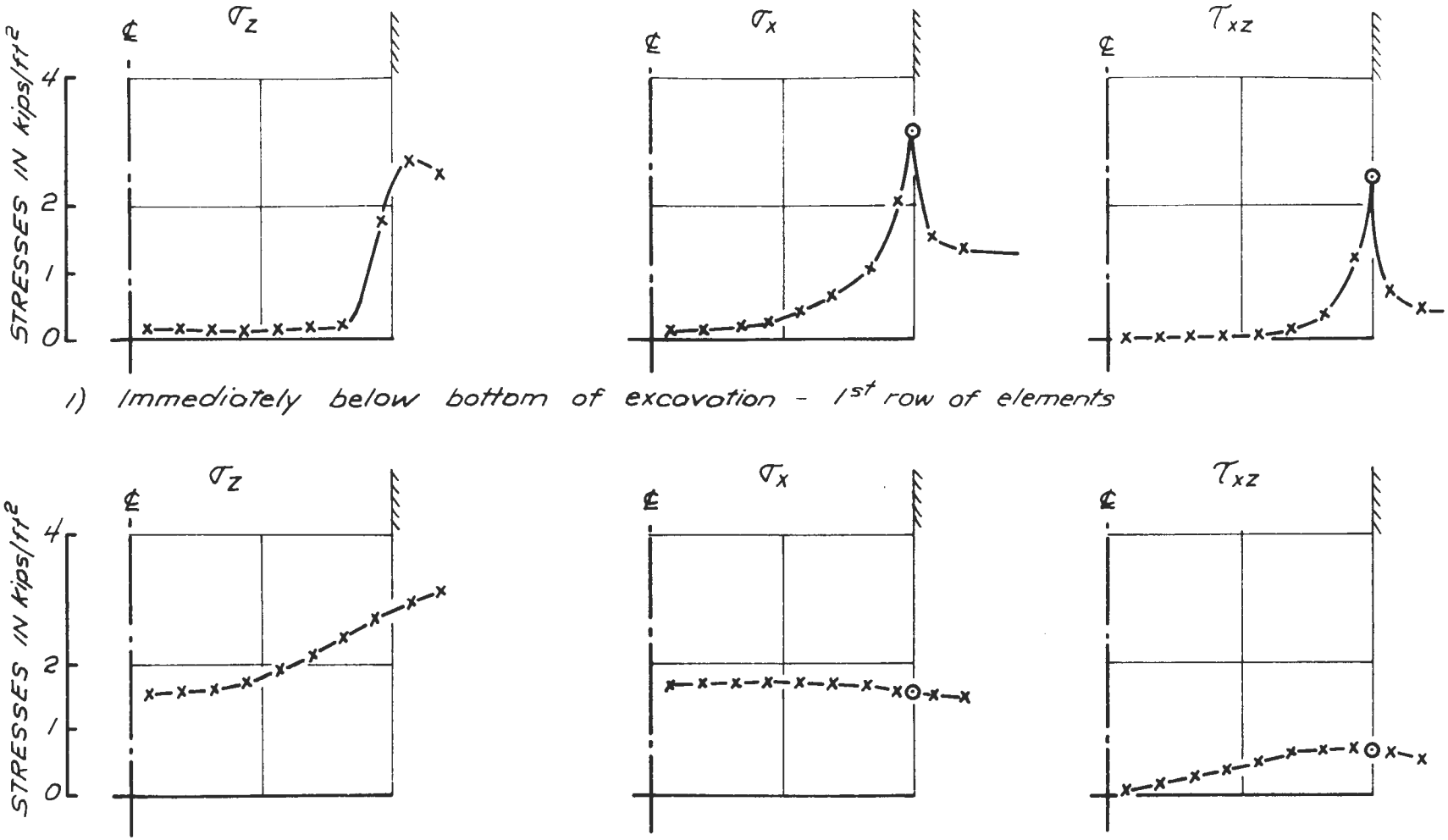

FIGURE 2.3.21 STRESS DISTRIBUTIONS IN HORIZONTAL ROWS OF ELEMENTS FOR EXCAVATION 20 FEET DEEP

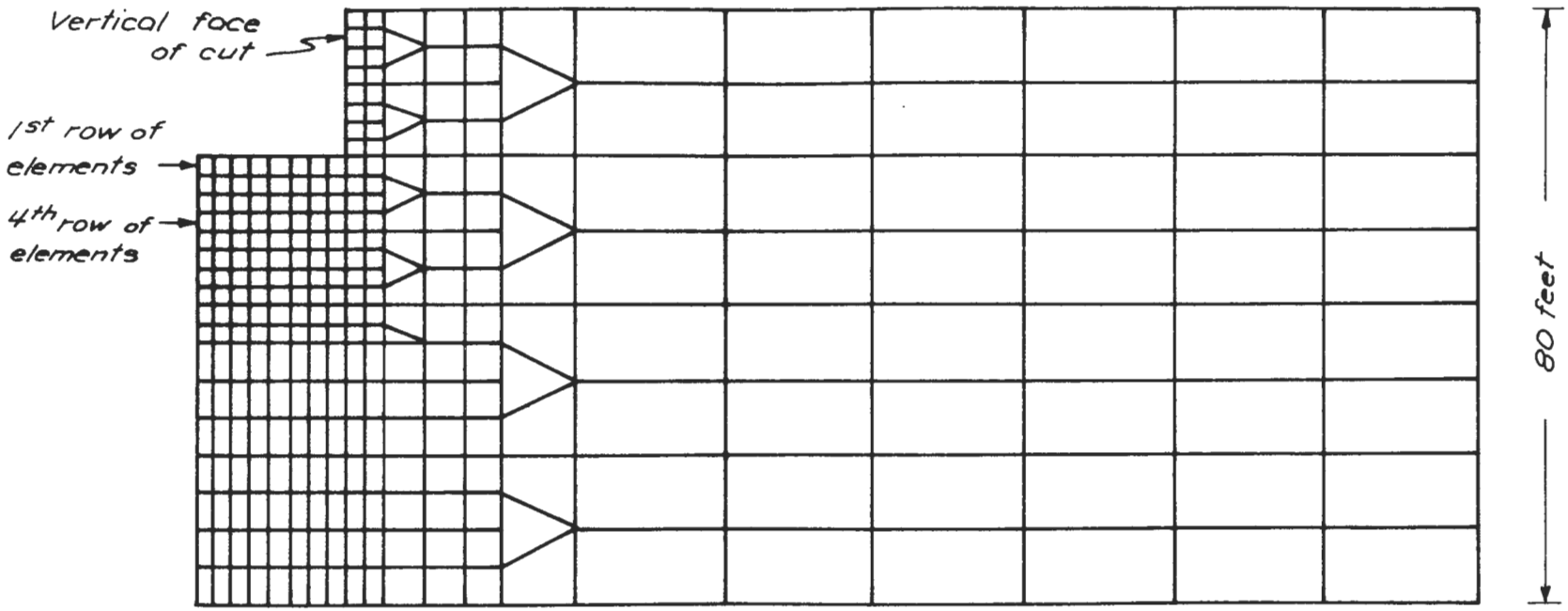

FIGURE 2.3.22 LOCATION OF TWO ROWS OF ELEMENTS BELOW BOTTOM OF EXCAVATION

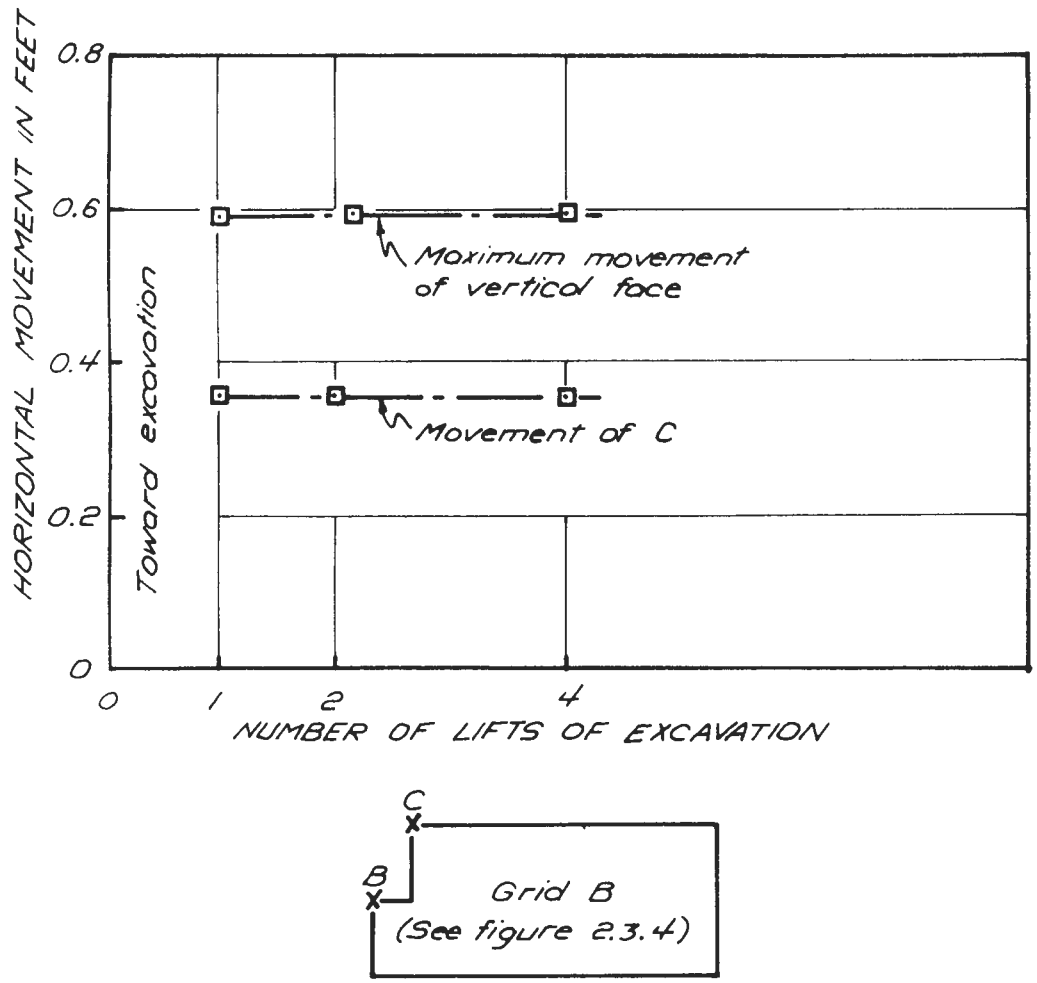

FIGURE 2.3.23 HORIZONTAL MOVEMENTS OF OPEN CUT STRESS RELEASE BY EXTRAPOLATION

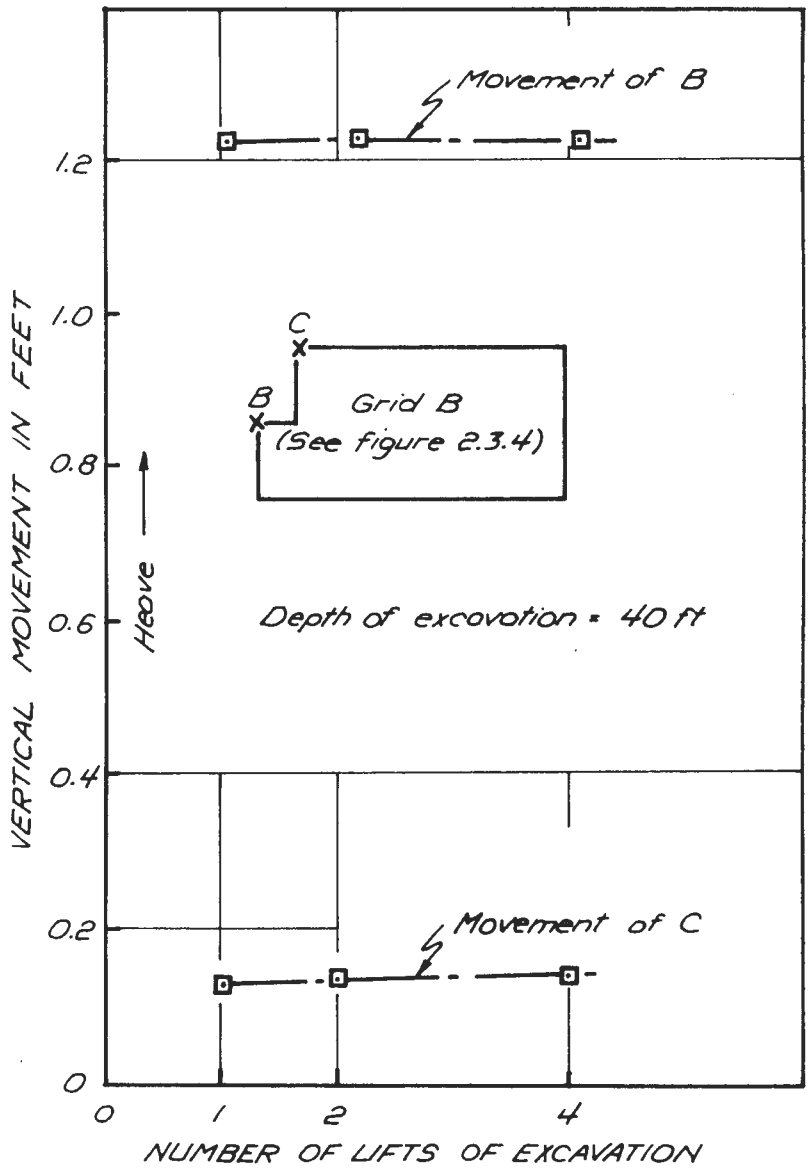

FIGURE 2.3.24 VERTICAL MOVEMENTS OF OPEN CUT STRESS RELEASE BY EXTRAPOLATION

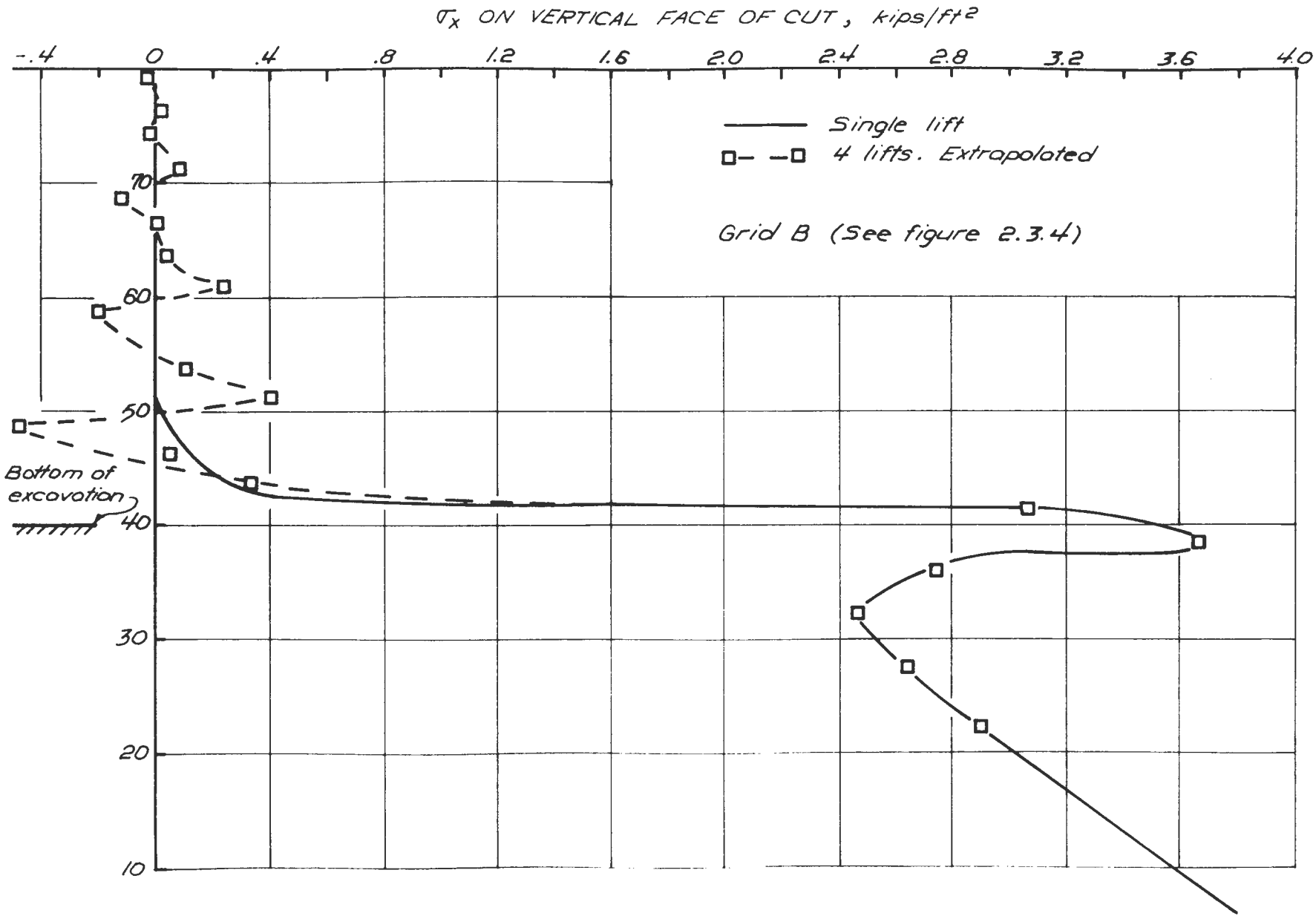

3.25 HORIZONTAL STRESS ACTING ON VERTICAL FACE OF OPEN

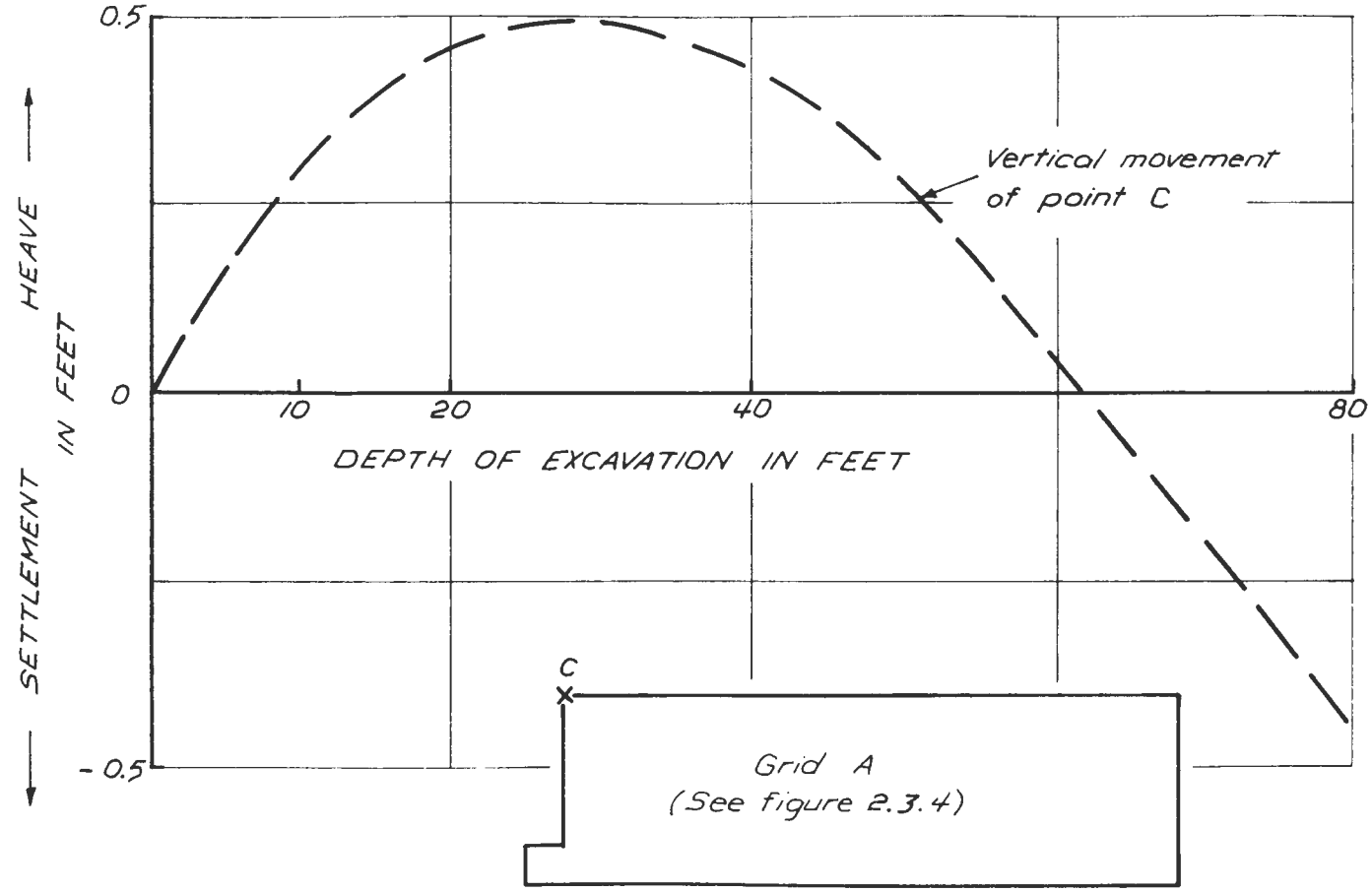

FIGURE 3.2.1 VERTICAL MOVEMENT OF OPEN CUTS WITH DEPTH OF INSTANTANEOUS EXCAVATION

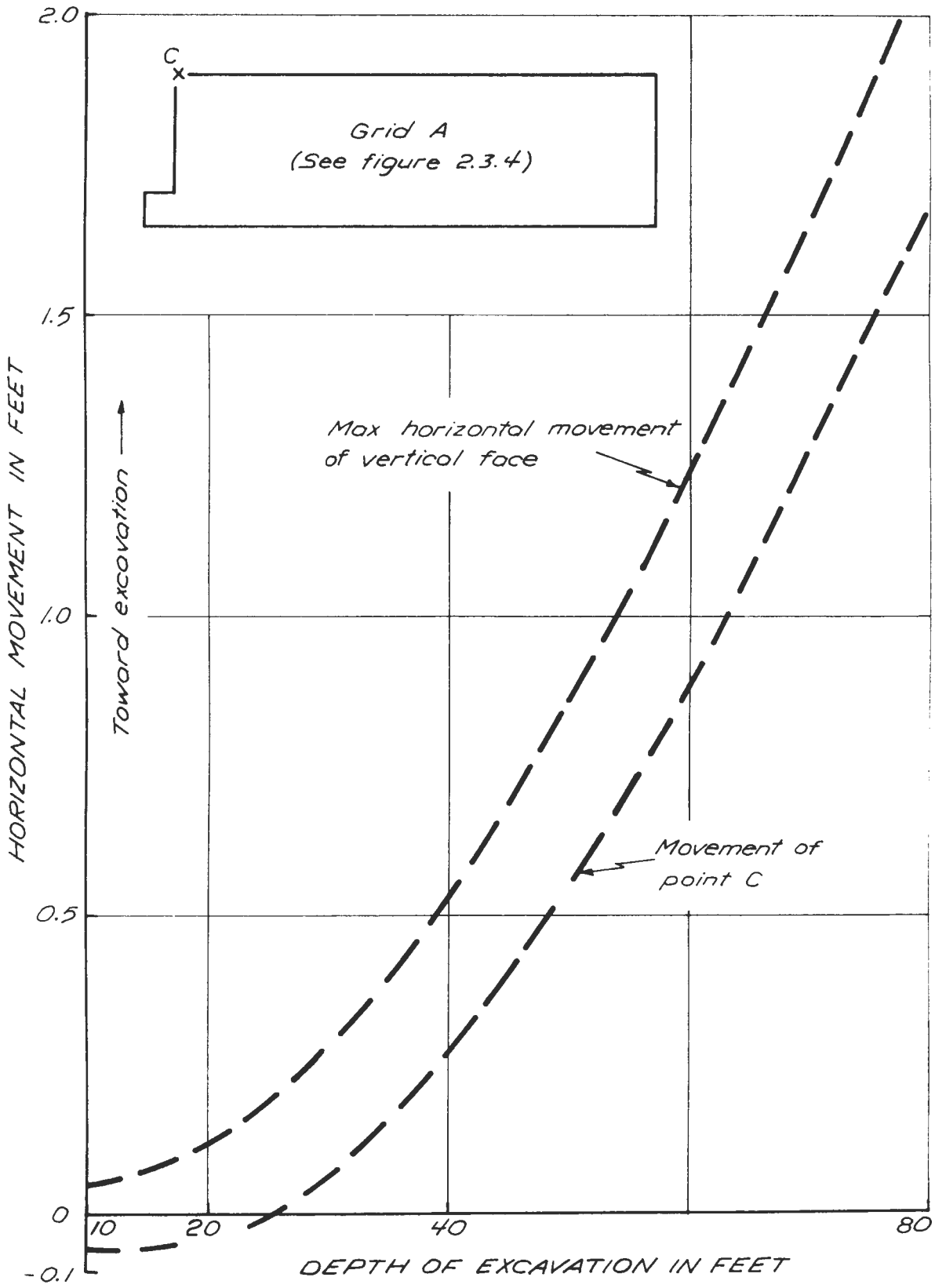

FIGURE 3.2.2 HORIZONTAL MOVEMENTS OF OPEN CUTS WITH DEPTH OF INSTANTANEOUS EXCAVATION

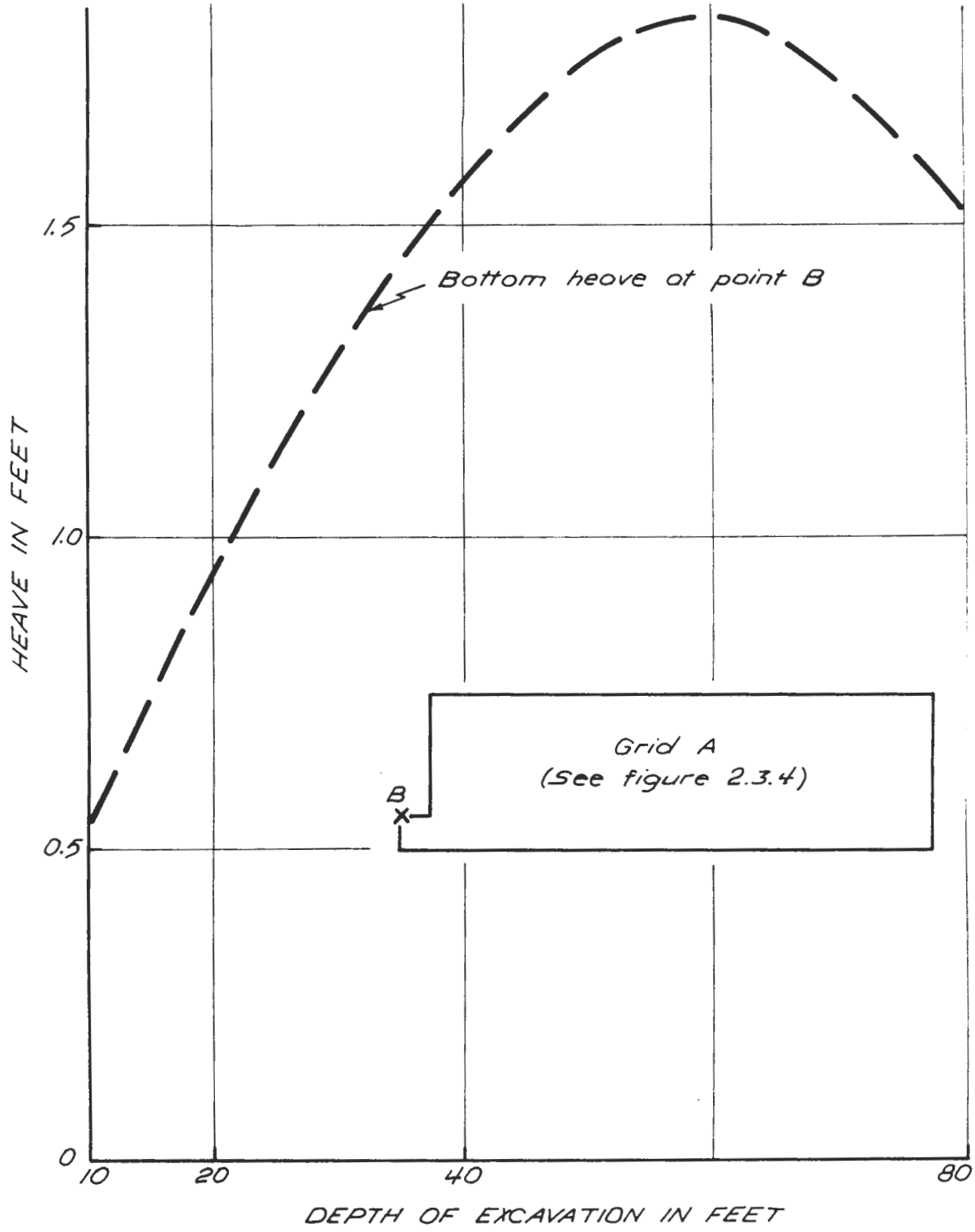

FIGURE 3.2.3 BOTTOM HEAVE OF OPEN CUTS WITH DEPTH OF INSTANTANEOUS EXCAVATION

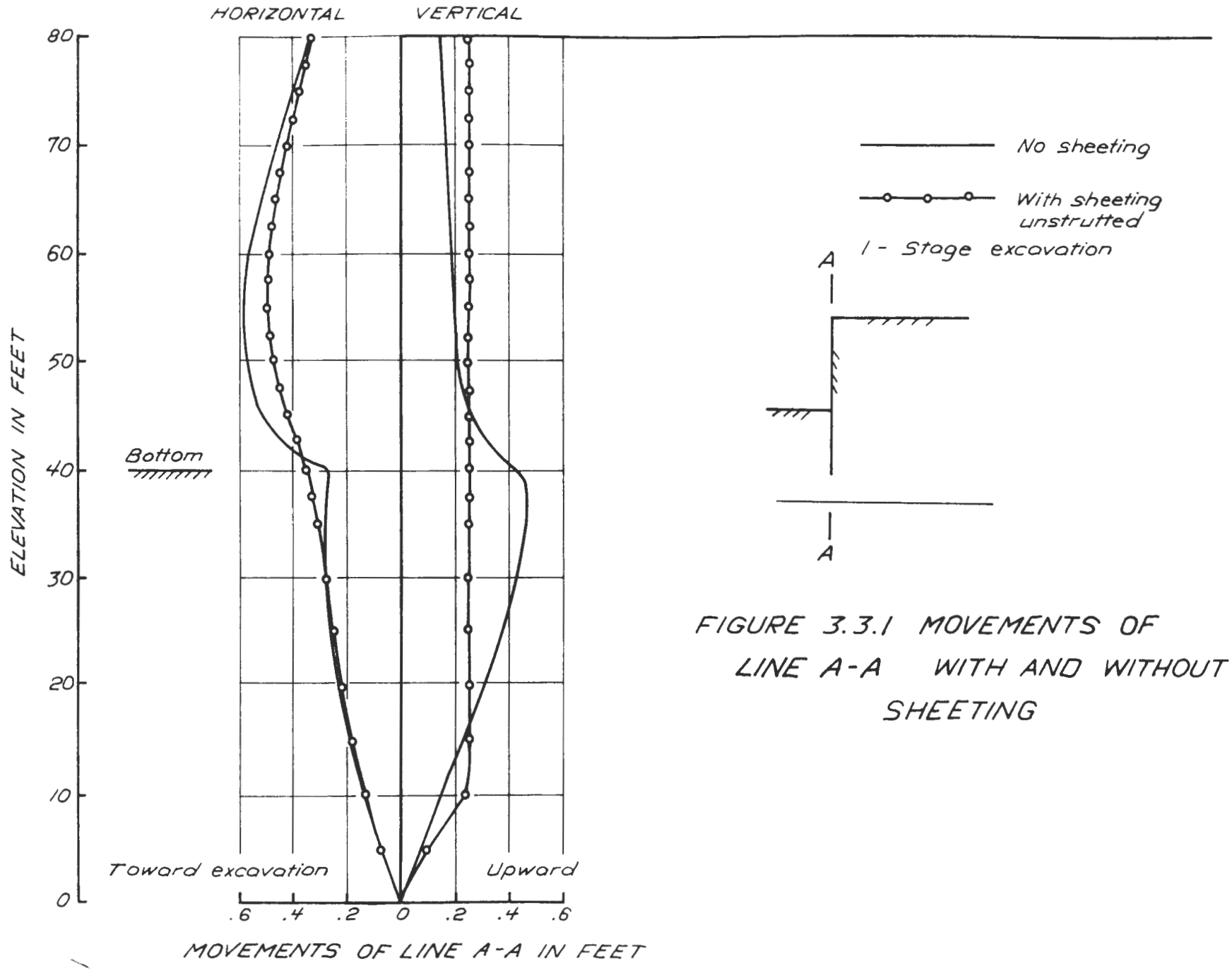

FIGURE 3.3.1 MOVEMENTS OF LINE A-A WITH AND WITHOUT SHEETING

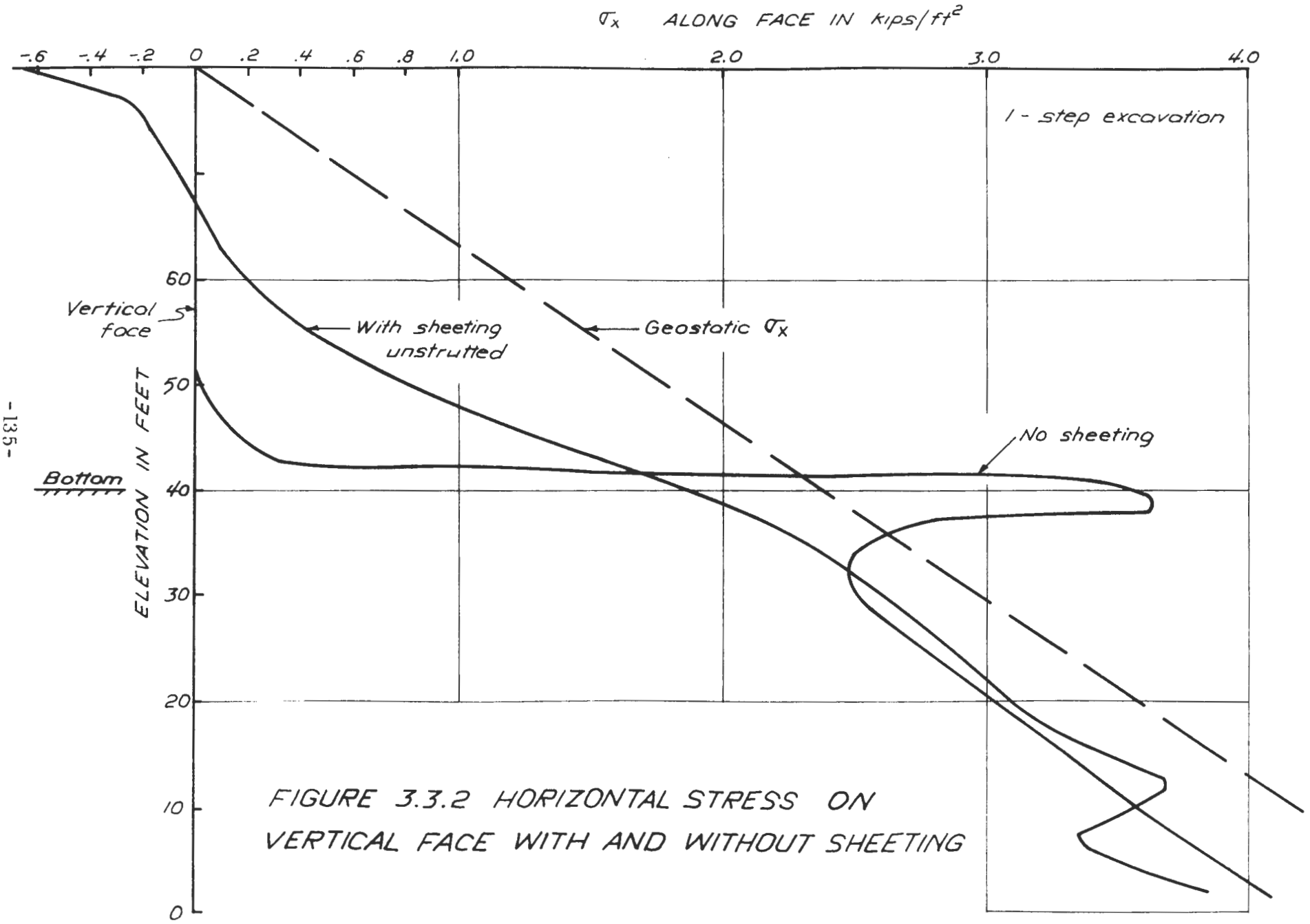

FIGURE 3.3.2 HORIZONTAL STRESS ON VERTICAL FACE WITH AND WITHOUT SHEETING

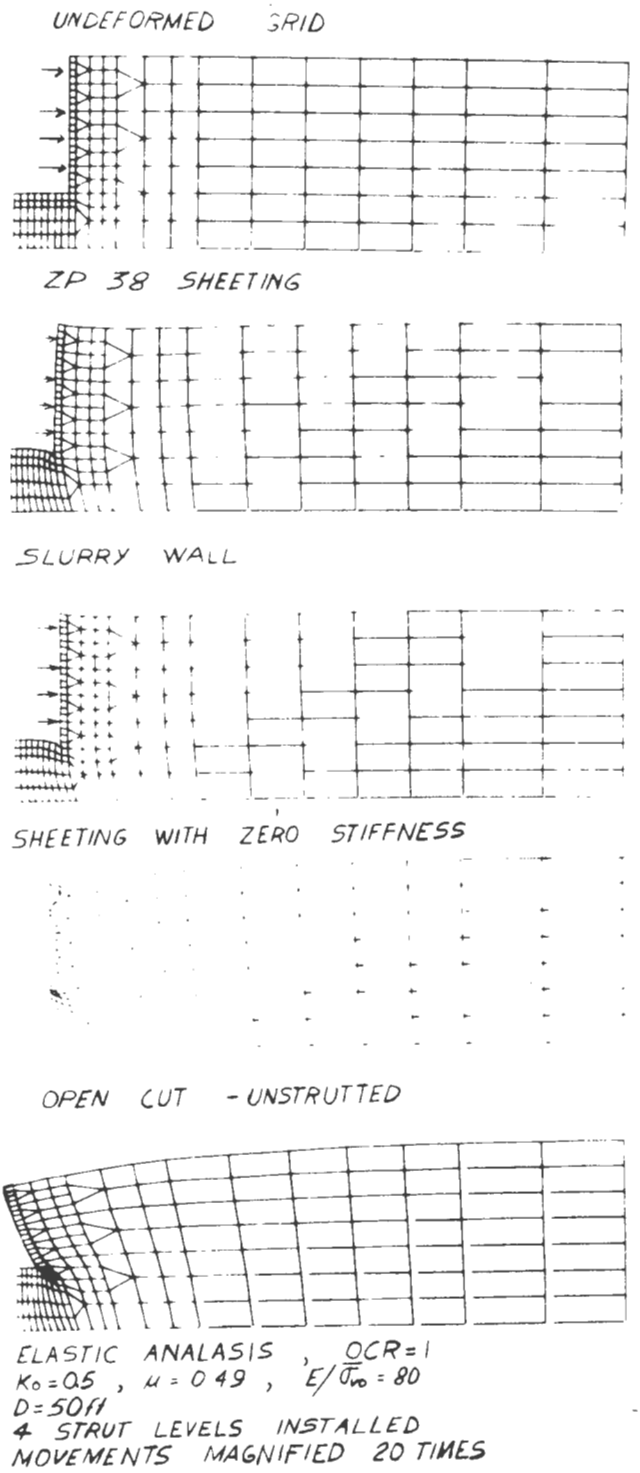

FIGURE 3.4.1 DEFORMED SOIL MASS LINEAR ELASTIC ANALYSIS

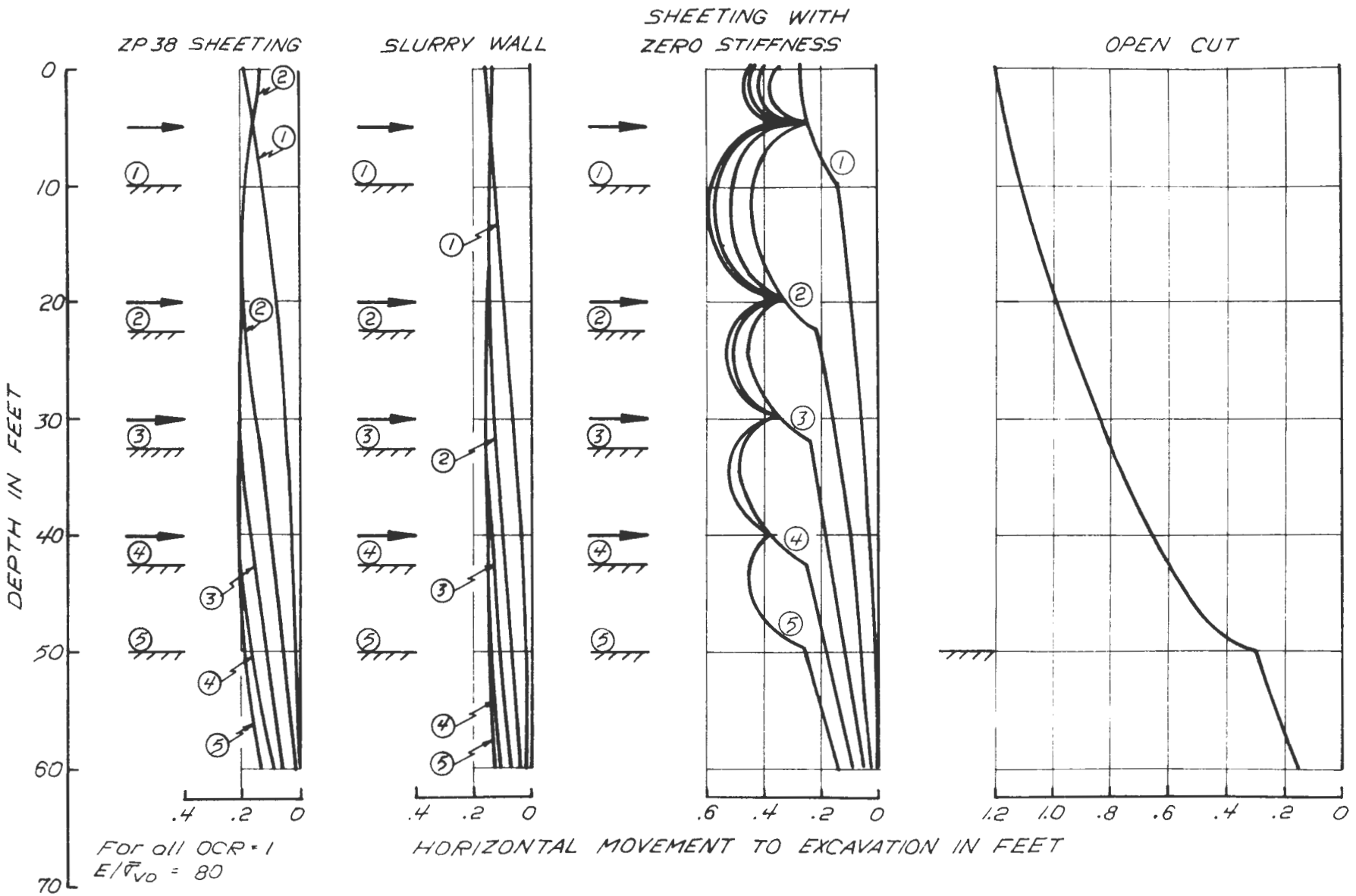

FIGURE 3.4.2 WALL MOVEMENTS TOWARD EXCAVATION LINEARLY ELASTIC ANALYSIS

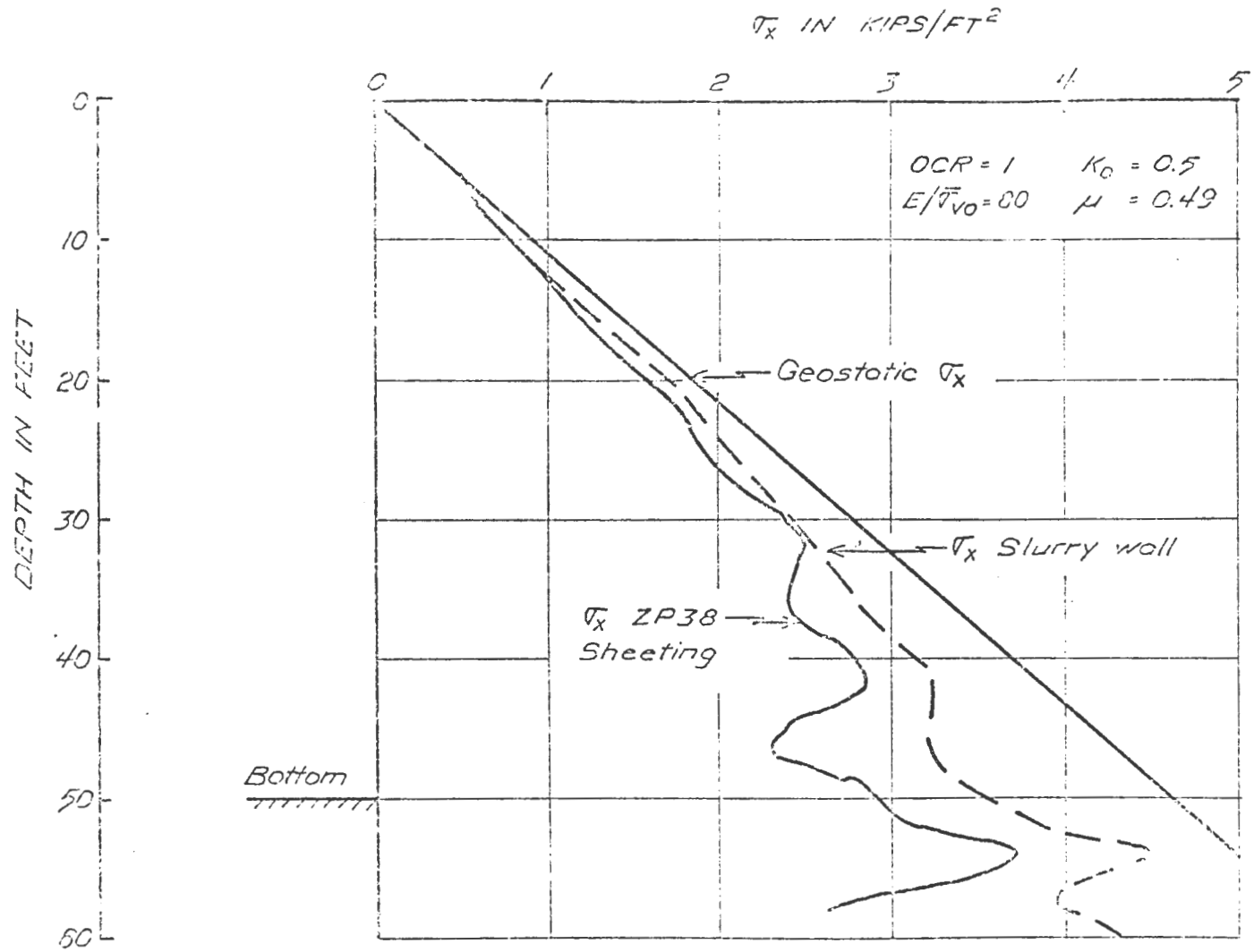

FIGURE 3.4.3 HORIZONTAL STRESS ON WALL

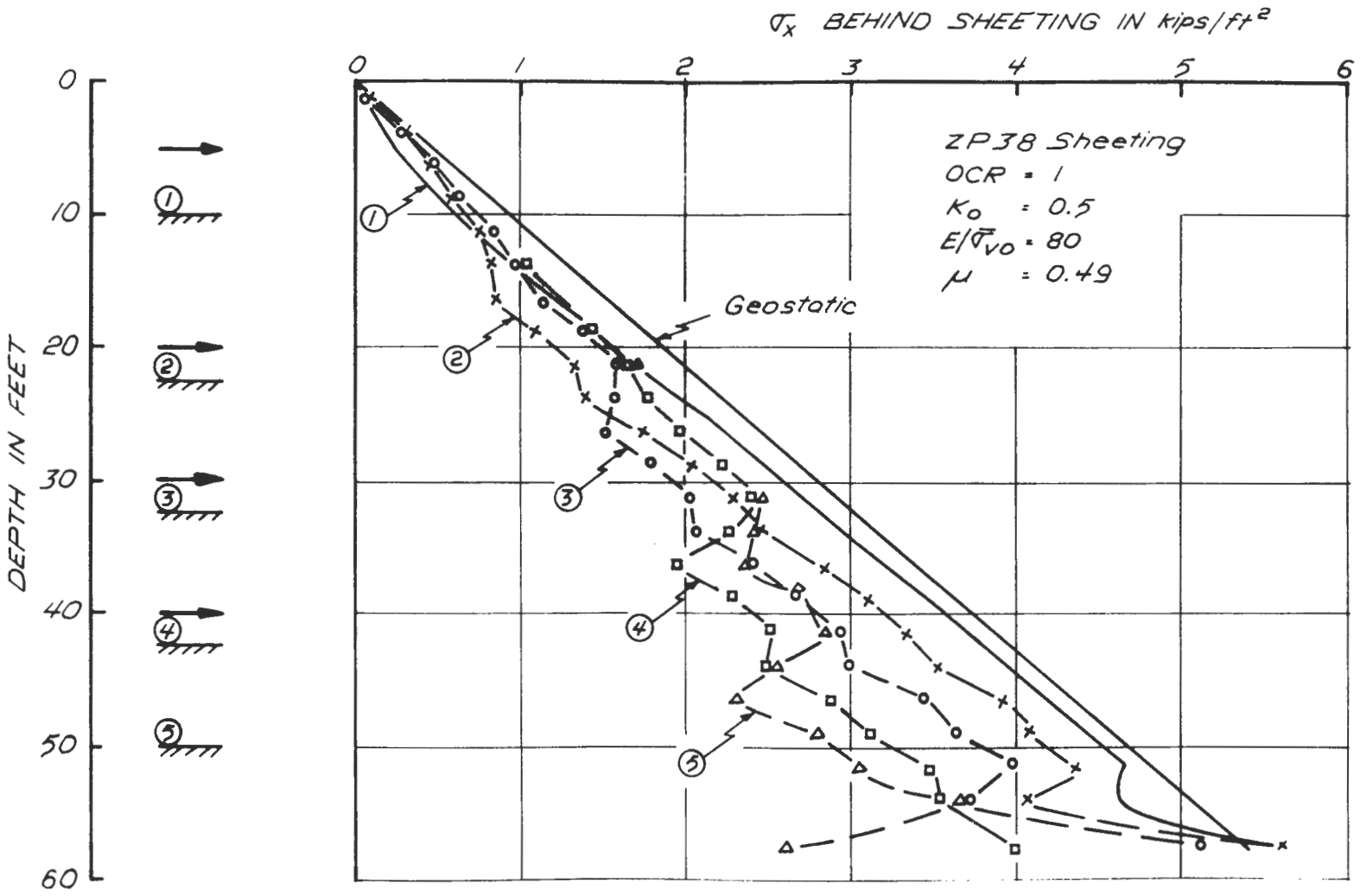

FIGURE 3.4.4 HORIZONTAL STRESS BEHIND SHEETING LINEARLY ELASTIC ANALYSIS

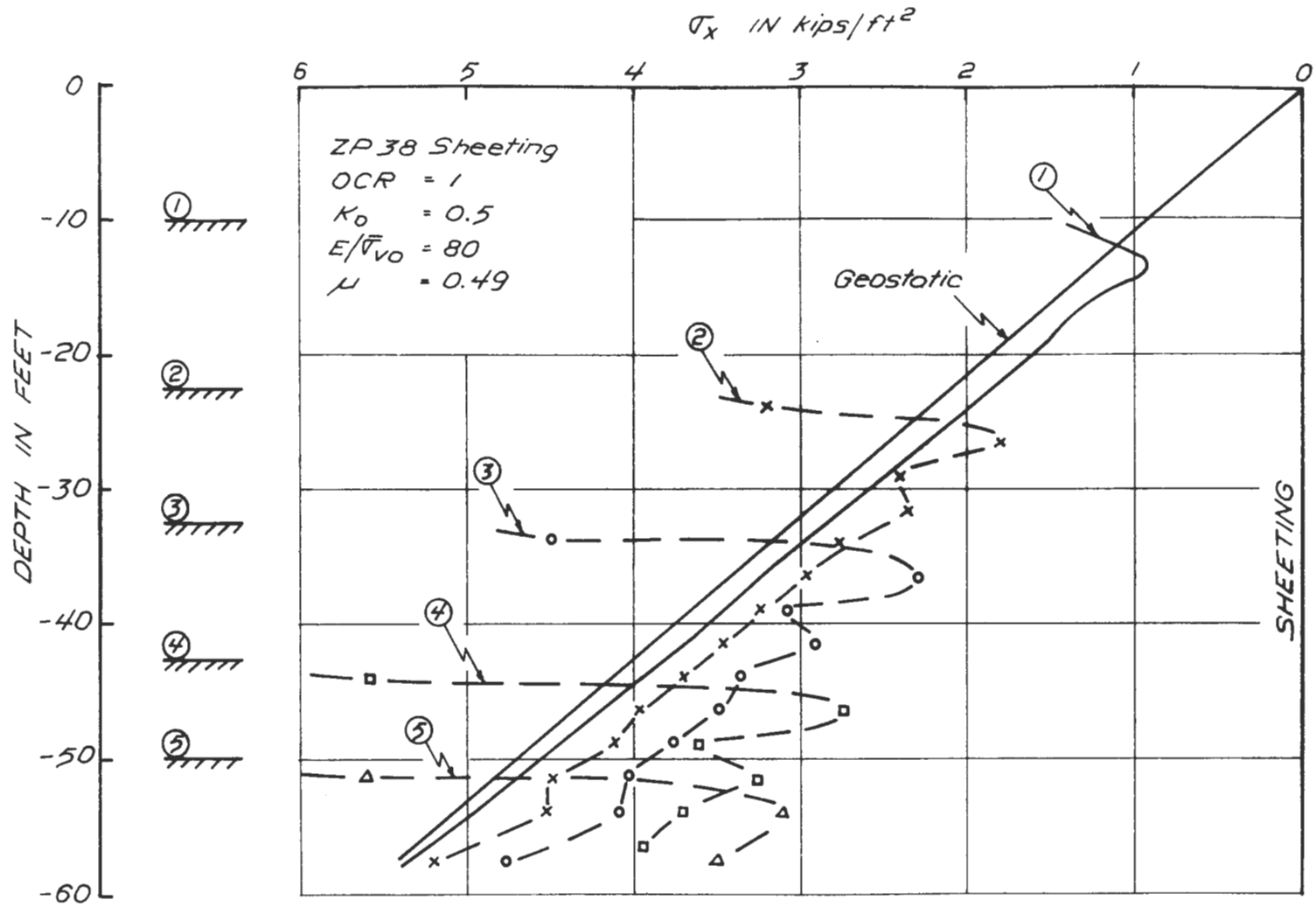

FIGURE 3.4.5 HORIZONTAL STRESS IN FRONT OF SHEETING LINEARLY ELASTIC ANALYSIS

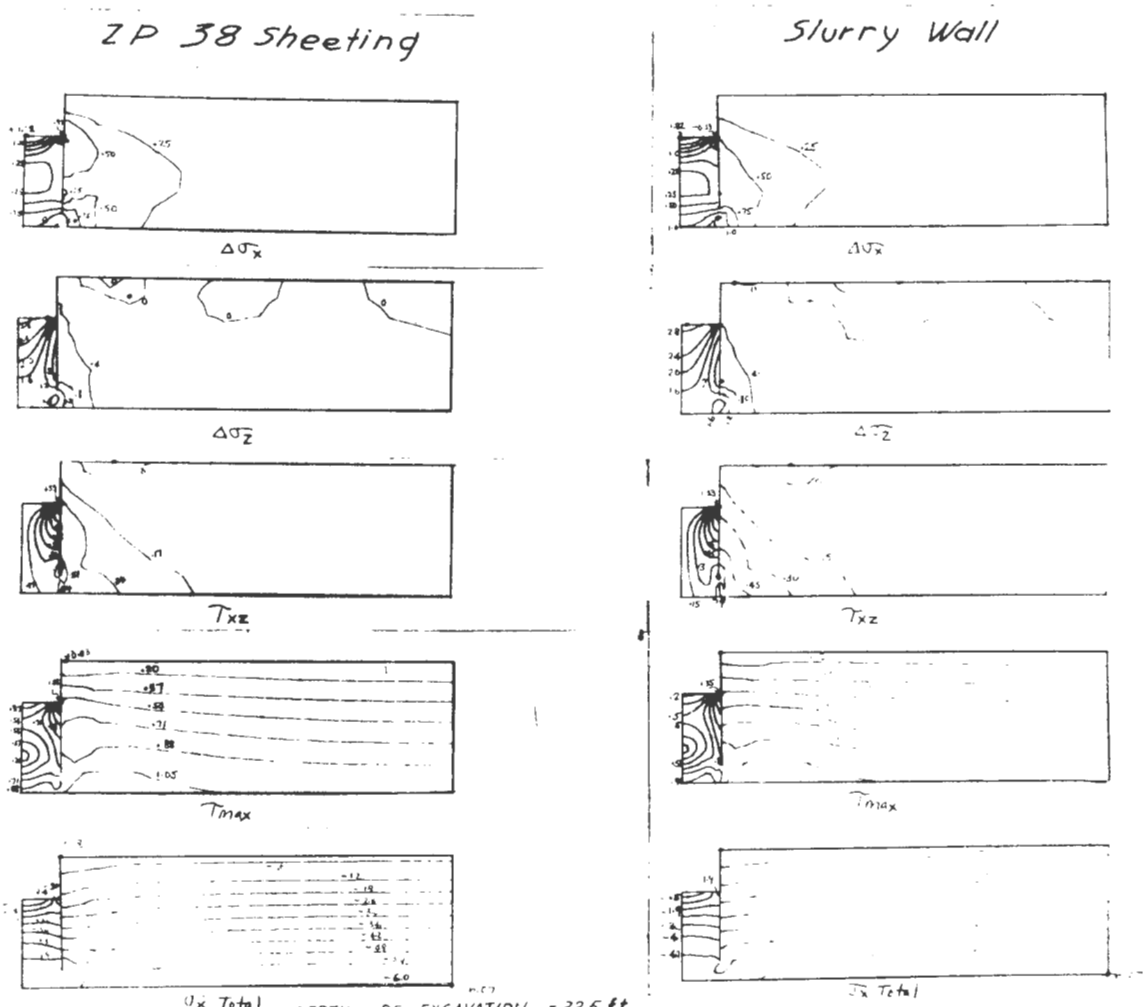

FIGURE 3.4.6 STRESSES IN SOIL MASS LINEARLY ELASTIC ANALYSIS

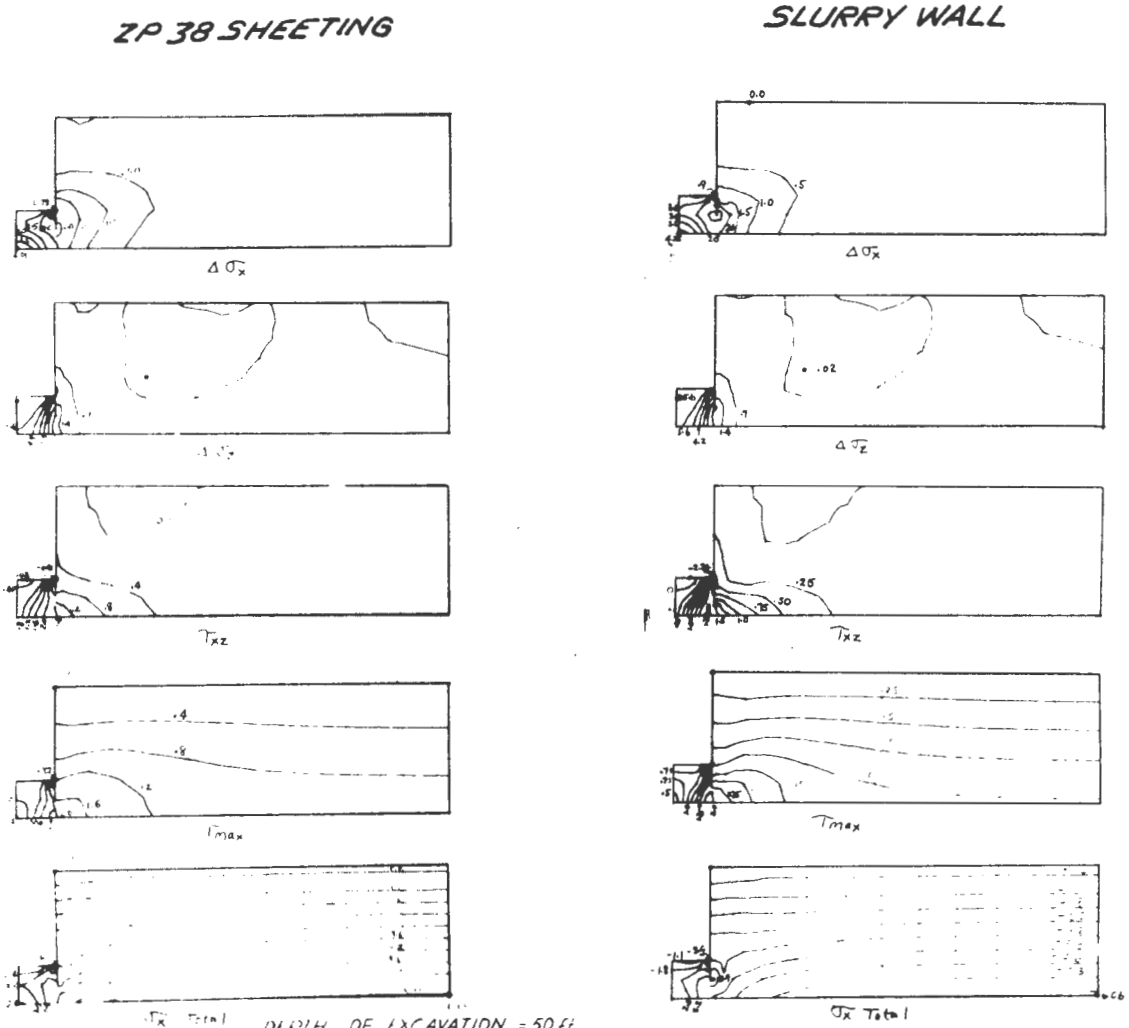

FIGURE 3.4.7 STRESSES IN SOIL MASS LINEARLY ELASTIC ANALYSIS

STAGE	LOAD IN STRUT KIPS/FT				TOTAL LOAD KIPS/FT	COMMENTS
	S1	S2	S3	S4		
2	8.76				8.76	Linear elastic ZP 38 Sheeting $\mu = 0.49$ $K_o = 0.5$ $E/\bar{\sigma}_{vo} = 80.0$
3	5.55	25.88			31.43	
4	6.79	16.79	39.34		62.92	
5	6.88	19.49	30.35	38.00	94.72	
2	14.14				14.14	Linear elastic Slurry wall $\mu = 0.49$ $K_o = 0.5$ $E/\bar{\sigma}_{vo} = 80.0$
3	4.65	36.75			41.40	
4	7.07	14.73	52.91		74.71	
5	6.82	19.80	32.34	45.90	104.86	

FIGURE 3.4.8 STRUT LOADS WITH DIFFERENT WALLS

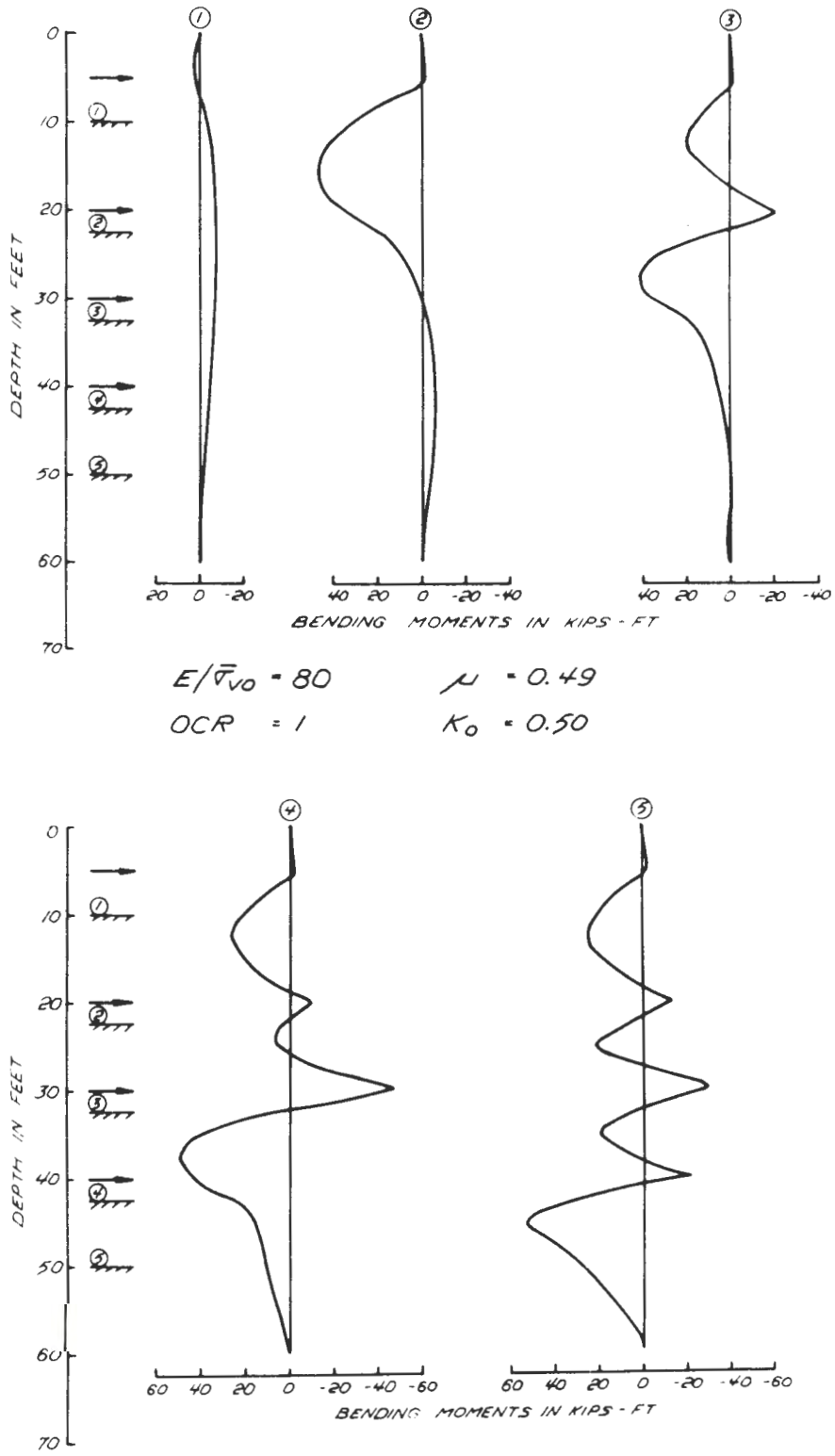

FIGURE 3.4.9 BENDING MOMENT IN SHEETING LINEARLY ELASTIC ANALYSIS

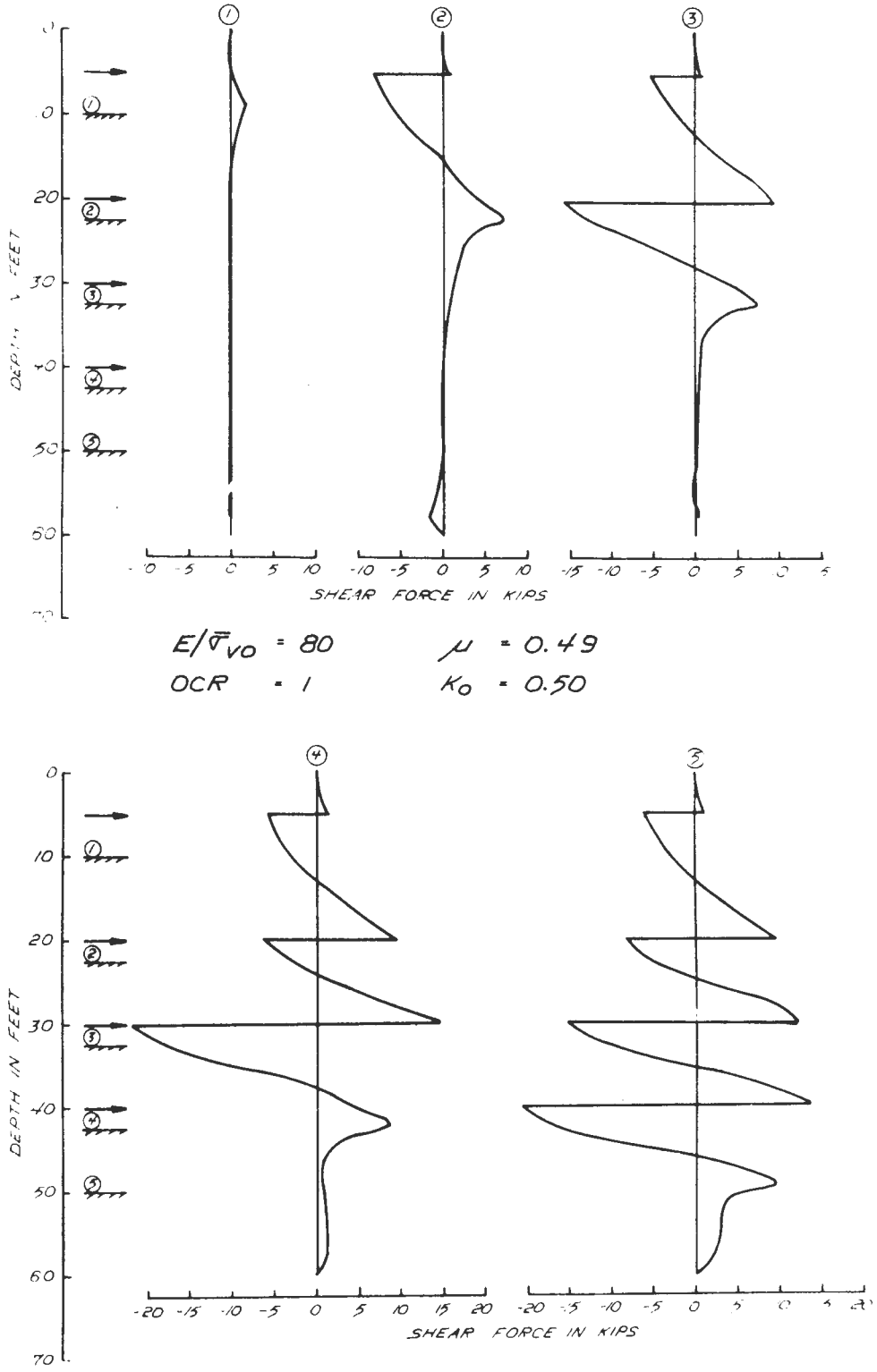

FIGURE 3.4.10 SHEAR FORCE IN SHEETING LINEARLY ELASTIC ANALYSIS

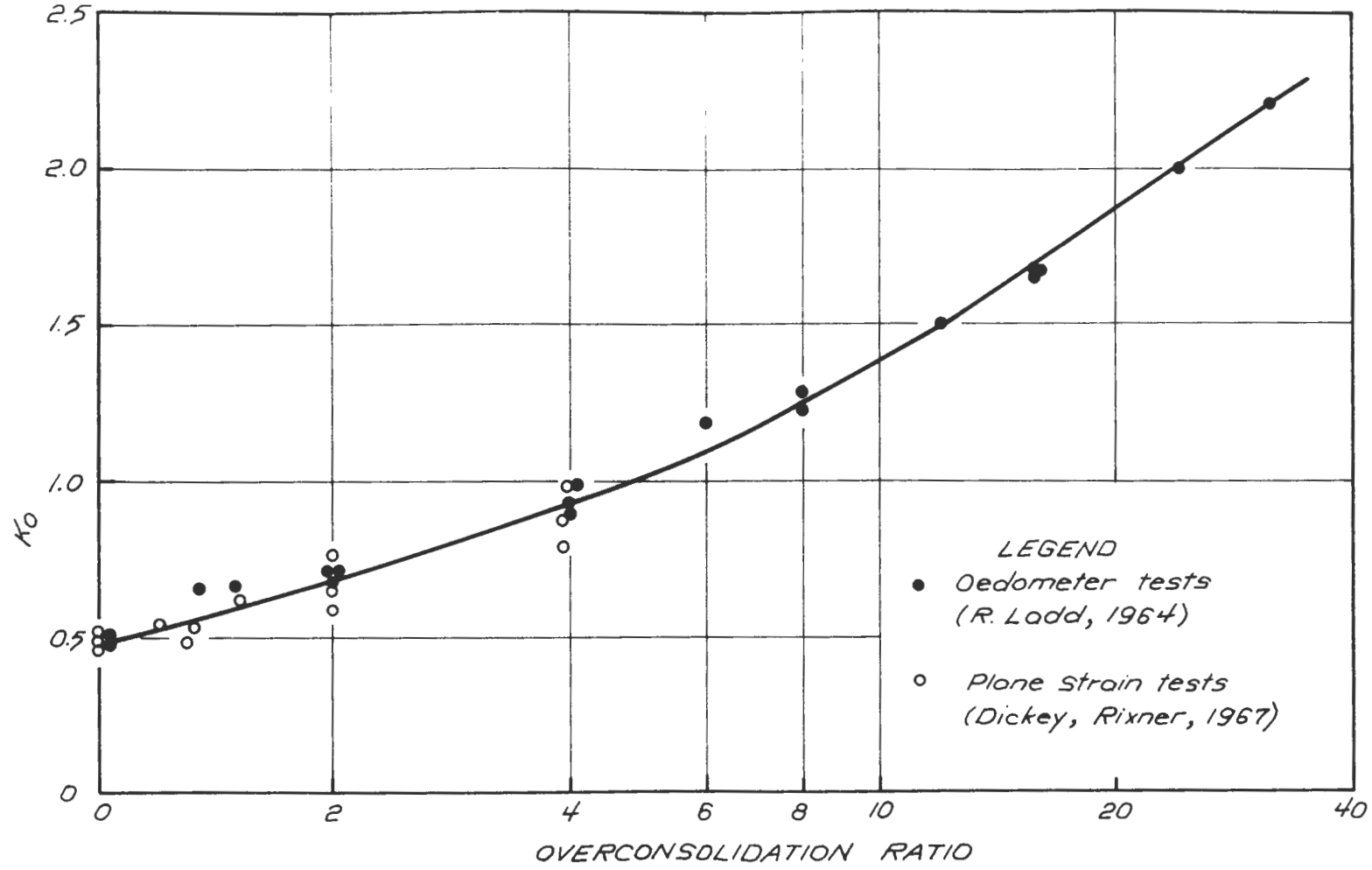

(After D'Appolonia and Lombe 1970)

FIGURE 3.5.1 K_o VS OVERCONSOLIDATION RATIO FOR BOSTON BLUE CLAY

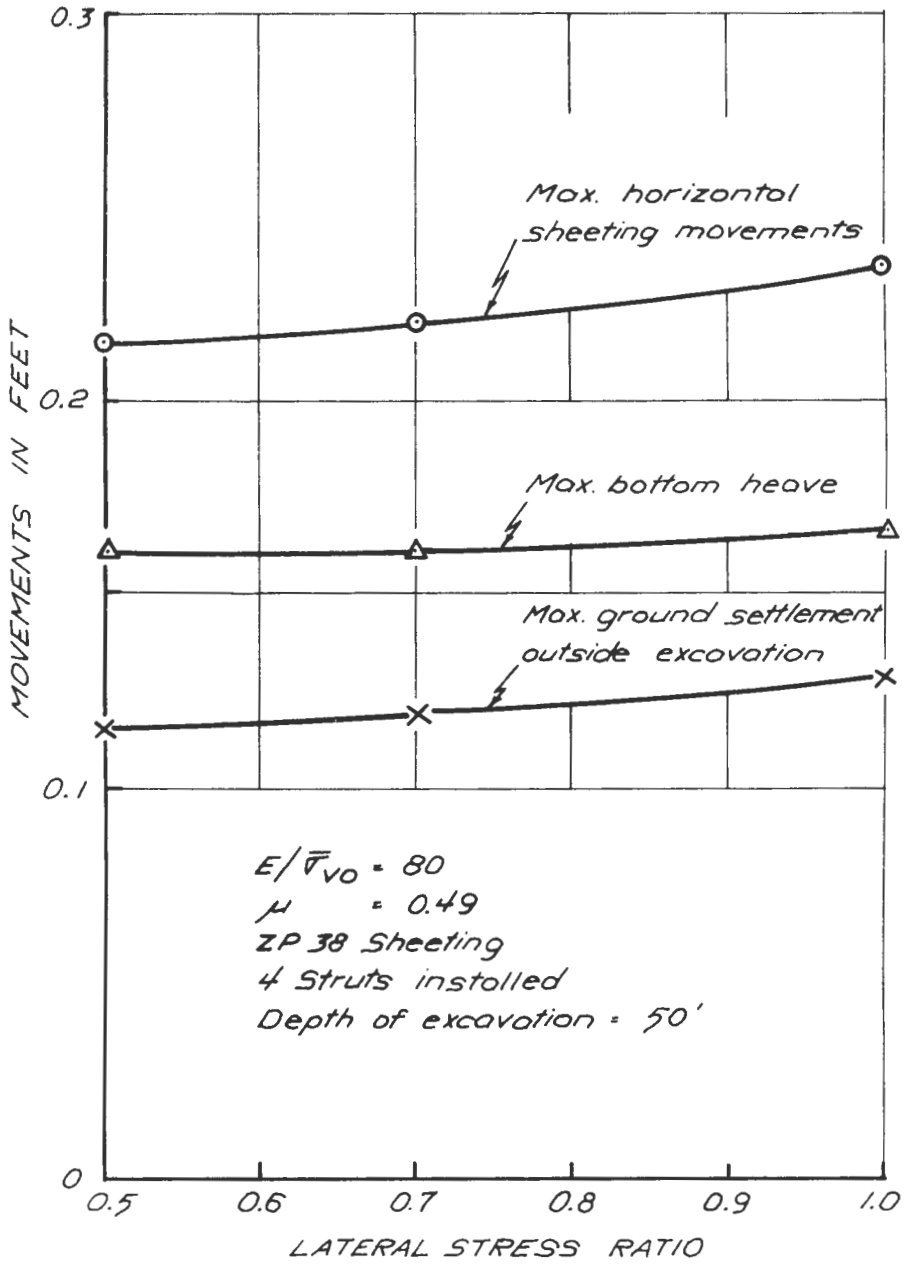

FIGURE 3.5.2 MOVEMENTS AT DIFFERENT OCR'S

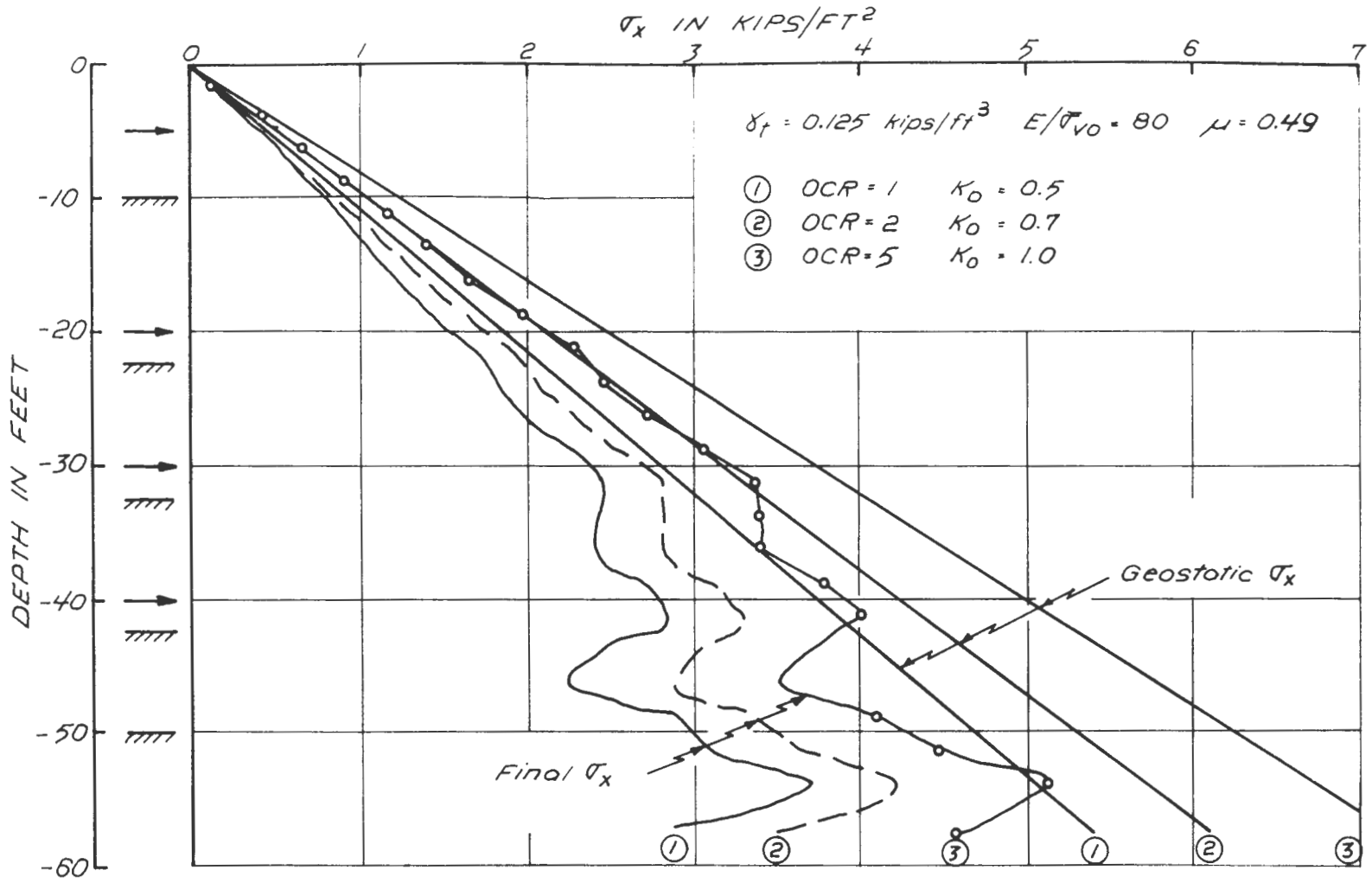

FIGURE 3.5.3 STRESSES ON SHEETING AT DIFFERENT OCR'S

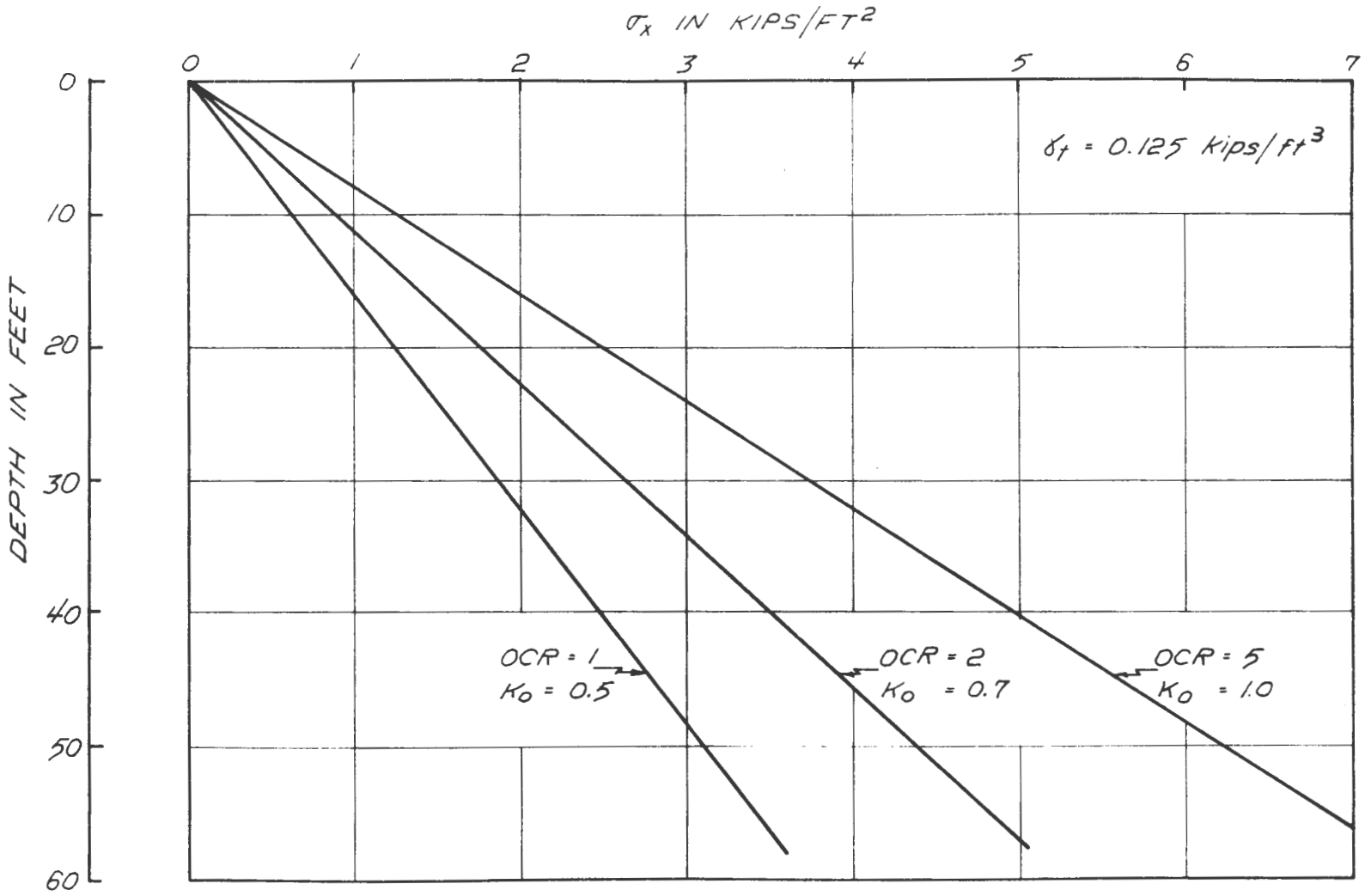

FIGURE 3.5.4 GEOSTATIC HORIZONTAL STRESSES IN DRY SOILS

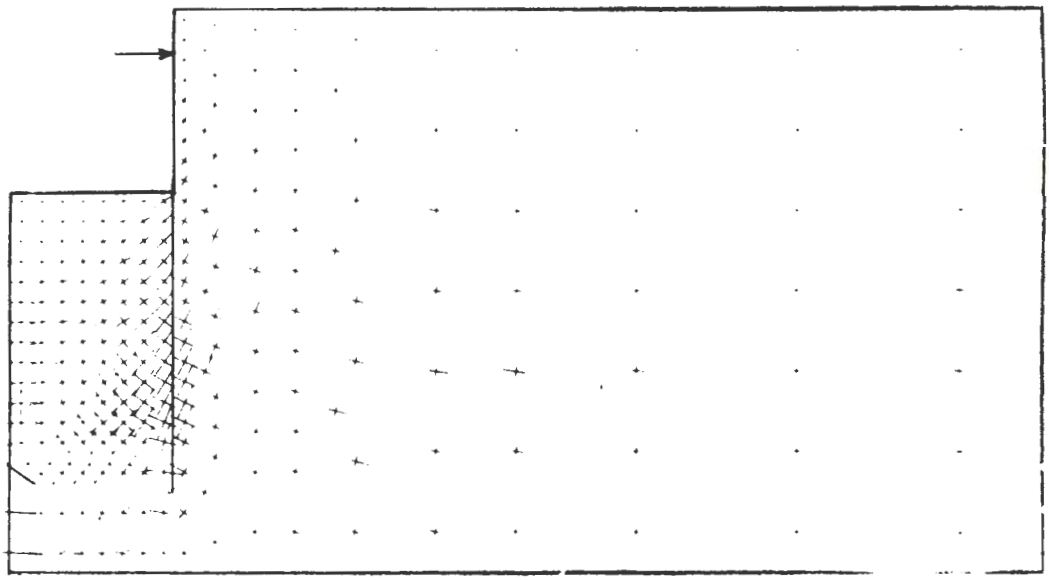

SECOND STAGE EXCAVATION D = 22.5 ft

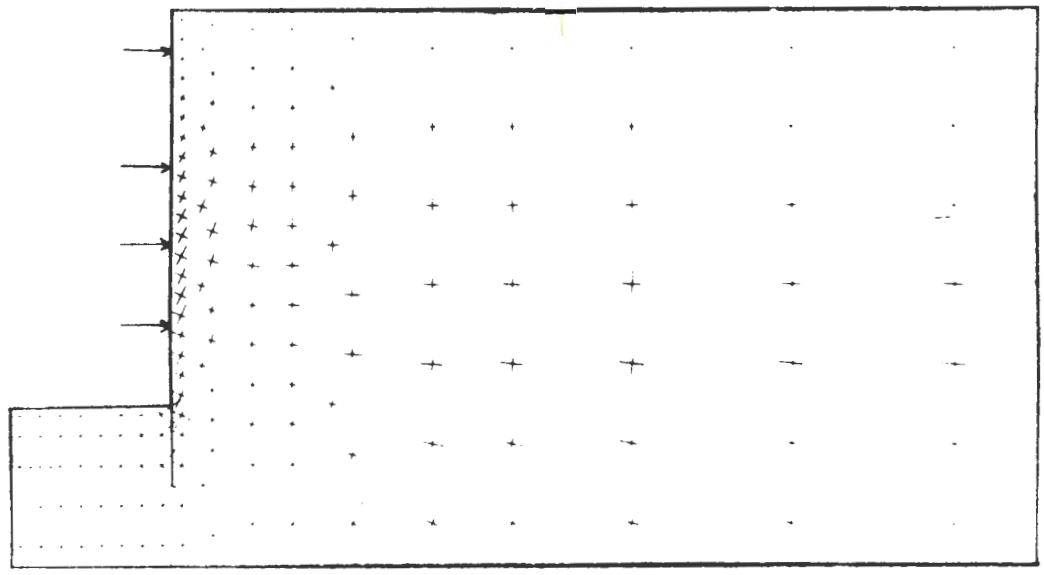

FIFTH STAGE EXCAVATION D = 50ft

ELASTIC ANALYSIS OCR = 2
$K_o = 0.7$ $\mu = 0.49$ $E/\overline{\sigma_{vo}} = 80$
ZP 38 SHEETING

FIGURE 3.5.5 ORIENTATION OF TOTAL PRINCIPAL STRESS
LINEARLY ELASTIC ANALYSIS OCR = 2

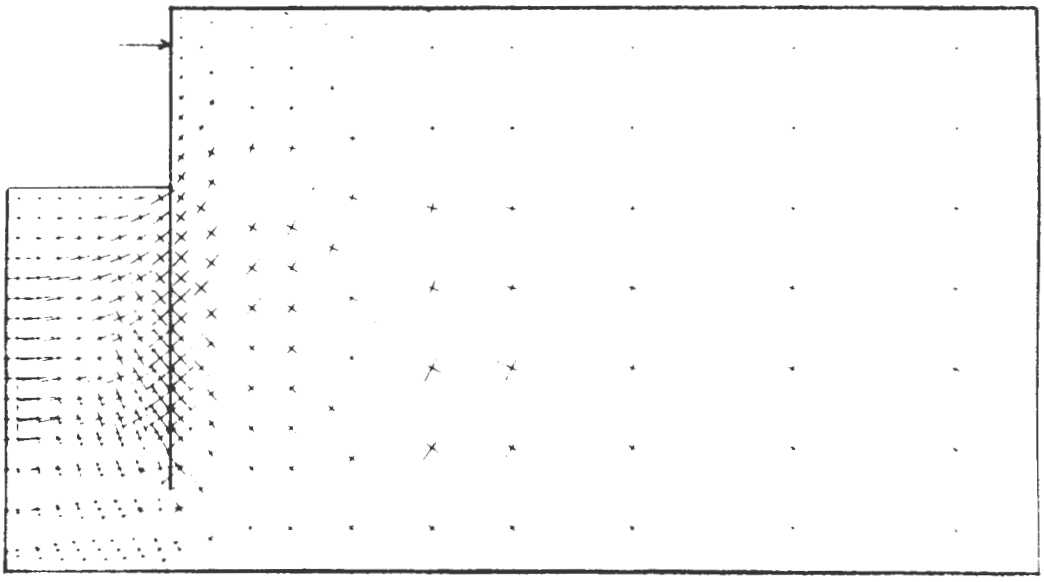

SECOND STAGE EXCAVATION D=22.5 ft

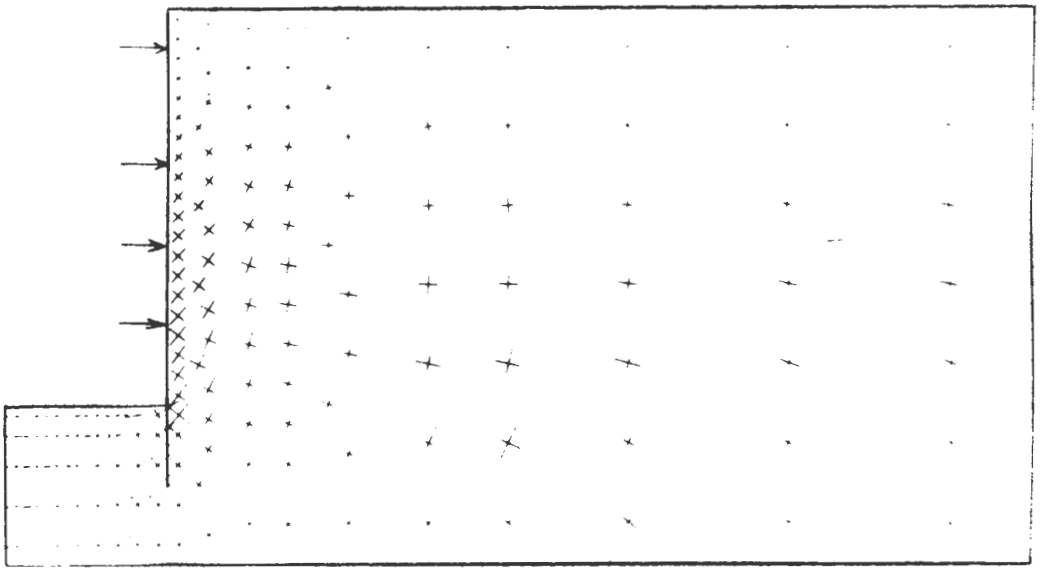

FIFTH STAGE EXCAVATION D=50 ft

ELASTIC ANALYSIS OCR=5
$K_o = 1.0$ $\mu = 0.49$ $E/\bar{\sigma}_{vo} = 80$
ZP 38 SHETTING

FIGURE 3.5.6 ORIENTATION OF TOTAL PRINCIPAL STRESSES
LINEARLY ELASTIC ANALYSIS OCR = 5

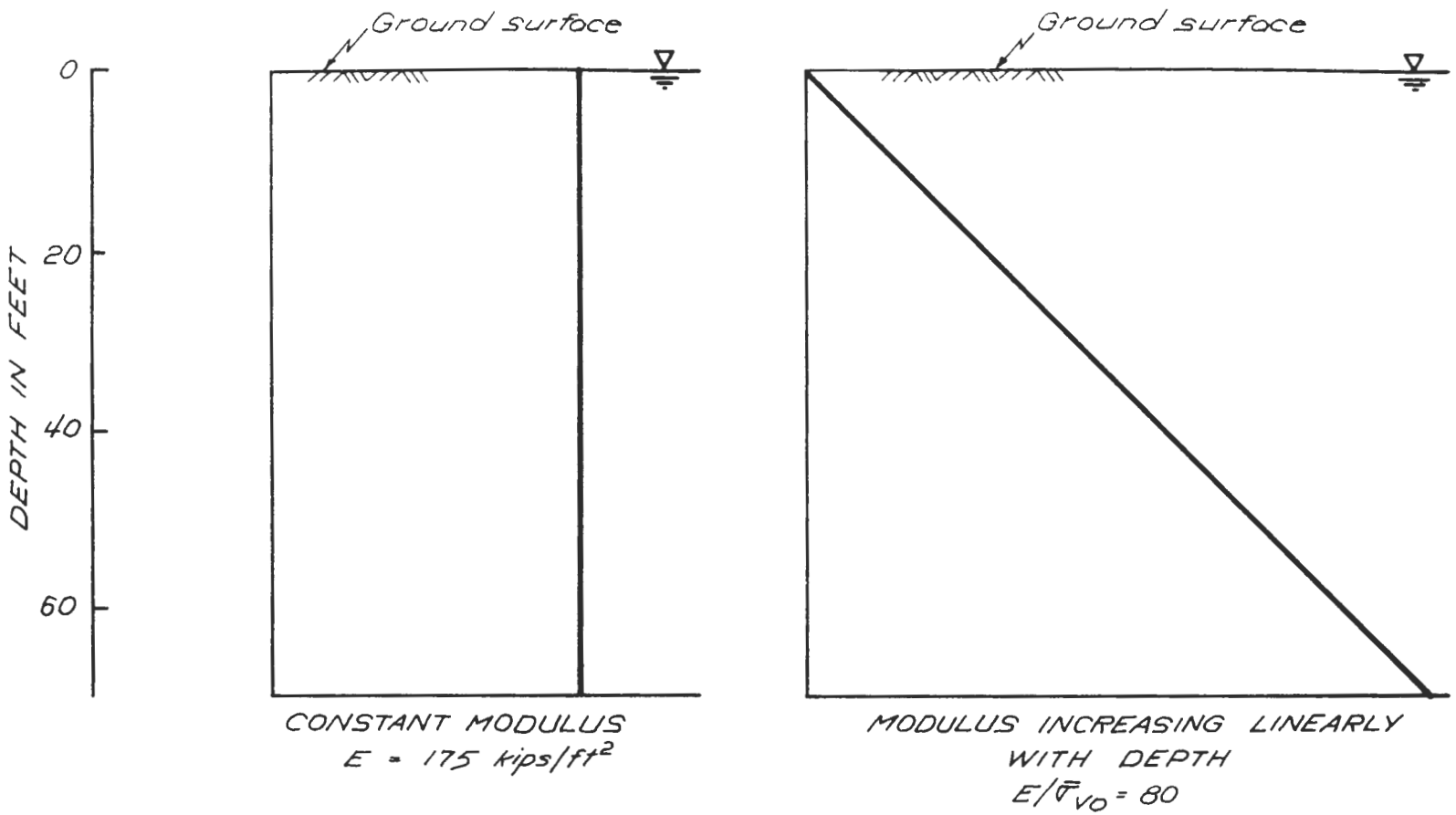

FIGURE 3.6.1 MODULUS VARIATIONS FOR LINEARLY ELASTIC ANALYSES

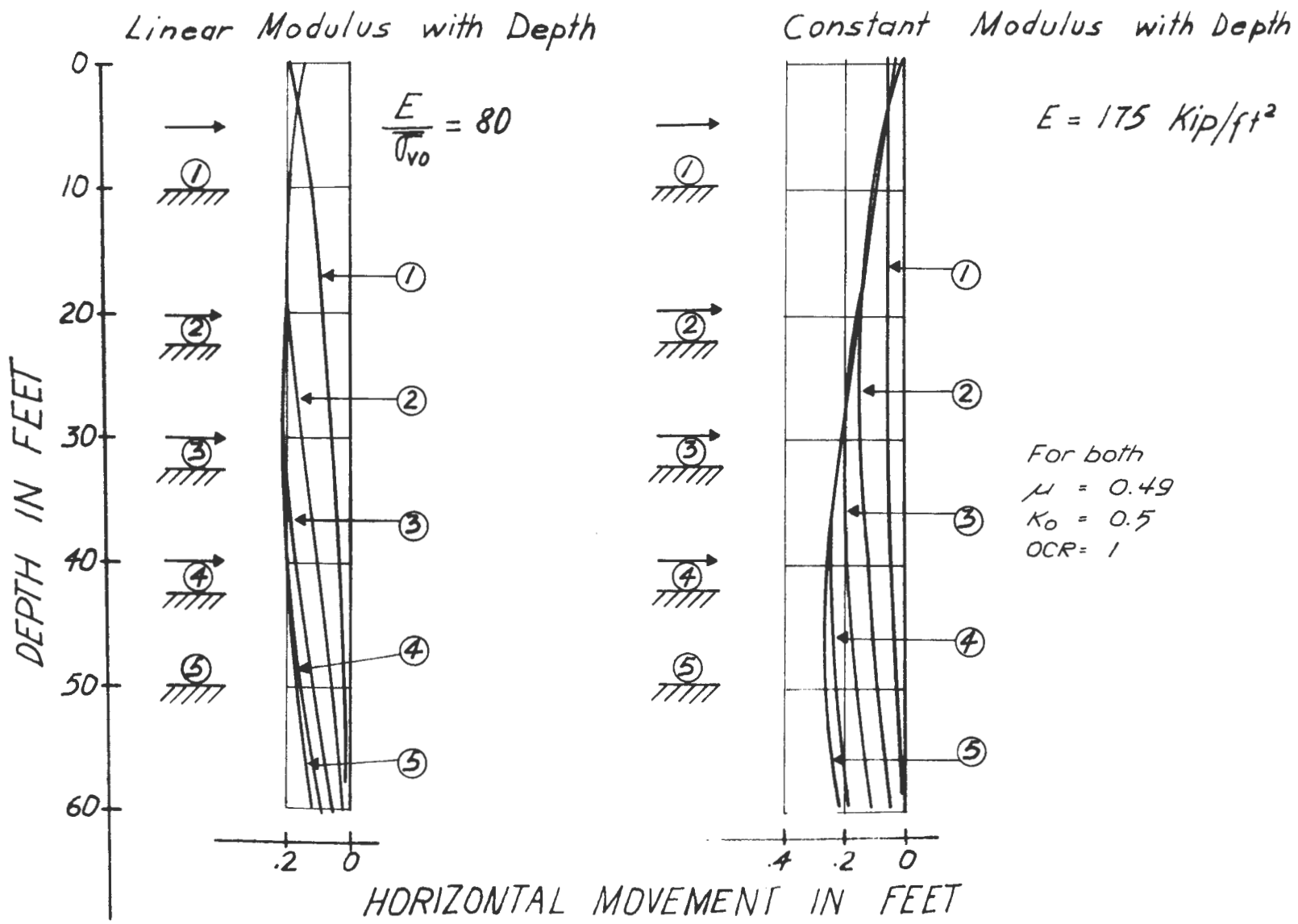

FIGURE 3.6.2 SHEETING MOVEMENT WITH DIFFERENT MODULUS VARIATIONS

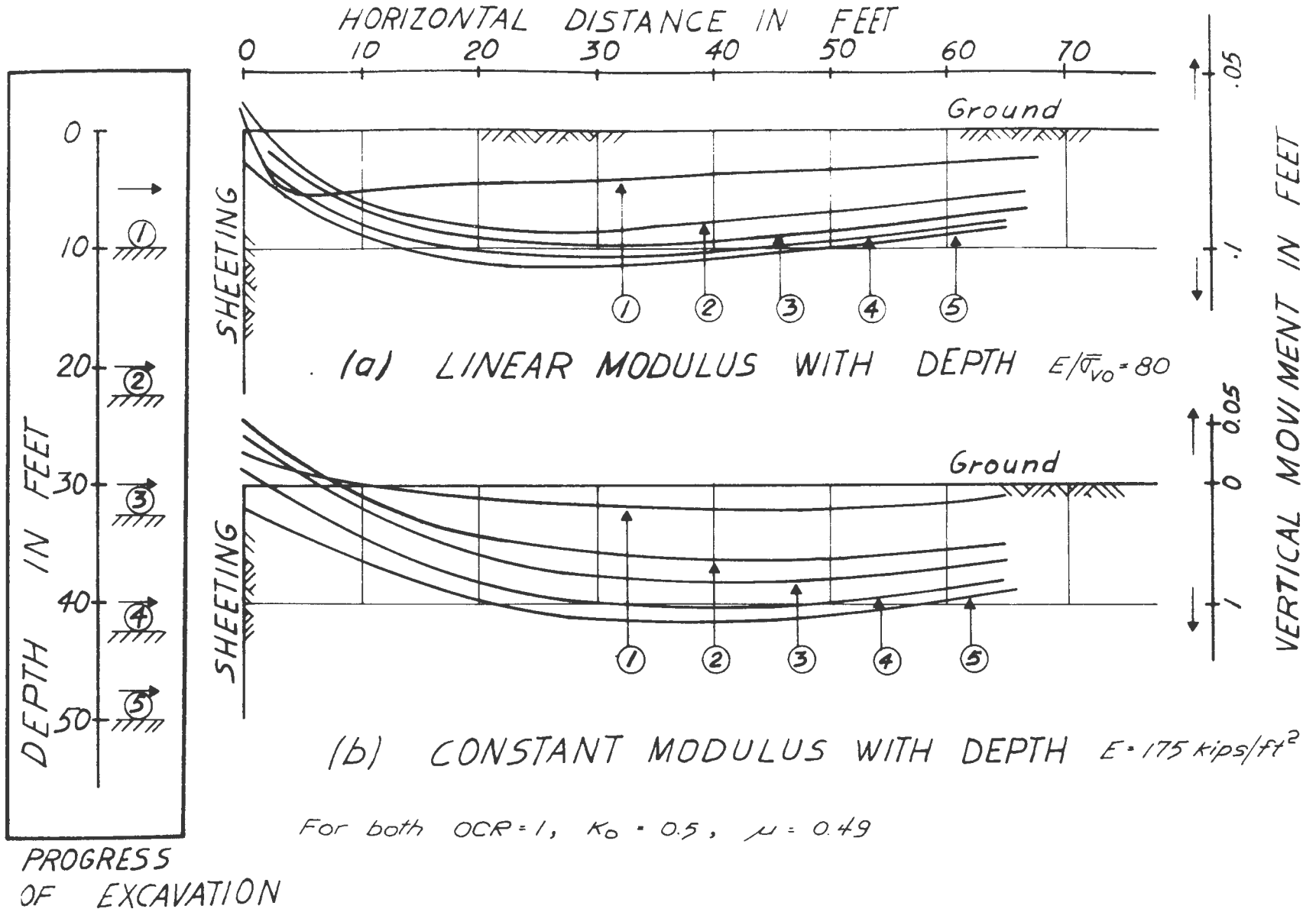

FIGURE 3.6.3 GROUND SETTLEMENT WITH DIFFERENT MODULUS VARIATIONS

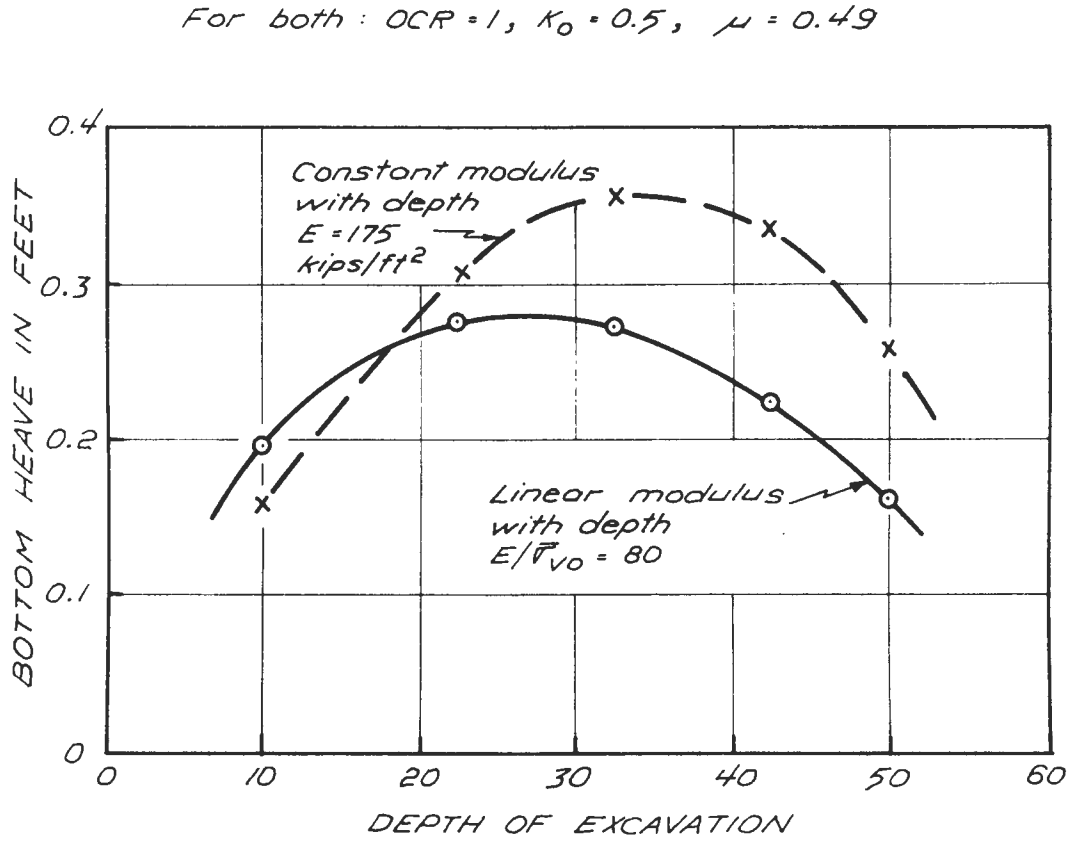

FIGURE 3.6.4 BOTTOM HEAVE WITH DIFFERENT MODULUS VARIATIONS

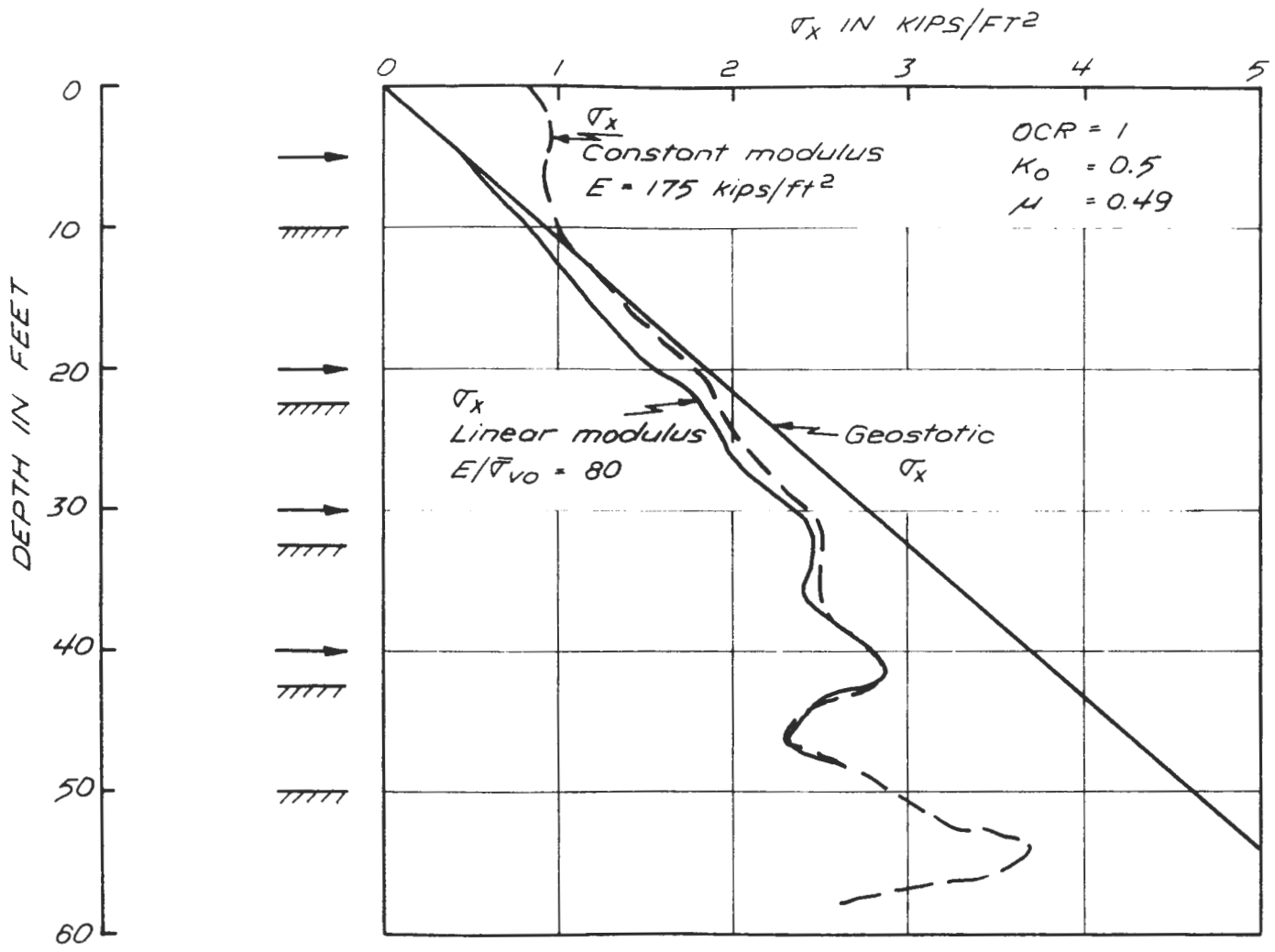

FIGURE 3.6.5 HORIZONTAL STRESS ON WALL ELASTIC ANALYSIS

STAGE	LOAD IN STRUT, kips/ft				TOTAL LOAD kips/ft	COMMENTS
	S1	S2	S3	S4		
2	8.76				8.76	Linear elostic ZP38 Sheeting $\mu = 0.49$ $K_o = 0.5$ $E/\bar{\sigma}_{vo} = 80.0$
3	5.55	25.88			31.43	
4	6.79	16.79	39.34		62.92	
5	6.88	19.49	30.35	38.00	94.72	
2	12.71				12.71	Linear elostic ZP38 Sheeting $\mu = 0.49$ $K_o = 0.5$ Constant modulus with depth, $E = 175$ kips/ft^2
3	9.58	29.48			39.06	
4	11.93	19.61	41.97		73.51	
5	12.92	22.45	31.87	38.53	105.77	

FIGURE 3.6.6 STRUT LOADS WITH DIFFERENT MODULUS VARIATIONS

CASE	MODULUS RATIO $E/\bar{\sigma}_{vo}$	MAX. MOVEMENTS IN FEET		MAX. MOVEMENTS OF CASE I OBTAINED FROM CASE II BY PROPORTIONALITY	
		SETTLEMENT	SHEETING MOVEMENT	SETTLEMENT	SHEETING MOVEMENT
I	80	0.1166	0.2156	0.1292	0.2388
II	300	0.0345	0.0637		

$\mu = 0.49$ $K_o = 0.5$ OCR = 1 $\gamma_t = 0.125$ kips/ft^3 D = 50 ft
ZP38 Sheeting

FIGURE 3.7.1 INFLUENCE OF SOIL STIFFNESS ON MOVEMENTS NEAR EXCAVATION

STAGE	LOAD IN STRUT - kips/ft				TOTAL LOAD kips/ft	COMMENTS
	S1	S2	S3	S4		
2	8.76				8.76	Linear elastic ZP 38 Sheeting μ = 0.49 K_o = 0.5 $E/\bar{\sigma}_{vo}$ = 80 OCR = 1
3	5.55	25.88			31.43	
4	6.79	16.79	39.34		62.92	
5	6.88	19.49	30.35	38.00	94.72	
2	6.4				6.4	Linear elastic ZP 38 sheeting μ = 0.49 K_o = 0.5 $E/\bar{\sigma}_{vo}$ = 300 OCR = 1
3	5.18	19.80			24.98	
4	6.01	16.01	28.32		50.34	
5	6.25	17.70	24.33	27.82	76.10	

FIGURE 3.7.2 STRUT LOADS WITH DIFFERENT MODULI

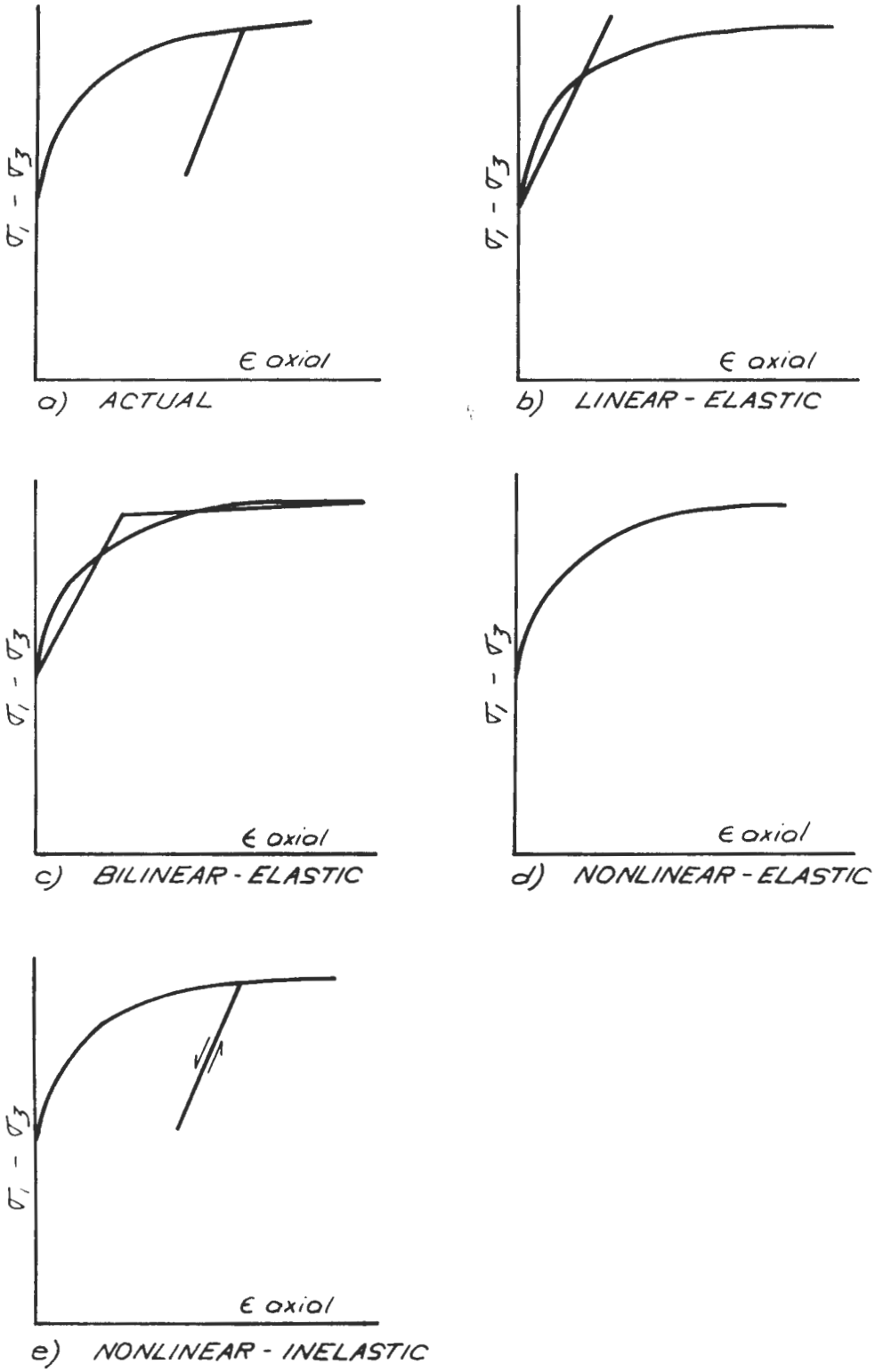

FIGURE 4.2.1 TIME INDEPENDENT IDEALIZATIONS OF STRESS-STRAIN BEHAVIOR OF SOILS

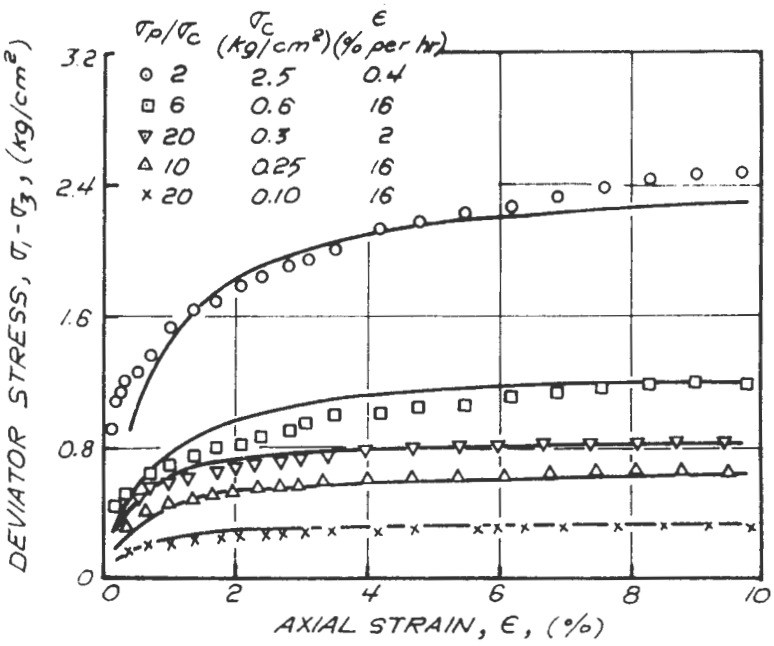

FIGURE 4.2.2 COMPARISON OF HYPERBOLIC PREDICTION EQUATION AND MEASURED RESPONSE FOR VARIOUS CONDITIONS (After Kondner, 1963)

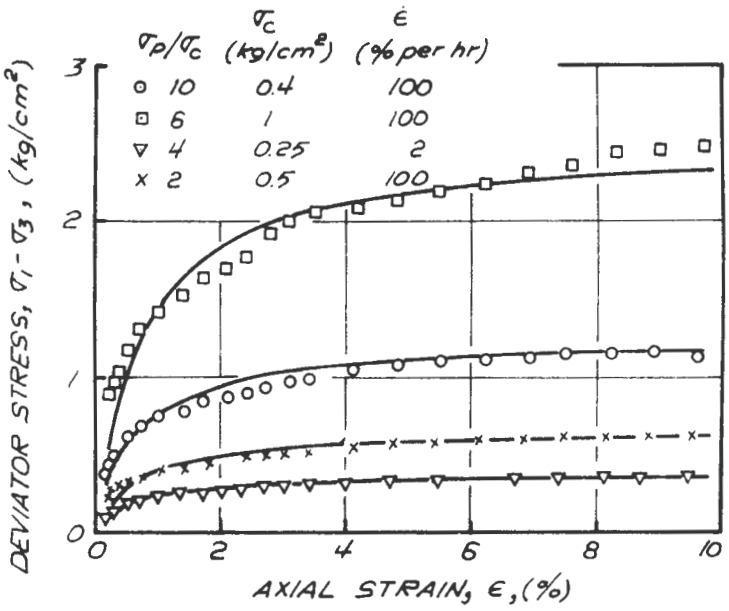

FIGURE 4.2.3 COMPARISON OF HYPERBOLIC PREDICTION EQUATION AND MEASURED RESPONSE FOR VARIOUS CONDITIONS (After Kondner 1963)

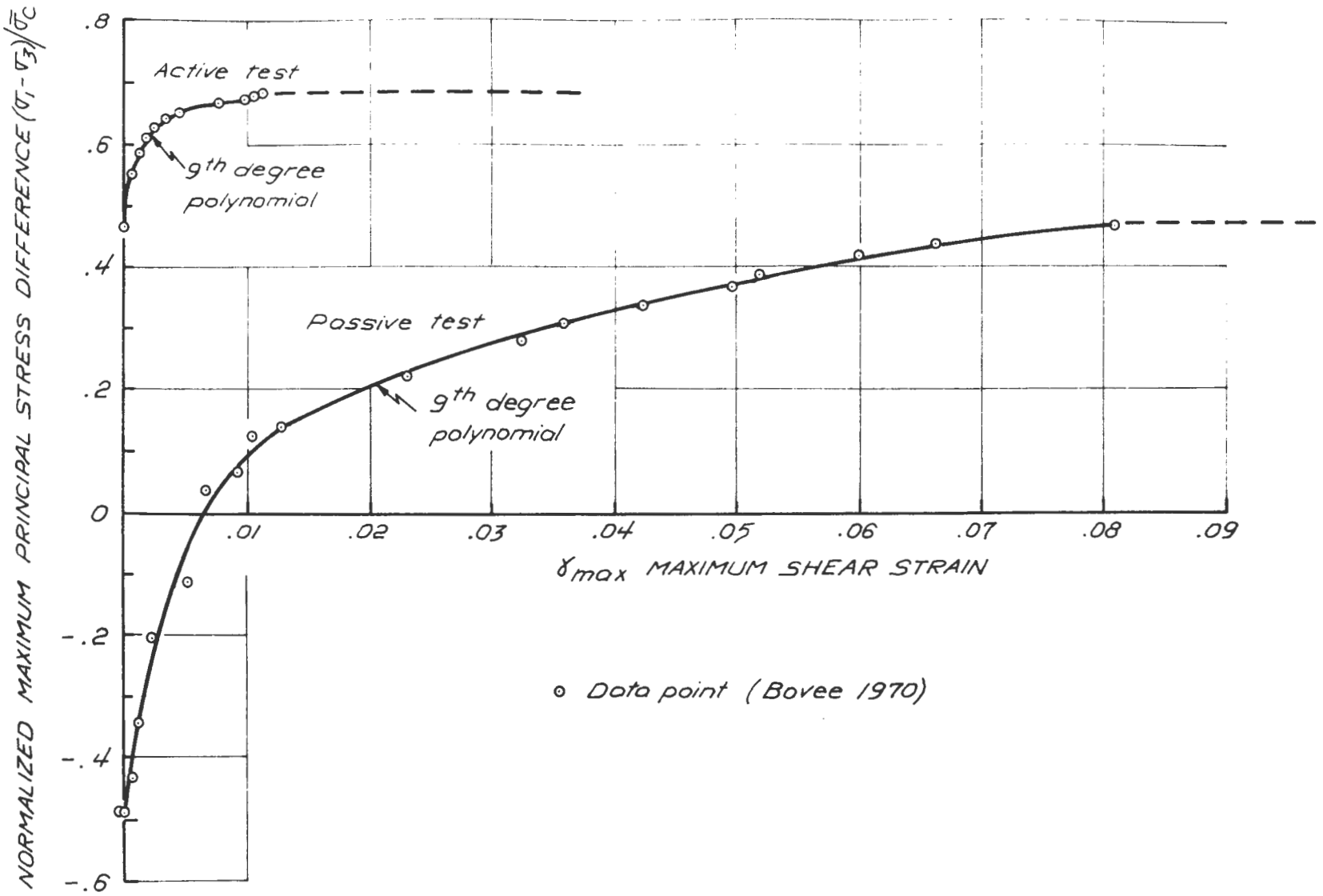

FIGURE 4.2.4 POLYNOMIAL APPROXIMATIONS OF STRESS-STRAIN BEHAVIOR
OCR = 1

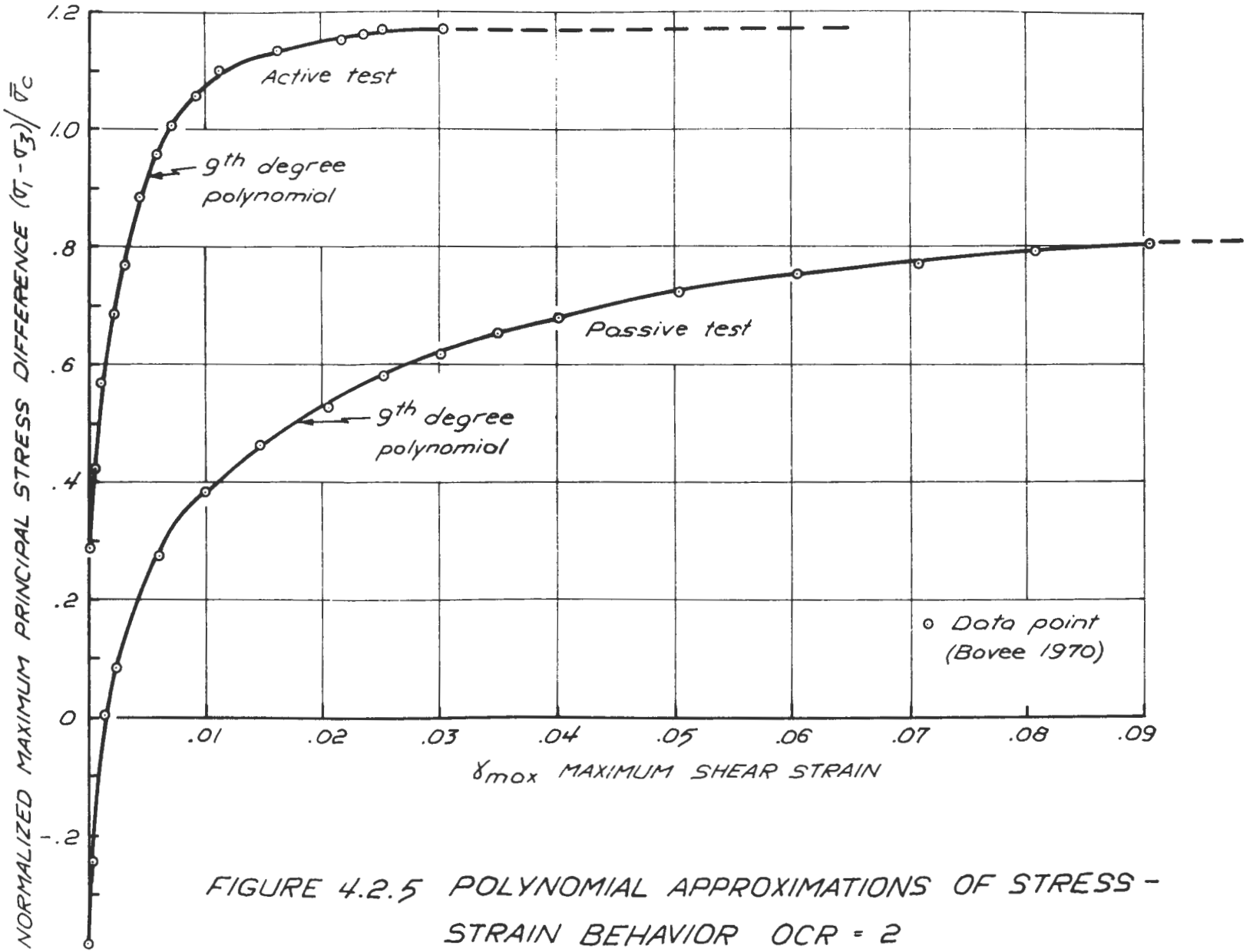

FIGURE 4.2.5 POLYNOMIAL APPROXIMATIONS OF STRESS-STRAIN BEHAVIOR OCR = 2

OCR	$S_u/\bar{\sigma}_{vo}$	K_o	μ	$E/\bar{\sigma}_{vo}$	$E^\circ/\bar{\sigma}_{vo}$
1	0.342	0.5	0.49	300	0.3
2	0.57	0.7	0.49	300	0.3
5	0.9	1.0	0.49	300	0.3
25	1.4 *	2.0	0.49	300	0.3

* Only 75% of full strength to account for loss with time.
Bulk modulus unchanged during yielding
E° = Young's modulus after yielding

FIGURE 4.3.1 SOIL PROPERTIES USED IN BILINEARLY ELASTIC ANALYSIS

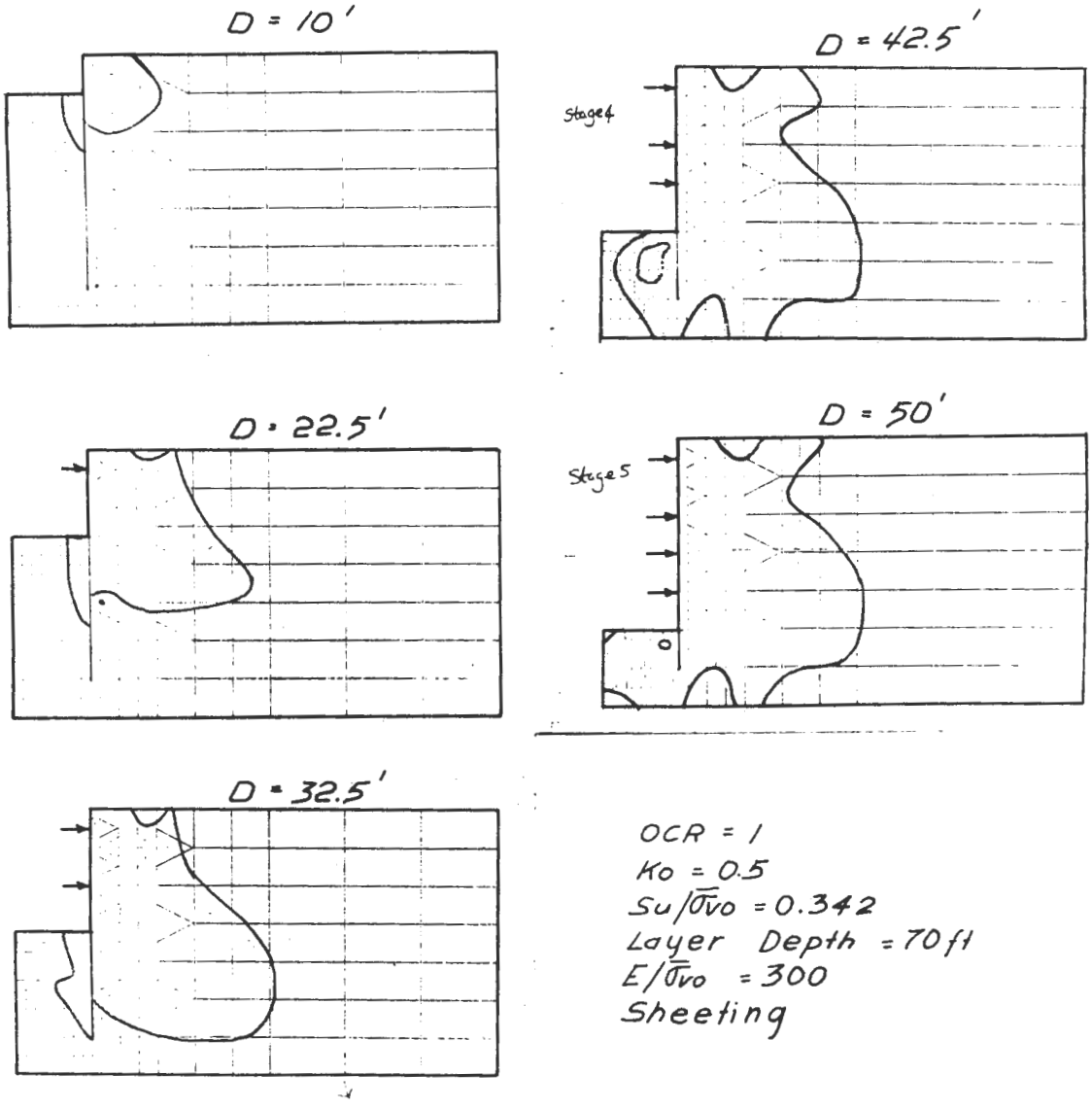

FIGURE 4.3.2 DEVELOPMENT OF YIELDED ZONES DURING EXCAVATION OCR = 1 WITH SHEETING

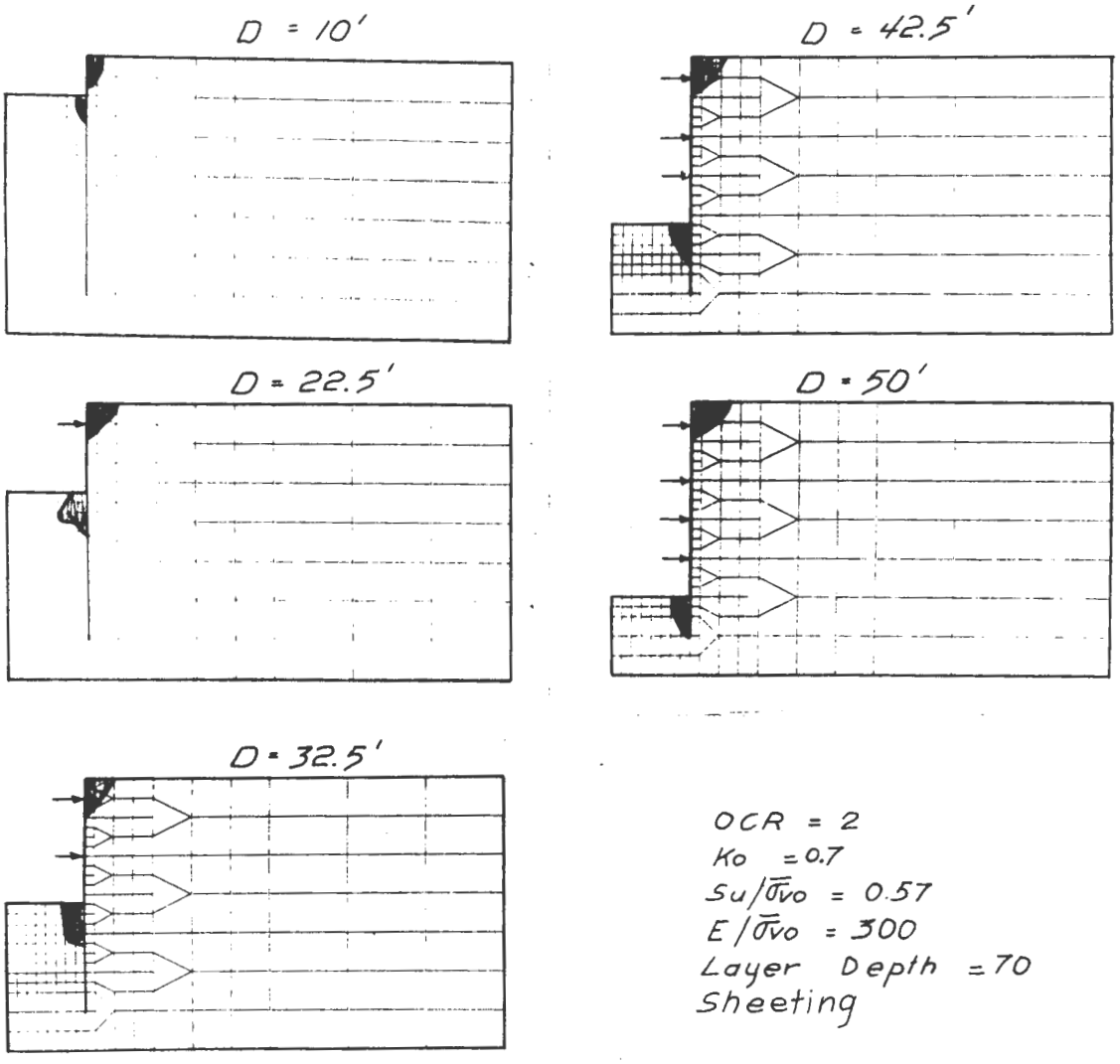

FIGURE 4.3.3 DEVELOPMENT OF YIELDED ZONES DURING EXCAVATION OCR = 2 WITH SHEETING

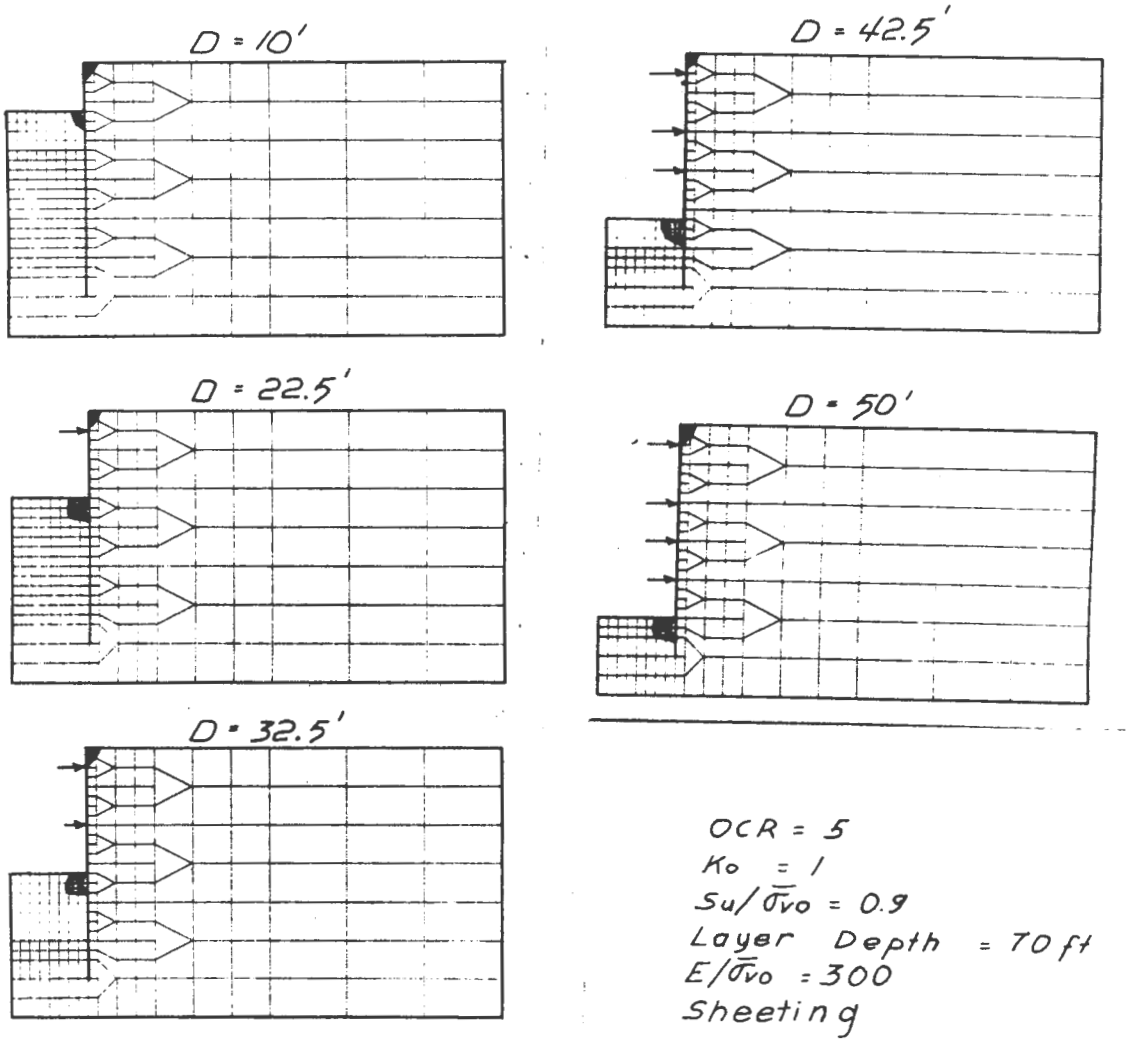

FIGURE 4.3.4 DEVELOPMENT OF YIELDED ZONES DURING EXCAVATION OCR = 5 WITH SHEETING

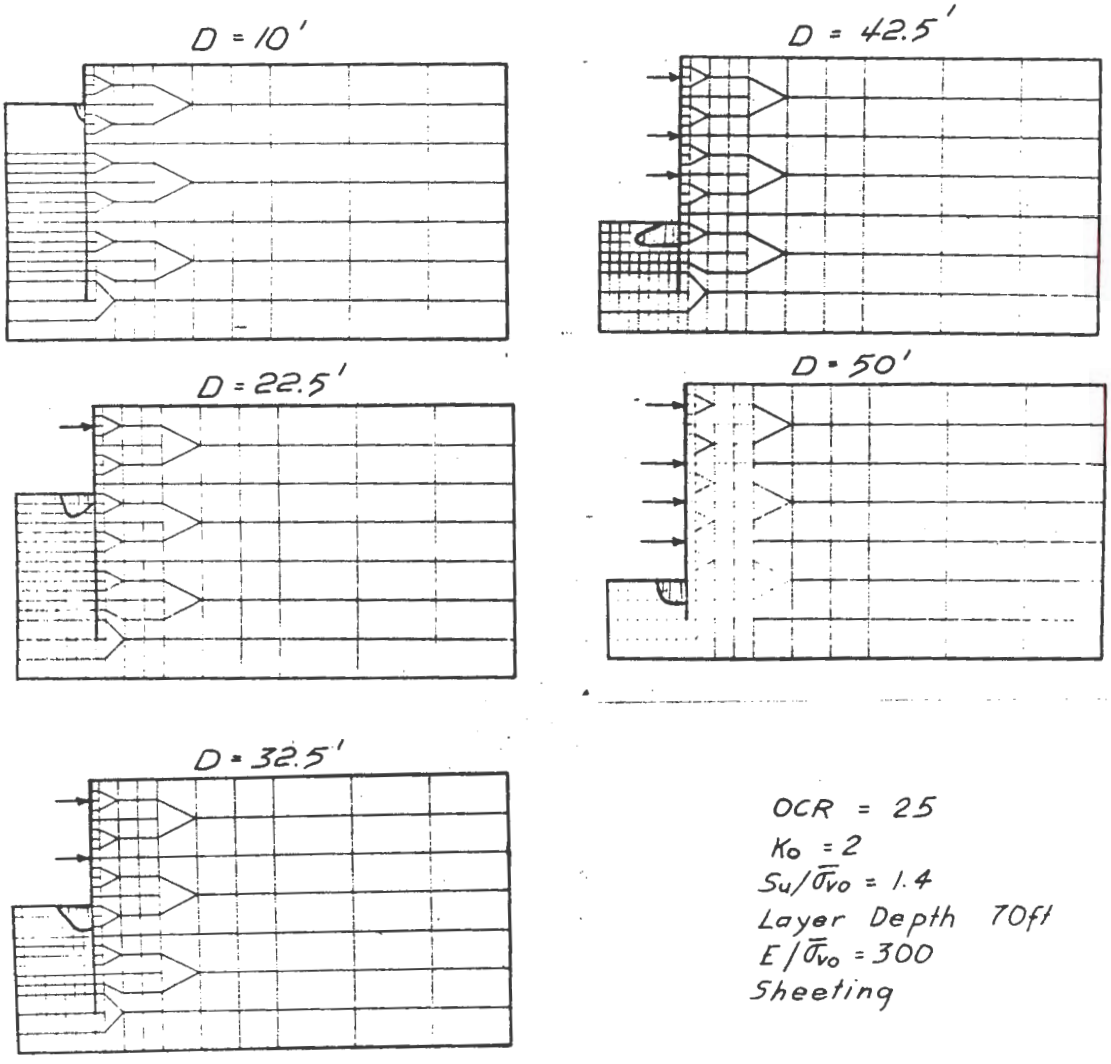

FIGURE 4.3.5 DEVELOPMENT OF YIELDED ZONES DURING EXCAVATION OCR = 25 WITH SHEETING

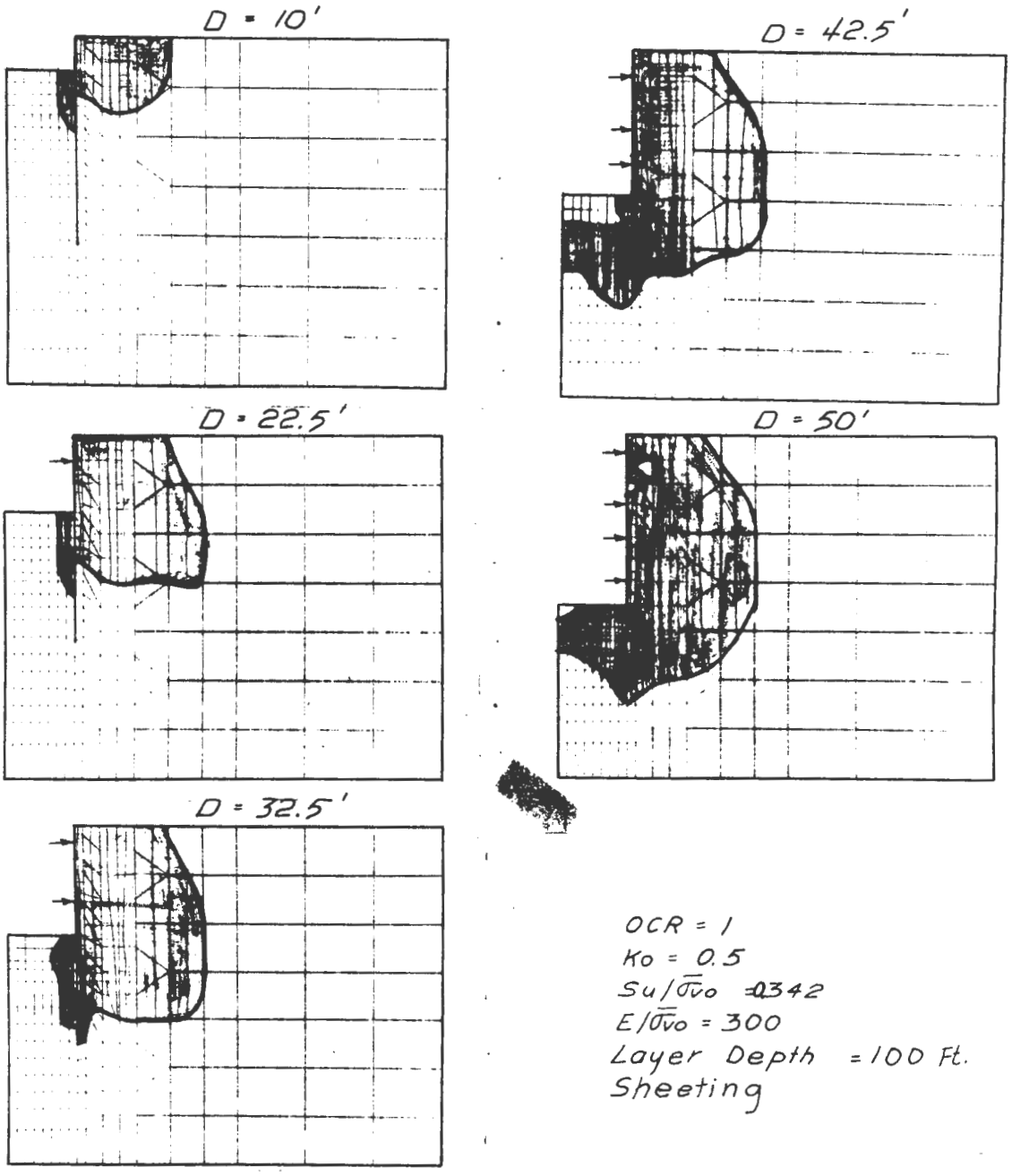

FIGURE 4.3.6 DEVELOPMENT OF YIELDED ZONES IN THICK LAYER DURING EXCAVATION OCR = 1

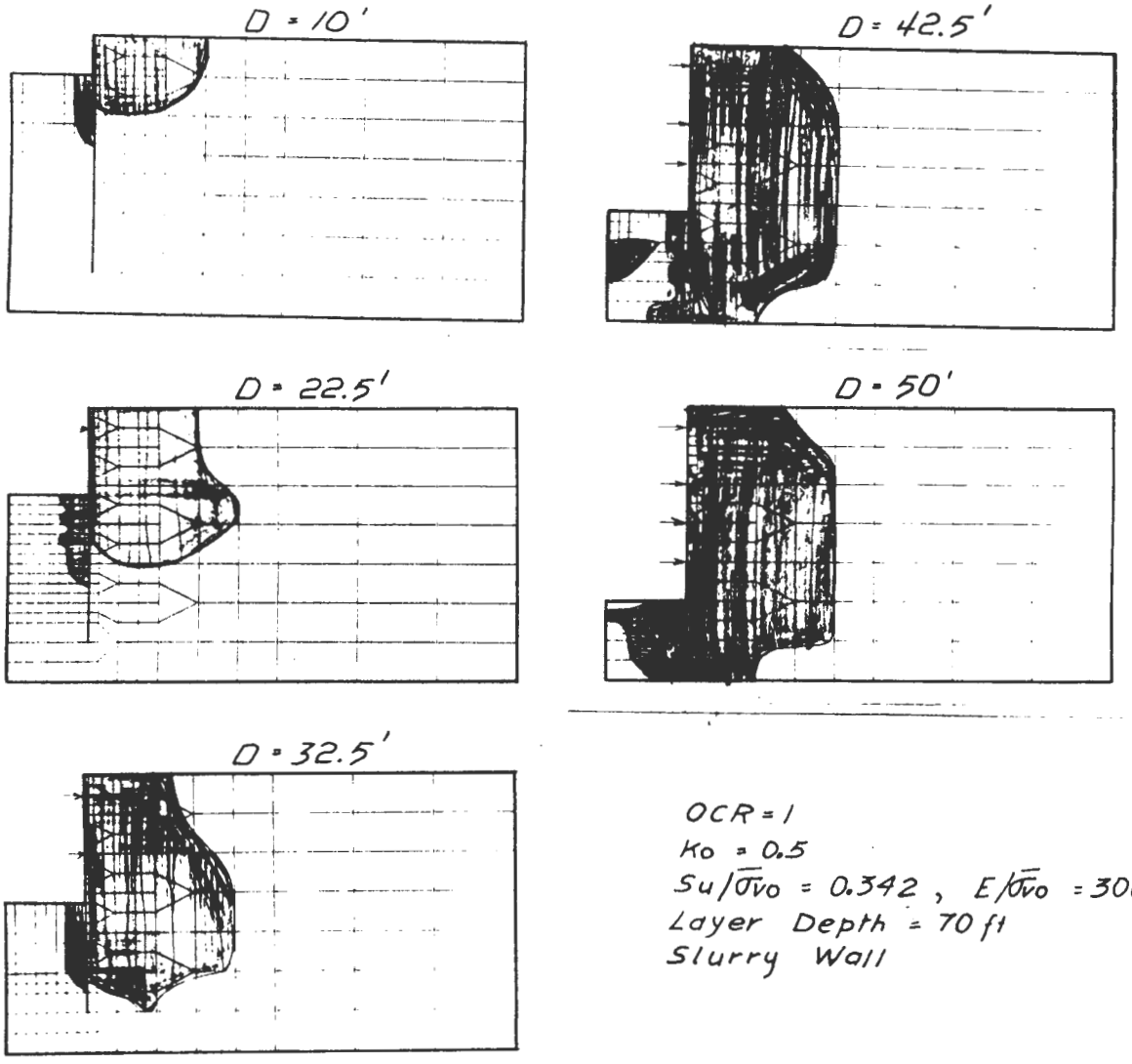

FIGURE 4.3.7 DEVELOPMENT OF YIELDED ZONES DURING EXCAVATION OCR = 1 WITH SLURRY WALL

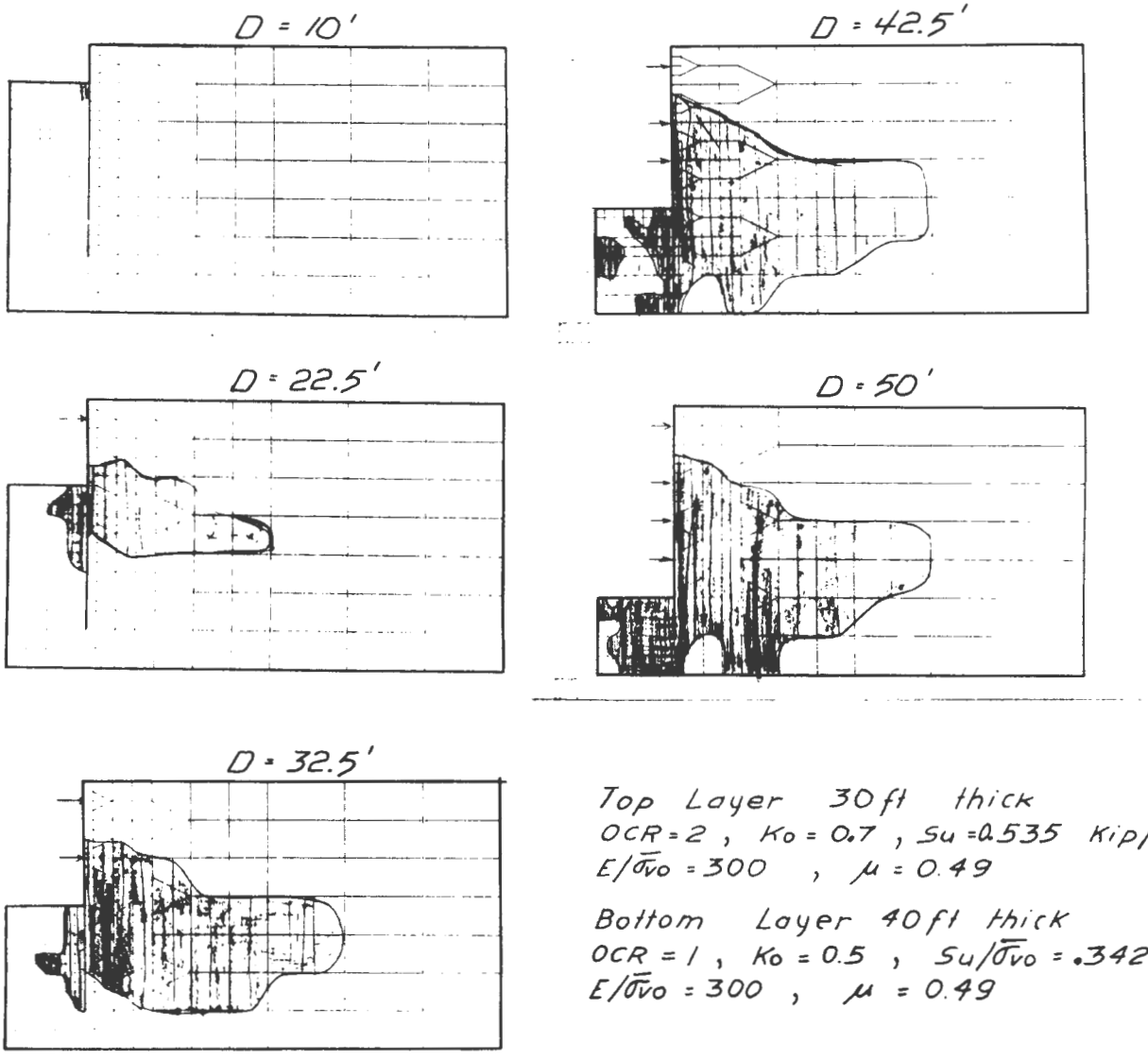

FIGURE 4.3.8 DEVELOPMENT OF YIELDED ZONES DURING EXCAVATION OCR = 1 WITH STIFF CRUST AND SHEETING

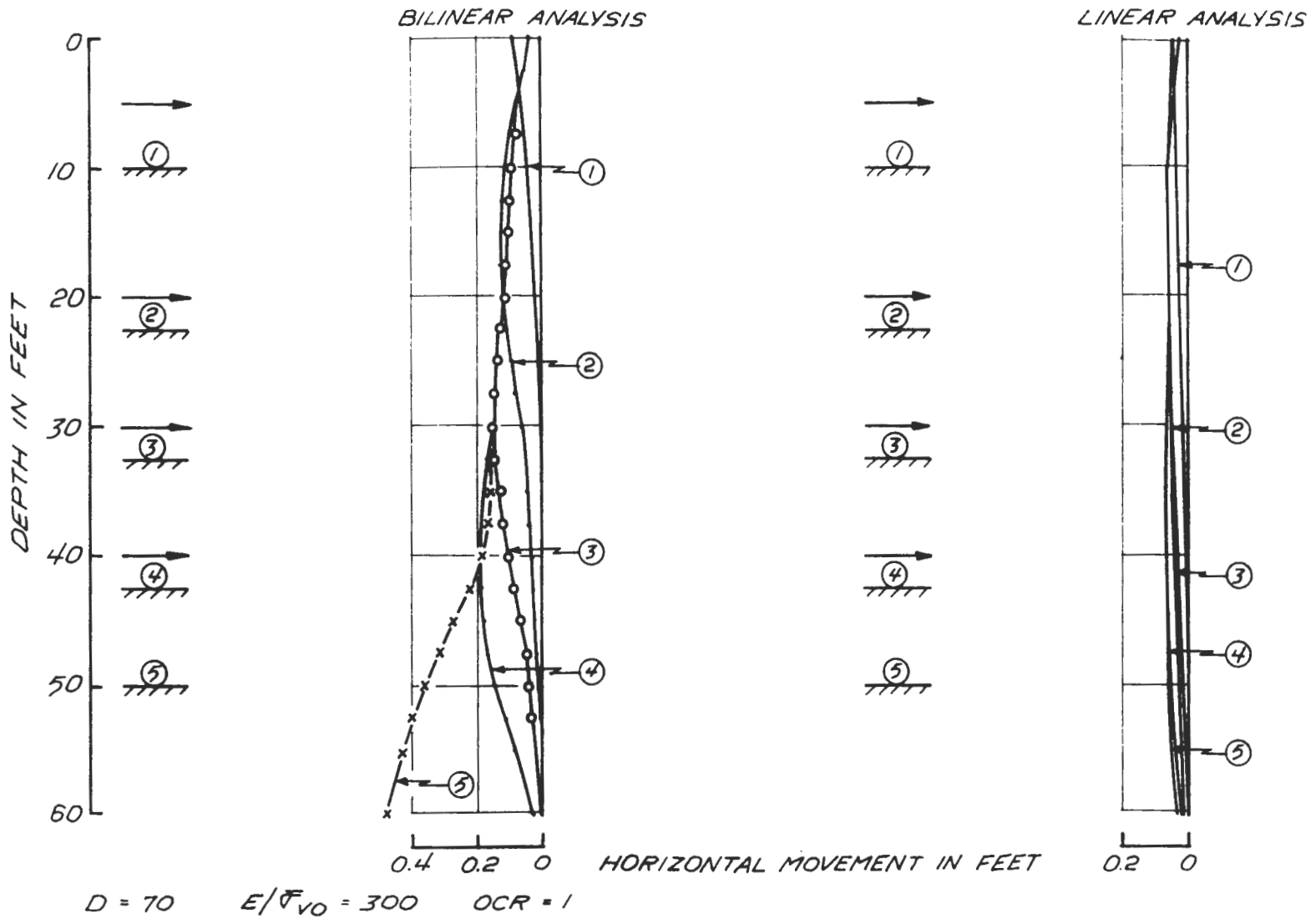

FIGURE 4.3.9 WALL MOVEMENTS LINEAR AND BILINEAR ANALYSES OCR = 1

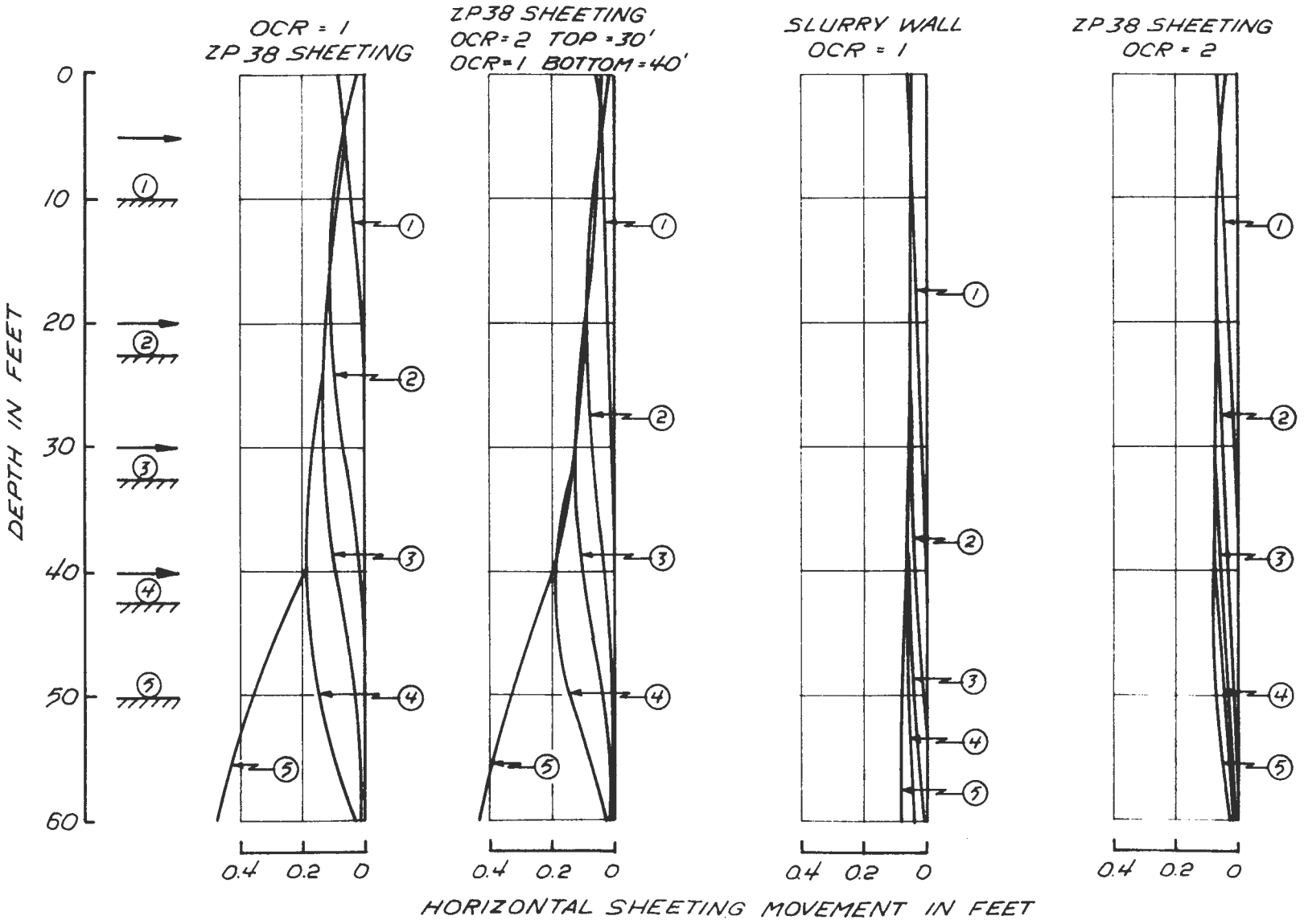

FIGURE 4.3.10 WALL MOVEMENTS FROM BILINEAR ANALYSIS

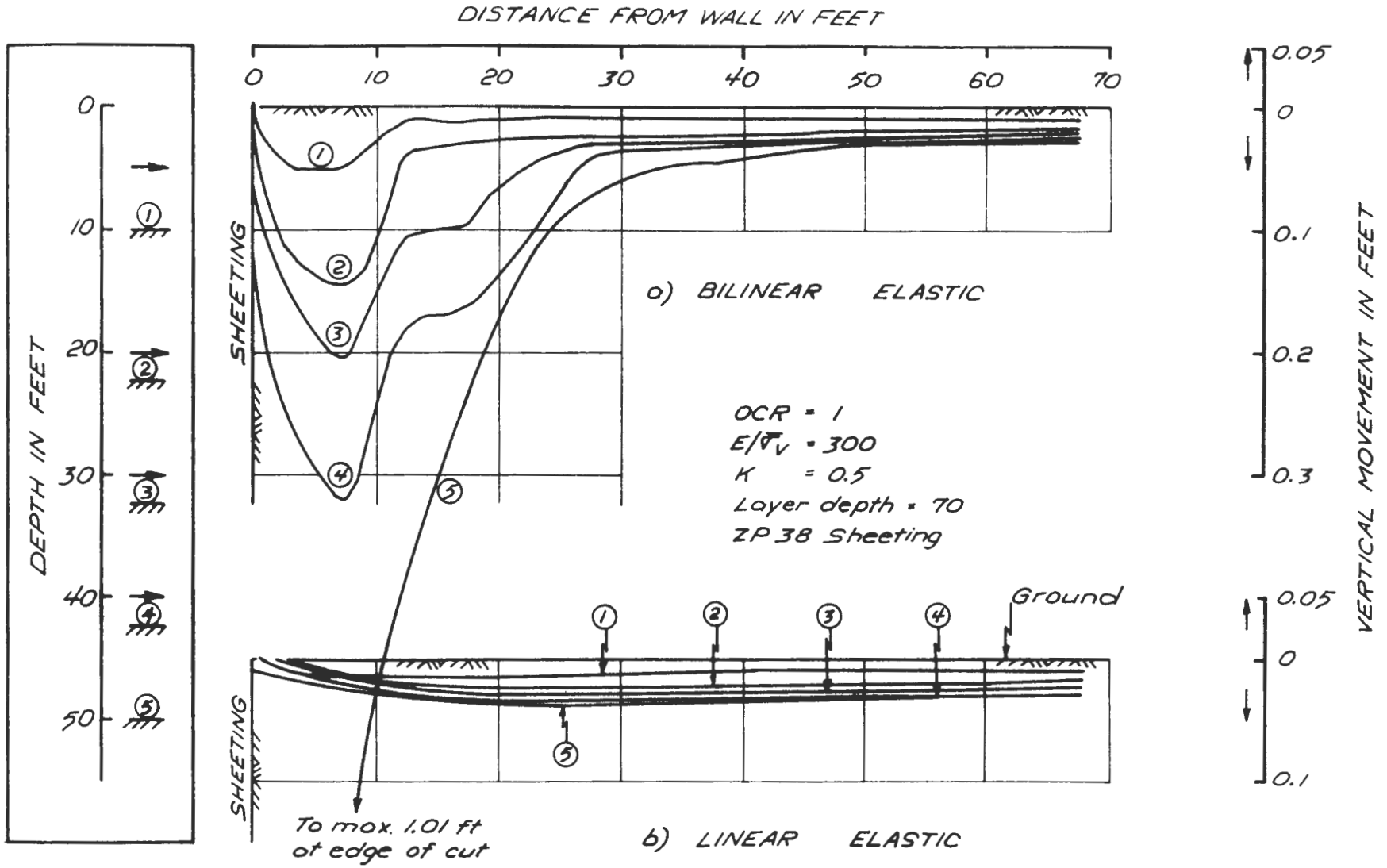

FIGURE 4.3.11 GROUND SETTLEMENT FROM LINEAR AND BILINEAR ANALYSES OCR=1

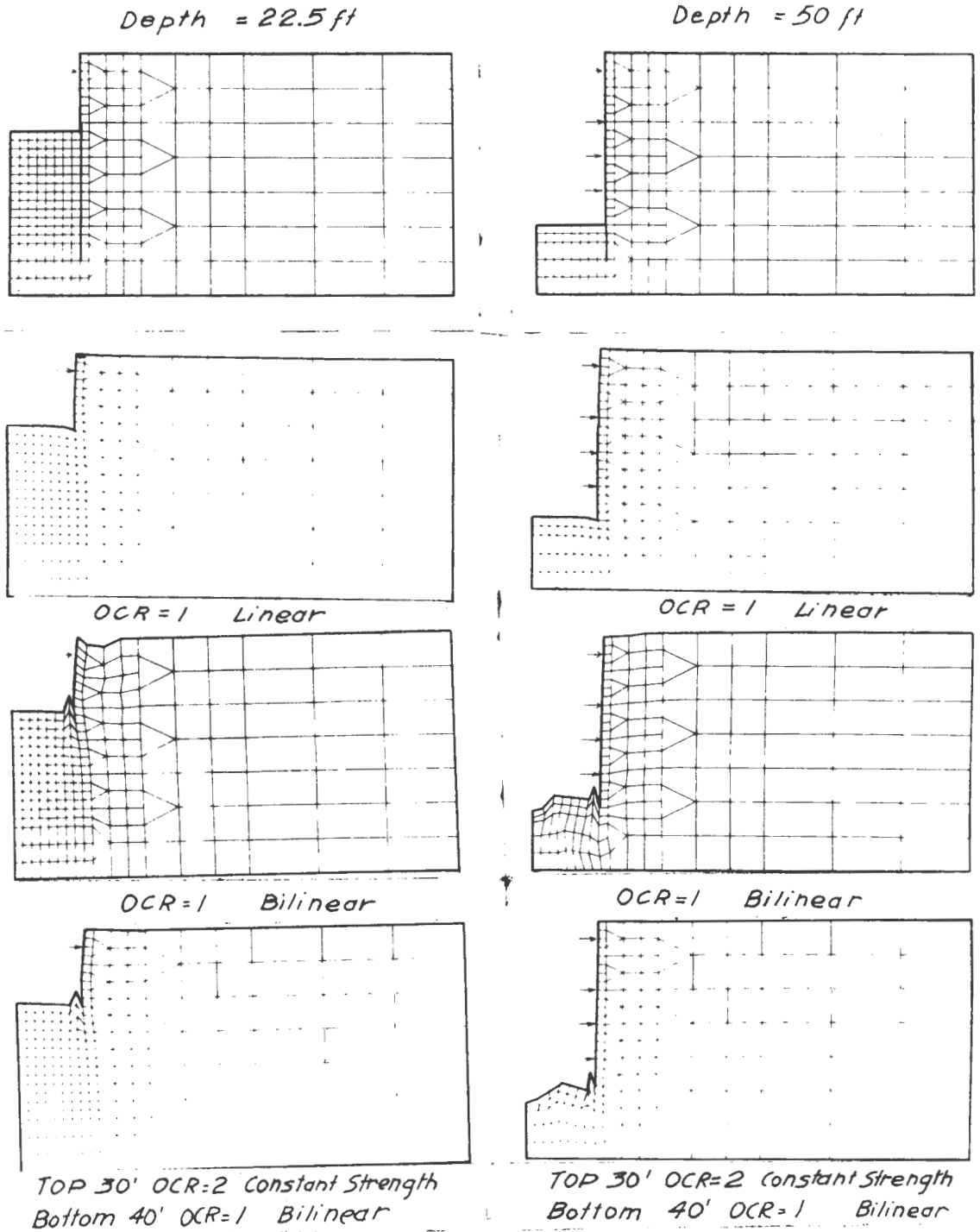

For OCR=1, $K_o = 0.5$ $S_u/\bar{\sigma}_{vo}$ 0.342
For OCR=2, $K_o = 0.7$ $S_u = 0.5$
For all $\mu = 0.49$, $E/\bar{\sigma}_{vo} = 300$
Magnification of Movements : 20 for all but 2 for Bilinear Analysis of 50ft cuts

FIGURE 4.3.12 DERFORMED SOIL MASS LINEARLY AND BILINEARLY ELASTIC ANALYSES

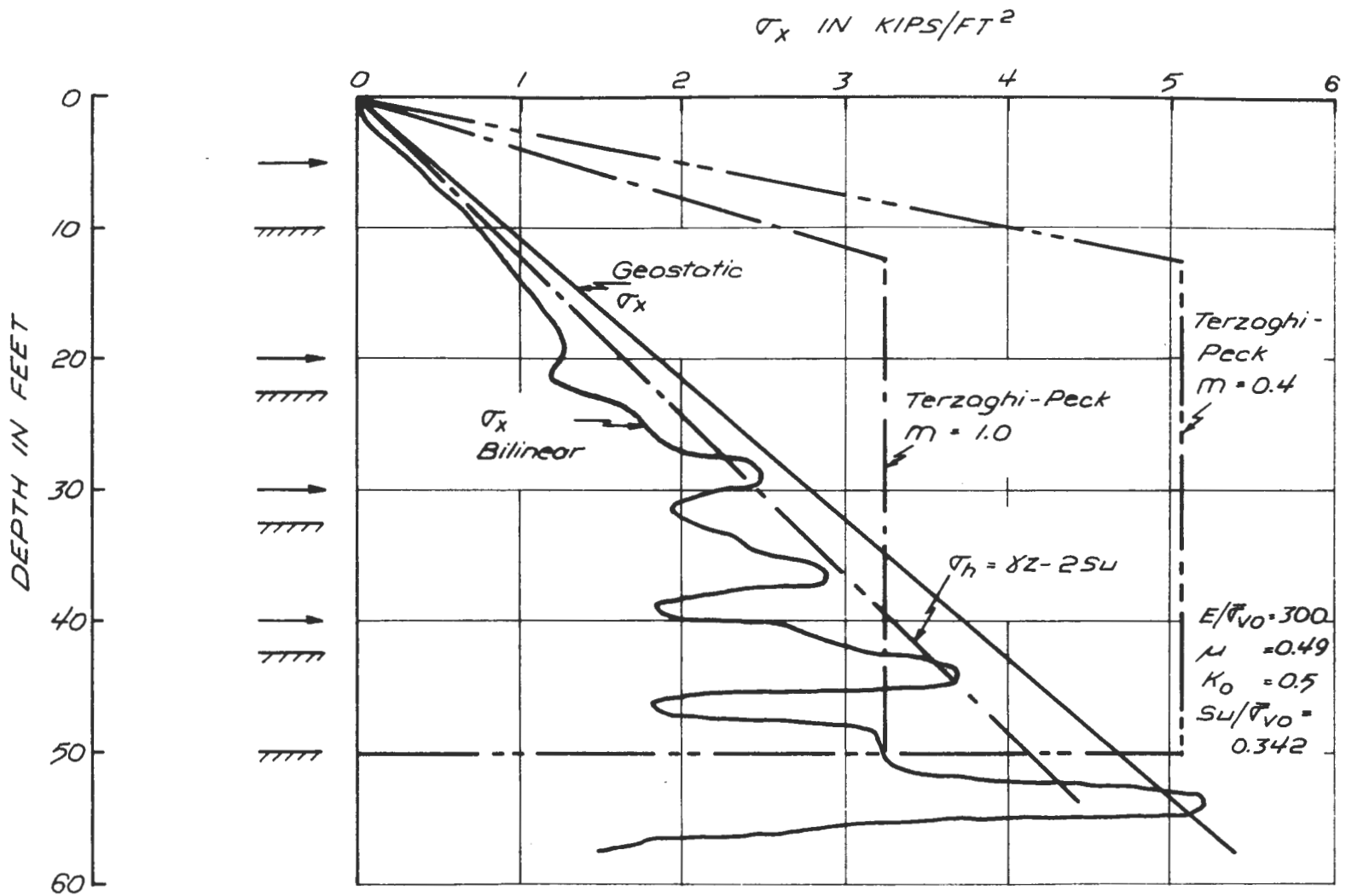

FIGURE 4.3.13 HORIZONTAL STRESSES ON SHEETING BILINEARLY ELASTIC ANALYSIS OCR = 1 WITH SHEETING

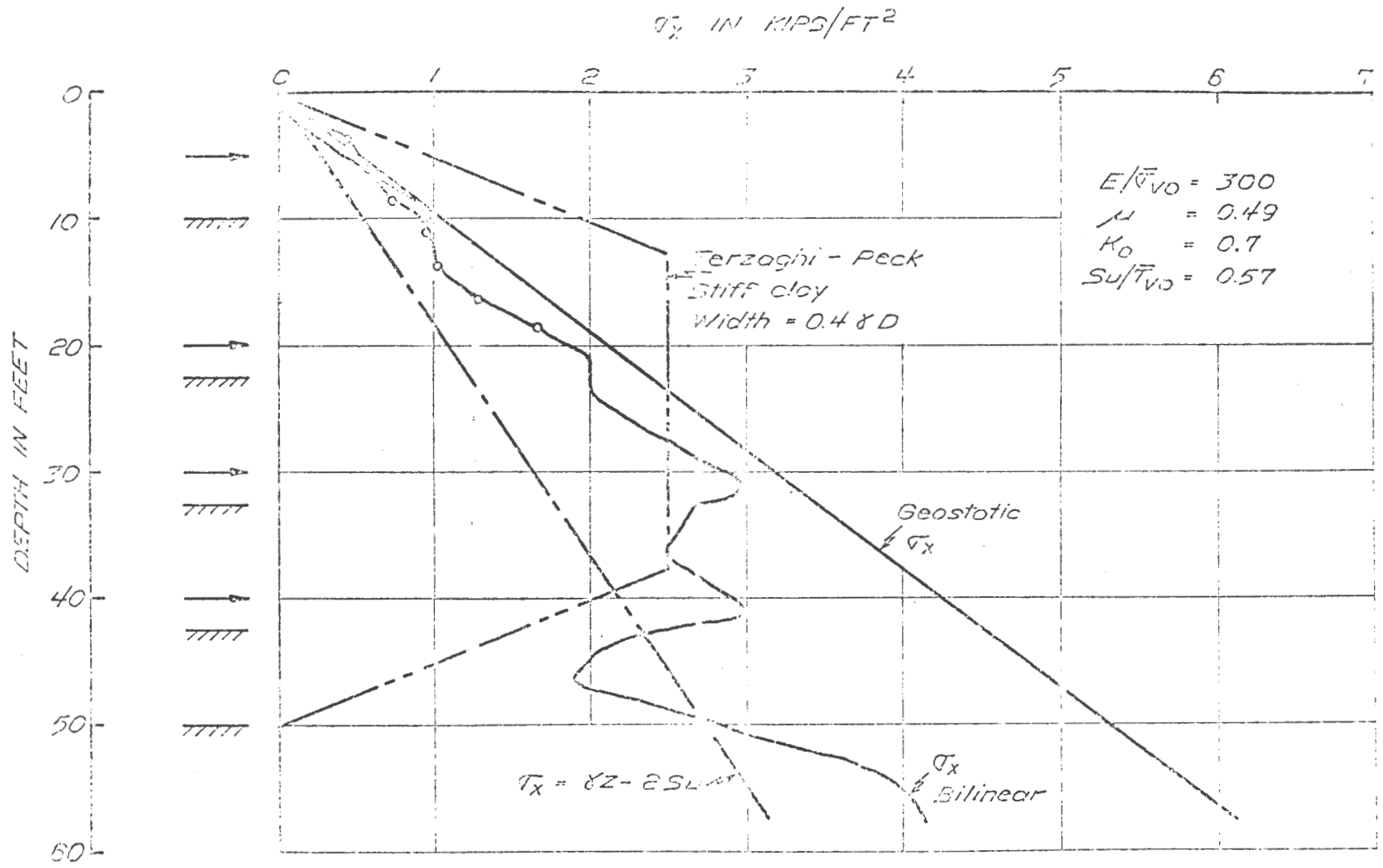

FIGURE 4.3.14 HORIZONTAL STRESSES ON WALL BILINEAR ANALYSIS
OCR = 2 WITH SWELLING

STAGE	LOAD IN STRUT, kips/ft				TOTAL LOAD kips/ft	COMMENTS
	S 1	S 2	S 3	S 4		
2	6.4				6.4	ZP 38 sheeting Linear elastic Strut fixed K = 0.5 OCR = 1 $E/\bar{\sigma}_{vo}$ = 300 Depth of layer = 70 ft
3	5.18	19.80			24.98	
4	6.01	16.01	28.32		50.34	
5	6.25	17.70	24.33	27.82	76.10	
2	7.94				7.94	ZP 38 Sheeting Bilinear elastic Depth of layer = 70 ft K_o = 0.5 $Su/\bar{\sigma}_{vo}$ = 0.342 $E/\bar{\sigma}_{vo}$ = 300 OCR = 1
3	3.33	22.13			25.46	
4	4.74	8.02	35.87		48.63	
5	3.96	16.32	-8.46	67.89	79.53	

FIGURE 4.3.15 STRUT LOADS IN LINEARLY AND BILINEARLY ELASTIC ANALYSES

CASE	SOIL TYPE	WALL	MOMENT OF INERTIA I IN FEET^4	HALF WIDTH IN FEET	MAX BENDING MOVEMENT AT LOWEST STRUT LEVEL Kips/ft	MAX FIBRE STRESS psf	MINIMUM YIELD STRESS psf
1	OCR = 1	ZP 38 sheeting	0.0135	0.5	156.5	5.8×10^6	5.2×10^6
2	Top 30' OCR = 2 Bottom 40', OCR = 1	ZP38 Sheeting	0.0135	0.5	132	4.9×10^6	5.2×10^6
3	OCR = 1	Slurry wall	2.25	1.5	89.54	6.0×10^4	1.4×10^5

FIGURE 4.3.16 MAXIMUM STRESSES DUE TO BENDING IN RETAINING WALL

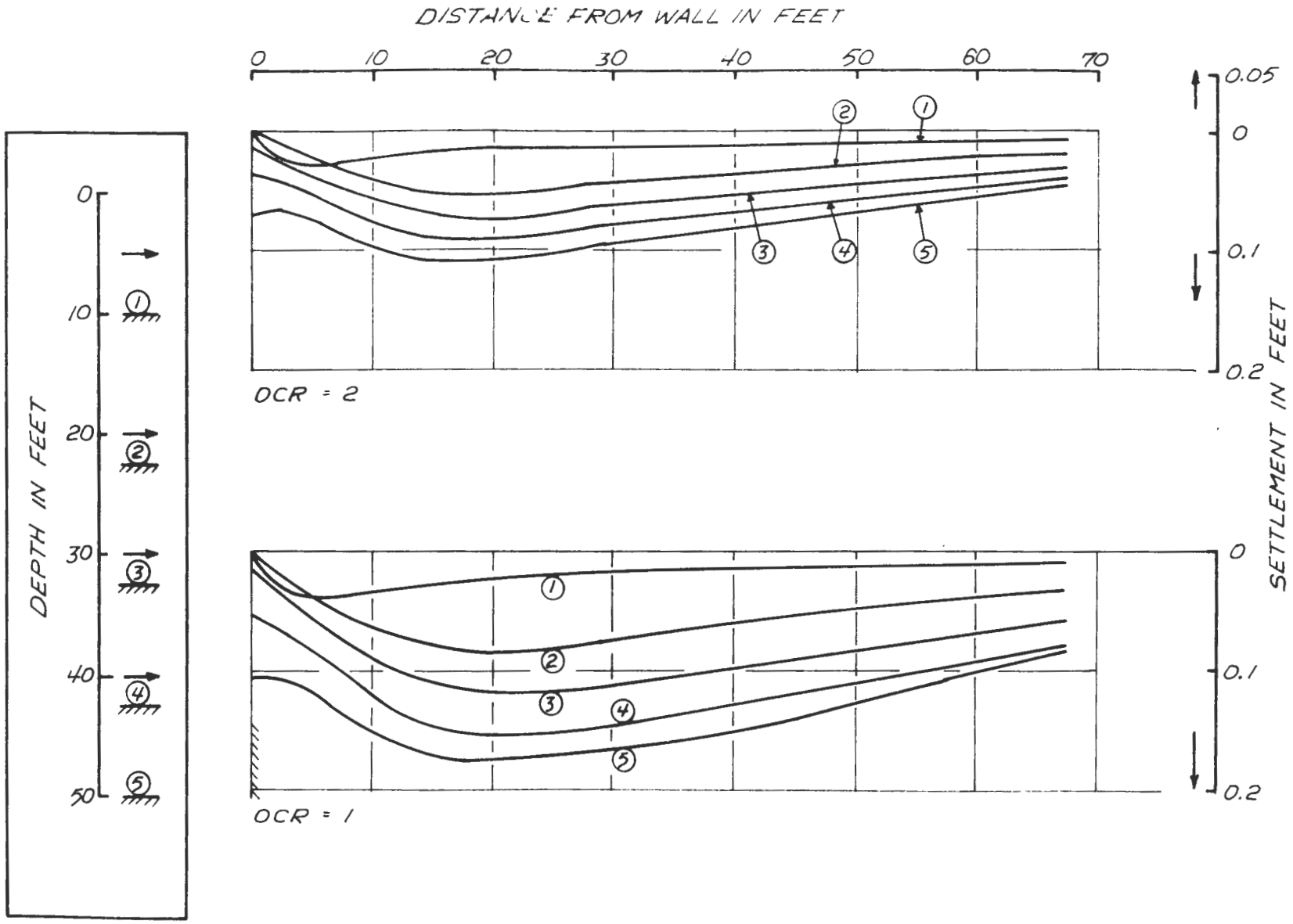

FIGURE 4.4.1 GROUND SETTLEMENT ANISOTROPIC NON-LINEARLY ELASTIC ANALYSIS

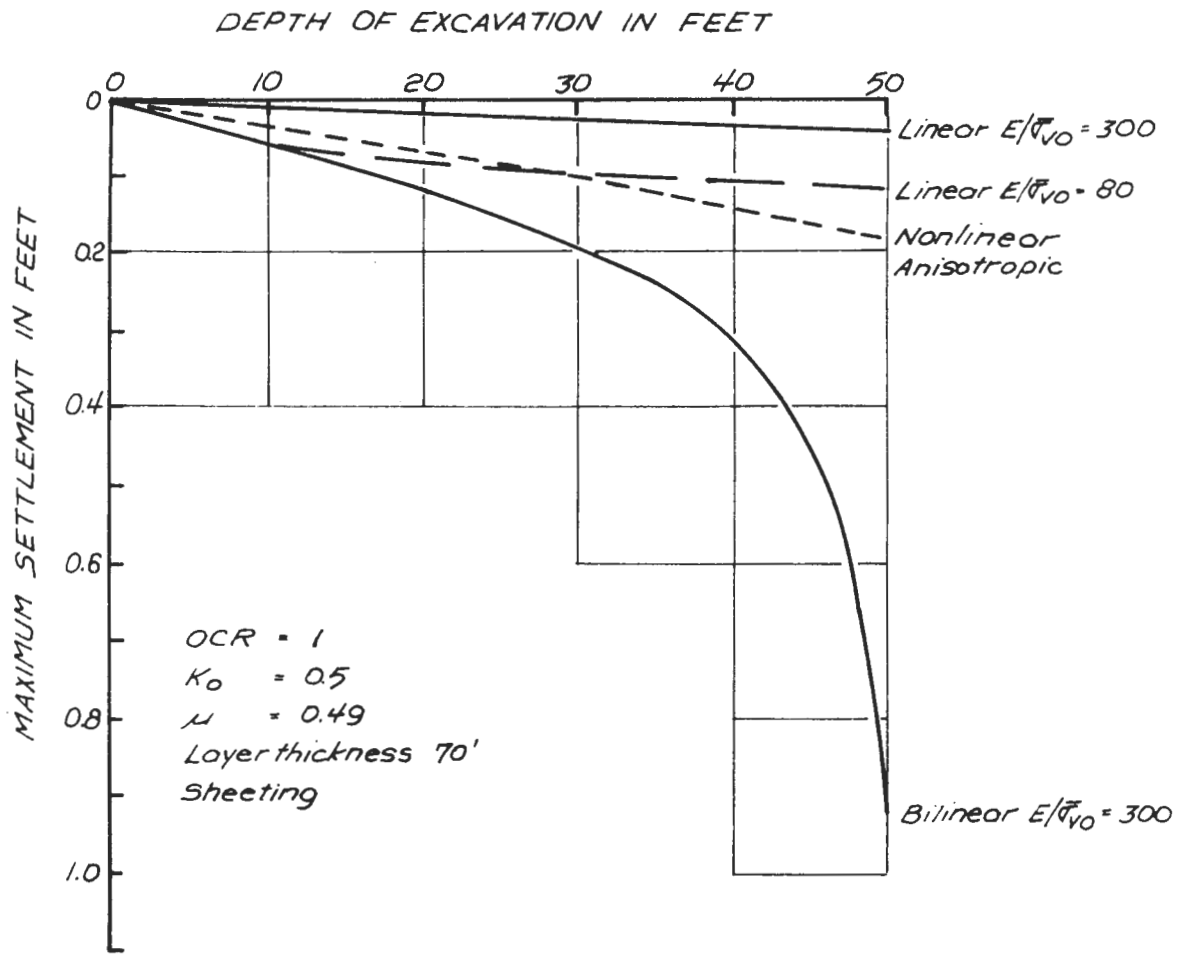

FIGURE 4.4.2 GROUND SETTLEMENT IN LINEARLY, BILINEARLY AND ANISOTROPIC NONLINEARLY ELASTIC ANALYSES

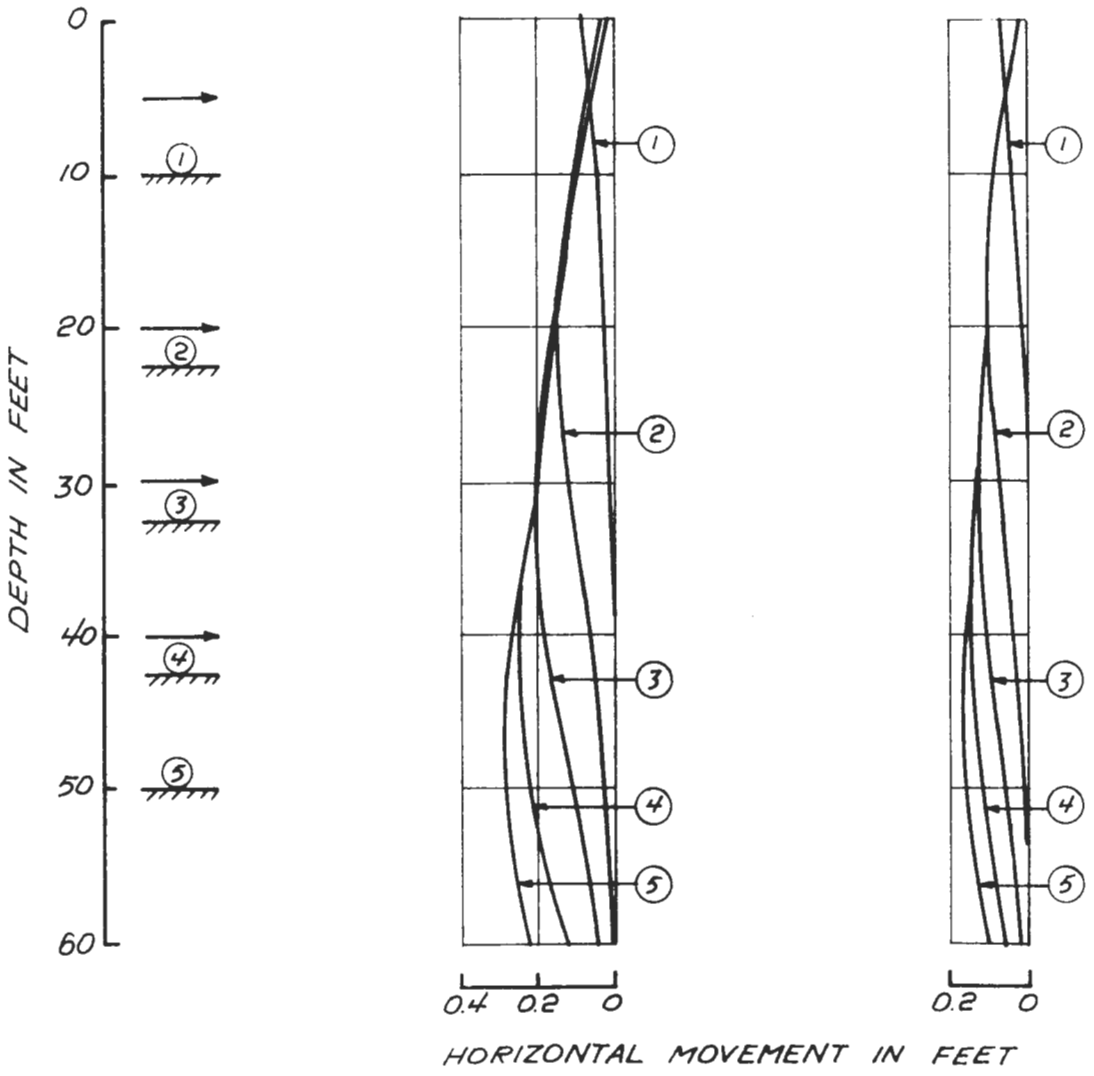

FIGURE 4.4.3 SHEETING MOVEMENT ANISOTROPIC NONLINEARLY ELASTIC ANALYSIS

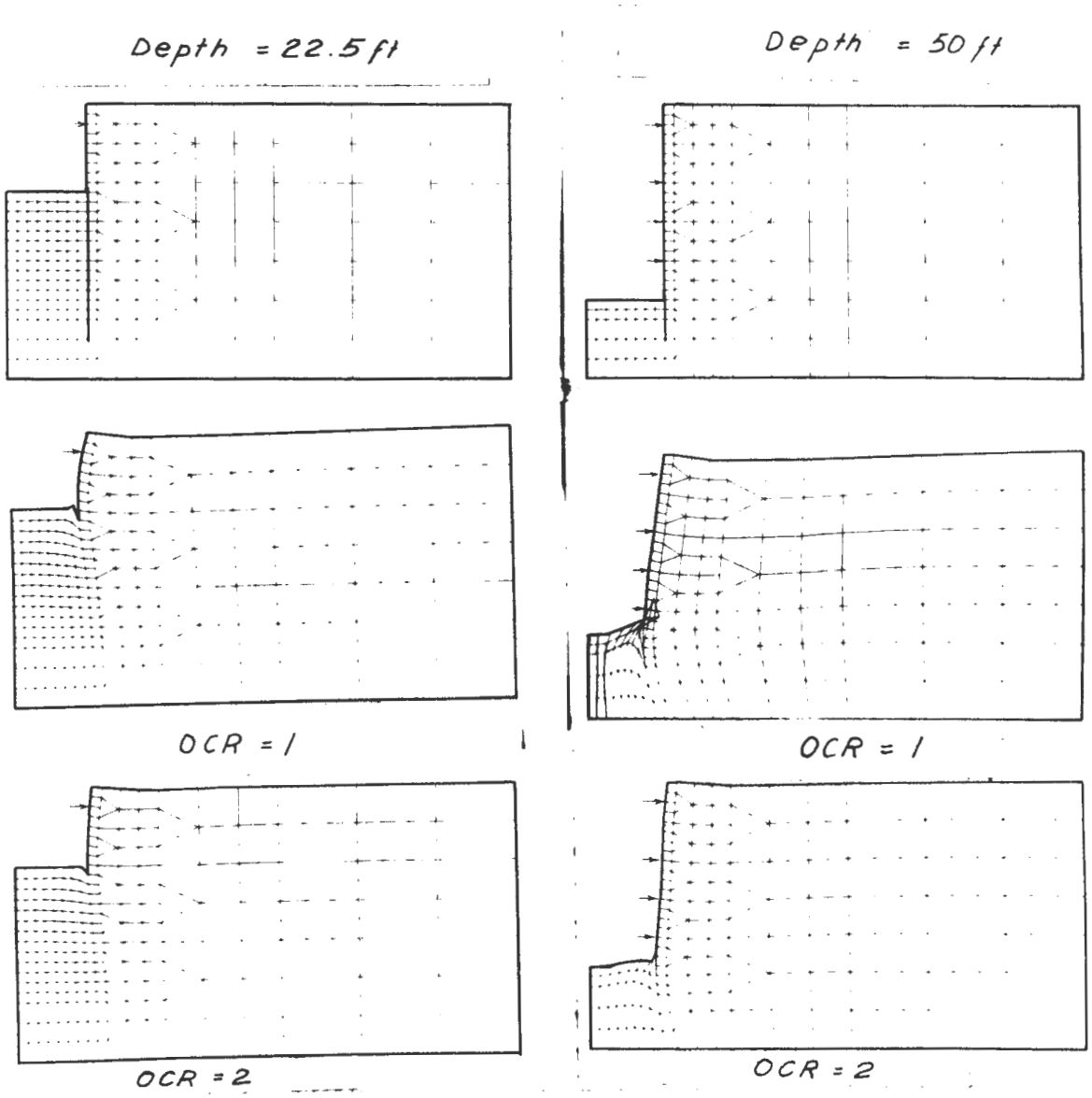

FIGURE 4.4.4 DEFORMED SOIL MASS ANISOTROPIC NONLINERLY. ELASTIC ANALYSIS

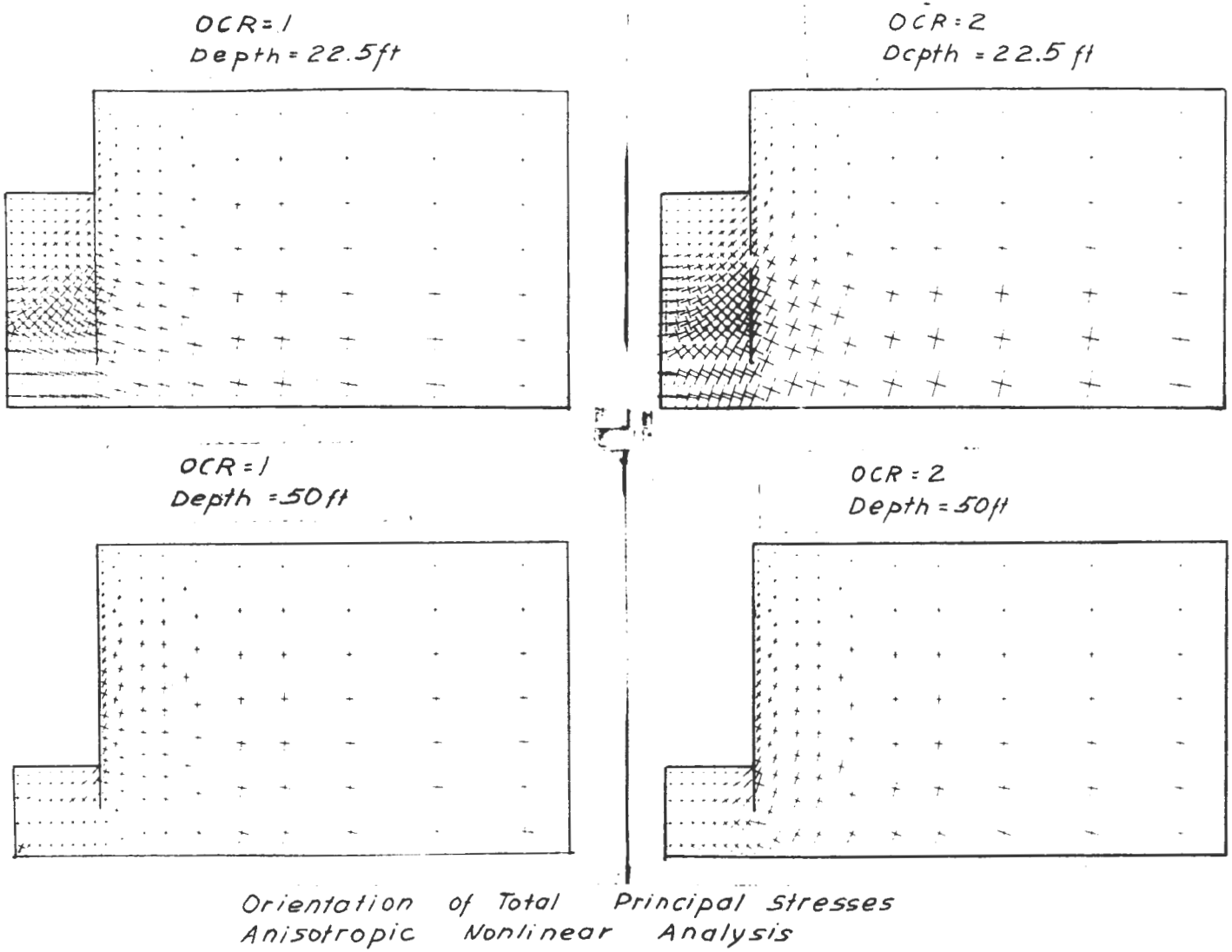

FIGURE 4.4.5 ORIENTATION OF TOTAL PRINCIPAL STRESSES ANISOTROPIC NONLINEARLY ELASTIC ANALYSIS

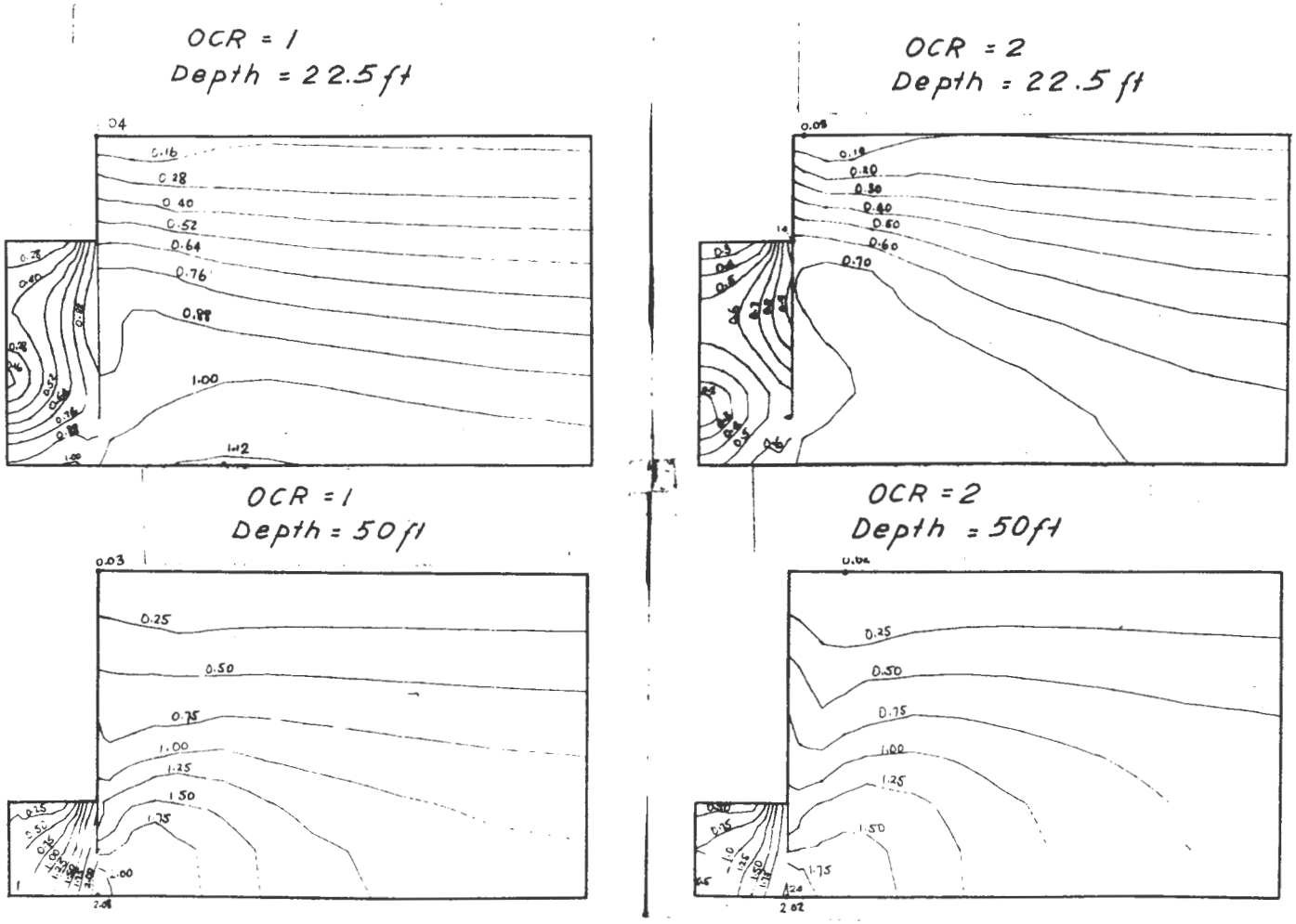

FIGURE 4.4.6 CONTOURS OF MAXIMUM SHEAR STRESS ANISOTROPIC NON-LINEARLY ELASTIC ANALYSIS

STAGE	LOAD IN STRUT, kips/ft				TOTAL LOAD kips/ft	COMMENTS
	S1	S2	S3	S4		
2	8.28				8.28	Nonlinear Anisotropic
3	3.32	25.04			28.36	OCR = 1
4	4.81	13.68	34.84		53.33	K_o = 0.5
5	5.16	17.10	24.15	34.78	81.19	$E_d/\bar{\sigma}_{vo}$ = 450 Layer = 70 ft ZP 38 Sheeting
2	7.50				7.50	Nonlinear Anisotropic
3	4.67	21.88			26.55	OCR = 2
4	5.88	14.27	31.25		51.40	K_o = 0.7
5	6.38	17.64	22.22	31.48	77.72	$E_d/\bar{\sigma}_{vo}$ = 450 Layer = 70 ft ZP 38 Sheeting

FIGURE 4.4.7 STRUT LOADS FROM ANISOTROPIC NONLINEARLY ELASTIC ANALYSIS

STAGE	LOAD IN STRUT, kips/ft²				TOTAL LOAD kips/ft²	COMMENTS
	S1	S2	S3	S4		
2	6.4				6.4	ZP 38 Sheeting Linear elastic Strut fixed K = 0.5 OCR = 1 $E/\bar{\sigma}_{vo}$ = 300 Depth of layer = 70 ft
3	5.18	19.80			24.98	
4	6.01	16.01	28.32		50.34	
5	6.25	17.70	24.33	27.82	76.10	
2	7.94				7.94	ZP 38 Sheeting Bilinear elastic K_o = 0.5 $S_u/\bar{\sigma}_{vo}$ = 0.342 $E/\bar{\sigma}_{vo}$ = 300 OCR = 1 Depth of layer = 70 ft
3	3.33	22.13			25.46	
4	4.74	8.02	35.87		48.63	
5	3.96	16.32	-8.46	67.89	79.53	
2	8.28				8.28	Nonlinear Anisotropic OCR = 1 K_o = 0.5 $E_o/\bar{\sigma}_{vo}$ = 450 Layer = 70 ft ZP 38 Sheeting
3	3.32	25.04			28.36	
4	4.81	13.68	34.82		53.33	
5	5.16	17.10	24.15	34.78	81.19	

FIGURE 4.4.8 STRUT LOADS FROM THREE ANALYSES

SOIL	PERMEABILITY $\times 10^{-6}$ CM/SEC	
FILL	500	
SLIGHTLY ORGANIC SILT	30	
BLACK ORGANIC SILT *	2.6	
TILL	130 HORIZONTALLY	13 VERTICALLY
SHEETING	0.1	

* Present of test section B only

FIGURE 5.2.1 PERMEABILITIES OF SUBSOILS NORTH STATION TEST SECTIONS A AND B

Sheeting Permeabilities	
Case	10^{-6} cm/sec
1	10
2	1
3	0.1
4	0.01
5	0.001

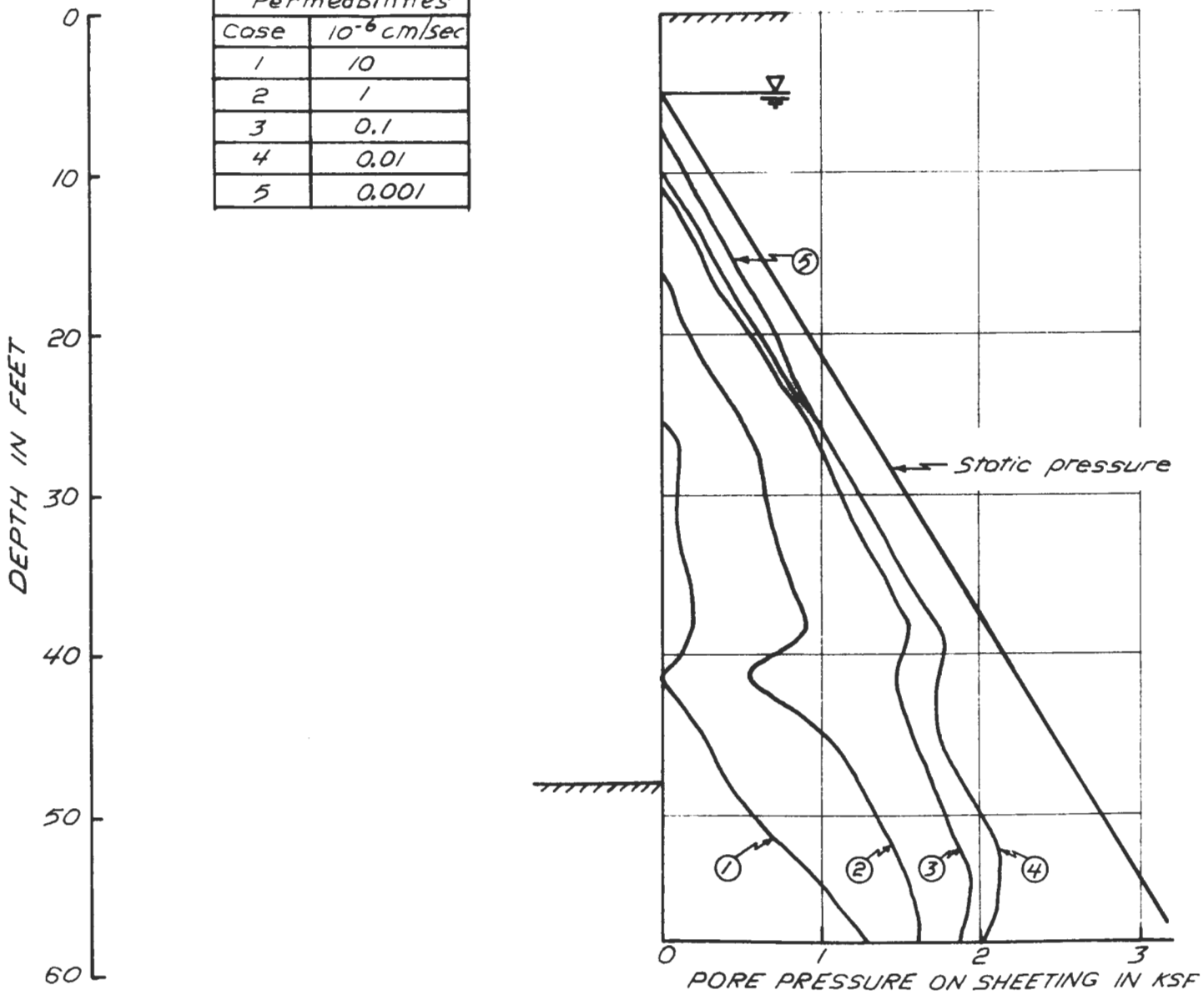

FIGURE 5.2.2 PORE PRESSURES ON SHEETING WITH DIFFERENT SHEETING PERMEABILITIES TEST SECTION B

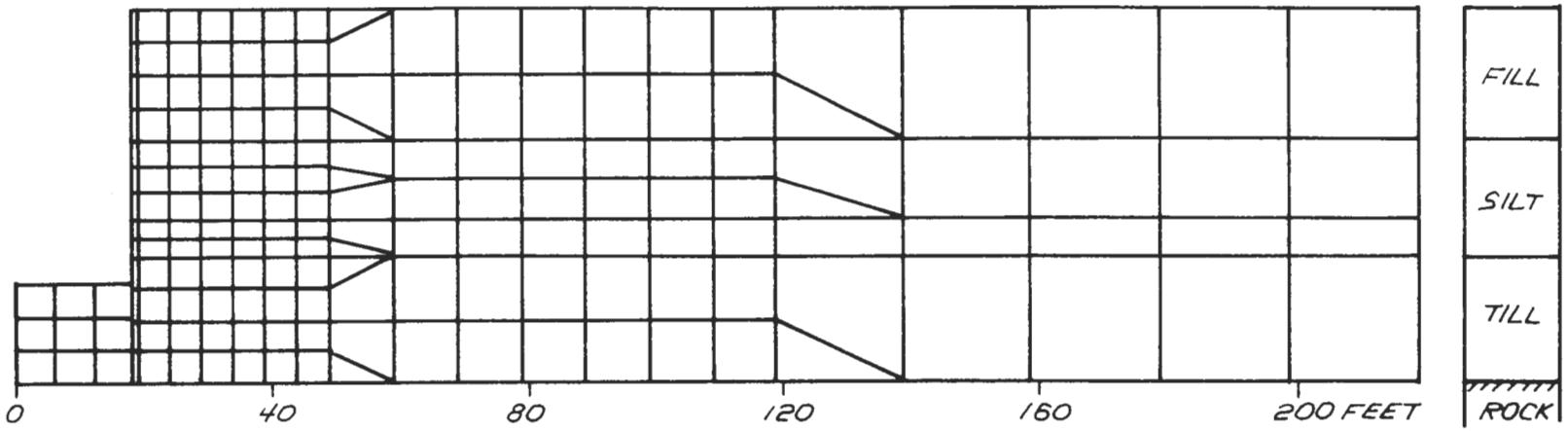

FIGURE 5.2.3 FINITE ELEMENT GRID FOR FEDAR SEEPAGE ANALYSIS
TEST SECTION B

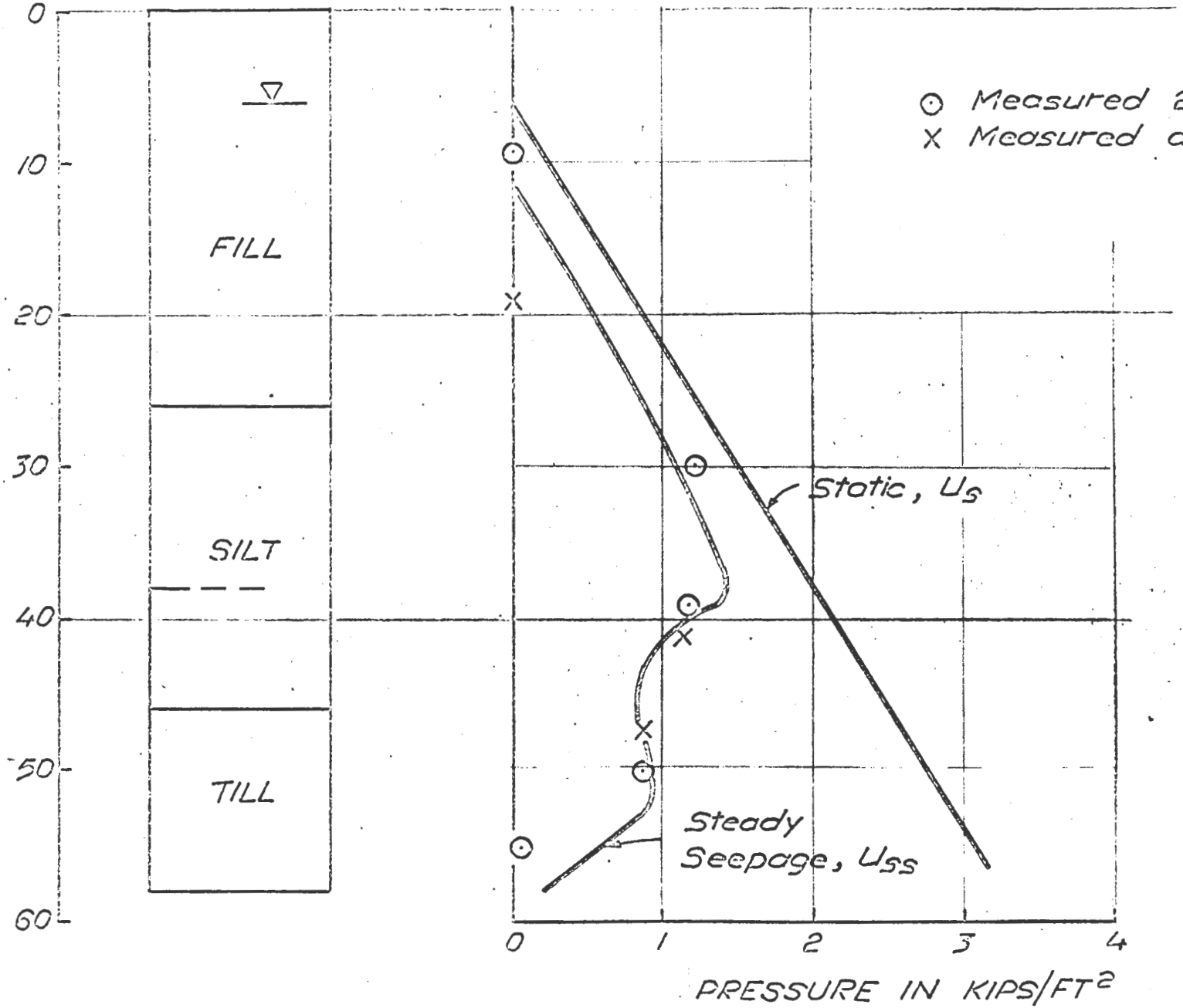

FIGURE 5.2.4 PORE PRESSURE ON SHEETING TEST SECTION B

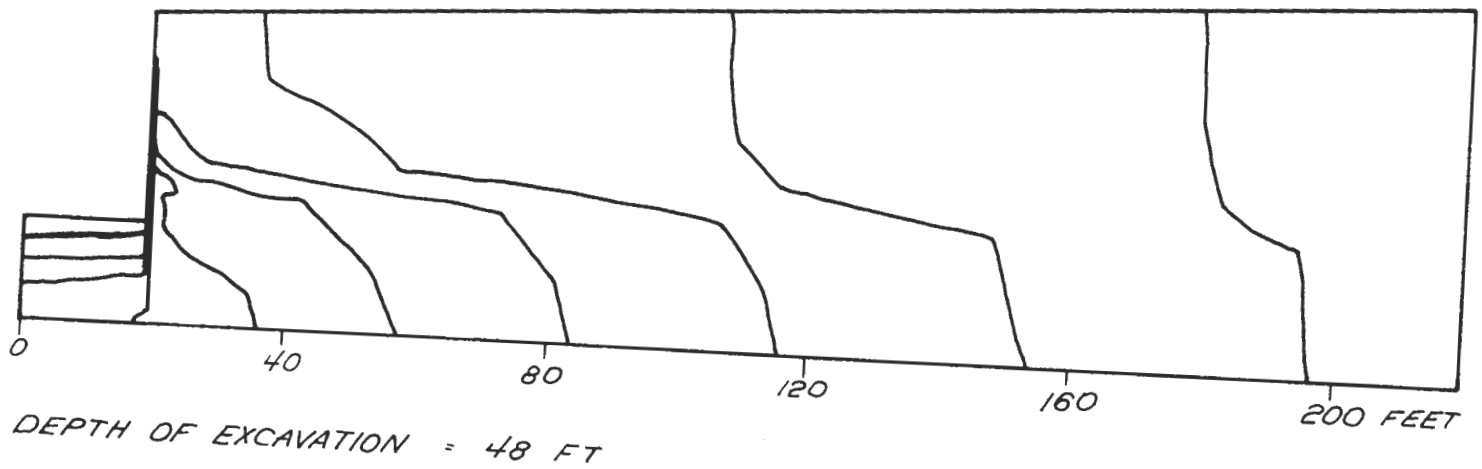

FIGURE 5.2.5 PREDICTED CONTOURS OF TOTAL HEAD TEST SECTION B

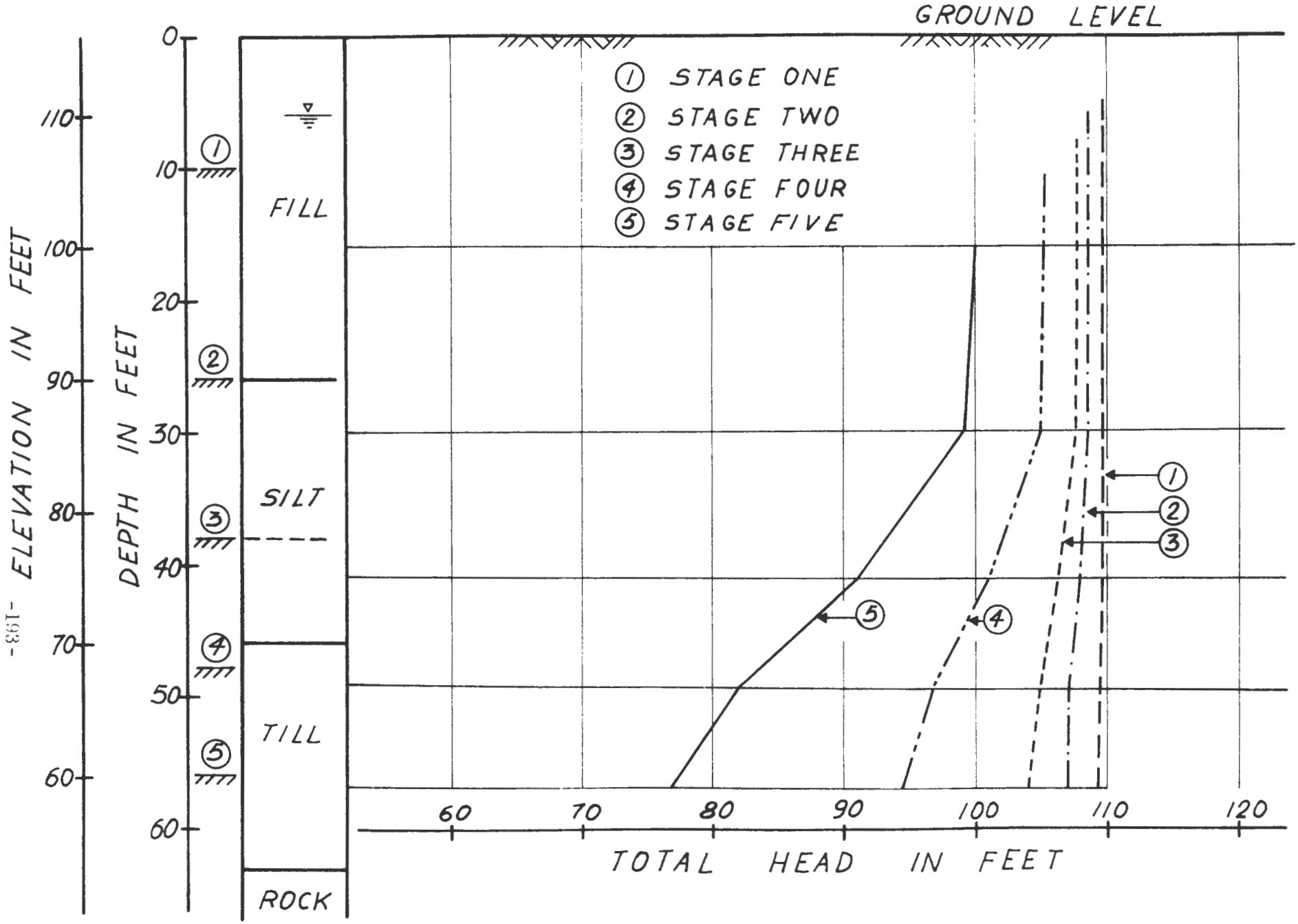

FIGURE 5.2.6 PREDICTED TOTAL HEAD 20 FT FROM WALL - TEST SECTION B

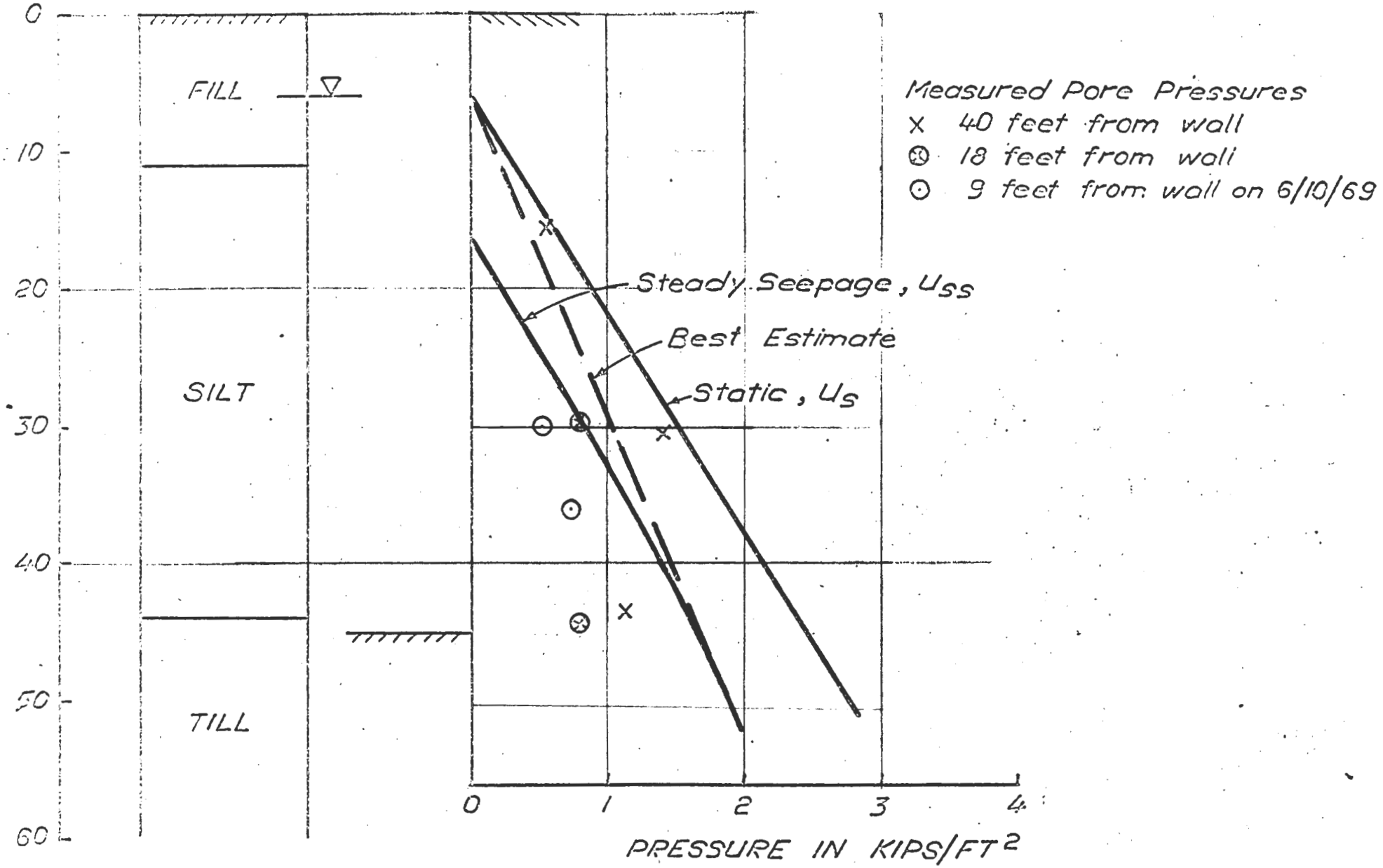

FIGURE 5.2.7 PORE PRESSURES ON WALL TEST SECTION A

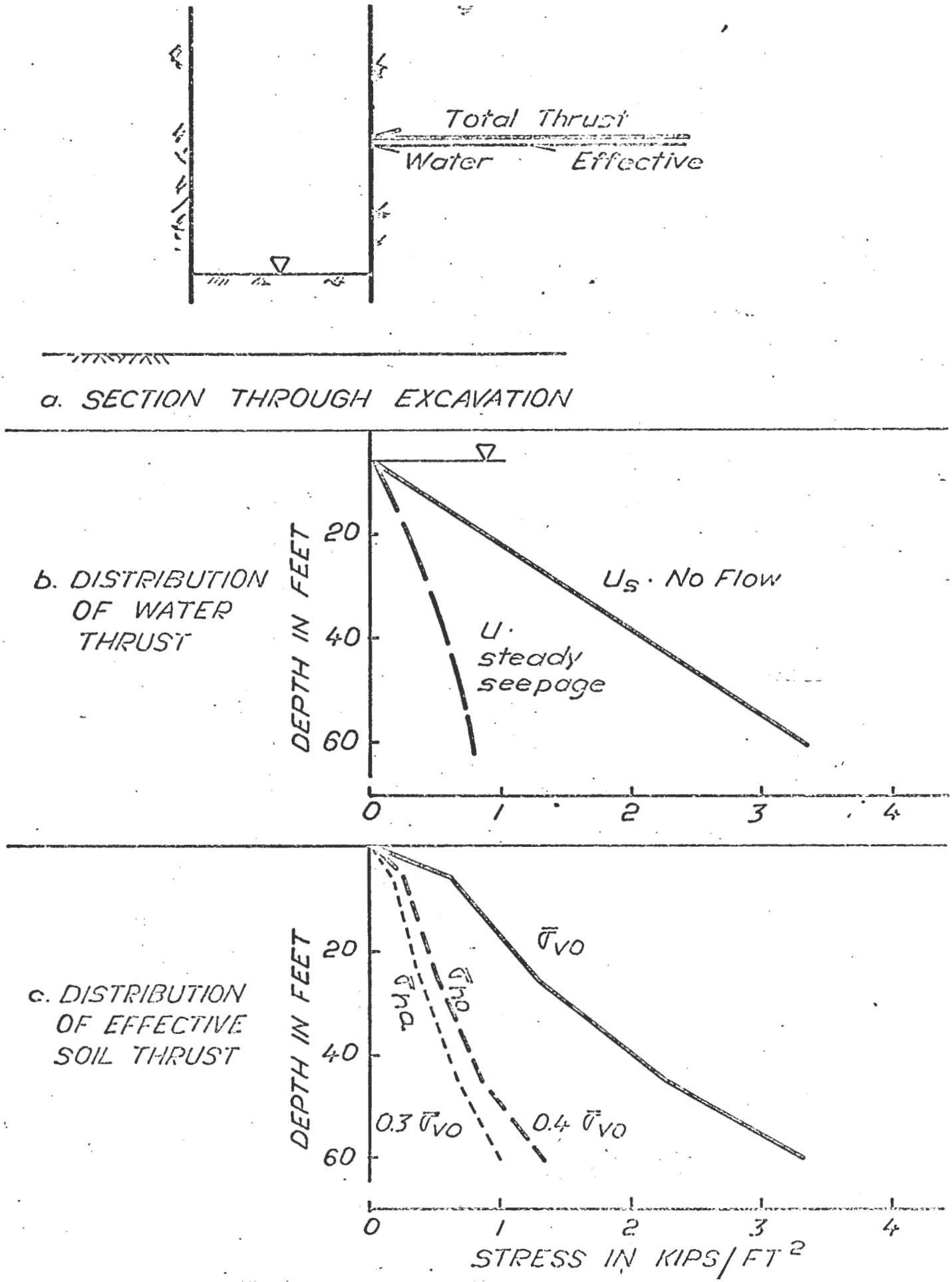

FIGURE 5.3.1 STRESS IN SOIL NEAR EXCAVATION
(After Lambe 1970)

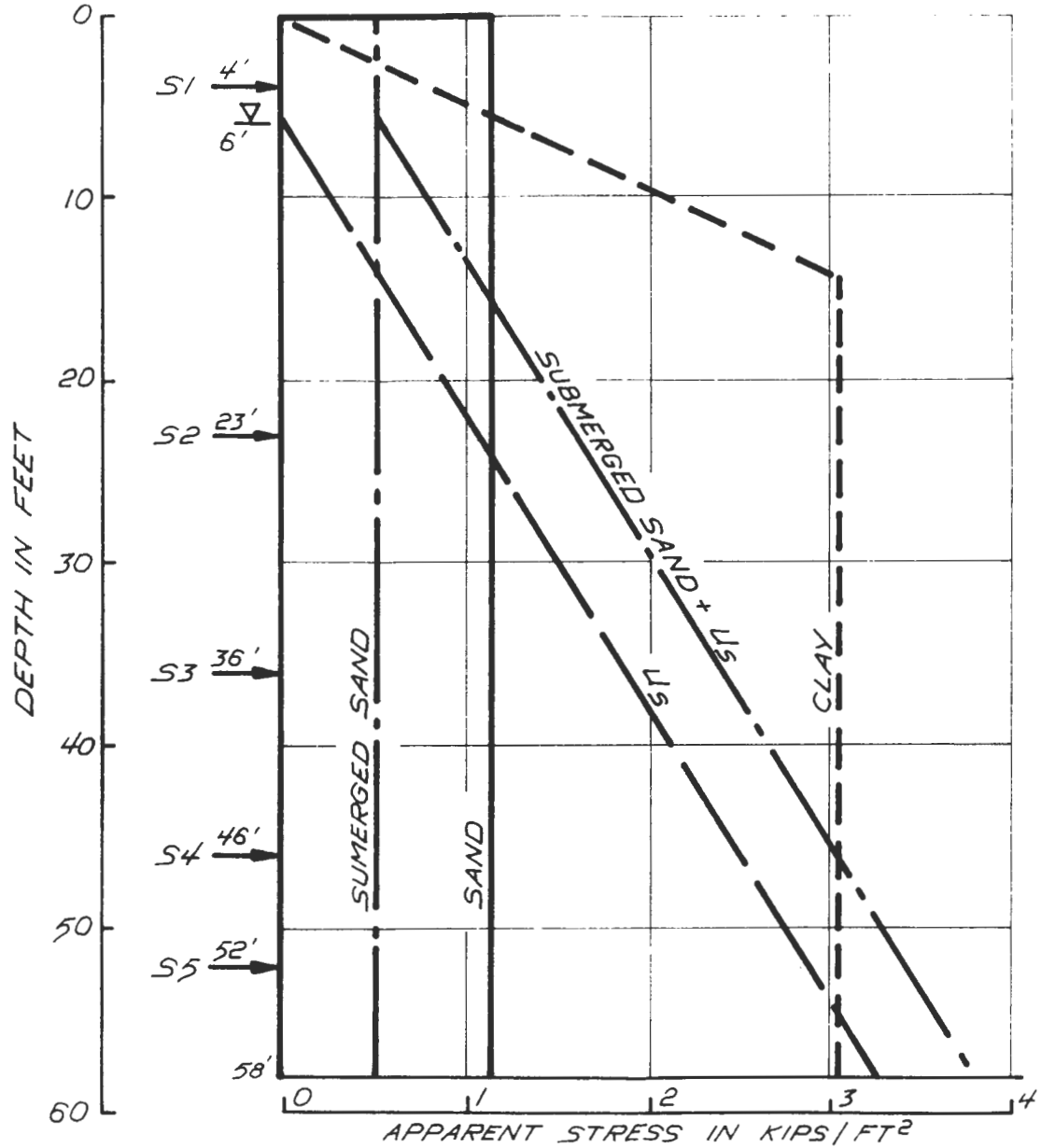

σ_h at bottom of excavation

Sand: $\sigma_h = 0.65\, K_o \gamma D$ (Average for profile)

$K_o = 0.26$

$\gamma = 0.114$ kips/ft³

$D = 58'$

$\sigma_h = (0.65)(0.26)(0.114)(0.58) = 1.12$

Clay: $\sigma_h = 1.0\, K_o \gamma D$

$K_o = 1 - \frac{4 S_u}{\gamma D} = 1 - \frac{4(.890)}{(.114)(58)}$

$= 0.46$

$\sigma_h = (1.0)(0.46)(0.114)(58) = 3.04$

Submerged Sand + U_s:

$\sigma_h = 0.65\, K_o (\gamma_t - \gamma_w) D +$

$U_s = (0.65)(0.26)$

$(0.0516)(58) + U_s$

$= 0.49 + 3.25$

$= 3.74$

FIGURE 5.3.2 TEST SECTION B ANALYSED BY TERZAGHI - PECK METHOD

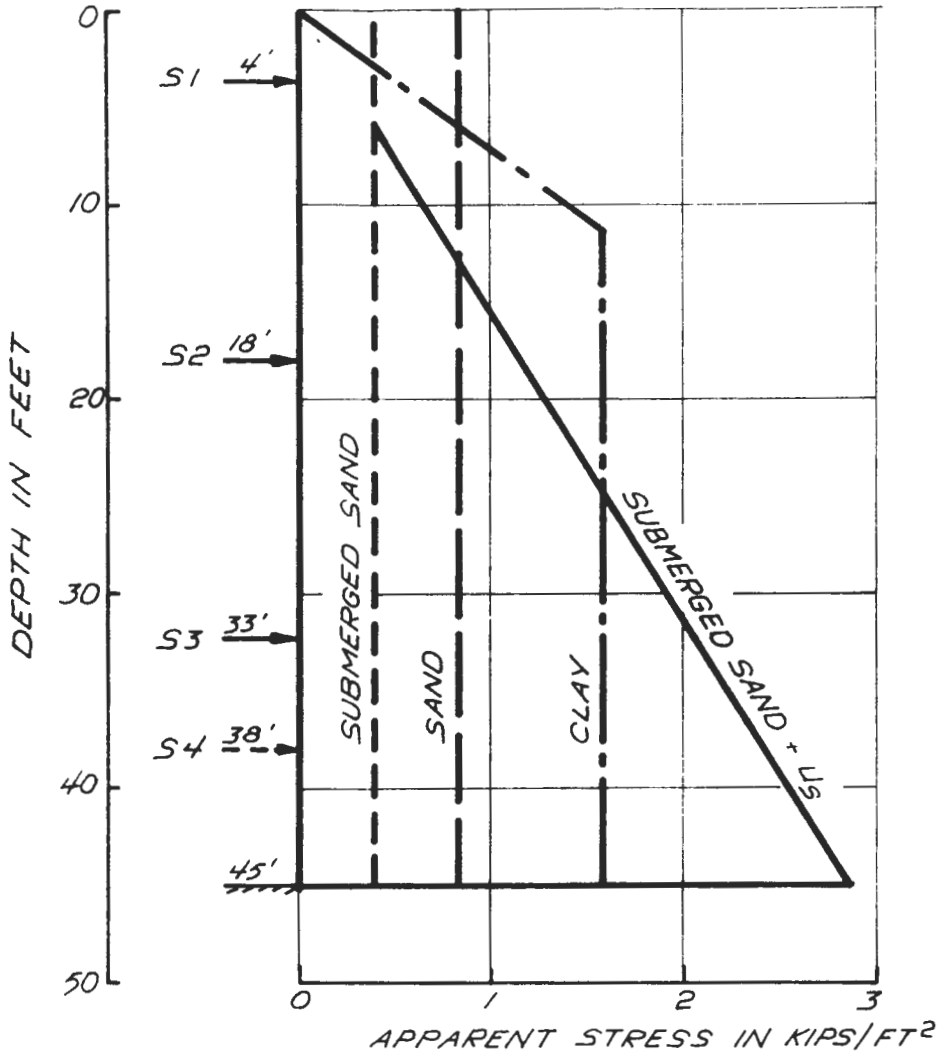

σ_h of bottom of excavation

Sand : $\sigma_h = 0.65\ K_a \gamma D$

$K_a = 0.26$

$\gamma = 0.114$ kips/ft³

$D = 45'$

$\sigma_h = (0.65)(0.26)(0.114)(45)$

$= 0.84$

Clay : $\sigma_h = 1.0\ K_a \gamma D$

$K_a = 1 - \frac{4S_u}{\gamma D} = 1 - \frac{4(0.890)}{(0.114)(45)}$

$= 0.3$

$\sigma_h = (1.0)(0.3)(0.114)(58)$

$= 1.52$

Submerged sand + U_s :

$\sigma_h = 0.65\ K_a (\gamma_t - \gamma_w) D + U_s$

$= (0.65)(0.26)(0.0516)(58)$

$+ U_s = 0.39 + 2.44$

$= 2.83$

FIGURE 5.3.3 TEST SECTION A ANALYSED BY TERZAGHI - PECK METHOD

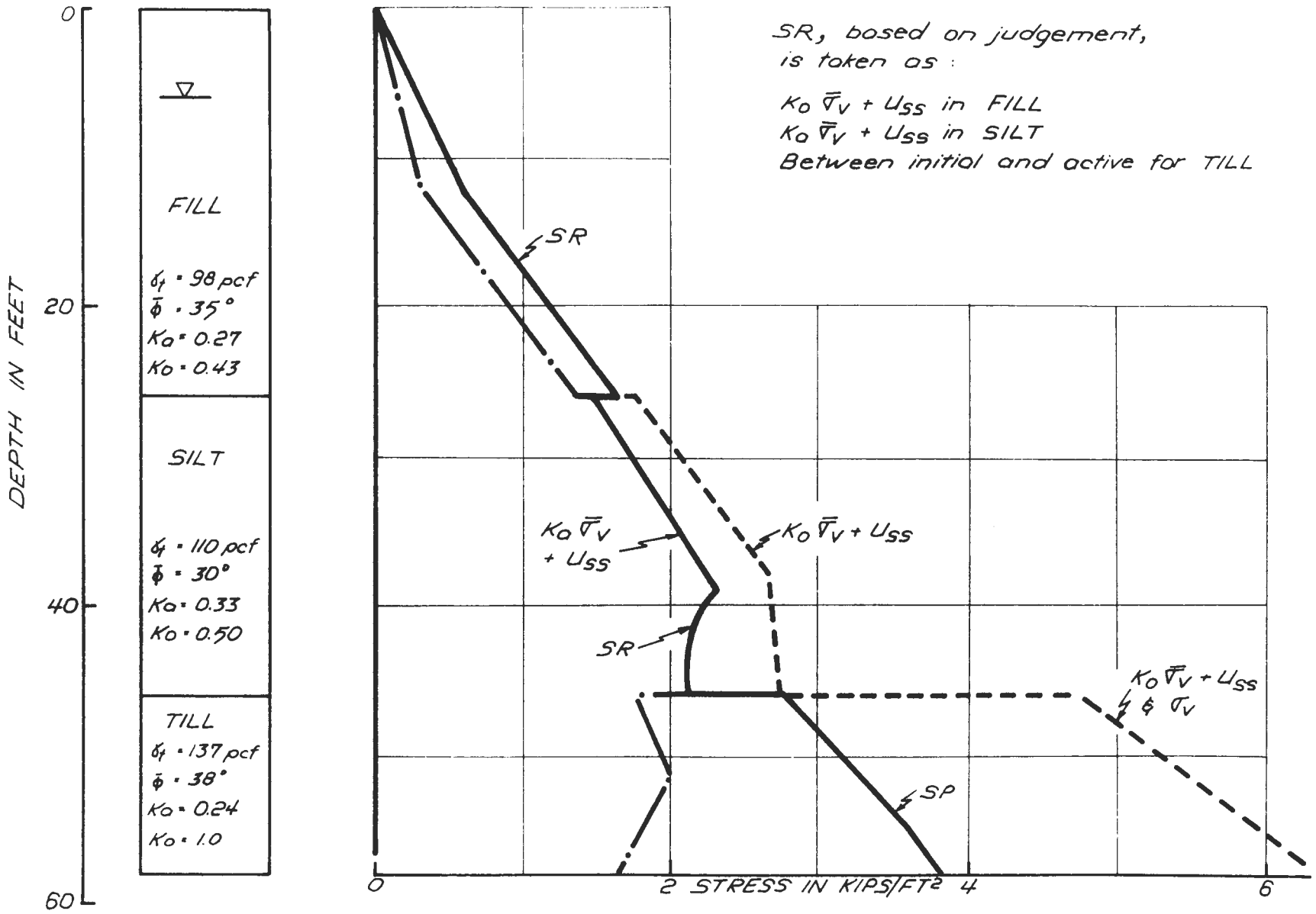

FIGURE 5.3.4 HORIZONTAL STRESSES ON WALL PREDICTED BY STRESS RATIO METHOD TEST SECTION B

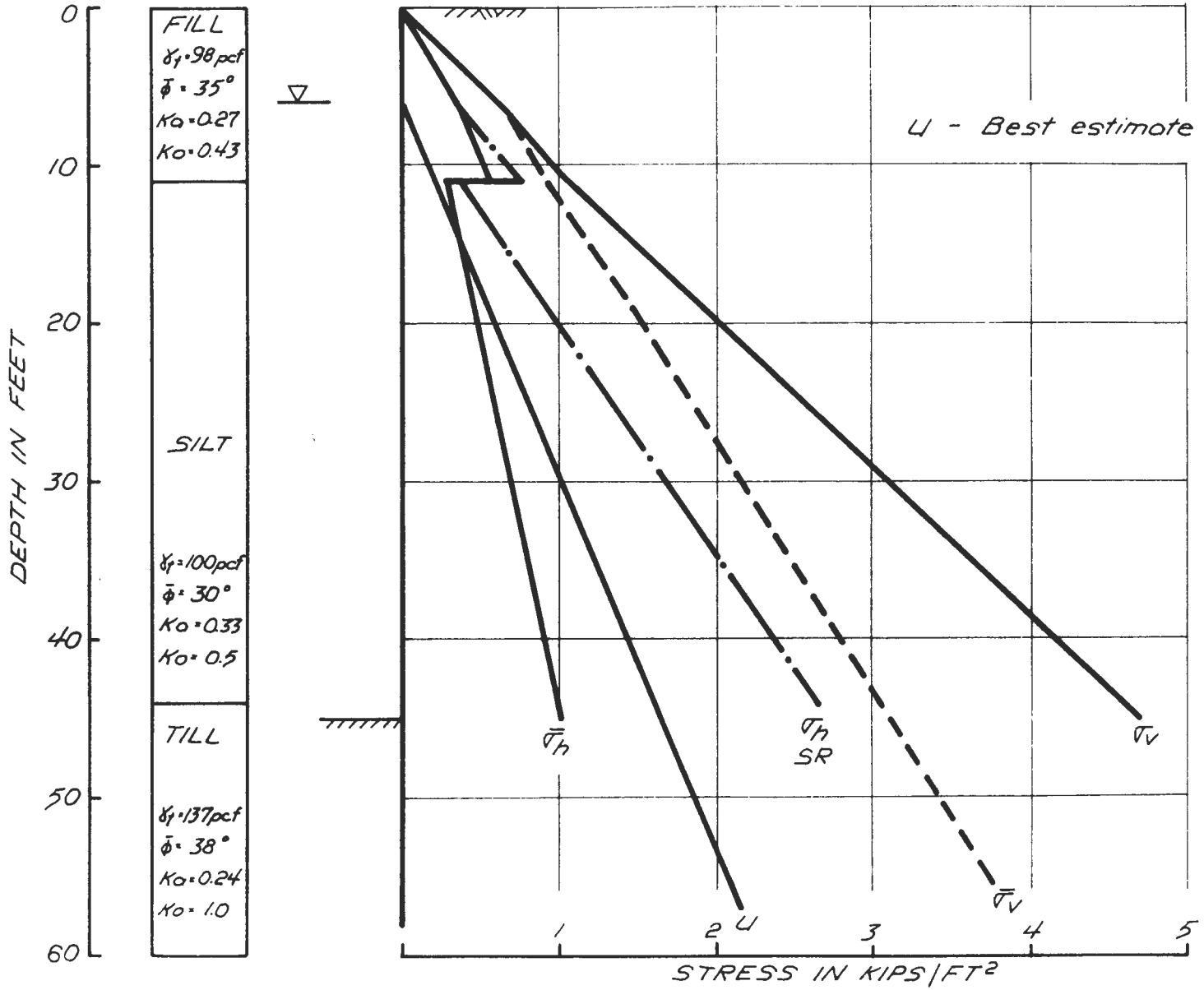

FIGURE 5.3.5 HORIZONTAL STRESSES ON WALL PREDICTED BY STRESS RATIO METHOD TEST SECTION A

STRUT NUMBERS	STRUT LOAD IN KIPS									
	TERZAGHI — PECK METHOD			SUBMERGED SAND + U_s TSCHEBOTARIOFF	CLAY NAVOOCK	STRESS RATIO	ELASTIC BEAM WITH SPRINGS	FINITE ELEMENT PROGRAM BRACE	MEASURED LOADS	DESIGN LOADS
	SAND	CLAY	SUBMERGED SAND + U_s							
S1	182	230	100	92	221	49	67	46	56	170
S2	215	580	279	290	580	206	176	176	210	493
S3	154	420	319	335	420	282	350	226	296	605
S4	108	292	280	288	290	233	147	256	266	566
S5	75	219	241	230	151	241	235	264	247	615

FIGURE 5.3.6 STRUT LOADS AT FULL EXCAVATION TEST SECTION B

STRUT NUMBERS	STRUT LOAD IN KIPS								
	TERZAGHI — PECK METHOD			SUBMERGED SAND + U_S TSCHEBOTARIOFF	CLAY NAVDOCK	STRESS RATIO	ELASTIC BEAM WITH SPRINGS	FINITE ELEMENT PROGRAM BRACE	MEASURED
	SAND	CLAY	SUBMERGED SAND + U_S						
S1	117	107	61	72	96	47	34	10	4
S2	140	272	201	222	258	150	200	198	196
S3	136	254	332	335	242	295	336	199	215

FIGURE 5.3.7 STRUT LOADS AT FULL EXCAVATION TEST SECTION A

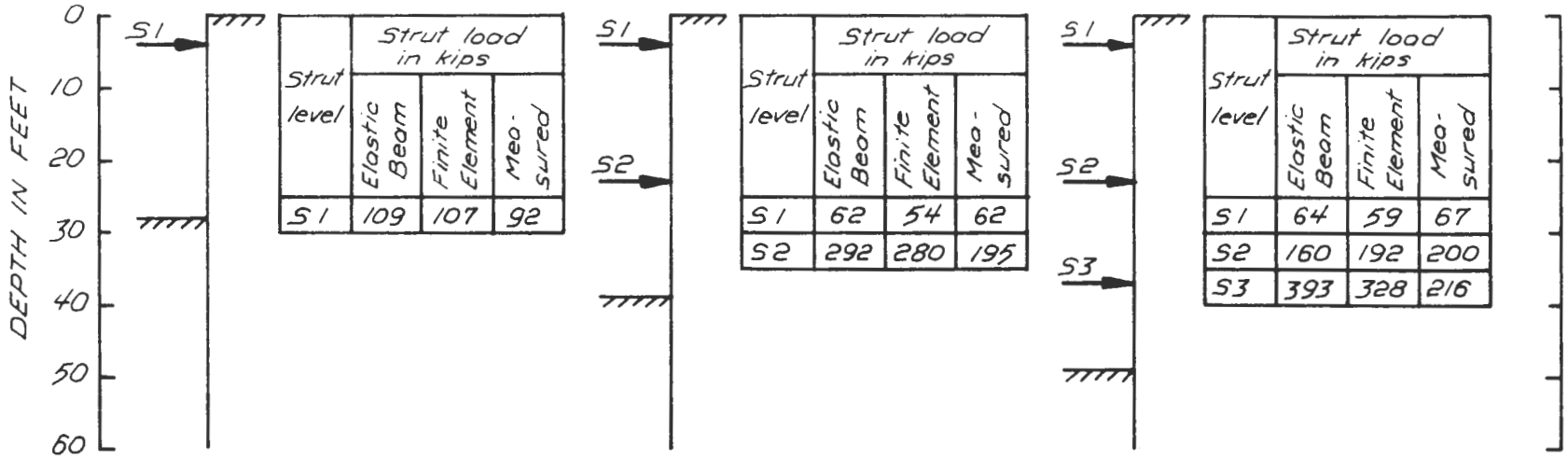

Note : Finite element method means the finite element computer program BRACE

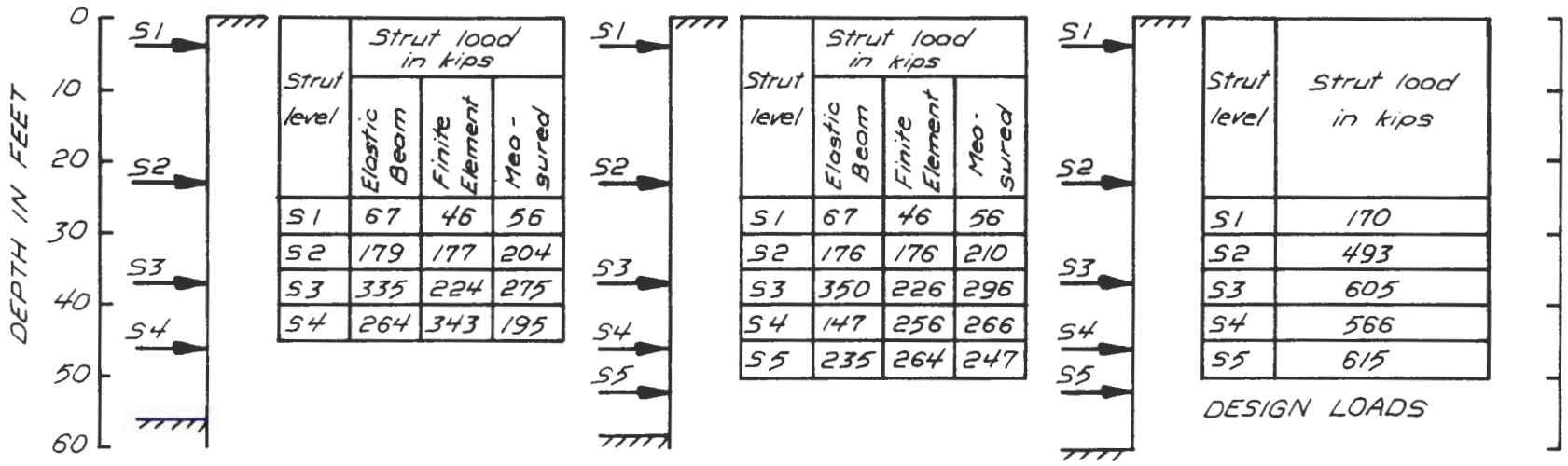

FIGURE 5.3.8 STRUT LOADS DURING EXCAVATION TEST SECTION B

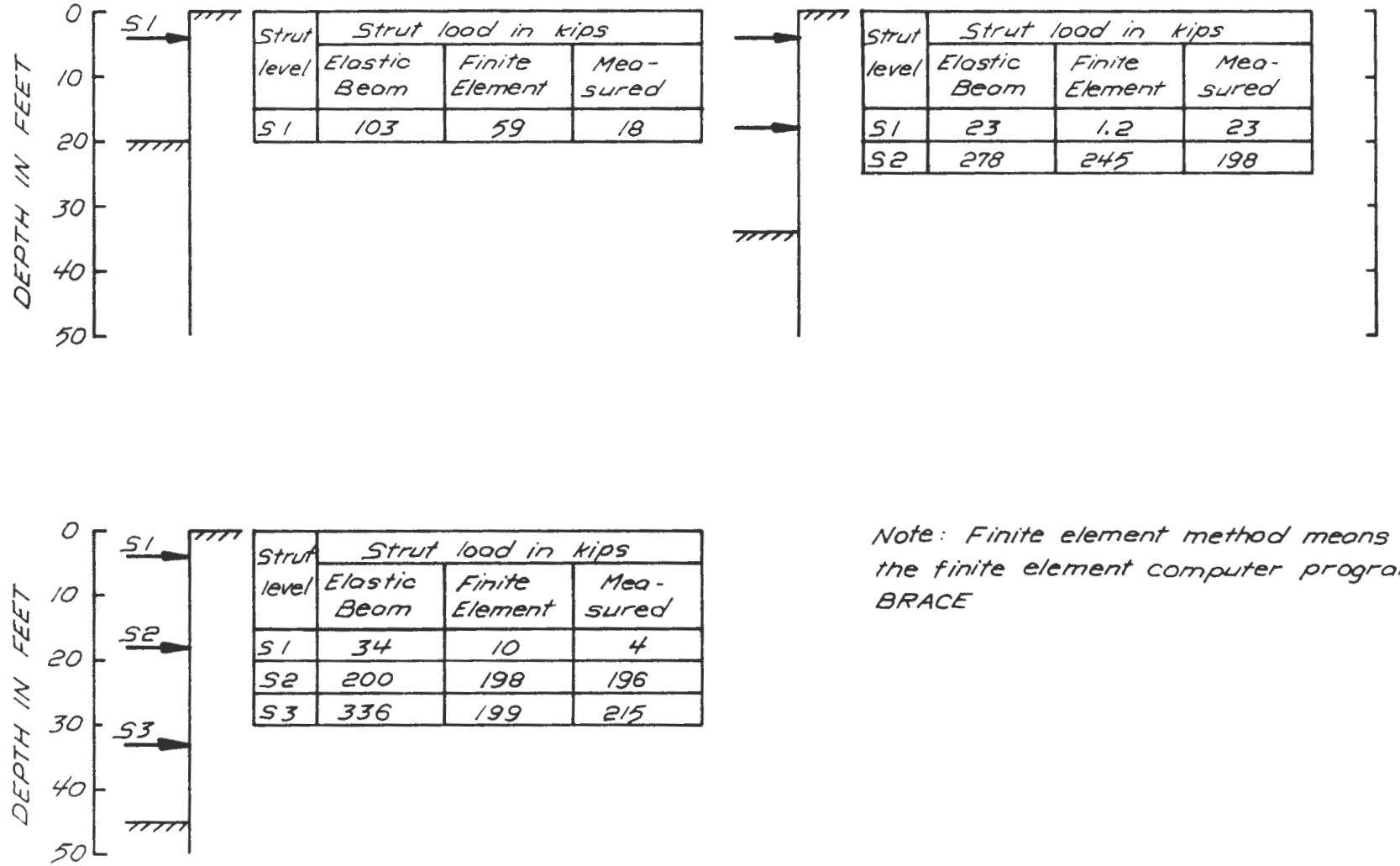

Strut level	Strut load in kips		
	Elastic Beom	Finite Element	Mea-sured
S1	103	59	18

Strut level	Strut load in kips		
	Elastic Beom	Finite Element	Mea-sured
S1	23	1.2	23
S2	278	245	198

Strut level	Strut load in kips		
	Elastic Beom	Finite Element	Mea-sured
S1	34	10	4
S2	200	198	196
S3	336	199	215

Note: Finite element method means the finite element computer program BRACE

FIGURE 5.3.9 STRUT LOADS DURING EXCAVATION TEST SECTION A

SOIL TYPE		YOUNG'S MODULUS E kips/ft²	POISSON'S RATIO μ	LATERAL STRESS RATIO AT REST K_o	STRENGTH PARAMETERS		YOUNG'S MODULUS AFTER YIELDING kips/ft²
					$S_u/\bar{\sigma}_{vo}$	$\bar{\phi}$	
FILL		70	0.3	0.43	0	35°	0.07
SILT	SLIGHTLY ORGANIC SILT	180	0.45	0.5	0.38	0	0.18
	BLACK ORGANIC SILT *	200	0.45	0.5	0.38	0	0.20
TILL		900	0.3	1.0	0	38°	0.90

* PRESENT AT TEST SECTION B ONLY

FIGURE 5.3.10 SOIL PROPERTIES USED IN BILINEARLY ELASTIC ANALYSES OF TEST SECTIONS A AND B BY BRACE

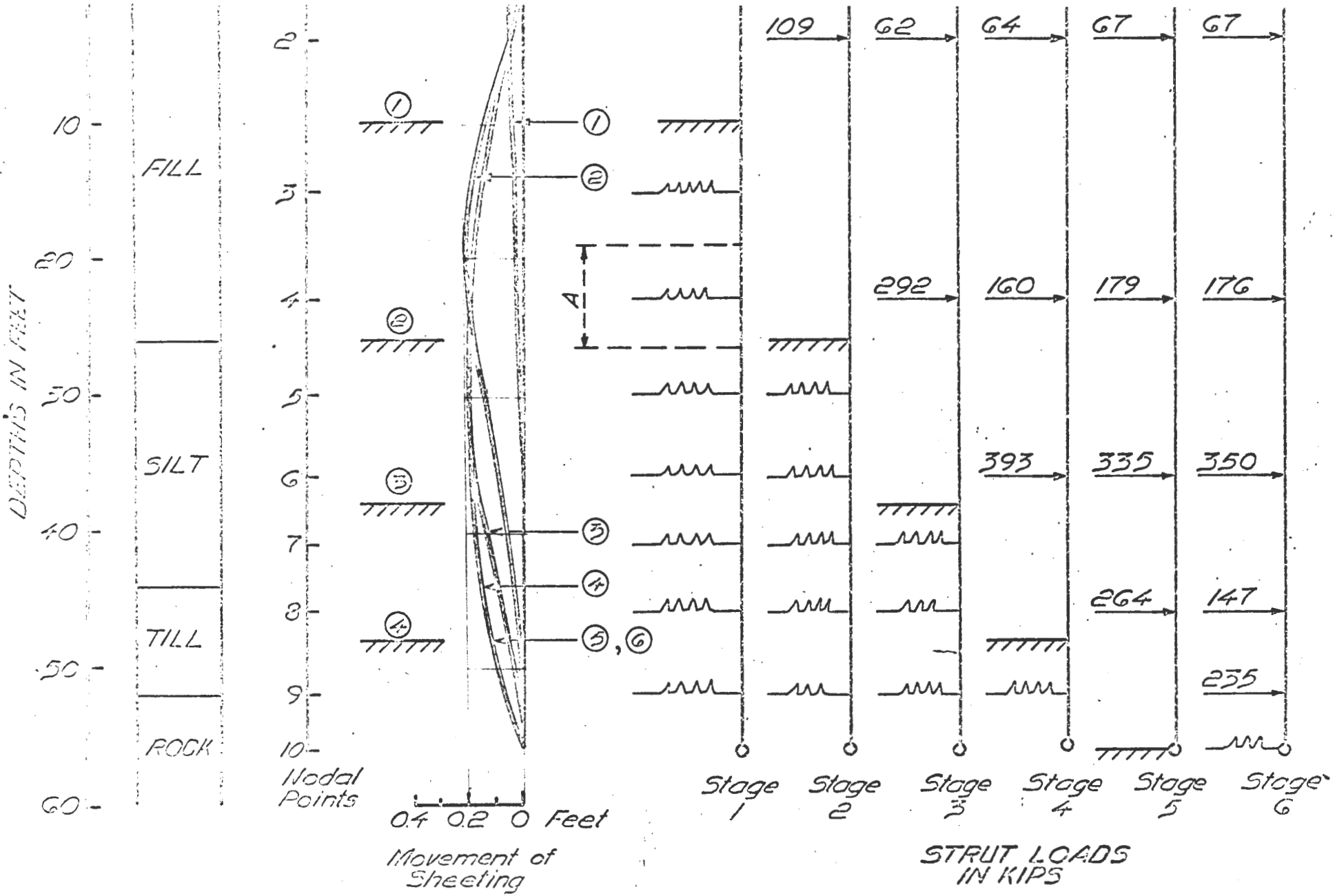

FIGURE 5.4.1 PREDICTED WALL MOVEMENT - ELASTIC BEAM WITH SPRINGS
TEST SECTION B

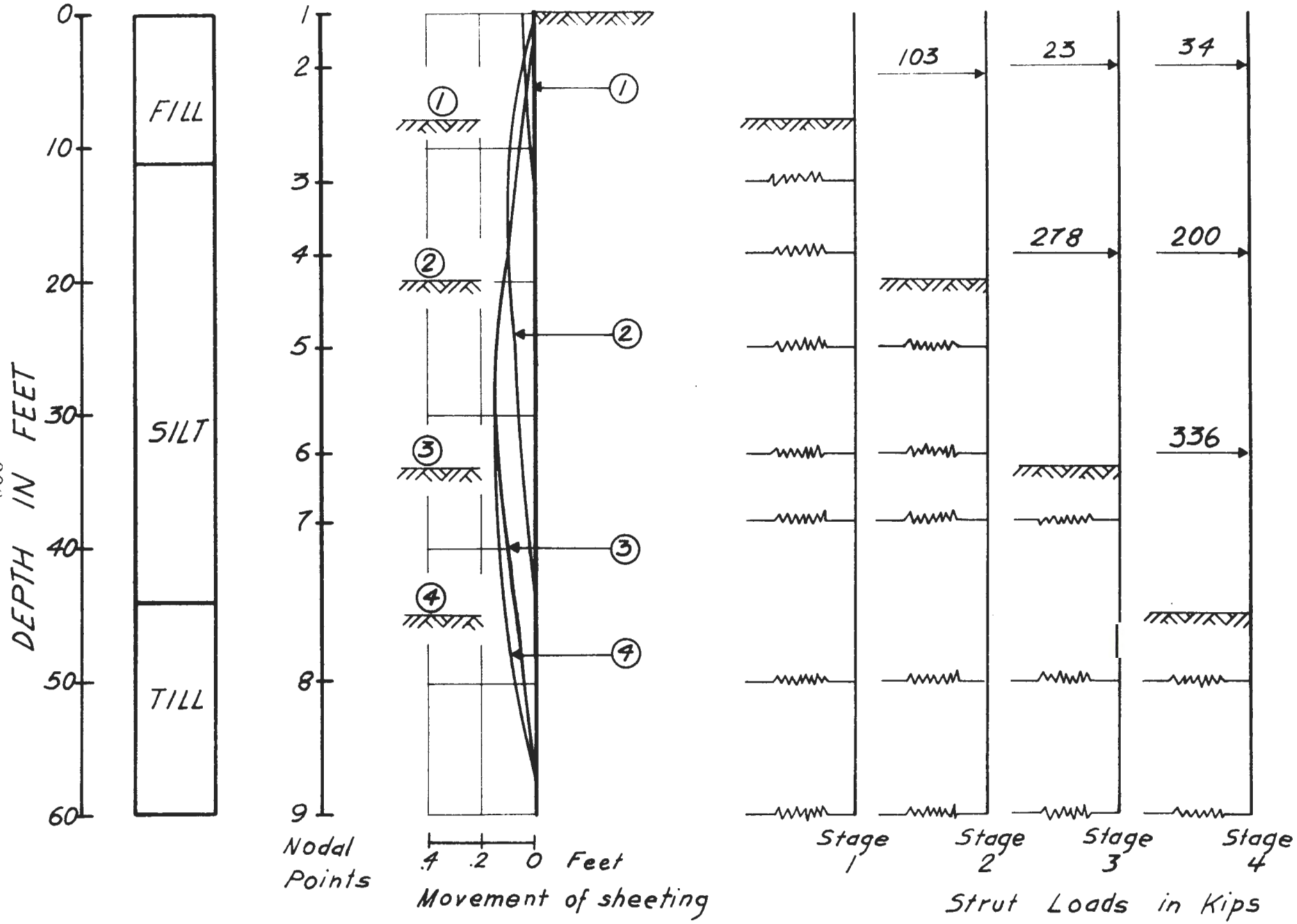

FIGURE 5.4.2 PREDICTED WALL MOVEMENT - ELASTIC BEAM WITH SPRINGS
TEST SECTION A

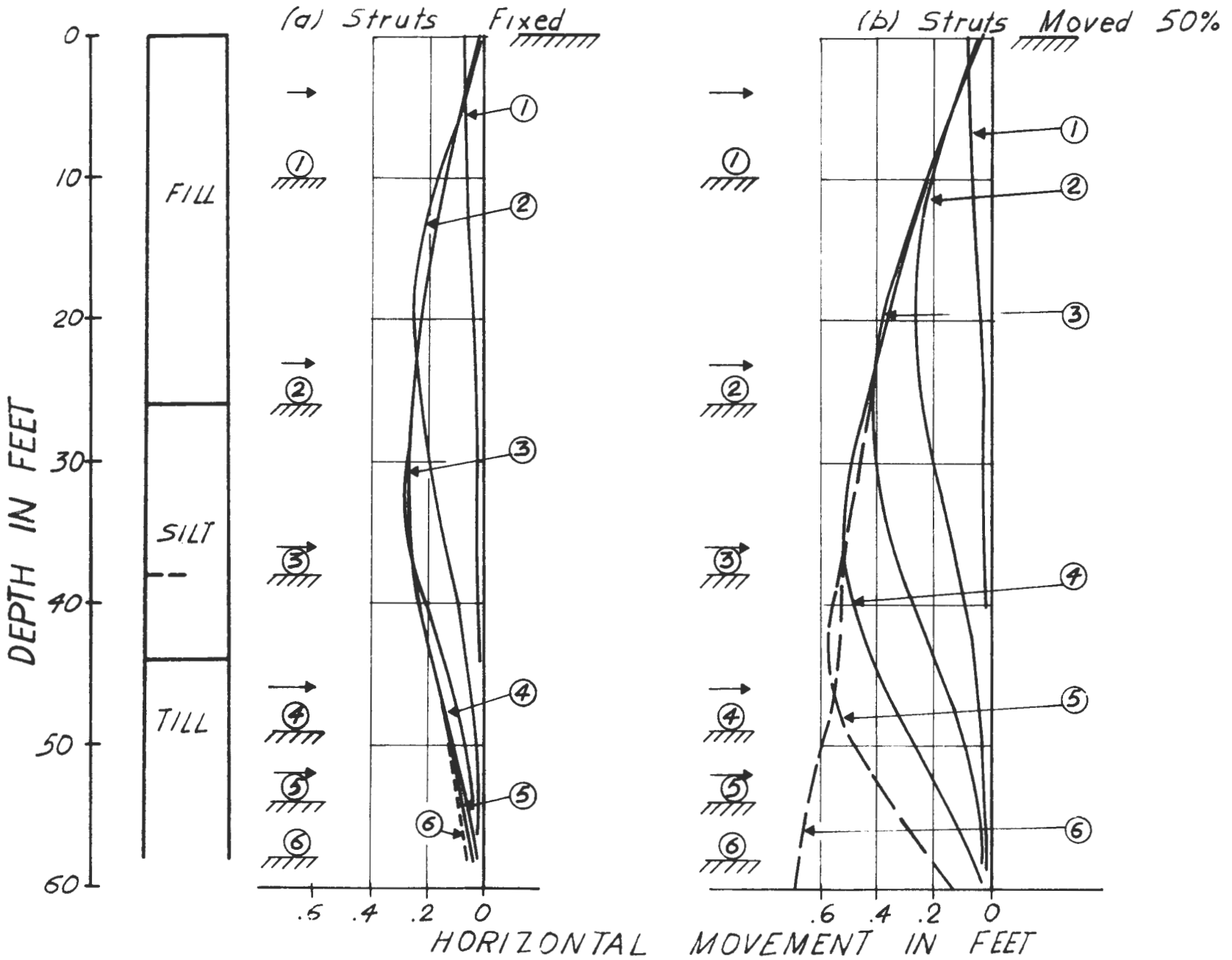

FIGURE 5.4.3 PREDICTED WALL MOVEMENTS - FINITE ELEMENT PROGRAM BRACE TEST SECTION B

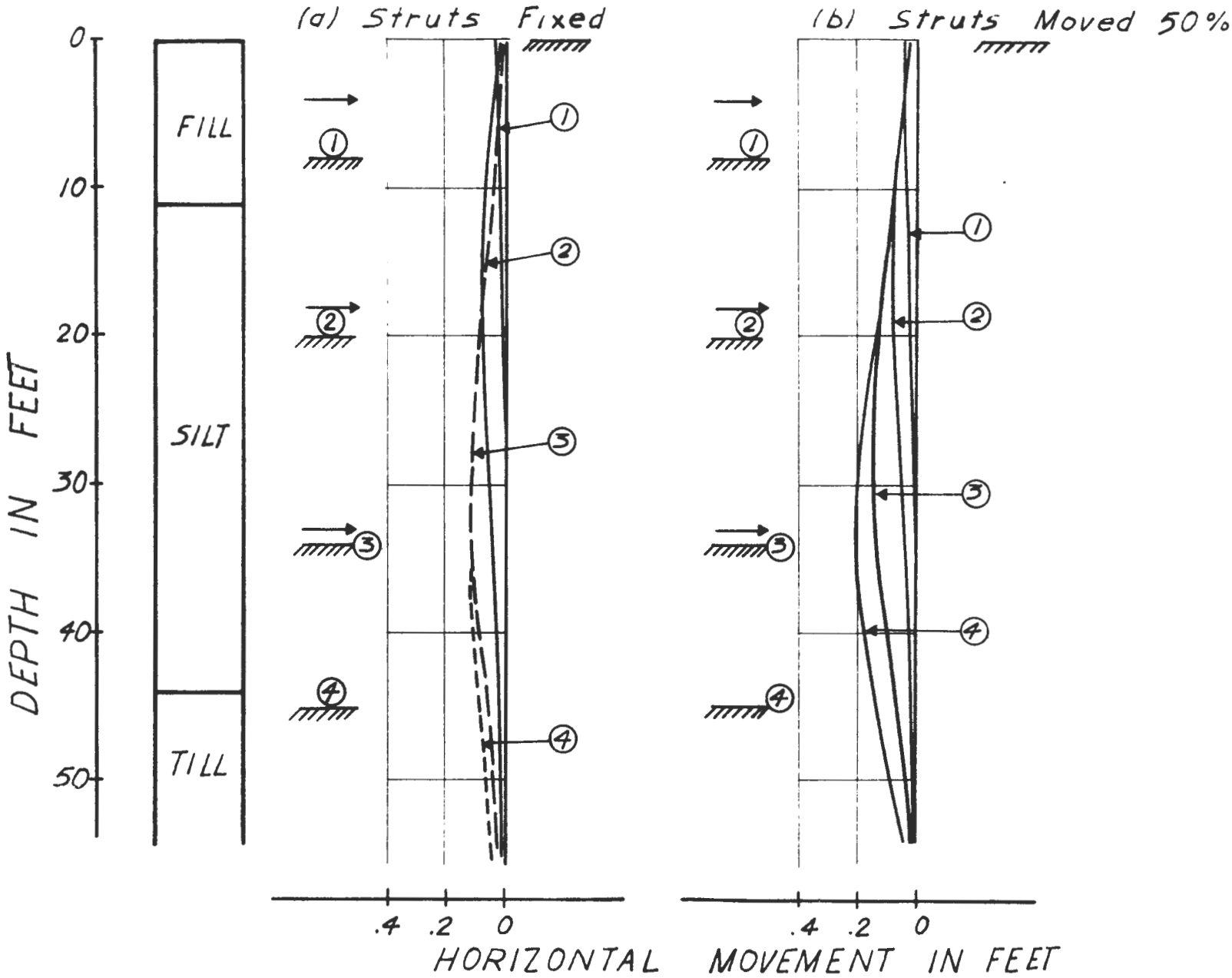

FIGURE 5.4.4 PREDICTED WALL MOVEMENT - FINITE ELEMENT PROGRAM
BRACE TEST SECTION A

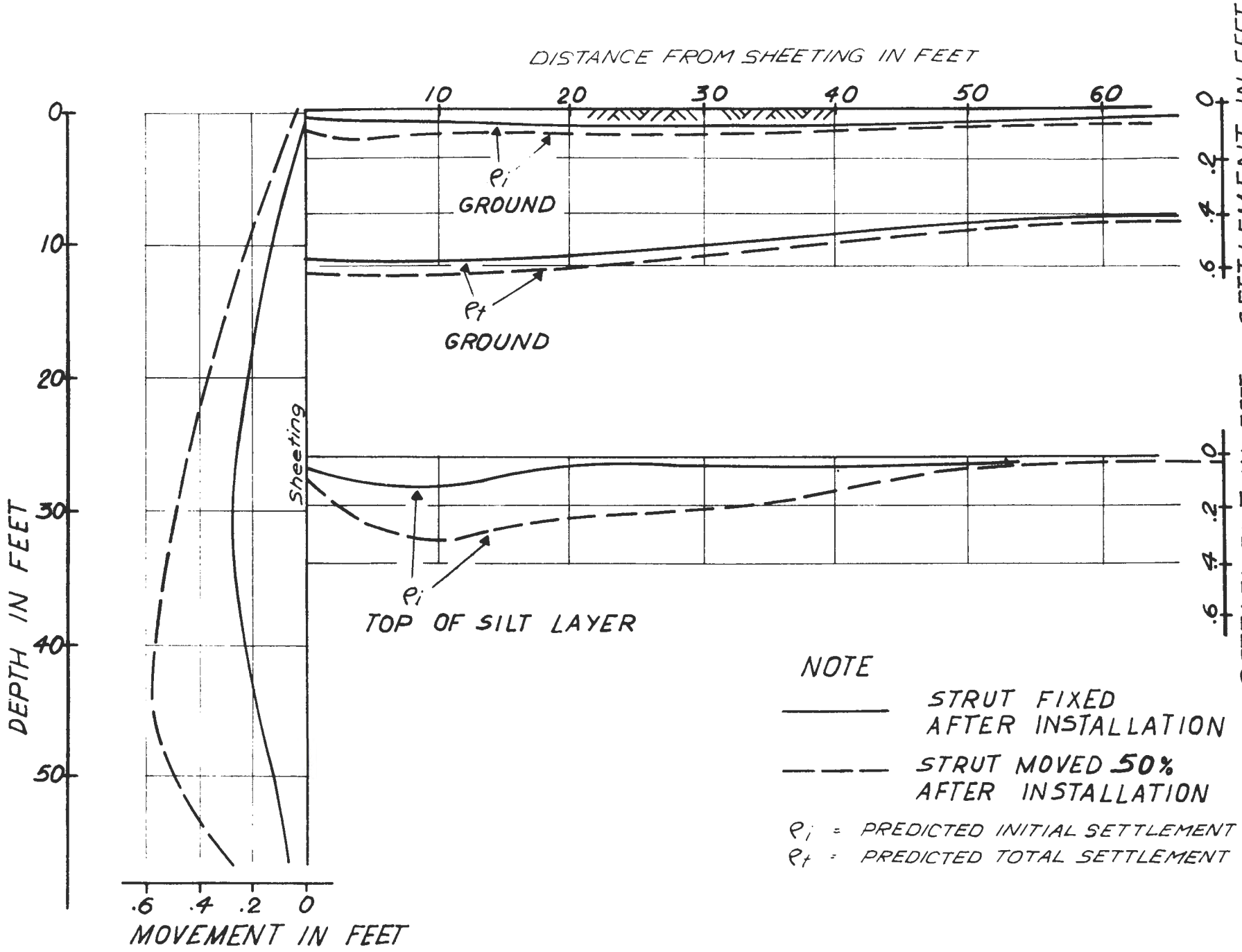

FIGURE 5.5.1 PREDICTED MOVEMENTS AT TEST SECTION B

STRUT NUMBERS	STRUT LOAD IN KIPS								
	TERZAGHI – PECK METHOD			TSCHEBOTARIOFF SUBMERGED SAND + Us	NAVDOCK CLAY	ELASTIC BEAM WITH SPRINGS	FINITE ELEMENT METHOD	MEASURED LOADS	DESIGN LOADS
	SAND	CLAY	SUBMERGED SAND + Us						
S1	182	230	100	92	221	109	107	92	170
S2	215	580	279	290	580	292	280	210	493
S3	154	420	319	335	420	393	326	296	605
S4	108	292	280	288	290	264	343	266	566
S5	75	219	241	230	151	235	264	247	615

FIGURE 5.6.1 MAXIMUM STRUT LOADS TEST SECTION B

STRUT NUMBERS	STRUT LOAD IN KIPS							
	TERZAGHI – PECK METHOD			TSCHEBOTARIOFF SUBMERGED SAND + LS	NAVDOCK CLAY	ELASTIC SPRING	FINITE ELEMENT	MEASURED
	SAND	CLAY	SUBMERGED SAND + LS					
S1	117	107	61	72	96	103	59	23
S2	140	272	201	222	258	278	245	198
S3	136	254	332	335	242	336	199	215

FIGURE 5.6.2 MAXIMUM STRUT LOAD - TEST SECTION A

PREDICTED BY FINITE ELEMENT PROGRAM BRACE			MEASURED
Moximum wall movement in feet			Maximum wall movement in feet
Strut fixed after installation		Strut moved 50% of prior sheeting movement after installation	Typical sheet pile
Test section B	0.29	0.6	0.42 (one particular sheetpile 0.75 ft)
Test section A	0.13	0.21	0.29

FIGURE 5.6.3 MEASURED AND PREDICTED WALL MOVEMENTS MAXIMUM VALUES

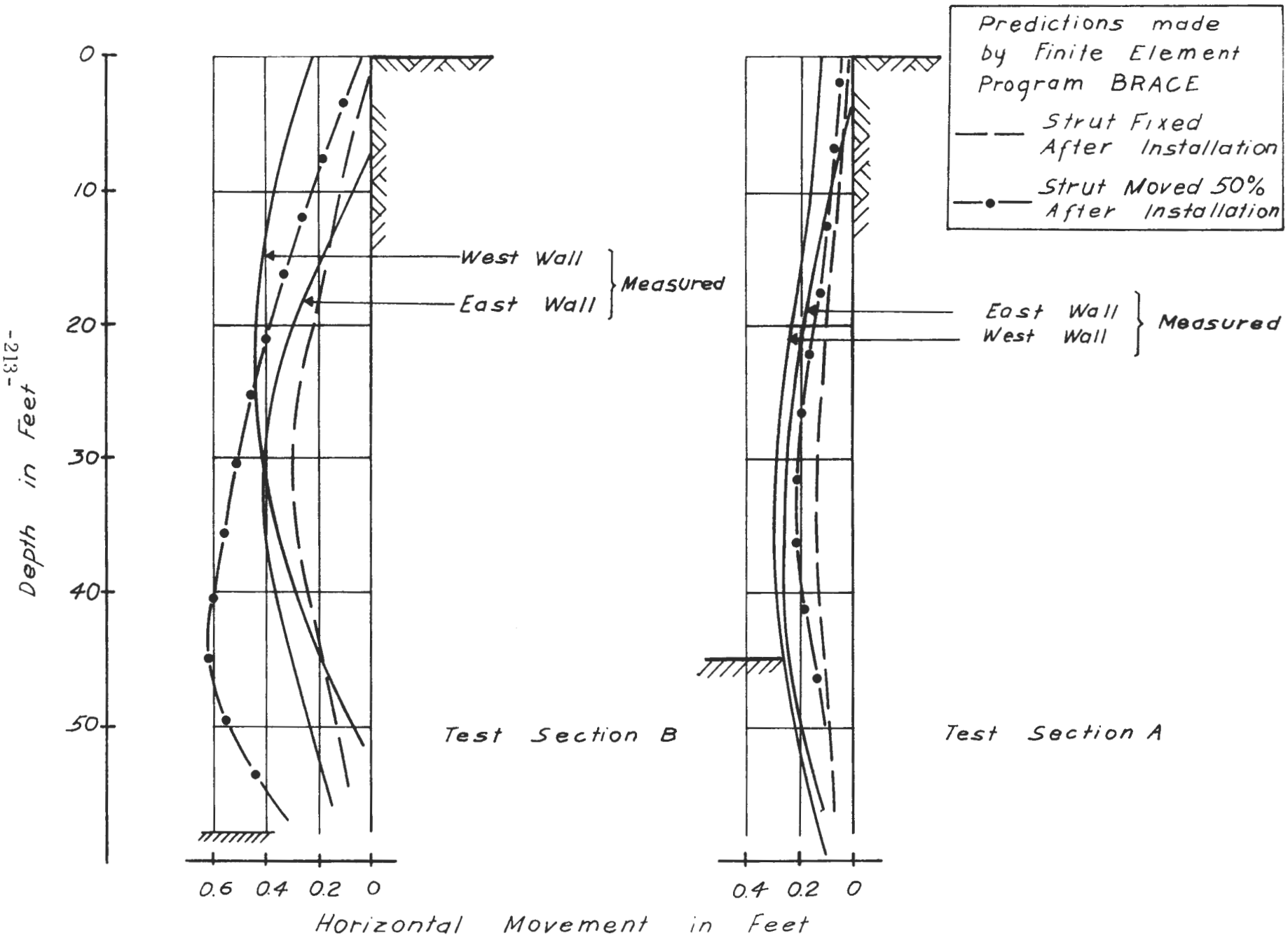

FIGURE 5.6.4 MEASURED AND PREDICTED WALL MOVEMENTS AT FINAL EXCAVATION

APPENDIX I-A

BRACE USER'S MANUAL

Massachusetts Institute of Technology
Department of Civil Engineering
Soil Mechanics Division

PROGRAM BRACE II

Date: December 1970

Modified: February 1972

Language: FORTRAN IV (G Level)

Programmer: J. T. Christian and I. H. Wong

Modified by: W. E. Jaworski and J. T. Christian

I. DESCRIPTION

BRACE II is a finite element program for analyzing braced excavations. It models excavation and bracing construction stages which include prestressing of struts and sheeting displacements due to the deformation of shims.

Problems are restricted to plane strain conditions. Constant strain triangles or quadrilaterals represent the soil mass. The sheeting is represented by one-dimensional bar elements. It is assumed that struts are installed horizontally and their deformations are neglected. Excavation stages are simulated by specifying soil elements and associated nodes to be removed.

Material properties for the soil may be considered as linearly or bilinearly elastic and isotropic or anisotropic. Yield moments can be specified for the sheeting. The program performs a linear elastic incremental load analysis for each construction stage. Total stress

analysis is used and pore pressures are evaluated on this basis. Incompressible materials cannot be specified. The program computes for each construction stage the strut loads, sheeting forces and soil stresses and deformations.

II. PROGRAM CAPABILITIES

The following restrictions are placed on the size of problem which can be input.

Nodal Points	- 290
Elements	- 260
Soil Types	- 20
Strut Sizes	- 2
Sheeting Elements	- 25

Soils must be input as layered systems. Initial stresses can be input for each element or generated by the program.

Plotted output can be obtained from a modified version of CNTRPLOT available at the Soil Mechanics Division, M.I.T.

Computer running time depends on the band width of the global stiffness matrix. For typical problems the running time varys between 1.0 and 1.75 minutes per load increment at each excavation stage and .25 to 1.0 minutes per bracing stage, the greater time resulting from specifying a prestress.

III. INPUT DATA FORMAT

A. Title Card - Format (18A4)

Any title or comment in card columns 1 through 72 will be reprinted at the top of the output. This card must be provided.

B. Control Card - Format (2015)

This card contains control information for the program as follows:

Card Column	Information
1 - 5	Number of Nodal Points in original configuration of problem before excavation (NUMNP) Maximum = 290
6 - 10	Number of Elements in original configuration (NUMEL) Maximum = 260
11 - 15	Number of soil materials (NUMMAT) Maximum = 20
16 - 20	Number of strutting materials (NMSMAT) Maximum = 2
21 - 25	Number of sheeting element (NSHEET) Maximum = 25 If NSHEET = 0 Omit Piling Material Card
26 - 30	Gravity Stress Indicator (IGRAV) If IGRAV = 0 initial stresses are set equal to 0. If IGRAV = 1 initial stresses are calculated from γ and K_o from Card D-1
31 - 35	Excess Pore Pressure Indicator (NPOREC) Put NPOREC = 1 if excess pore pressures due to total stress changes are to be computed for any one or all layers
36 - 40	Initial Pore Pressure Indicator (NPORE) -1 hydrostatic initial pore pressure 0 no initial pore pressure 1 nonstatic initial pore pressure

41 - 45	Plotting Indicator (IPLOT) IPLOT should be $\neq 0$ even if no plot is to be generated before excavation is initiated (see Instruction Card).
46 - 50	Surface loading card (ILOAD) ILOAD = 1 surface load present before excavation and before sheeting is driven. Deformations due to these surface loads will not be superposed to deformations after sheeting is driven. ILOAD = 2 surface load present before excavation and after sheeting is driven.
51 - 55	Settlement Indicator (ISETLE) If ISETLE $\neq 0$ Parameters needed to compute I D settlement or heave due to dissipation of excess pore pressure will be read in.
56 - 60	Anisotropic Strength Indicator Set NDELSU = 1 for card E 1 to be read in.
61 - 65	Soil sheeting Interface Card. If NADD > 0 slipping between soil and sheeting is allowed.
66 - 70	Number of load increments (NLDINC) NLDINC should be ≥ 1. At each increment the load applied will be total load/NLDINC.
71 - 75	Capillarity Indicator (ICAPIL) If ICAPIL $\neq 0$, capillary pore pressures will be considered in calculating effective vertical stresses.
75 - 80	Nodal Point Update Indicator (IUPDAT) If IUPDAT > 0, nodal coordinates are updated.

C. Piling Material Card - Format (3F10.0)

Omit if NSHEET = 0

Card Column	Information
1 - 10	Young's Modulus, E
11 - 20	Moment of Inertia
21 - 30	Cross Section Area
31 - 35	(IVSC) Axial Stiffness = 0 if IVSC = 1
36 - 45	Sheeting Yield Moment (YMOM) If YMOM = 0 the sheeting has no rotational stiffness.

D. Soil Material Cards - Format (I5, F5.0, 3F10.0, 2F5.0, 2F10.0, 2F5.0)

One card per soil type from number (one) to a maximum number of 20. Cards to be input sequentially.

Card Column	Information
1 - 5	Soil Number
6 - 10	K_o
11 - 20	Unit Weight, γ
21 - 30	Young's modulus in the Vertical Direction, E_v
31 - 40	Young's modulus in the Horizontal Direction, E_h
41 - 45	Poisson's ratio from Vertical to Horizontal, ν_{VH}
46 - 50	Poisson's Ratio from Horizontal to Horizontal, ν_{HH}

51 - 60	Blank
61 - 70	Cohesion, C or undrained shear strength when the major principal stress is vertical (S_{uv})
71 - 75	Friction angle, $\bar{\phi}$
76 - 80	Yield Factor

Notes: If E_H is input as zero, an isotropic material is assumed with $E = E_V$, and $\nu = \nu_{VH}$. For anisotropic soils the modulus for an element is a function of the angle (θ) between the major principle stress and the vertical plane and is taken as

$$E_\theta = E_H - (E_H - E_V) \cos^4 \theta.$$

E. Material Properties - Second Set - Card (15, 5X 5F10.0, 512)

If (NPOREC ≠ 0) this set of cards will be read in. One card per soil type from number 1 to a maximum number of 20. Input cards sequentially.

Card Column	Information
1 - 5	Information
5 - 10	Blank
11 - 20	Shear strength when major principal stress is rotated 90° (S_{uh})
21 - 30	Shear strength when major principal stress is rotated 45° (S_{u45}). If left blank: $S_{u45} = \frac{1}{2}(S_{uv} + S_{uh})$. The shear strength $S_{u\theta}$ of an element is dependent on the angle θ between the major principle stress and the vertical plane. An elliptical strength variation is used (Davis and Christian, 1970) in the program. The equation describing the yield criterion is: $\left(\frac{\sigma_y - \sigma_x}{2} - \frac{S_{uv} - S_{uh}}{2}\right)^2 + \tau_{xy}^2 \frac{a^2}{b^2} = a^2$

where $b/a = \dfrac{S_{u45}}{\sqrt{S_{uv} S_{uh}}}$

$$a = \frac{S_{uv} + S_{uh}}{2}$$

31 - 40	Henkel pore pressure parameter a. a is a constant $\Delta U = \Delta\sigma_{oct} + a\Delta\tau_{oct}$
41 - 50	Blank
51 - 60	Yielded Poisson's ratio
61 - 62	Modulus Indicator 1 Modulus normalized with respect to $\bar{\sigma}_v$ 0 Constant modulus with depth 1 Modulus normalized with respect to $\bar{\sigma}_{oct}$
63 - 64	Strength indicator 1 Strength normalized with respect to σ_v 0 Constant with depth -1 Strength normalized with respect to σ_{oct}
65 - 66	Pore Pressure Curve Indicator 1 Henkel parameter a will be a continuous function with maximum shear strains
67 - 68	Yield Poisson's Ratio Indicator 1 Bulk modulus computed using yielded Poisson's ratio 0 Bulk modulus constant during shear
69 - 70	Anisotropic Strength Indicator If zero, isotropic shear strength is used for that material

E.1 Nonuniform Henkel Parameter Card - (2I5, 2F10.0)

If column 65 - 66 in Card E is nonzero, the following set of cards will immediately follow that card for that material.

Card Column	Information
1 - 5	Number of data points of maximum shear strains to be read in.
6 - 10	Number of data points of Henkel's pore pressure coefficients a to be read in.
11 - 20	Constant Henkel's pore pressure coefficient a.
21 - 30	Maximum shear strain beyond which Henkel's coefficient a is constant.

F. One-Dimensional Settlement Card (I5, 5X, 5F10.0)

If Column 51 - 55 (ISETLE) $\neq 0$, the following cards must be supplied, one for each material.

Card Column	Information
1 - 5	Soil Number
6 - 10	Blank
11 - 20	Void Ratio at ℄ of Layer
21 - 30	Virgin Compression Index
31 - 40	Compression Index in 0 - C range
41 - 60	Effective stress at ℄ of Layer

G. Strutting Material Card - Format (I5, 2F10.0)

If no strutting material is desired, NMSMAT should be set to zero and this card may be omitted. No more than two types of strutting can be used.

Card Column	Information
1 - 5	Material Number
6 - 15	Young's modulus
16 - 25	Cross-sectional area

II. Nodal Point Cards - Format (15, F5.0, 4F10.0, 15)

Cards should be input in increasing order of number of nodal points. If cards are omitted, the nodal points will be generated along a straight line between the two points before and after the omitted ones. All such generated points will be unrestrained and will have no load on them except as caused by gravity stress and excavation or bracing.

Card Column	Information
1 - 5	Nodal Point Number (N)
6 - 10	Loading Code:
	Code
	0 — UX(N) is a force; UZ(N) is a force
	1 — UX(N) is a displacement; UZ(N) is a force
	2 — UX(N) is a force; UZ(N) is a displacement
	3 — UX(N) is a displacement; UZ(N) is a displacement
11 - 20	X coordinate (X (N))
21 - 30	Z coordinate (X (N))
31 - 40	UX(N) if necessary
41 - 50	UX(N) if necessary
51 - 55	KOD If $\neq 0$, all generated succeeding points will have the same code.

I. Soil Element Cards - Format (615)

Cards should be input in order of increasing element number. If cards are omitted elements will be generated by adding one to each of the nodes of the preceeding element. Material

numbers are kept constant in the generation. The last element must be input.

Card Column	Information
1 - 5	Element Number (M)
6 - 10	Node Number I
11 - 15	Node Number J
16 - 20	Node Number K
21 - 25	Node Number L
26 - 30	Material Number

Note: Nodes must be numbered in a rotational order from the positive X to positive Z (axes), i.e., counter clockwise for the usual convention of Z positive upwards and X positive to the right. Triangular elements are described by making K = L. The maximum difference between nodes for any element must not exceed 26.

J. Sheeting Element Cards - (615)

If NSHEET = 0, omit this card.

Card Column	Information
1 - 5	Element Number
6 - 10	Nodal Number I
11 - 15	Nodal Number J

Intermediate Element Cards will be generated. Only end Cards need be input. Maximum allowable difference between first and last sheeting node number is 26.

K. Plot Control Card - Format (I2, F9.4, F5.1, 6F8.3)

This card is used only if plots are requested.

Card Column	Information
1 - 2	Integers '01'

3 - 11	Blank
12 - 16	Distortion Factor for displaced mesh, DMESH. Displacements are multiplied by this factor to obtain an exaggerated plot.
17 - 22	Vector scale factor for principal stress plots, SPLOT. Value is length of largest vector in grid units.
23 - 28	Delta Sigma X contour plot code
29 - 34	Delta Sigma Z contour plot code
35 - 40	Tau XZ contour code
41 - 46	Tau maximum contour code
47 - 52	Maximum shear strain contour code
53 - 58	Excess Pore Pressure contour code

The contour codes are interpreted thus:

59 - 64	Total Sigma X contour plot code
65 - 70	Total Sigma Z contour plot code

0. or blank - no contour plot desired

Positive - value is the interval between contours

Negative - value is the number of desired contours

The plotting program will find a suitable, even interval.

After these cards are read the computer sets up the problem and solves for any initial loads, displacements or stresses. The following input can follow:

L. Grid Reduction Card - (2F10.0)

To restrict the contours to region of interest. Omit if no plot is wanted.

Card Column	Information
1 - 10	Extreme Left X-coordinate of grid to be shown
11 - 20	Extreme Right X-coordinate of grid to be shown.

M. Pore Fluid Card (2F10.0)

If NPORE (Column 36 - 40, Card B) is -1, this card must be supplied.

Card Column	Information
1 - 10	Depth to water table below ground surface as a positive number
11 - 20	Unit weight of water

Or if NPORE is 1, the following card must be supplied.

Card M-1 (I5, IPE12.4)

Card Column	Information
1 - 5	Element number
6 - 17	Pore Pressures

Card M-1 must be repeated for every element for which there is non-zero pore pressures.

N. Layer Thickness Cards - Format (8F10.0)

These cards are used only if IGRAV is not zero, that is, if initial stresses are to be calculated. Each card contains up to eight numbers, each of which describes the thickness of one layer of soil. The layer numbers correspond to the soil material numbers on cards D-1 and E-1 and must increase with decreasing depth. Thus, soil 1 is the top layer, soil 2 the next and so on. A maximum of three cards may be needed to describe all twenty permitted layers. The first would read:

Card Column	Information
1 - 10	Thickness of soil 1
11 - 20	Thickness of soil 2
21 - 30	Thickness of soil 3

and so on.

O. Instruction Card - Format (18A4)

This card must have one of the following five sets of characters in card columns 1 through 4:

a. '****' This signals end of problem, if the next four columns also contain '****' execution ends. Otherwise a new problem is read starting with card A.

b. 'EXCA' This means excavation will occur as described under cards P through T below.

c. 'BRAC' This means bracing will occur as described under cards U and V below.

d. 'LOAD' This means new surface loads are input.

e. 'STLE' This means 1-D settlement or heave will be calculated due to dissipation of excess pore pressure.

P. Excavation Control Card (815, 2F10.0, 15)

Card Column	Information
1 - 5	Number of elements to be removed
6 - 10	Number of nodes to be removed
11 - 15	Number of new surfaces exposed by excavation (one surface per element exposed)
16 - 20	Plotting indicator for new configuration, IPLOT
21 - 25	Highest degree of polynomial used for extrapolating stresses at sheeting surfaces. The maximum permissible value is the number of elements in a horizontal row to be removed minus 2 (set = 1 for first 'EXCA')
26 - 30	Number of Load Increments (≥ 1)
31 - 35	Element number for the corner element between old surface and sheeting

36 - 40	Highest degree of polynomial used for corner element. (Cannot exceed the value in cc 21-25 above).
41 - 50	Z-coordinate above which slipping between sheeting and soil occurs. If NADD = 0 leave blank
51 - 60	Normalizing factor for plots.
61 - 65	Output control. If ≥ 1 results for each load increment output. If blank only results from final load increment output.

Q. Elements Removed - Format (815)

Numbers of the elements to be removed are listed, up to 8 per card. As many cards as are necessary are used.

R. Nodal Points Removed - Format (815)

Numbers of the nodal points to be removed are listed, up to 8 per card. As many cards are used as are necessary. If no nodal points are removed the card should be omitted.

S. New Surfaces Exposed - Format (215)

Card Column	Information
1 - 5	First node
5 - 10	Second node

Repeat S for each new surface.

T. Boundary Cards - Format (1615)

These are needed only if plots are requested. The number of nodes at the end of straight lines on the boundaries are listed, 16 per card, on as many cards as needed, up to IPLAT nodes.

Cards P through T should follow the 'EXCA' card. The program will solve for the effects of excavation, print output, and read the next card O.

U. Bracing Card - Format (215, F10.0, 15, F10.0, 2I5)

Card Column	Information
1 - 5	Node at which strut is installed
6 - 10	Strutting material number
11 - 20	Prestress in bracing program computes preload for strut. Input stress in positive direction as negative value

Input stresses as σ_x 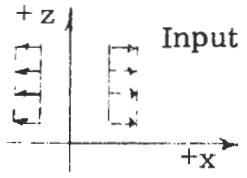 Input stresses as $-\sigma_x$

21 - 25	Plotting indicator, as in 16 - 20 for card P
26 - 35	Crushing of timber wedges at % of movement already occurred at strut level
36 - 40	Load Increment (≥ 1)
41 - 45	Output control. If set ≥ 1 results for each load increment output. If blank only results for final load increment output.

V. Boundary Card - Format (1615)

These are needed only if plots are requested and are identical to card T.

Cards U and V should follow the 'BRAC' card. This program will solve for the effects of the bracing, print output and read the next card O.

If "load" in card O, cards W and X will be read in.

W. Loading Control Card - (15)

Card Column	Information
1 - 5	Total number of nodes subject to external loads

6 - 10	Plotting Indicator as in CC-16-20 for card P
11 - 15	Number of Load Increments (NLDINC)
	If NLDINC = 0, only the nodal codes are changed.

X. Loading Cards

Card Column	Information	
1 - 5	Node number	See Card H
6 - 10	Nodal Code	
31 - 40	UX(N)	
41 - 50	UX(N)	

As many cards are needed as number of loading points.

If 'STLE' in card O, the following cards will be read in.

Cards Y-2 - (1615)

Element numbers in a string which contribute to heave of settlement. As many cards as needed.

Cards Y-3 - (15)

Card Column	Information
1 - 5	Total number of nodes in a string which heave or settle.

Cards Y-4 - (1615)

Node numbers in a string which heave or settle . As many cards as needed.

Hardware Requirements

The program required that scratch discs or tapes be set up on logical units 8, 11, 12 and 13. If plots are desired the required data can be written on data set reference number 7, as described by Job Control Language (JCL) cards or the

required cards punched. The program requires 450K bytes of computer core.

Recommended JCL cards for the 370-M155 IBM computer at the MIT Information Processing Center are as follows:

```
//  'Name', CLASS=B, REGION=450K
/*MITID  USER=((MMMMM, NNNN)
/*SRI
/*MAIN  TIME=TT, LINES=LL, CARDS=CC
//C.SYSIN  DD  *
  SOURCE DECK
/*
//G.FT08F001  DD  UNIT=SYSDA, SPACE=(816, (1200, 200)),
//  DCB=BLKSIZE=816
//G.FT11F001  DD  UNIT=SYSDA, SPACE=(1280, (600, 100)),
//  DCB=BLKSIZE=1280
//G.FT12F001  DD  UNIT=SYSDA, SPACE=(0312, (034, 010)),
//  DCB=BLKSIZE=0312
//G.FT13F001  DD  UNIT=SYSDA, SPACE=(0560, (110, 030)),
//  DCB=BLKSIZE=0560
```

DATA

```
/*
```

Where

MMMMM = Problem Number, NNNN = Programmer Number

TT = Maximum time to run problem

LL = Maximum lines of output, thousands

CC = Maximum cards output, hundreds.

APPENDIX I-B

DETAILS OF ONE-DIMENSIONAL BAR ELEMENTS USED FOR THE SIMULATION OF WALL

This appendix describes the details of the one-dimensional bar elements used for the simulation of the retaining wall.

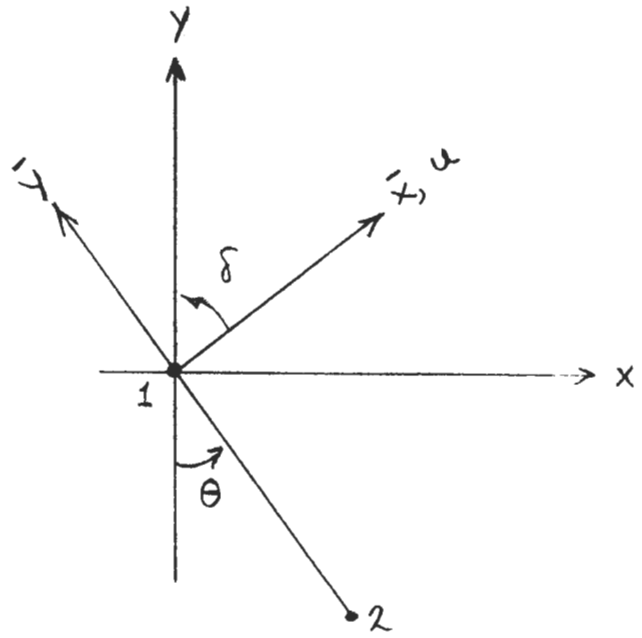

x, y is the global coordinate system.

$\bar{x}$, $\bar{y}$ is the local coordinate system.

Figure B-1 Arbitrarily Oriented Element

For an arbitrarily oriented one-dimensional bar element (Fig. B-1) carrying combined bending and axial loading, the element stiffness matrix [S] is as follows:

$$[S] = \frac{E}{L}\begin{bmatrix}
u_1 & v_1 & u_2 & v_2 & \delta_1 & \delta_2 \\
\frac{12I}{L^2}\mu^2 + A\lambda^2 & (\frac{12I}{L^2} - A)\lambda\mu & -(\frac{12I}{L^2}\mu^2 + A\lambda^2) & -(\frac{12I}{L^2} - A)\lambda\mu & -\frac{6I}{L}\mu & -\frac{6I}{L}\mu \\
 & \frac{12I}{L^2}\lambda^2 + A\mu^2 & -(\frac{12I}{L^2} - A)\lambda\mu^2) & -(\frac{12I}{L^2}\lambda^2 + A\mu^2) & -\frac{6I}{L}\lambda & -\frac{6I}{L}\lambda \\
 & & (\frac{12I}{L^2}\mu^2 + A\lambda^2) & (\frac{12I}{L^2} - A)\lambda\mu & -\frac{6I}{L}\mu & -\frac{6I}{L}\mu \\
 & & & -(\frac{12I}{L^2}\lambda^2 + A\mu^2) & -\frac{6I}{L}\lambda & -\frac{6I}{L}\lambda \\
 & & & & 4I & 2I \\
 & \text{Symmetrical} & & & & 4I
\end{bmatrix}$$

where

$\mu = \cos\theta, \quad \lambda = \sin\theta$

A = area of cross section of element

E = Young's modulus of element

L = axial length of element

I = moment of inertia of element

u and v are the translations in the $\bar{x}$ and $\bar{y}$ directions and δ is the rotation

Subscripts 1 and 2 refer to the nodes.

For a system of m bar elements the total stiffness [H] is

$$[H] = \sum_{1}^{m} [S]$$

The equilibrium equations for the system of m bar elements involve 3(m+1) equations and are written in the following partitioned matrix form:

$$\left[\begin{array}{c} q_t \\ \hline q_r \end{array}\right] = \left[\begin{array}{c|c} H_{tt} & H_{tr} \\ \hline H_{rt} & H_{rr} \end{array}\right] \left[\begin{array}{c} u_t \\ \hline u_r \end{array}\right] \qquad \text{(B.1)}$$

where (q) is the nodal force vector and (u) is the nodal displacement vector. The subscripts t and r represent respectively the translational and the rotational degress of freedom. $[H_{tt}]$ has a "half-band" width of 4 and $[H_{rr}]$ has a "half-band" width of 2.

Equation B.1 may be written as two matrix equations or

$$(q_t) = [H_{tt}]\ (u_t) + [H_{tr}]\ (u_r)$$

$$(q_r) = [H_{tr}]\ (u_t) + [H_{rr}]\ (u_r)$$

Eliminating (u_r) we get

$$(\bar{q}_t) = [\bar{H}_{tt}]\ (u_t)$$

where

$$[\bar{H}_{tt}] = [H_{tt}] - [H_{tr}]\,[H_{rr}]^{-1}\,[H_{tr}]$$

and

$$(\bar{q}_t) = (q_t) - [H_{tr}]\,[H_{rr}]^{-1}\,[q_r]$$

Now $[\bar{H}_{tt}]$ is a fully populated 2(m+1) x 2(m+1) matrix. It is the statically condensed stiffness matrix expressing the stiffness of the wall in terms of the translational degree of freedom.

In the finite element computer program BRACE the stiffness matrix [T] for the complete system of n soil elements and m wall elements is given by the summation

$$[T] = \sum_{1}^{n} [K] + [\overline{H}_{tt}] .$$

Note that in Chapter Two [SH] is used to represent the total stiffness matrix of the wall both before and after static condensation.

The computer program BRACE contains an option through which the stiffness of the wall element in the axial direction is reduced to the initial modulus of the soil element adjacent to it if the soil element has yielded. In this way slippage between soil and wall is considered.

It is not possible to assess at this stage the effect of the lack of compatibility between a wall element and a soil element on the accuracy of the solution obtained. This is a topic for future investigation.

Haliburton (1968) analyzes retaining walls using the finite difference method and the theory of beams on elastic foundations. His method of analysis considers the nonlinear stress-strain response of the soil. However, its application to braced excavation problems is restricted as it does not simulate excavation and strut installation in a sequential manner and does not solve for the movements of the soil adjacent to the excavation.

APPENDIX I-C

ESTIMATION OF SOIL PARAMETERS USED FOR THE PREDICTION OF THE PERFORMANCE OF TEST SECTIONS A AND B MADE BY BRACE

This appendix explains how the soil parameters used for the prediction of the performance of Test Sections A and B made by BRACE were estimated. These parameters are shown in Fig. 5.3.10.

The undrained shear strength of the silt was the peak value obtained from $\overline{CIU}$[1] triaxial tests. The friction angle of the fill was obtained from a CID triaxial test. The friction angle for the till was based on empirical correlations between standard penetration resistance and friction angles for granular soils (Peck et al, 1953 and Teng, 1962) and on representative values of friction angles for granular soils (Sowers and Sowers, 1951 and Terzaghi and Peck, 1967). The strength parameters chosen for the fill, silt and till have been reported by Golder et al (1970) and Lambe et al (1970). In the predictions made by BRACE, the strength of the fill and of the till varied with the effective confining pressure, but the strength of the silt was independent of the confining pressure during shear.

The lateral stress ratios at rest for the fill and for the silt were computed from $K_o = 1 - \sin \phi$. The till was overconsolidated and its K_o value was guessed to be 1.0.

The Young's modulus (E) of the slightly organic silt was computed from $E = 300\ S_u$ where S_u was the undrained shear strength from unconfined compression tests (Bjerrum, 1964). For the black organic silt E was estimated in two ways. The first was to use $E = 300\ s_u$. The second way was to calculate the secant modulus at 1% axial strain from stress-strain curves based on $\overline{CIU}$ triaxial tests.

---

[1] $\overline{CIU}$ means isotropically consolidated undrained tests with pore pressure measurements and CID means isotropically consolidated drained tests.

The modulus used for the black organic silt was the average of the values based on these two methods. The modulus of the fill was computed at 0.5% axial strain from the stress-strain curve obtained from a CID triaxial test. The modulus of the till was estimated (guessed) in two ways. The first way was to treat the till as a granular material and to obtain the average modulus from a range of values listed in Table 12.3 in Lambe and Whitman (1969). The second way was to compute the average of the undrained active and passive moduli from stress-strain curves obtained in plane stress tests performed by Bocee (1970) on samples of Boston blue clay having an OCR of 4. The moduli were the secant moduli from the K_o condition to the stress level equal to 50% of the stress level at failure. The drained modulus was computed from the average undrained modulus using the expression

$$E_{drained} = \frac{1+\mu_{drained}}{1+\mu_{undrained}} \times E_{undrained}.$$

As the till consisted of layers of clay, sand, and gravel the average of the moduli for the sand and for the clay was used as the modulus for the till.

The Poisson's ratio of 0.3 used for the fill and the till was typical for drained soils. The Poisson's ratio of 0.45 used for the silt was to account for some partial drainage. After an element yielded its modulus was reduced to one thousandth of its initial modulus.

The samples of the fill and silt used in the triaxial tests were obtained from Test Section B. The moduli shown in Fig. 5.3.10 were calculated for the center line of the soil layers at Test Section B. For Test Section A the same values were used except for the loosely dumped sand backfill in the trench behind the sheeting where a

guessed modulus of one tenth that of the fill layer and a guessed friction angle of 28^{o} were used.

PART II - EXPERIMENTAL WORK

PART II

LIST OF FIGURES

Figure No.	Title
1.1	Plan View of Subway Extension
1.2	Cross Section at Test Section B
1.3	Cross Section of Test Section A
2.1	Soil Properties at Test Section B
3.1	Plan View of Test Section B
3.2	Plan View of Test Section A
3.3	Section ll Looking North Test Section B
3.4	Section pp Looking North Test Section A
4.1	Water Flowing into Excavation
4.2	Water Flowing Through Holes in Sheeting - Test Section A
4.3	Water Flowing Through Ruptured Joints in Sheeting - Test Section B
4.4	Crushing of Timber Wedges
5.1	Measured Total Head of Middle of Section nn - Test Section B
5.2	Total Head Along Section II - Test Section B
5.3	Test Section A - Total Head
5.4	Pore Pressures - Test Section B
6.1	Measured Loads in Struts - Test Section B
6.2	Measured Loads in Struts - Test Section A
6.3	Apparent Total Horizontal Stresses
7.1	Movements Near Excavation - Test Section B
7.2	Measured Horizontal Movements - Test Section B

Figure No.	Title
7.3	Measured Horizontal Wall Movements - Test Section A
7.4	Settlement of Anelex Building
7.5	Comparison of Maximum Wall Movements Near Test Sections A and B

EXPERIMENTAL WORK

MEASURED PERFORMANCES OF TEST SECTIONS A AND B, NORTH STATION, BOSTON

I. INTRODUCTION

Part II reports the measured performances of two test sections of braced excavations in Boston. These two test sections have been instrumented and studied by the Department of Civil Engineering of the Massachusetts Institute of Technology as part of a research project under a contract with the Massachusetts Bay Transportation Authority (MBTA).

The principal researcher in this project is Professor T. William Lambe. Dr. L. A. Wolfskill heads the M.I.T. field instrumentation staff who installed and read the instruments. Appendix A describes the details of the instrumentation at Test Sections A and B, and presents uninterpreted plots of the measurements obtained. Owing to a lack of space, repetitive data obtained with similar instruments are not shown. The complete data collected under this project are available in Room 1-339 at M.I.T. Appendix B describes the data acquisition and management system that was developed to handle the enormous amount of data generated in this research project.

The two test sections are called Test Sections A and B. Their locations are shown in Fig. 1.1. They were part of the braced excavation along Accolon Way for the MBTA subway extension between Haymarket Square and Charlestown.

The cross section of Test Section B is shown in Fig. 1.2. It

was 37 feet wide and 58 feet deep and five levels of struts were used. The cross section of Test Section A is shown in Fig. 1.3. It was 35 feet wide and 45 feet deep. Three levels of struts were used. Test Section B was located between a low building and vacant land, but Test Section A was located between two large buildings.

Excavation at Test Section B started in September 1967 and finished in November 1968. Excavation at Test Section A started in January 1969 and finished in May 1969.

2. SOIL PROFILE

Figures 1.2 and 1.3 show the soil profiles at Test Section B and A, respectively. The thickness of the soil layers were different in the two sections. As a whole, the soil profiles at the two test sections were very heterogeneous, particularly at Test Section B. Slightly different profiles for Test Section B are used in some figures of Part I and Part II showing the writer's judgment in selecting the appropriate profiles for different analyses.

At both sections the stratigraphy from the top down included fill, silt, till and rock. The fill was a loose mixture of gravel, sand, silt and clay. At Test Section B the silt graded from light gray slightly organic silt to black organic silt containing shells. At Test Section A it consisted of the slightly organic silt only. The till consisted of layers of sandy silt or clay, sand and gravel, and sandy clay. The fill layer was much thicker and the till layer much thiner at B than at A. The rock was jointed.

At Test Section A the sheeting was driven to the designed depth of about 60 feet. At Test Section B it hit bedrock at 56 feet. However, northward from Station 76+30 (see Fig. 3.1), the till increased rapidly in thickness and the sheeting was driven to its

designed depth.

Figures 1.2 and 2.1 present the soil properties based on laboratory tests on undisturbed soil samples. The permeability values of the soils were obtained from field sensitivity tests on piezometers and deep observation wells.

3. LAYOUT OF FIELD INSTRUMENTS

Figures 3.1 and 3.2 are plan views of Test Sections B and A, respectively.

The devices installed at the two test sections included hydraulic and electrical piezometers, slope indicator tubes, strain gauges, stress cells, and settlement points. The hydraulic piezometers were the double tube Casagrande type (Casagrande 1949). The electrical piezometers were the Genor vibrating wire type (Bjerrum et al, 1965). The slope indicator tubes (Wilson and Hancock, 1960) were installed both on the sheeting and in the soils behind the sheeting. Several of those on the sheeting were perforated to enable them to function as observation wells. Figures 3.3 and 3.4 show the elevations of the sensors of the piezometers and of the tips of the slope indicator tubes in Test Sections B and A, respectively. At Test Section A, two bench marks were installed to the till.

The strain gauges were of the Geonor vibrating wire type (Bjerrum et al, 1965), and were used to measure strut loads. At Test Section B all the struts in six vertical sections and at Test Section A all the struts in nine vertical sections were instrumented. The strain gauges and the electrical piezometers were wired to a switching terminal in an instrumentation shack nearby.

All the stress cells were damaged and rendered inserviceable

during the hard driving of the sheet piles.

Settlement pins were installed on columns of Anelex and North Station Buildings and settlement points were installed under Anelex Building. At Test Section B settlement points were installed.

4. CONSTRUCTION PROCEDURE

Terzaghi and Peck (1967) have shown that details of construction procedure can greatly influence the behavior of a braced excavation. The following are some features of construction important to the behavior of Test Sections B and A.

4.1 Depth of Sheeting

At Test Section B the original design called for driving the sheeting to about 10 feet below the bottom of excavation. However, owing to the presence of the bedrock it was driven only to a depth of 56 feet, while the bottom of excavation was 58 feet deep.

4.2 Control of Ground Water

Water was pumped from a sump to keep the site dry for work. To minimize settlements of nearby buildings, the contractor was required to maintain the total head in the till outside the excavation at or about +95 feet. Despite the recharge wells placed in the till, the total head at both test sections dropped markedly (See Figs. 5.2 and 5.3), particularly at Test Section B. Calculations presented in Part I of this report show that these decreases in total head influenced both strut loads and ground surface settlements.

4.3 Wedging Details

The Contractor was required to preload all struts except the top level of struts to half their design loads. However, owing to the

crushing of timber wedges placed between the wale and the sheeting, a loss in the strut preload occurred upon removal of the jacks. This fact can be detected from Fig. 6.1 which presents the measured strut loads at Test Section B. Figure 4.4 shows some crushed timber wedges.

4.4 Excavation Progress

Excavation progressed longitudinally in a terraced fashion rather than in horizontal lifts. At Test Section B, some stages of excavation proceeded deeper than were necessary to install the struts. Sometimes as much time as two weeks elapsed before the strut was installed after an excavation. At Test Section A, the undercut below each strut level was limited to about 2 feet and the time lapse between excavation and strut installation reduced to 2 or 3 days.

4.5 Underpinning

At Test Section A, the front row of columns of the Anelex and the North Station Buildings were underpinned before the subway excavation started to forestall damage. To do the underpinning a trench 15 feet deep and 5 feet wide was dug in front of each building. These trenches were later backfilled with sand. The backfill was not compacted and was loose. This explains the low loads measured in the first level of struts at Test Section A (see Fig. 6.2).

5. PORE PRESSURE NEAR EXCAVATIONS

As shown in Figs. 4.1 through 4.3, significant seepage into the excavation occurred at both Test Sections A and B.

The ground water problem was caused by (a) a highly pervious gravel stratum in the till, (b) cracks in the rocks at Test Section B,

(c) ruptured joints between sheet piles, (d) holes in the sheet piles, and (e) three-dimensional seepage of water in the till as the till was not of uniform thickness and the sheet piles were not of uniform length.

Figure 5.1 shows the change in total head with time twenty feet from the east wall at Test Section B. Initially, the total head was nearly constant with depth and was between +108 and +110 feet. As excavation proceeded, the total head dropped drastically despite recharging efforts. At the final stage of excavation the total head was as low as +62 feet.

Figure 5.2 shows the contours of the measured total head outside the east wall. It shows that even as far away as 70 feet from the excavation there was a very marked decrease in total head in the till.

At Test Section A many more recharge wells to the till were installed. Still a significant decrease in total head occurred outside the excavation (Fig. 5.3).

Figure 5.4 again shows that the pore pressures on the wall and near the wall were far below static at Test Section B.

At the two test sections grout was used in an attempt to control the seepage, but these grouting efforts were largely unsuccessful as the total heads continued to drop.

6. HORIZONTAL STRESSES AND STRUT LOADS

Figure 6.1 shows the design strut loads and measured strut loads during various stages of excavation for Test Section B, and Fig. 6.2 shows those for Test Section A. At Test Section B the same six struts and at Test Section A the same nine struts were instrumented at each horizontal level.

At Test Section A, north of Strut 8 (Fig. 3.2), a fourth level of struts was installed, and three of these struts were instrumented. The strut loads reported in Fig. 6.2 were measured prior to the installation of the fourth struts.

Figure 6.3 shows the "apparent" pressure diagrams for Test Sections B and A at final excavation. They were backfigured from the measured strut loads by considering the sheeting to consist of independent vertical segments. These diagrams suggest that the distributions of total horizontal stresses against the wall were approximately triangular in shape.

7. MOVEMENTS NEAR EXCAVATION

Figure 7.1 shows the horizontal movements of the sheeting and the settlements of the ground surface outside the excavation at Test Section B. It shows the levels of excavation at various dates as well as the dates of installation of the struts. Figure 7.2 shows the horizontal movements of the sheeting and of slope indicator tubes in the soil twenty feet from the excavation.

Figure 7.1 shows that the maximum horizontal movement towards the excavation of the sheeting was about 5 inches. This movement was typical of the movements of the sheeting at Test Section B. One slope indicator (SIB-7), however, showed a movement of the west sheeting equal to 9 inches. Figure 7.1 also shows large settlements of the ground outside the excavation. The maximum settlements were 5 inches east of the excavation and 10 inches west of the excavation. Calculations presented in Part I of this report show that these settlements were caused both by excavation and by dewatering.

Figure 7.3 shows the horizontal movements of the sheeting at Test Section A as well as the levels of excavation at various dates

and the dates of strut installation. Figure 7.4 shows the contours of the settlements of the Anelex Building, which was a 13-story structure 5 feet from the east sheeting line. The maximum settlement was 0.7 inch.

Figure 7.5 compares the maximum movements of the sheeting toward the excavation at the two test sections, at approximately similar depths of excavation. It is seen that the movements at Test Section A were smaller than at Test Section B. This could be explained by the smaller undercutting at each strut level and the smaller time lag between excavation and strut installations, as noted in Subsection 4.4.

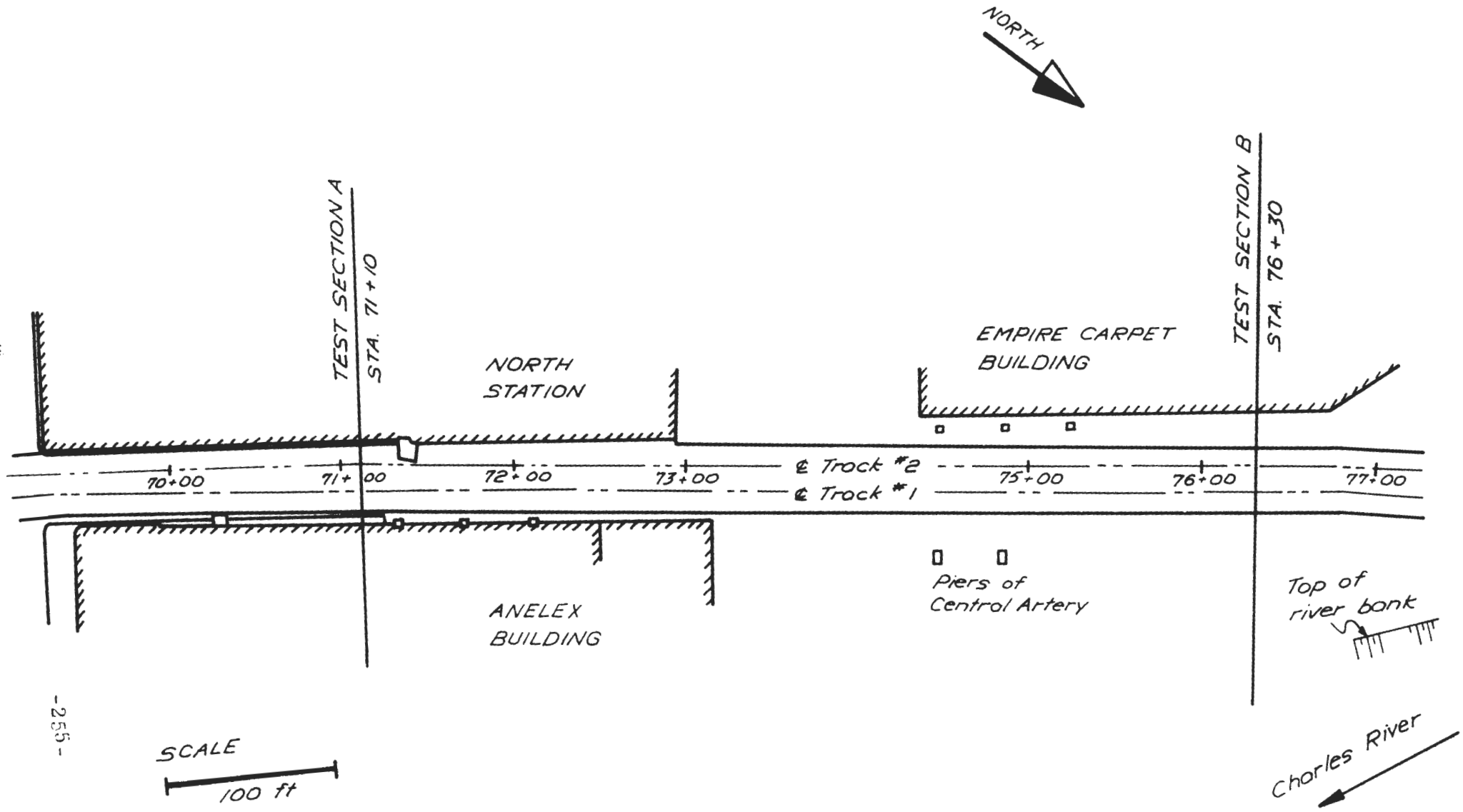

FIGURE 1.1 PLAN VIEW OF SUBWAY EXTENSION

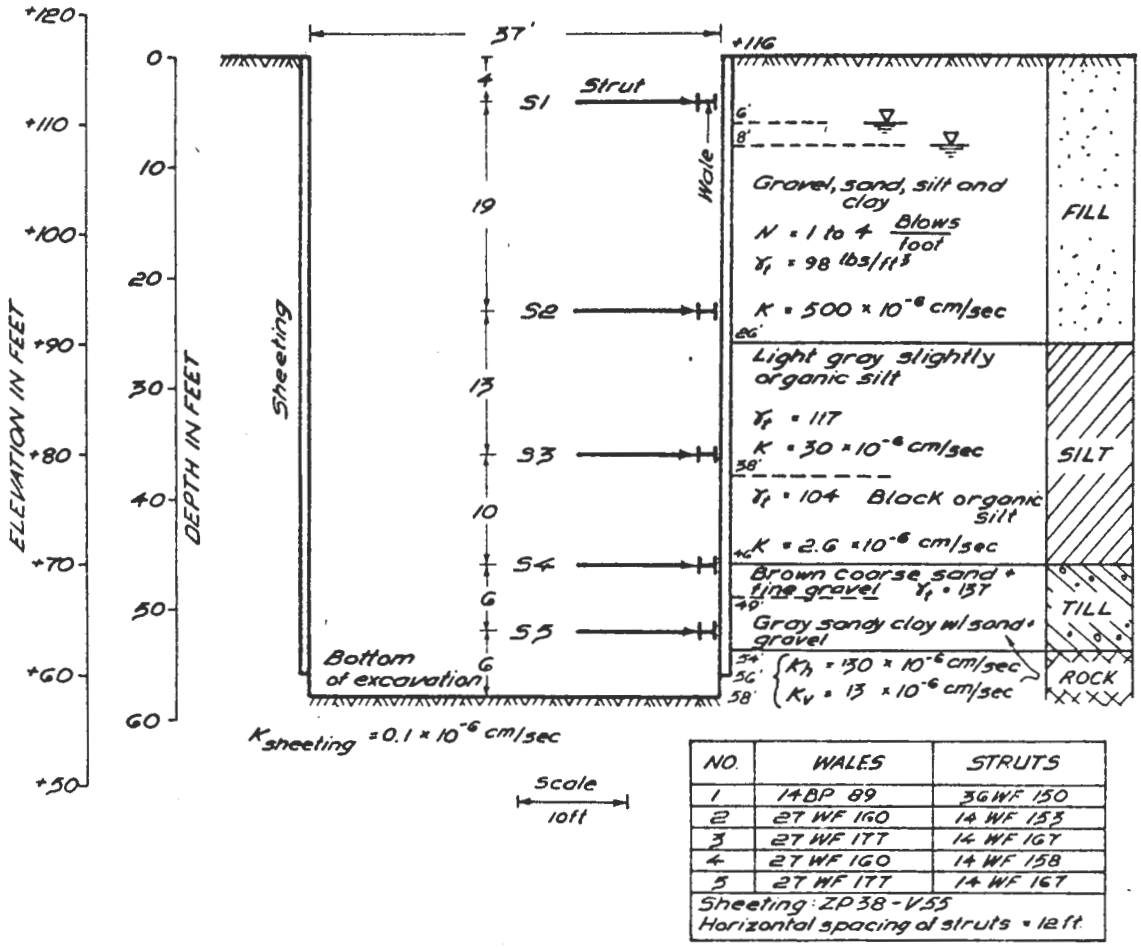

NO.	WALES	STRUTS
1	14BP 89	36WF 150
2	27 WF 160	14 WF 153
3	27 WF 177	14 WF 167
4	27 WF 160	14 WF 158
5	27 WF 177	14 WF 167

Sheeting: ZP38 - V55
Horizontal spacing of struts = 12 ft.

FIGURE 1.2 CROSS SECTION AT TEST SECTION B

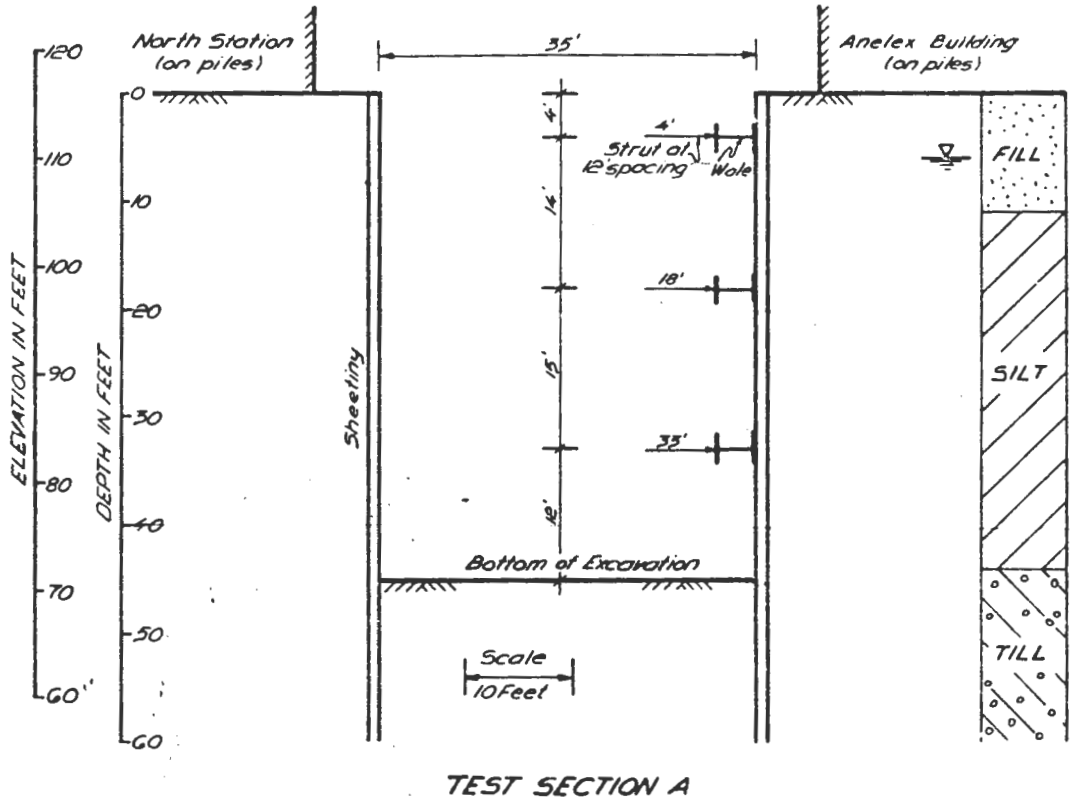

TEST SECTION A

FIGURE 1.3 CROSS SECTION AT TEST SECTION A

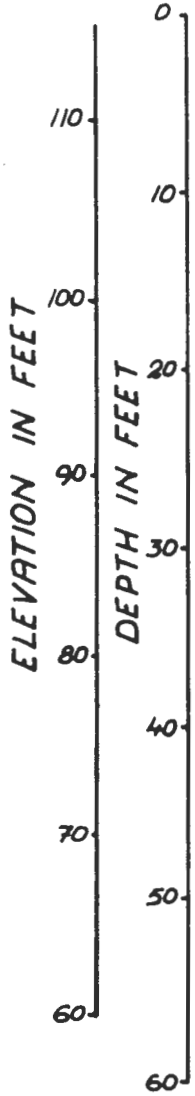

Classification	G_s	γ_t lb/ft³	Natural water content %	Liquid limit w_L (%)	Plastic limit w_P (%)	Plasticity index PI (%)	Percent passing 2mm	Percent passing .06mm	Percent passing .002mm	Unconfined strength, s_u p_u psf	Unconfined strength, s_u ε_f (%)	Unconfined strength, s_u S_T	$\frac{s_u}{\bar{\sigma}_{1c}}$	$\bar{c}$ psf	$\bar{\phi}$
FILL		95	5.1			NP	82	3	0						
		102	10.3			NP								0	35°
			30	34	19	15	89	68	13						
SILT	2.73		26	29.5	21.8	7.7	100	22	5						
			31							795	8.4	2.6			
										1020*	16.3*				
			42												
	2.46	104	80	123	61	62	100	85	33	860	3.3	2.8	.38	408	30°
TILL															
			12.1	23	12	11	36	11	2					0	38°
ROCK		134													

* UU test at $\bar{\sigma}_c$ = 2040 psf

FIGURE 2.1 SOIL PROPERTIES AT TEST SECTION B
(After Lambe, Wolfskill and Wong, 1970)

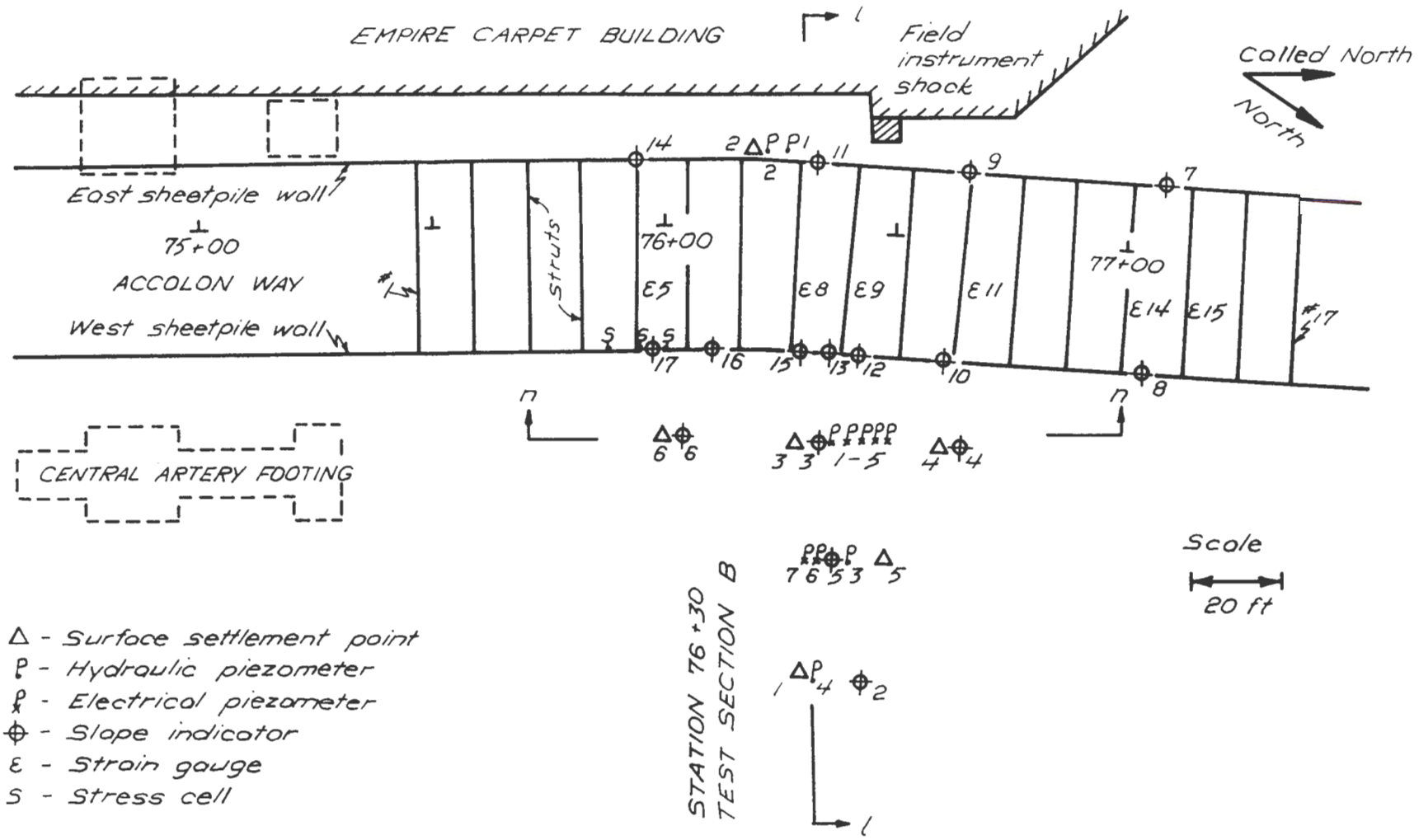

FIGURE 3.1 PLAN VIEW OF TEST SECTION B

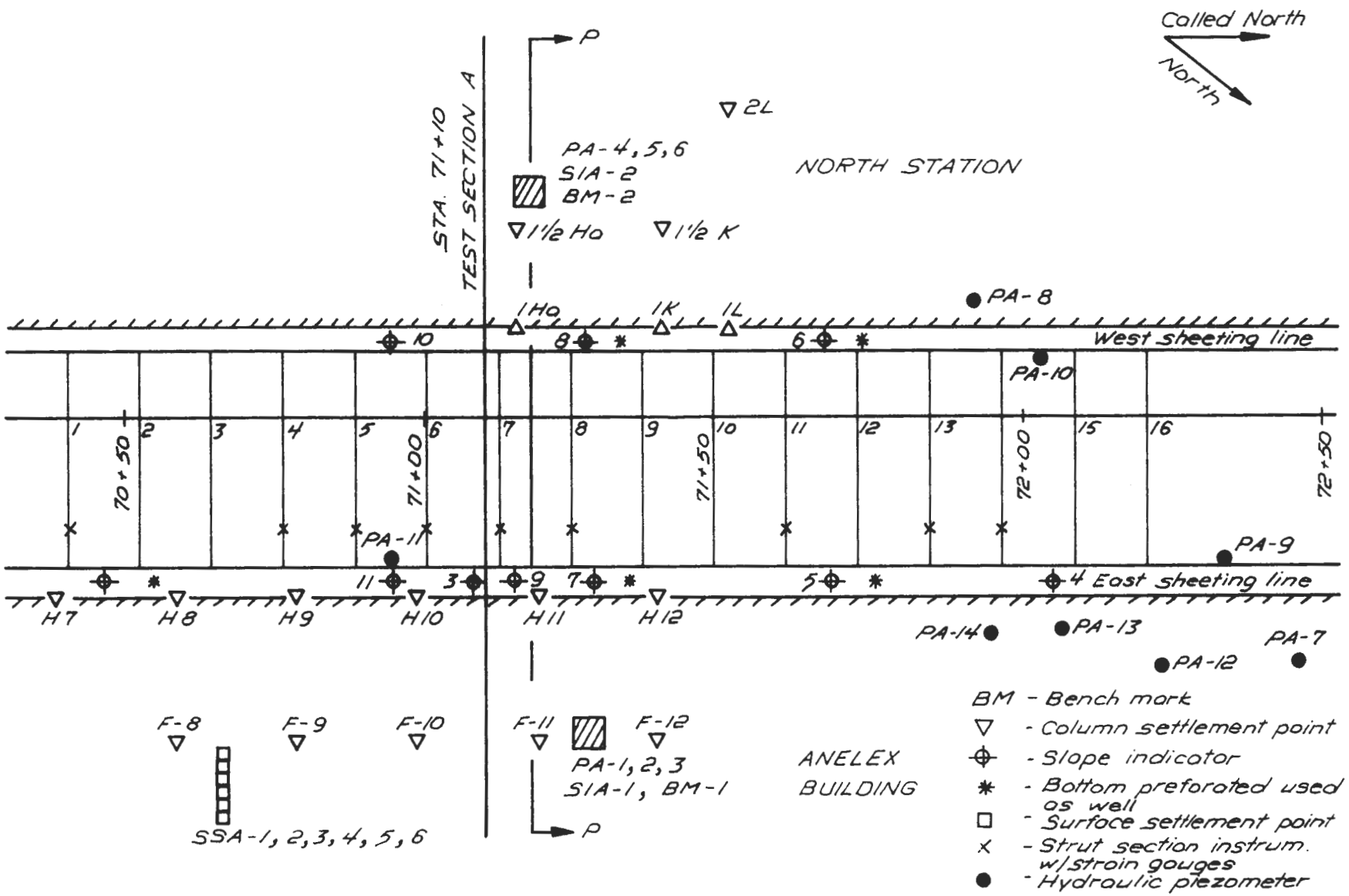

FIGURE 3.2 PLAN VIEW OF TEST SECTION A

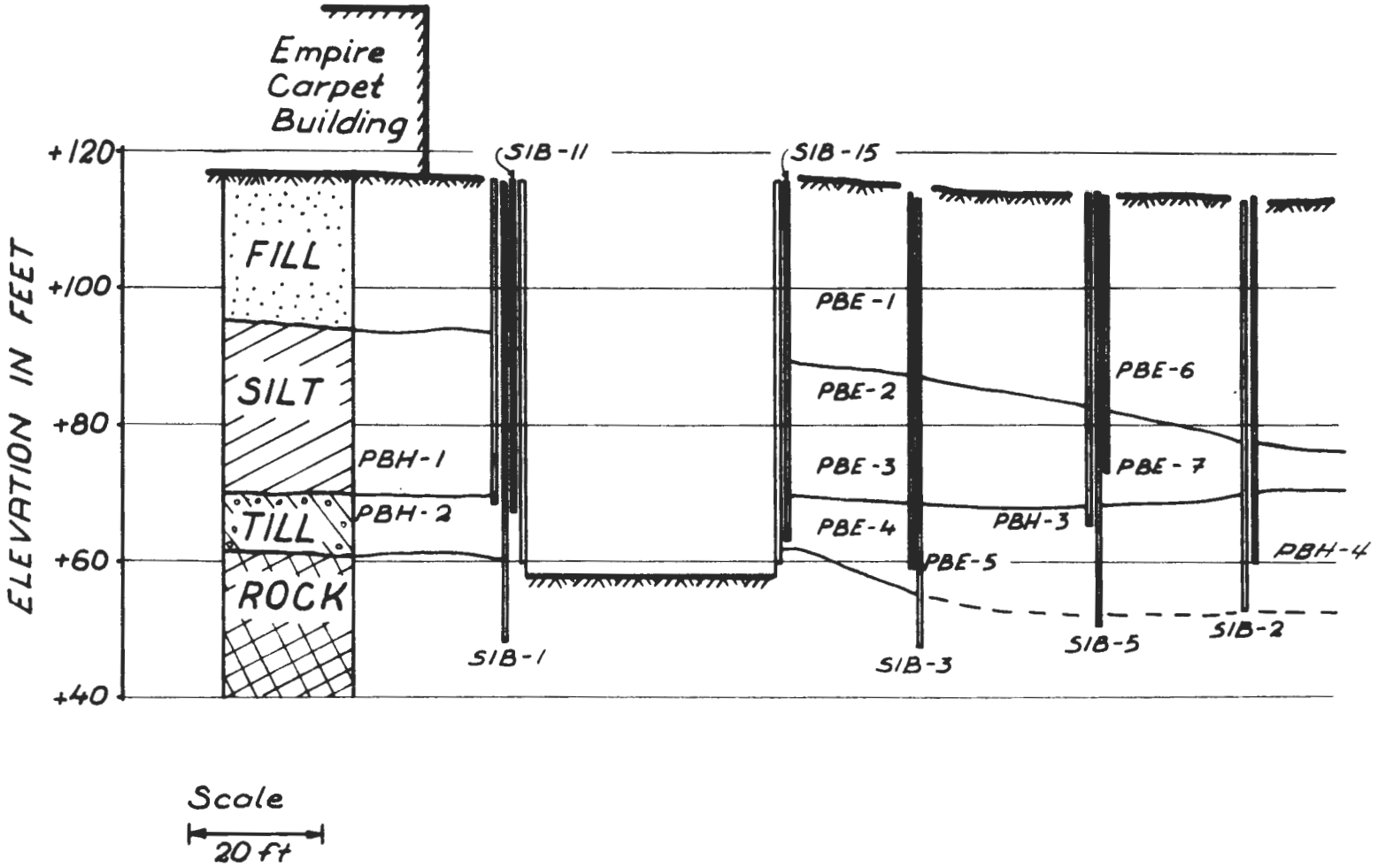

FIGURE 3.3 SECTION II LOOKING NORTH - TEST SECTION B
(After Lambe, Wolfskill and Wong, 1970)

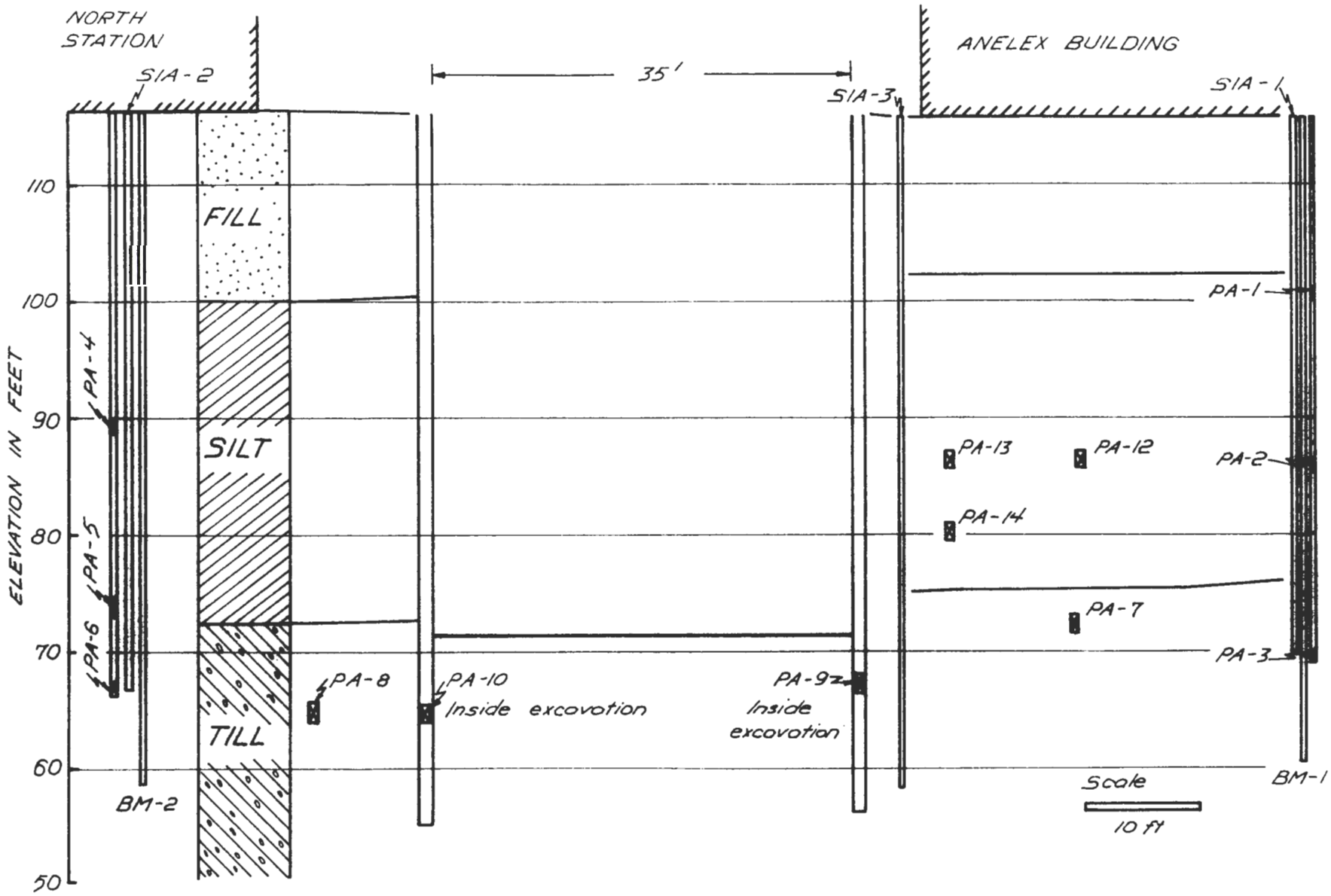

FIGURE 3.4 SECTION pp LOOKING NORTH - TEST SECTION A

WATER FLOWING INTO EXCAVATION
(Looking south from station 76+33, 12/17/68)

FIGURE 4.1 WATER FLOWING INTO EXCAVATION
(After Lombe, Wolfskill and Wong, 1970)

FIGURE 4.2 WATER FLOWING THROUGH HOLES IN SHEETING TEST SECTION A

FIGURE 4.3 WATER FLOWING THROUGH RAPTURED JOINTS IN SHEETING TEST SECTION B (COMPLIMENTS OF MBTA)

FIGURE 4.4 CRUSHING OF TIMBER WEDGES

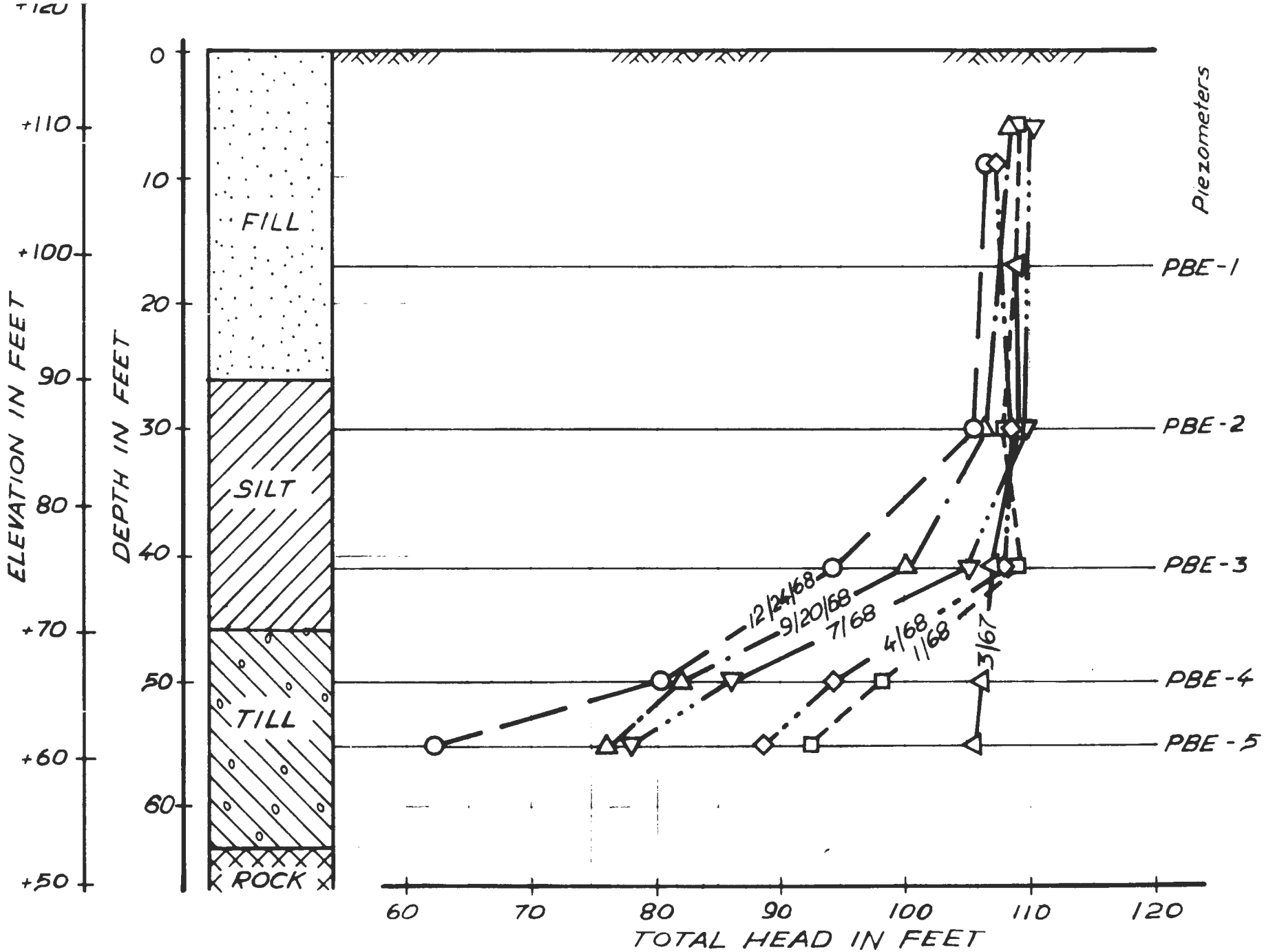

FIGURE 5.1 MEASURED TOTAL HEAD AT MIDDLE OF SECTION nn
TEST SECTION B (After Lombe, Wolfskill and Wong, 1970)

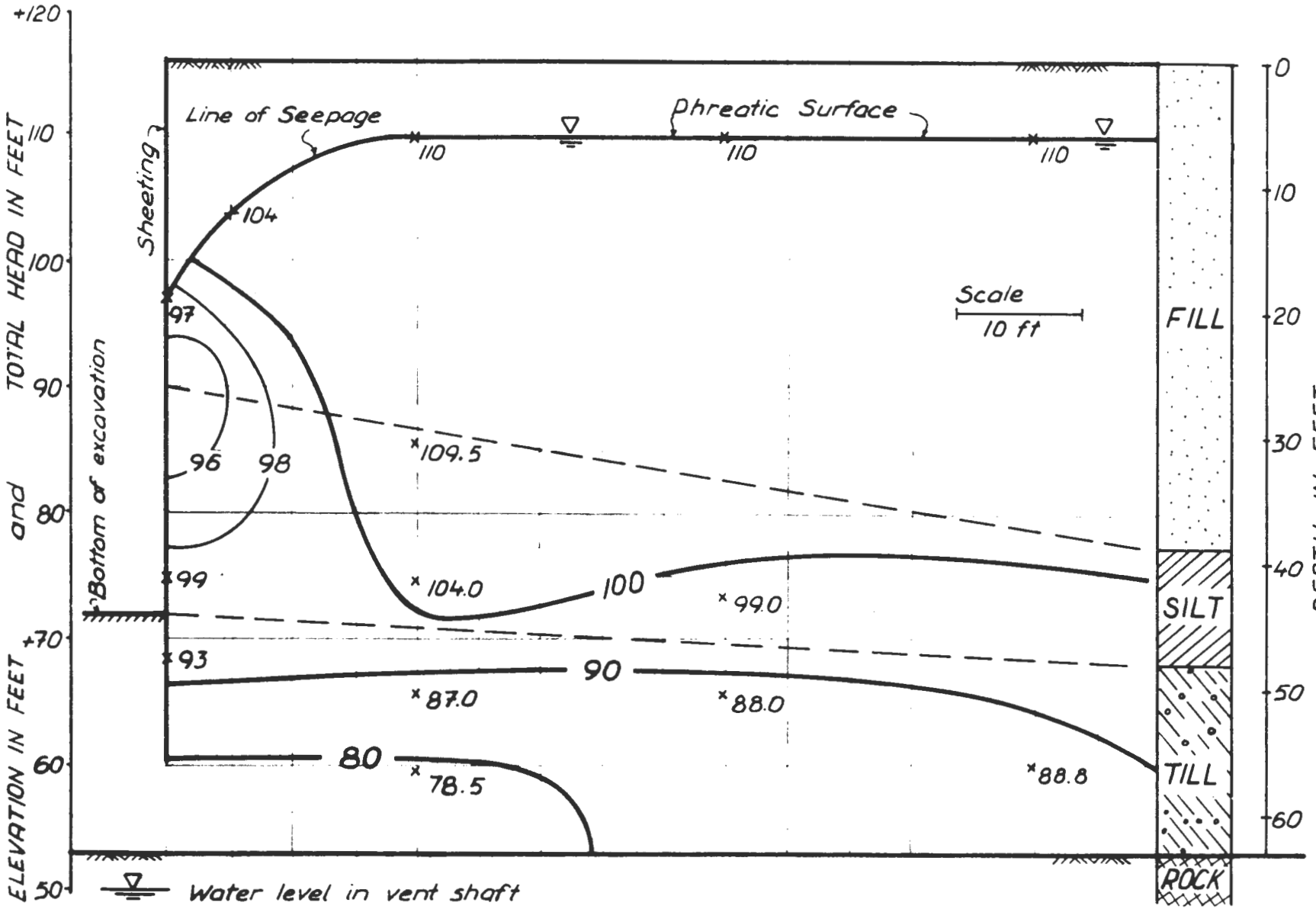

FIGURE 5.2 TOTAL HEAD ALONG SECTION II TEST SECTION B
(HEAD MEASURED ON JULY 19, 1968)
(After Lombe, Wolfskill and Wong, 1970)

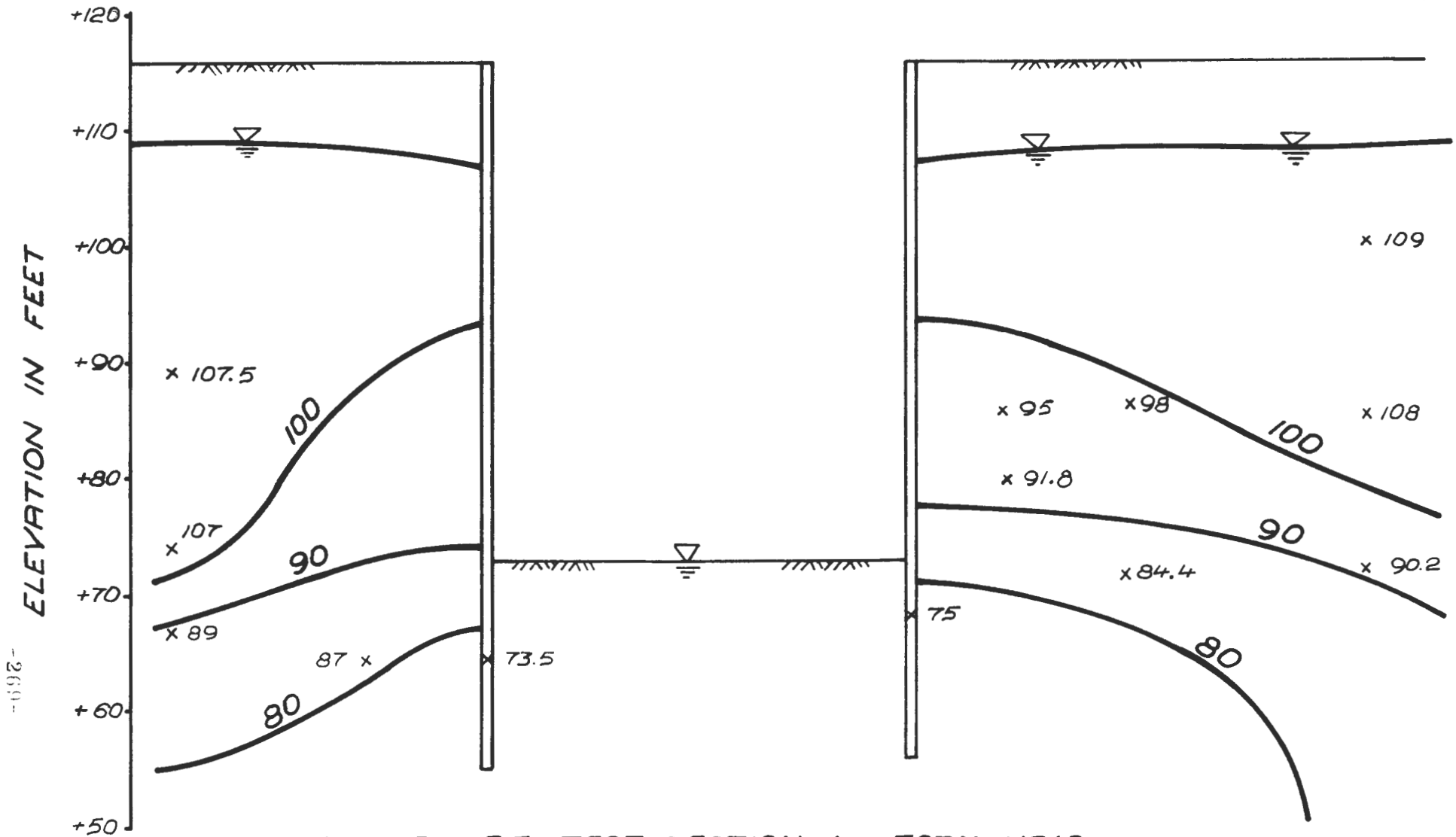

FIGURE 5.3 TEST SECTION A - TOTAL HEAD
(ON 10 JUNE 1969)

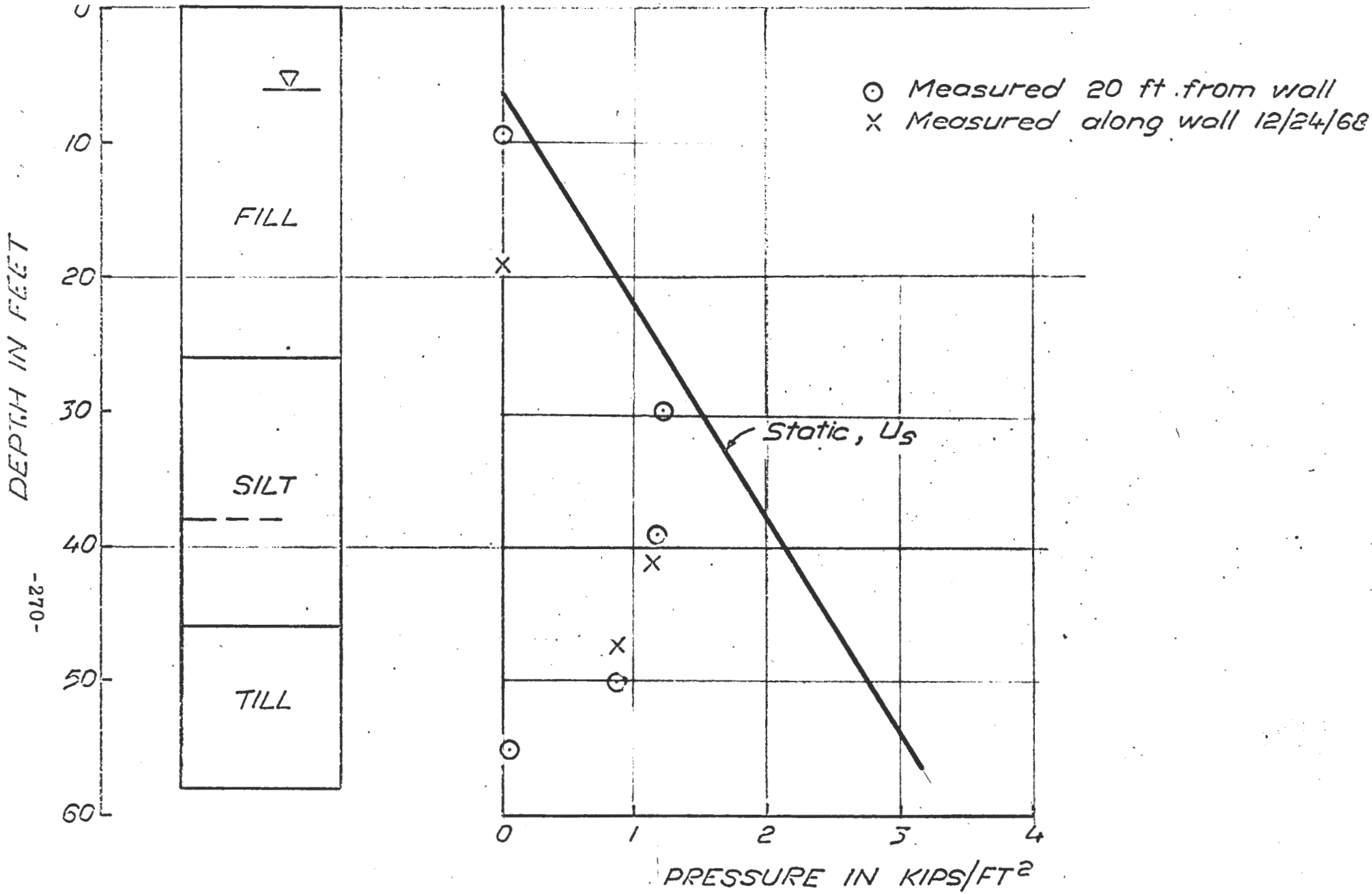

FIGURE 5.4 PORE PRESSURESTEST SECTION B

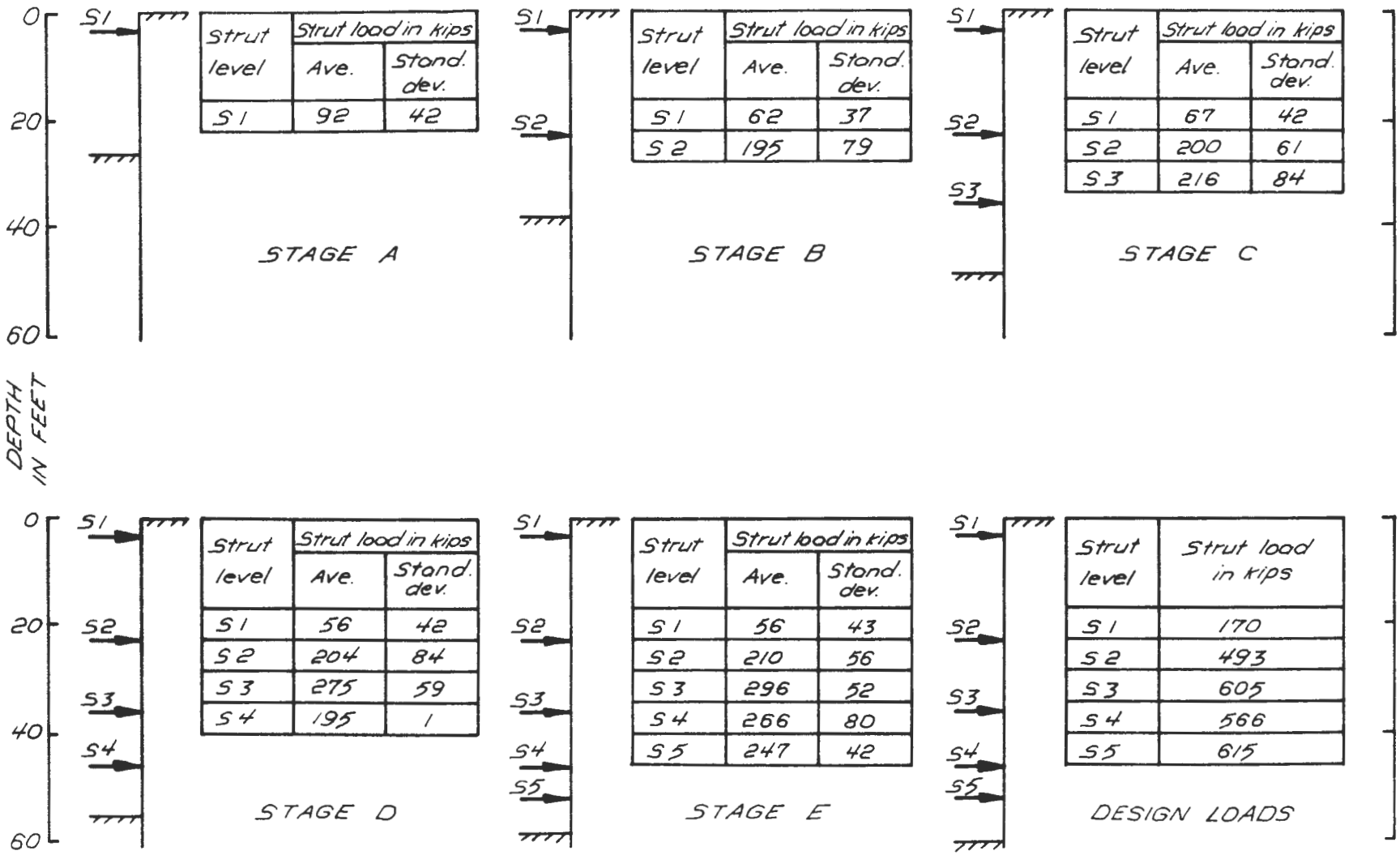

Strut level	Strut load in kips	
	Ave.	Stond. dev.
S 1	92	42

Strut level	Strut load in kips	
	Ave.	Stond. dev.
S 1	62	37
S 2	195	79

Strut level	Strut load in kips	
	Ave.	Stond. dev.
S 1	67	42
S 2	200	61
S 3	216	84

Strut level	Strut load in kips	
	Ave.	Stond. dev.
S 1	56	42
S 2	204	84
S 3	275	59
S 4	195	1

Strut level	Strut load in kips	
	Ave.	Stond. dev.
S 1	56	43
S 2	210	56
S 3	296	52
S 4	266	80
S 5	247	42

Strut level	Strut load in kips
S 1	170
S 2	493
S 3	605
S 4	566
S 5	615

FIGURE 6.1 MEASURED LOADS IN STRUTS - TEST SECTION B

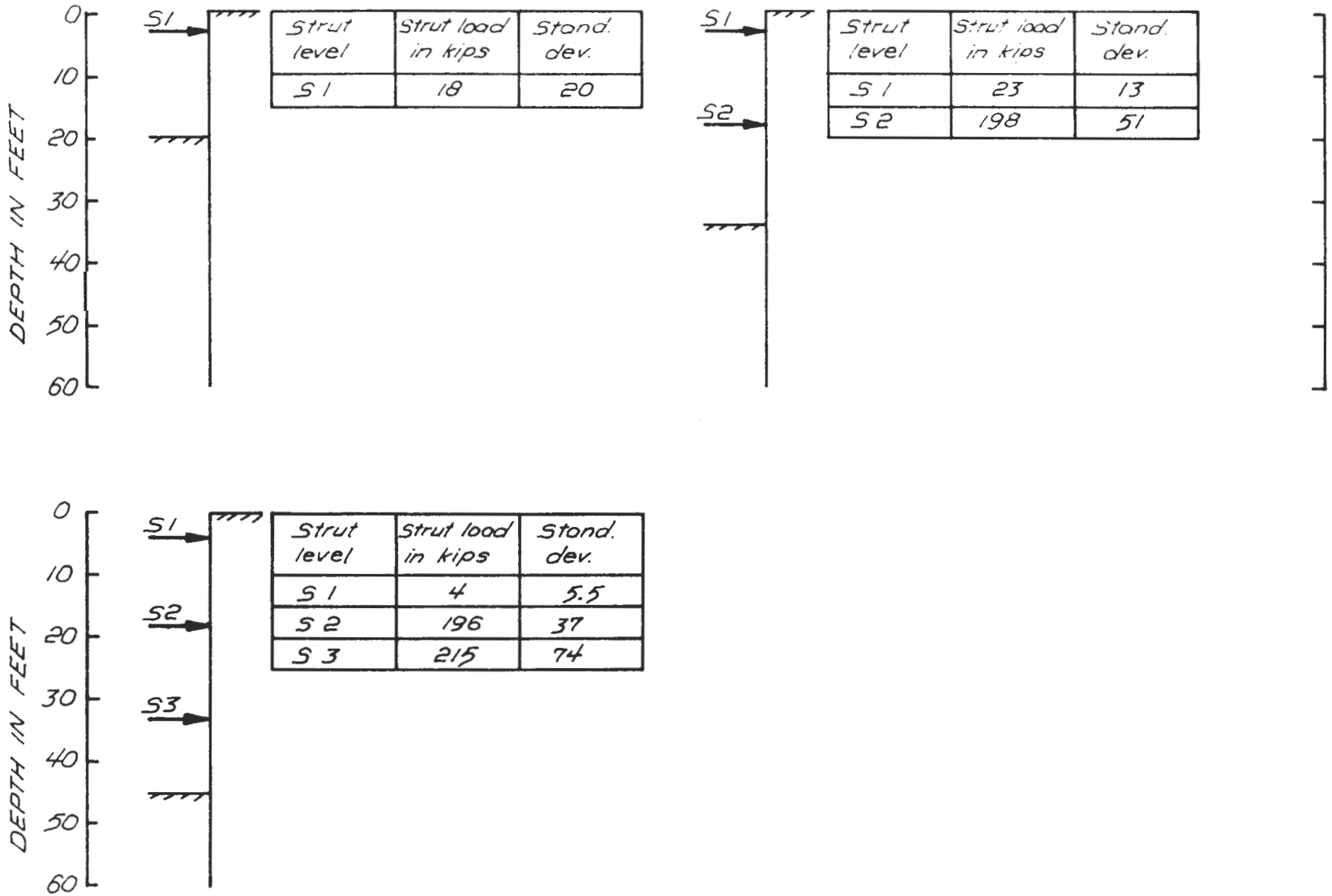

Strut level	Strut load in kips	Stand. dev.
S 1	18	20

Strut level	Strut load in kips	Stand. dev.
S 1	23	13
S 2	198	51

Strut level	Strut load in kips	Stand. dev.
S 1	4	5.5
S 2	196	37
S 3	215	74

FIGURE 6.2 MEASURED LOADS IN STRUTS - TEST SECTION A

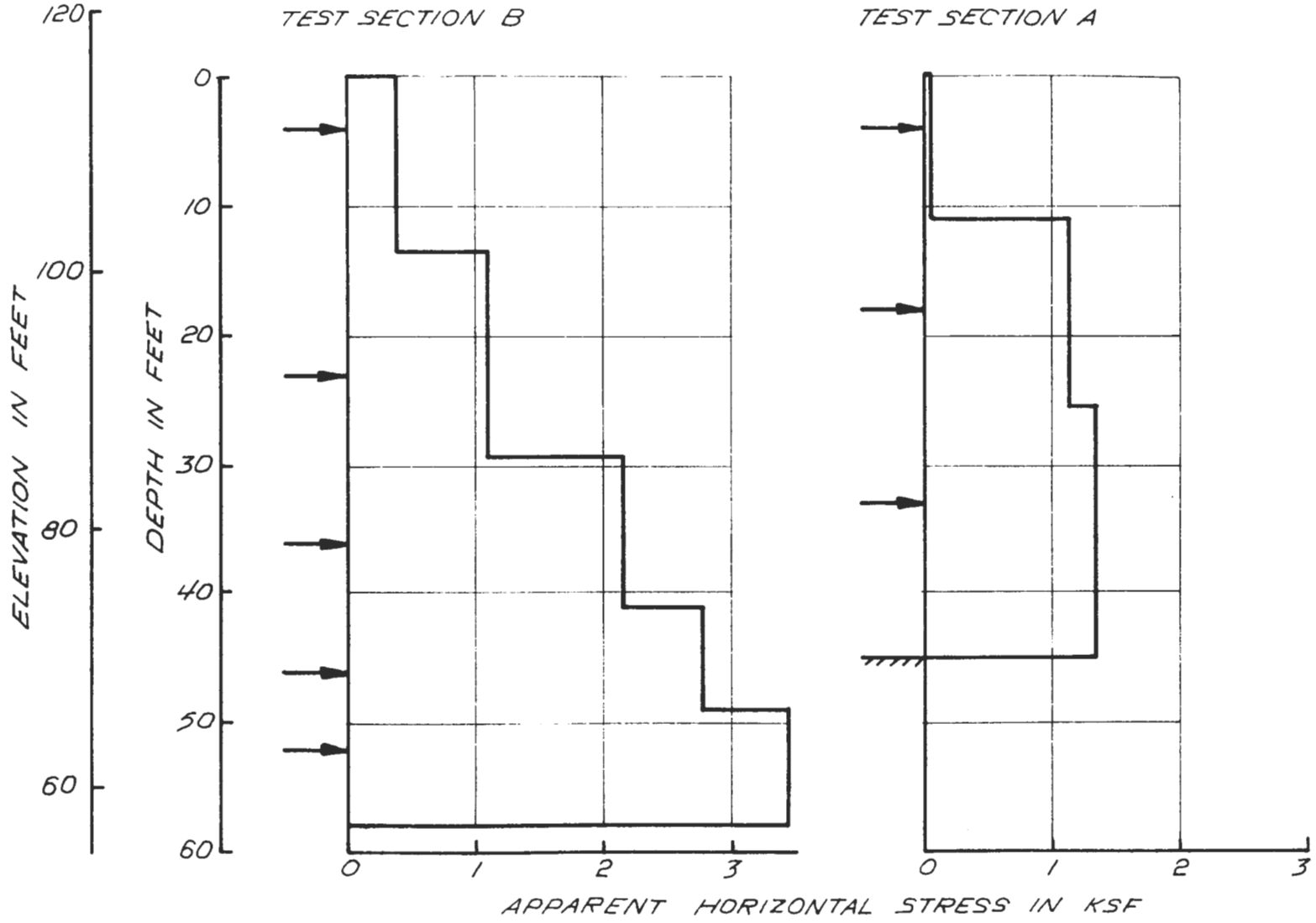

FIGURE 6.3 APPARENT TOTAL HORIZONTAL STRESSES

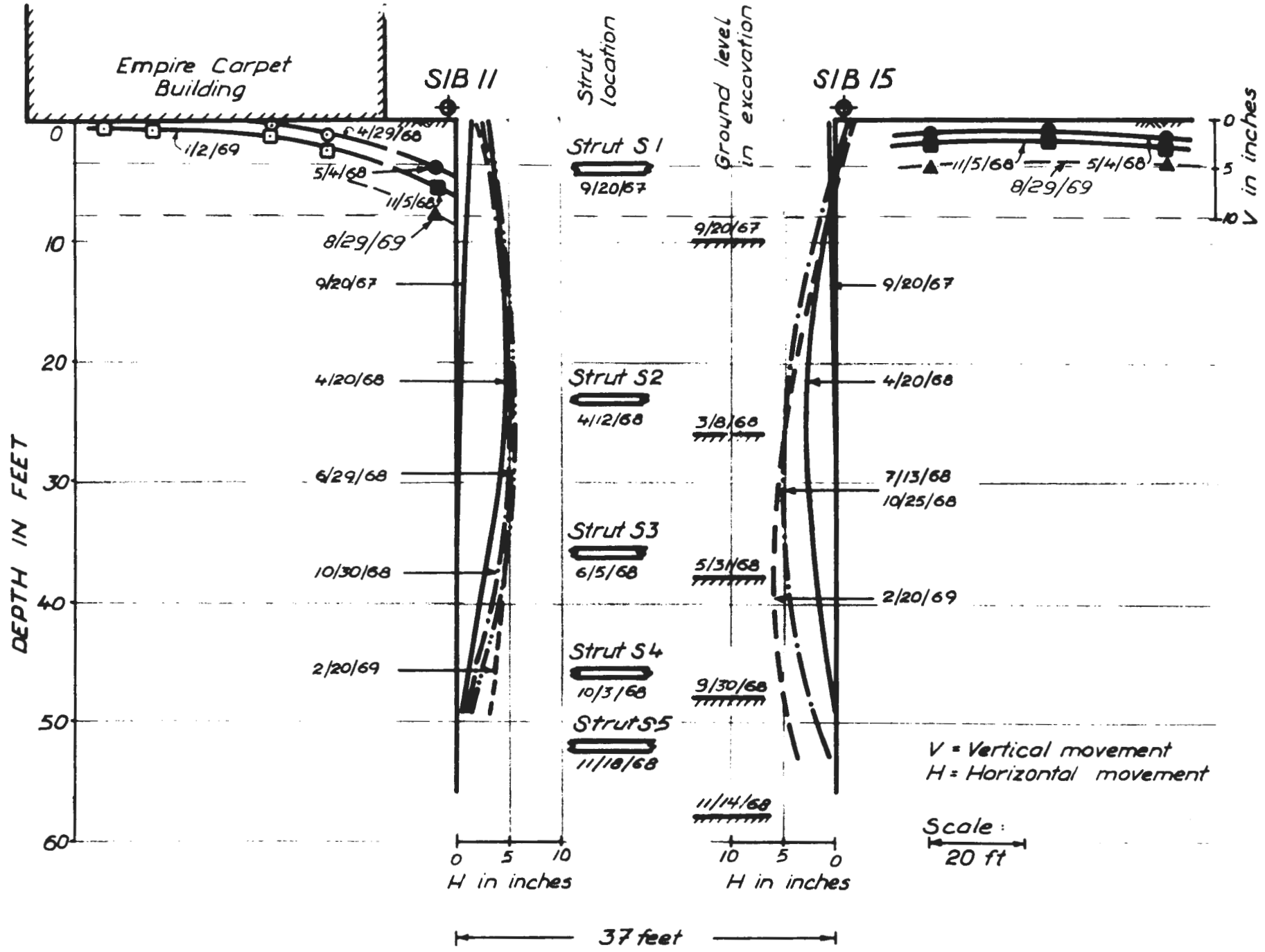

FIGURE 7.1 MOVEMENTS NEAR EXCAVATION TEST SECTION B

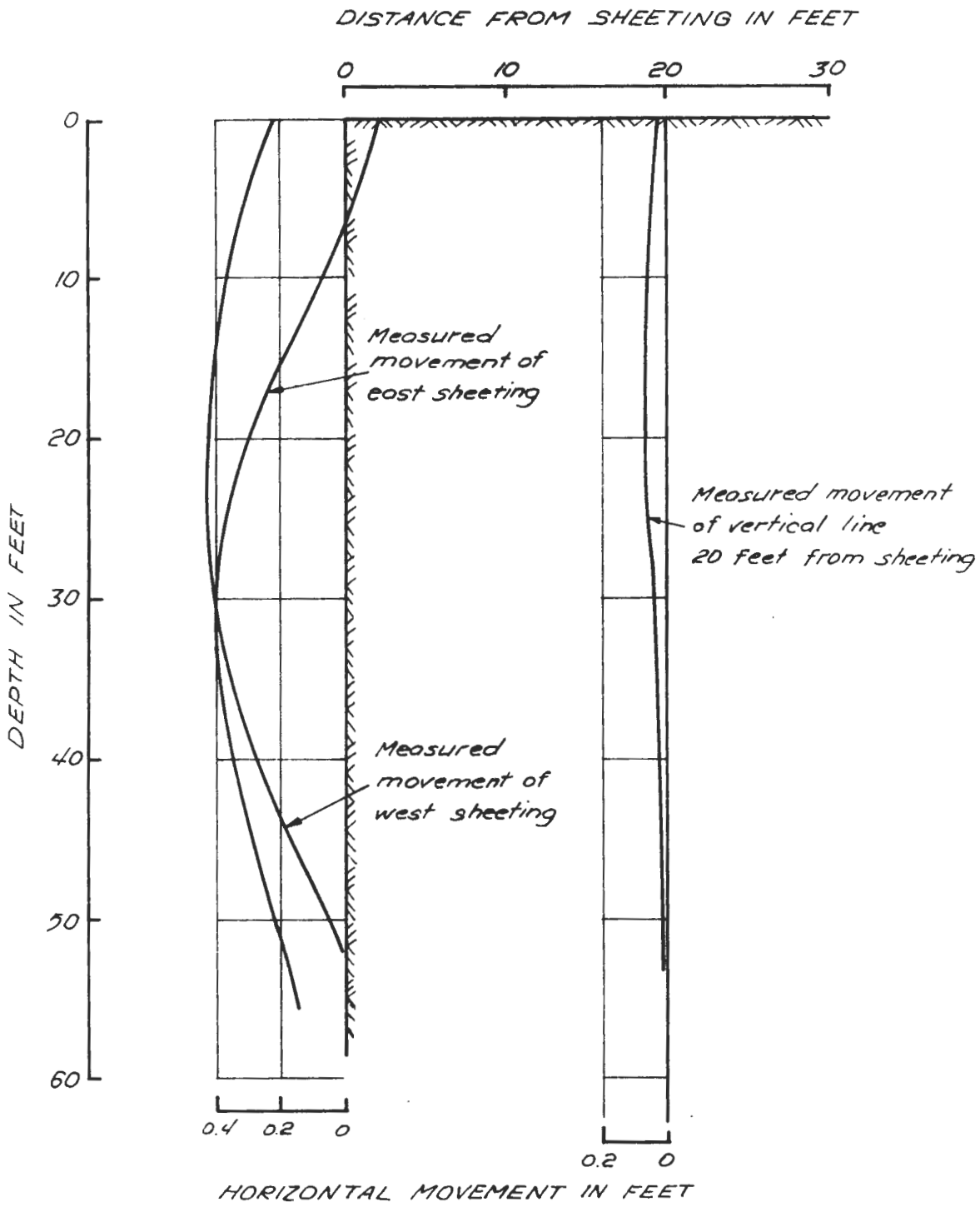

FIGURE 7.2 MEASURED HORIZONTAL MOVEMENTS
TEST SECTION B

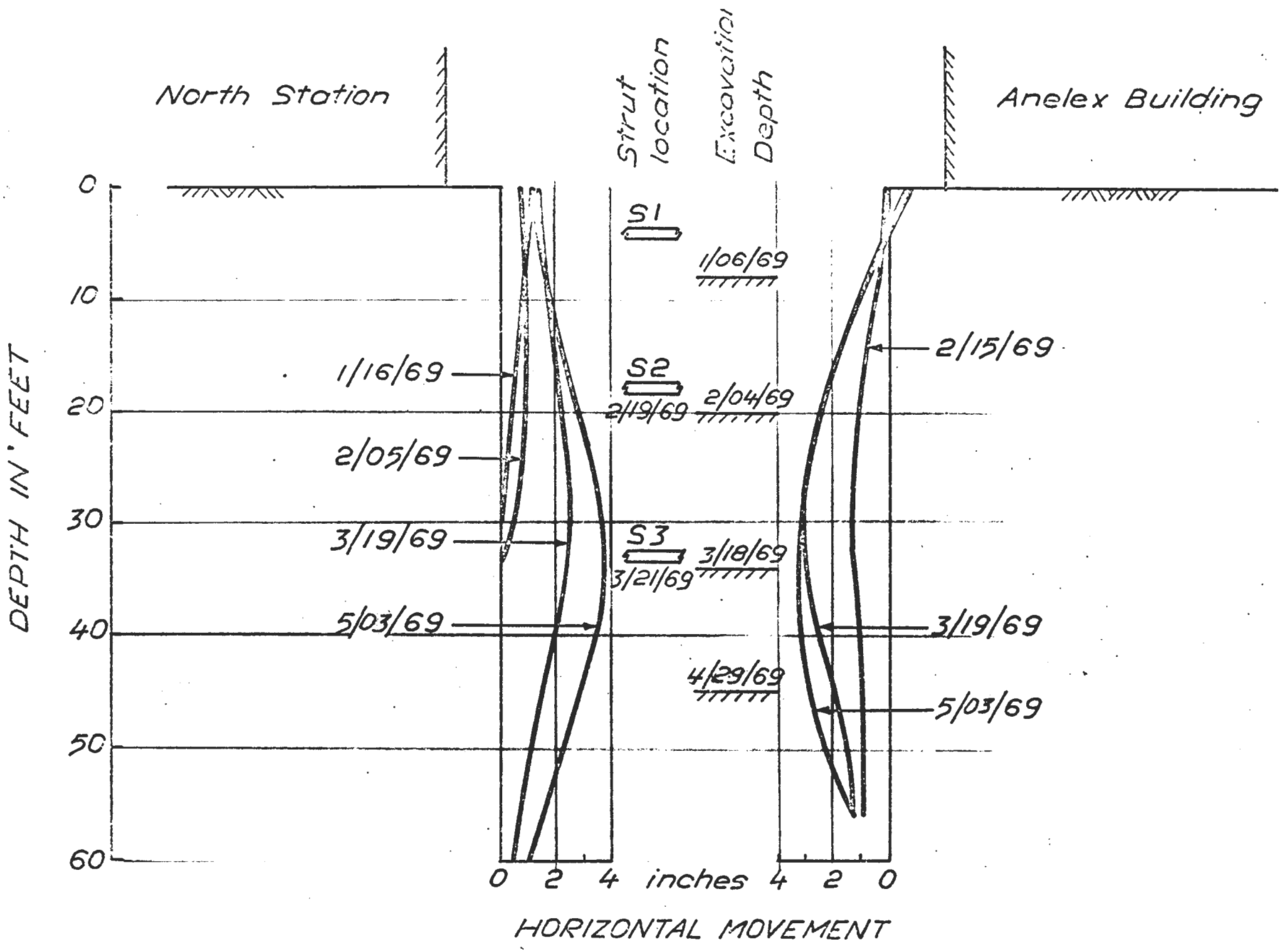

FIGURE 7.3 MEASURED HORIZONTAL WALL MOVEMENT - TEST SECTION A

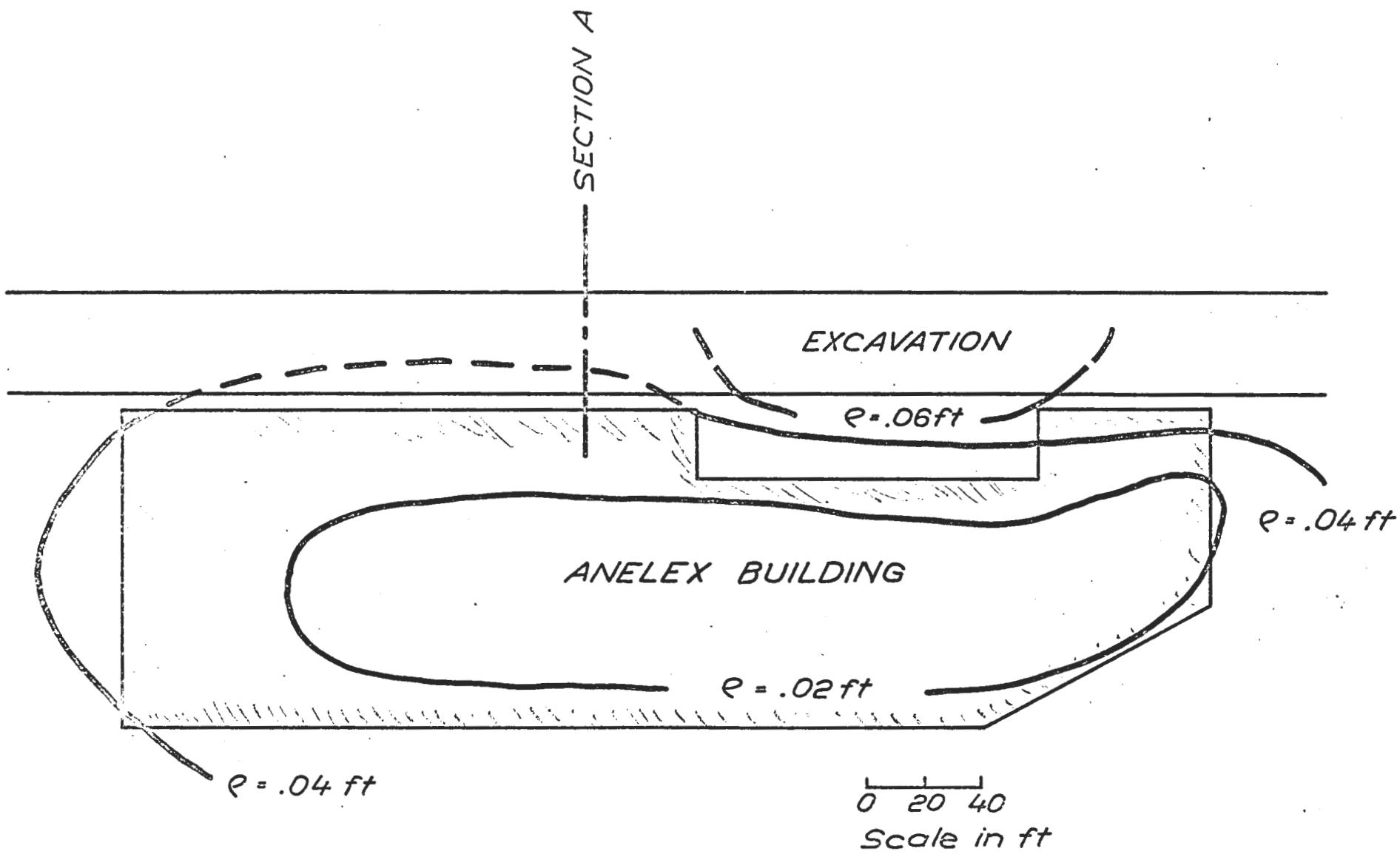

FIGURE 7.4 SETTLEMENT OF ANELEX BUILDING

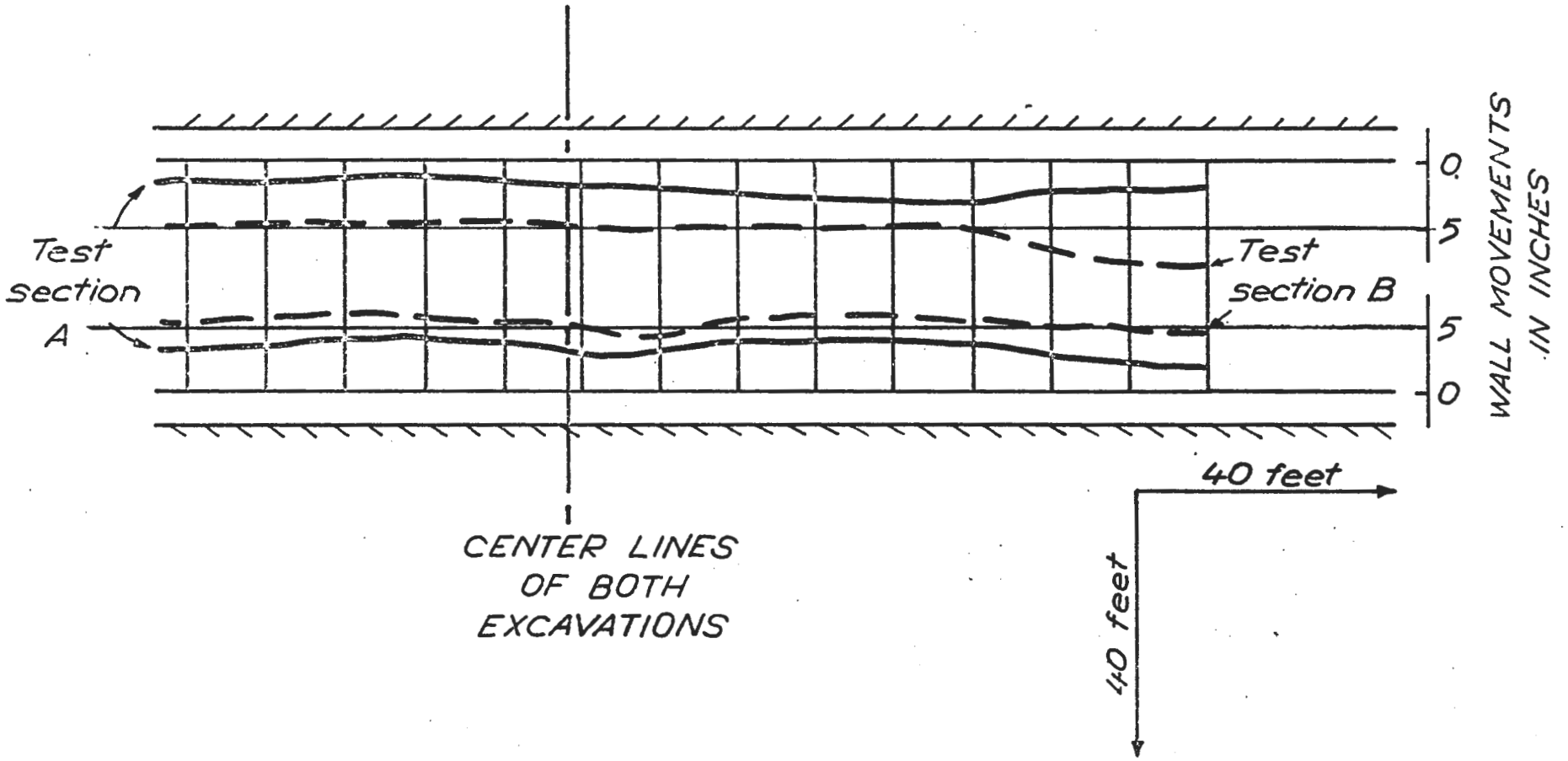

FIGURE 7.5 COMPARISON OF MAXIMUM WALL MOVEMENTS NEAR TEST SECTIONS A & B

APPENDIX II-A

INSTRUMENT DETAILS AND SUMMARY OF DATA

LIST OF TABLES

APPENDIX II-A

Table No.	Title
A-1	Instruments Installed
A-2	List of Strain Gauges - Test Section A
A-3	List of Strain Gauges - Test Section B
A-4	List of Slope Indicators
A-5	List of Hydraulic Piezometers
A-6	List of Vibrating Wire Piezometers
A-7	List of Vibrating Wire Stress Cells
A-8	List of Surface Settlement Points

LIST OF FIGURES

APPENDIX II-A

Figure No.	Title
A-1	Vibrating Wire Strain Gauge
A-2	Vibrating Wire Strain Gauge Installation
A-3	Vibrating Wire Strain Gauge Installation Report
A-4	Daily Strain Gauge Report - Test Section A
A-5	Daily Strain Gauge Report - Test Section B
A-6	Hydraulic Piezometer Installation Report
A-7	Geonor Vibrating Wire Piezometer
A-8	Vibrating Wire Piezometer Installation Report
A-9	Column Pin
A-10	Settlement Screw
A-11	Location of Settlement Screws and Column Pins - North Station
A-12	Location of Settlement Screws and Column Pins - Anelex Building
A-13	Surface Settlement Point Installation Report
A-14	Detail of Slope Indicator
A-15	Slope Indicator Well Installation Report
A-16	Slope Indicator Well Installation
A-17	Geonor Vibrating Wire Stress Cell
A-18	Vibrating Wire Stress Cell Installation Report
A-19	Permanent Bench Mark
A-20	Bench Mark Installation Report
A-21A to A-21K	Strut Load Measurement

LIST OF FIGURES (cont.)

Figure No.	Title
A-22A to A-22C	Pore Pressure Measurements
A-23A to A-23B	Settlement Measurements - Test Section A
A-24A	Wall Movement - Test Section A
A-24B	Wall Movement Measurement - Test Section B

PART II

APPENDIX II-A

INSTRUMENTATION DETAILS AND SUMMARY OF DATA

This appendix describes the details of the instrumentation at Test Sections A and B, and presents uninterpreted plots of the measurements obtained.

Tables A-1 through A-8 list all the instruments installed at the two test sections. Figures A-1 through A-20 show the details of each type of instrument and an example of the installation report for each type of instrument. Figures A-3 and A-4 show examples of the daily strain gauge reports for the two test sections. Figures A-11 and A-12 show the location of the settlement screws and column pins at Test Section A.

Figures A-21 through A-24 show uninterpreted plots of the measurements obtained by a certain number of instruments. Owing to a lack of space, repetitive data obtained with other instruments are not shown.

All of the stress cells were damaged during the pile driving and therefore no earth pressure data was collected. The hammer used was a Vulcan 11B3 hammer operating a 1 blow/second.

The damages were caused when 1) the membrane disc moved in and out perpendicular to the sheeting face and hit the back of the cell, and 2) the screws fastening the magnet became loosened and caused tipping or complete disconnection of the magnet, and 3) the Allen screw fastening the wire became loosened and caused the wire to be unfastened.

Table A-1 Instruments Installed

Instrument Type	Number Installed		
	Section A	Section B	Total
Open Hydraulic Piezometer	15	4	19
Vibrating Wire Piezometer	0	7	7
Slope Indicator	12	17	29
Permanent Bench Mark	2	0	2
Settlement Reference Screws	51	0	51
Settlement Reference Pins	43	0	43
Surface Settlement Points	6	6	12
Vibrating Wire Strain Gauges	54	54	108
Vibrating Wire Stress Cells	0	13	13

Table A-2 List of Strain Gauges - Test Section A

Strut No.	Gauge No.	Initial Zero Freq.	Final Zero Freq.	Beam Size	Date of Installation	Date of Removal
1-A	1-1	1404	NG *	36WF150	12/12/68	3/10/70
	1-2	1273	1281 *			
1-B	1-3	1026.5	877 *	14BP89	1/31/69	11/19/69
	1-4	1017	1022 *			
3-C	3-5	1200	1053 * *	14WF111	3/22/69	7/9/69
	3-6	1282	1255 *			
4-A	4-1	1048.5	NG *	36WF150	12/2/68	4/10/70
	4-2	1242.5	1369 *			
4-B	4-3	986.5	1060 * *	14BP89	1/31/69	11/20/69
	4-4	923	948 *			
4-C	4-5	1094	1168 * *	14WF111	3/22/69	7/9/69
	4-6	1136.5	1216 *			
5-A	5-1	1214.5	1327 *	36WF150	12/2/68	4/9/70
	5-2	1343.5	NG			
5-B	5-3	1103	1048 * *	14BP89	1/23/69	11/20/69
	5-4	1071	1049 *			
5-C	5-5	1207	1284 * *	14WF150	3/11/69	7/9/69
	5-6	1023	1006 *			
6-B	6-3	1011	946 *	14BP89	1/23/69	11/20/69
	6-4	1073	1023 *			
6-C	6-5	1367.5	1326 *	14WF150	3/11/69	7/9/69
	6-6	1319	1150			
7-A	7-1	1275.5	1508 * *	36WF150	12/2/69	4/10/70
	7-2	1165.5	958 *			
7-B	7-3	1214	926 *	14BP89	1/23/69	11/20/69
	7-4	1025	792 *			
7-C	7-5	1047	1149 * *	14WF150	3/11/69	7/9/69
	7-6	1148	1129 *			
8-A	8-1	1026.5	1062 * *	36WF150	1/7/69	4/23/70
	8-2	1000	1072 *			
8-B	8-3	1064.5	NG * *	14BP89	1/23/69	11/20/69
	8-4	1302	1511 *			

Table A-2 List of Strain Gauges - Test Section A (Continued)

Strut No.	Gauge No.	Initial Zero Freq.	Final Zero Freq.	Beam Size	Date of Installation	Date of Removal
8-C	8-5	1080	1097*	14WF150	3/11/69	7/22/69
	8-6	1115	1137*			
11-A	11-1	1320	1328*	36WF150	1/7/69	4/7/70
	11-2	1320	1167*			
11-B	11-3	1017	1027*	14WF142	2/6/69	11/20/69
	11-4	1037	1052			
11-C	11-5	1183	1165*	14WF111	3/18/69	7/22/69
	11-6	1147	1152*			
12-D	12-7	1355	1357	14WF119	4/29/69	7/22/69
	12-8	1200	1245			
13-B	13-3	1276	1370*	14WF142	2/18/69	11/24/69
	13-4	1325	1387*			
13-C	13-5	1364	1895*	14WF119	3/27/69	7/24/69
	13-6	1195	1009*			
13-D	13-7	1094	1110	14WF119	4/29/69	7/22/69
	13-8	1130	1113			
14-B	14-3	1366	1463	14WF142	2/18/69	11/24/69
	14-4	1196	1252*			
14-C	14-5	1286	1317*	14WF111	3/21/69	7/24/69
	14-6	1090	1132			
14-D	14-7	1221	1431	14WF119	4/28/69	7/22/69
	14-8		1130			

* Denotes frequency used.
NG = No Good.

Table A-3 List of Strain Gauges - Test Section B

Strut No.	Gauge No.	Initial Zero Freq.	Final Zero Freq.	Beam Size	Date of Installation	Date of Removal
5-1	5-1	1000	1017*	36WF150	9/27/67	3/16/70
	5-2	958	953*			
5-2	5-3	1337*	1532	14WF202	4/5/68	3/9/70
	5-4	1553*	1342			
5-3	5-5	1339*		14WF202	6/18/68	
	5-6	1351				
8-1	8-1	1524	1502*	36WF150	12/6/67	3/12/70
	8-2	1067	1071*		12/8/67	3/12/70
8-2	8-3	1533*		14WF202	4/3/68	
	8-4	1415*			4/5/68	
8-3	8-5	1334	1346*	14WF202	6/4/68	3/17/69
	8-6	1570	1604*		6/4/68	3/19/69
9-1	9-1	953*	862*	36WF150	9/12/67	3/12/70
	9-2	1564	1574*			
	9-3	1111*	1134*			
	9-4	1455*	1360			
9-2	9-5	NG		14WF202	3/12/68	3/9/70
	9-6	1599				
	9-7	1582				
	9-8	1402				
	9-9	1355	1462			
	0-1	1550	1465			
9-3	9-11	1448	1446*	14WF167	6/5/68	3/17/69
	9-12	1319	1353*		6/3/68	3/17/69
9-4	9-13	1593	1634*	14WF167	10/2/68	1/27/69
	9-14	1396	1393			
9-5	9-15	1098	1024*	14WF167	11/15/68	1/3/69
	9-16	1333	1297*		11/16/68	1/3/69
11-1	11-1	1226*	NR	36WF150	12/5/67	3/12/70
	11-2	1107*	1052			
11-2	11-3	1302*		14WF202	3/12/68	3/10/70
	11-4	1520*				

Table A-3 List of Strain Gauges - Test Section B (Continued)

Strut No.	Gauge No.	Initial Zero Freq.	Final Zero Freq.	Beam Size	Date of Installation	Date of Removal
11-3	11-5	1507	1487*	14WF167	5/23/68	4/1/69
	11-6	1489	1496*			
11-4	11-7	1440*	OCS	14WF167	10/2/68	1/2/69
	11-8	1482*	OCS			
11-5	11-9	1116	783*	14WF167	11/15/68	1/3/69
	11-10	1357	1314*			
14-1	14-1	1447*	1402	36WF150	12/7/67	3/10/70
	14-2	1291*	1271			
14-2	14-3	1047	1176*	14WF158	2/27/68	9/12/69
	14-4	1173	1167*			
14-3	14-5	1248	1252*	14WF202	5/5/68	4/22/69
	14-6	1588	1667*		5/2/68	4/22/69
14-4	14-7	1246	1248*	14WF158	9/18/68	12/23/68
	14-8	1287	1229*			
14-5	14-9	1472	1455*	14WF167	10/18/68	11/29/68
	14-10	1194	1130*			
15-3	15-3	1463	1489*	14WF202	5/2/68	4/22/69
	15-4	1456	1463*			
15-4	15-5	1461		14WF158	7/9/68	12/23/68
	15-6	1498	1544*			
15-5	15-7	1567	1496*	14WF167	9/25/68	12/23/68
	15-8	1376	1206*			

* Denotes frequency used.

Table A-4 List of Slope Indicators

Instrument No.	Date of Installation	Bottom Elevation (ft.)	Test Section	Location	Bottom 20' of 4" Pipe Perforated?
SIA-1	1/30/67	+69.43*	A	In Soil	
SIA-2	1/25/67	+66.18	A	In Soil	
SIA-3	2/5/67	+62.93	A	In Soil	
SIA-4	1/10/69	+60.22	A	On Sheeting	No
SIA-5	1/2/69	+58.36	A	On Sheeting	Yes
SIA-6	8/26/68	+59.98	A	On Sheeting	Yes
SIA-7	8/29/68	+61.75	A	On Sheeting	Yes
SIA-8	9/12/68	64.26	A	On Sheeting	Yes
SIA-9	8/27/68	58.24	A	On Sheeting	No
SIA-10	11/30/68	66.39	A	On Sheeting	No
SIA-11	8/29/68	58.20	A	On Sheeting	No
SIA-12	8/16/68	60.74	A	On Sheeting	Yes
SIB-1	2/28/67	48.05	B	In Soil	
SIB-2	1/26/67	52.02	B	In Soil	
SIB-3	2/21/67	47.58	B	In Soil	
SIB-4	2/26/67	54.50	B	In Soil	
SIB-5	2/21/67	51.11	B	In Soil	
SIB-6	3/3/67	52.60	B	In Soil	
SIB-7	7/24/67	54.20	B	On Sheeting	Yes

* Boston City Datum +100.000 ft.

Table A-4 List of Slope Indicators (Continued)

Instrument No.	Date of Installation	Bottom Elevation (ft.)	Test Section	Location	Bottom 20' of 4" Pipe Perforated?
SIB-8	7/24/67	47.86	B	On Sheeting	No
SIB-9	7/21/67	55.75	B	On Sheeting	Yes
SIB-10	7/19/67	49.87	B	On Sheeting	No
SIB-11	8/25/16	67.16	B	On Sheeting	Yes
SIB-12	8/22/67	61.96	B.	On Sheeting	No
SIB-13	8/22/67	62.47	B	On Sheeting	No
SIB-14	8/25/67	61.63	B	On Sheeting	Yes
SIB-15	8/22/67	62.93	B	On Sheeting	No
SIB-16	8/23/67	62.30	B	On Sheeting	No
SIB-17	8/23/67	62.64	B	On Sheeting	Yes

Table A-5 List of Hydraulic Piezometers

Instrument No.	Date of Installation	Sensor** Elevation (ft.)	Test Section	Type of Leads*
PA-1	1/5/67	+100.51	A	Double
PA-2	1/14/67	+ 85.622	A	Double
PA-3	1/21/67	+ 72.17	A	Double
PA-4	1/12/67	+ 89.29	A	Double
PA-5	1/13/67	+ 74.00	A	Double
PA-6	1/13/67	+ 66.88	A	Double
PA-7	4/12/69	+ 71.7	A	Double
PA-8	4/17/69	+ 64.8	A	Double
PA-9	4/12/69	+ 67.90	A	Double
PA-10	4/15/69	+ 64.35	A	Double
PA-11	4/29/69	+ 75.0	A	Single
PA-12	6/3/69	+ 86.4	A	Double
PA-13	6/3/69	+ 85.9	A	Double
PA-14	6/2/69	+ 80.0	A	Double
PA-15	6/19/69	+ 65.46	A	Double
PBH-1	1/15/67	+ 75.21	B	Double
PBH-2	1/14/67	+ 68.63	B	Double
PBH-3	1/17/67	+ 65.63	B	Double
PBH-4	1/15/67	+ 60.26	B	Double

* Double tube type consists of 3/8" inner diameter tube and 1/4" inner diameter tube. Single tube type consists of one 3/8" inner diameter bube.

** Boston City Datum + 100.000 feet.

Table A-6 List of Vibrating Wire Piezometers

Instrument No.	Date of Installation	Sensor* Elevation (ft.)	Test Section	Hard or Soft Ground Installation
PBE-1	1/17/67	+98.52	B	Hard
PBE-2	10/31/67	+87.47	B	Hard
PBE-3	1/18/67	+74.70	B	Soft
PBE-4	1/19/67	+65.61	B	Hard
PBE-5	1/16/67	+59.36	B	Hard
PBE-6	8/11/67	+87.48	B	Soft
PBE-7	9/5/67	+73.56	B	Soft

* Boston City Datum + 100.000 feet.

Table A-7 List of Vibrating Wire Stress Cells

Instrument No.	Date of Installation	Sensor* Elevation (ft.)	Test Section
σ-158-1	8/1/67	+113.77	B
σ-158-2	8/1/67	+107.79	B
σ-158-3	8/1/67	+101.77	B
σ-158-4	8/11/67	+ 95.88	B
σ-158-5	8/1/67	+ 88.79	B
σ-158-6	8/1/67	+ 83.79	B
σ-158-7	8/1/67	+ 80.28	B
σ-158-8	8/1/67	+ 74.78	B
σ-158-9	8/11/67	+ 69.79	B
σ-158-10	8/11/67	+ 65.29	B
σ-158-11	8/11/67	+ 61.29	B
σ-162-1	8/11/67	+ 93.94	B
σ-166-1	8/11/67	+ 88.00	B

*Boston City Datum + 100.000 feet.

Table A-8 List of Surface Settlement Points

Instrument No.	Date of Installation	Sensor** Elevation (ft.)	Test Section
SSA-1	1/18/69	+120.791	A
SSA-2	1/18/69	+121.347	A
SSA-3	1/18/69	+121.097	A
SSA-4	1/18/69	+121.274	A
SSA-5	1/18/69	+120.975	A
SSA-6	1/18/69	+120.767	A
SSB-1	11/1/67	+113.270	B
SSB-2	11/1/67	+115.074	B
SSB-3*	11/1/67		B
SSB-4	11/1/67	+113.670	B
SSB-5	11/1/67	+112.833	B
SSB-6	11/1/67	113.885	B

Datum: MBTA BM-1

*Abandoned

**Boston City Datum + 100.000 feet.

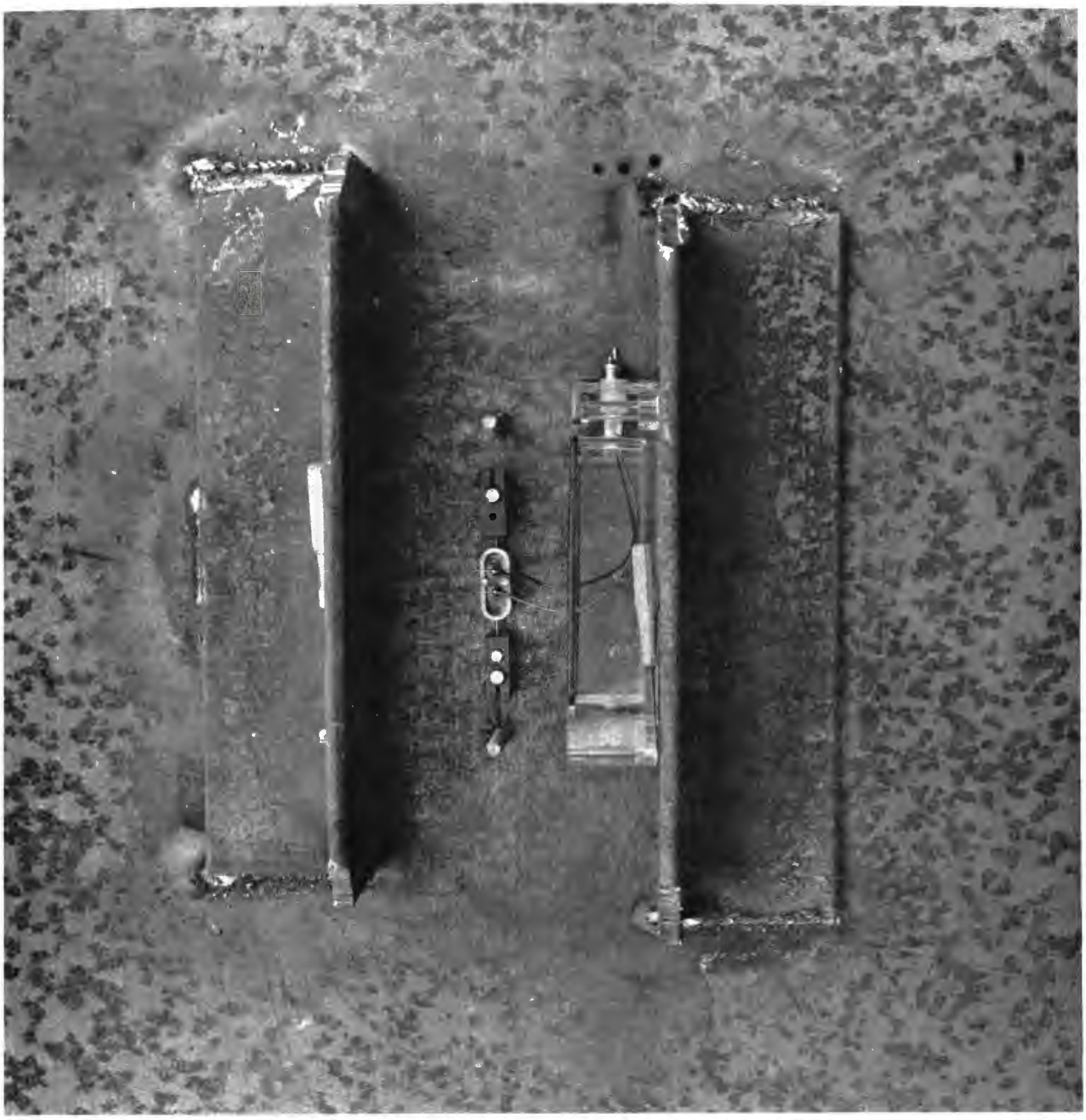

FIGURE A-2 VIBRATING - WIRE STRAIN GAUGE INSTALLATION

VIBRATING-WIRE STRAIN GAUGE INSTALLATION

Project [illegible] Test [illegible] Gauge No. [illegible]

Location: Strut No. 14 Level No. [illegible]

[illegible] 10 ft [illegible]

Direction of Measurement [illegible]

Date Installed 18 Sept [illegible] By [illegible]

Zero Frequency (initial)

Date	Time	Temp	f_o	Comments	By
[illegible]	[illegible]	66°F	1257.8	[illegible]	[illegible]
	[illegible]	66°F	125[illegible]	[illegible]	[illegible]
	[illegible]	66°F	[illegible]	[illegible] simply supported	
[illegible]	[illegible]	[illegible]°F	124[illegible]		
[illegible]	[illegible]	66°F	1245	[illegible]	
[illegible]	[illegible]	66°F	1246	[illegible]	

Zero Frequency (end-of-job)

Date	Time	Temp	f_o	Comments	By
03 Dec 68		39°F	1248	On ground [illegible]	

Strut Size:

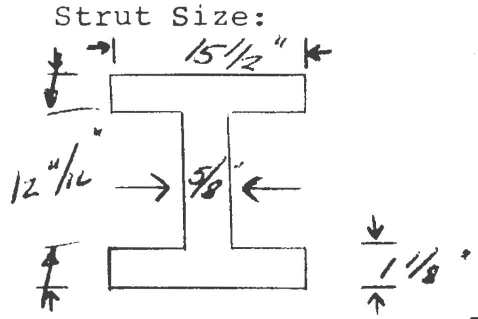

14 WF 158

Readout Location ______________

FIGURE A-3 VIBRATING-WIRE STRAIN GAUGE INSTALLATION REPORT

Time 0730
Date 8 APRIL 1969
Reader J.SKLARZ
Weather CLEAR
Temp (above ground)
°F Hi
R 420
Lo

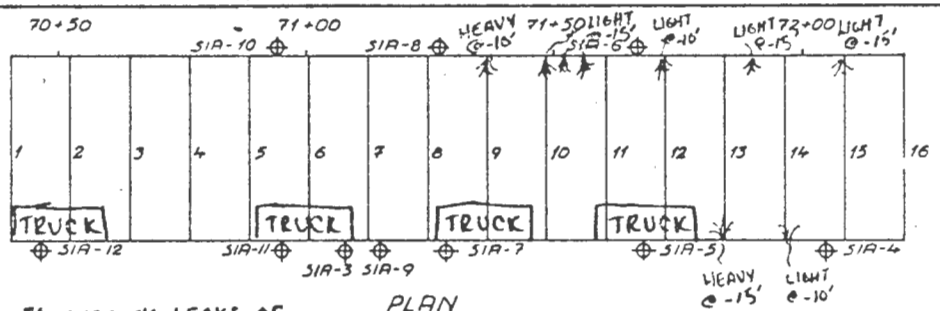

PLAN

SHEETING LEAKS OF 4-8-69 @ 0800

WEST

MBTA - MIT

TEST SECTION A

DAILY STRAIN GAUGE REPORT

EAST

Comments :

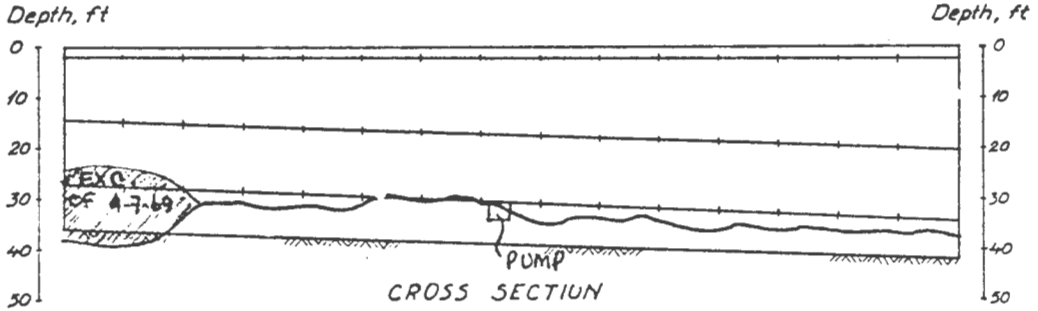

CROSS SECTION

Indicate :
Depth of excavation, water level location of cranes, decking, surcharge loads, etc.

Circle all struts installed since date of last reading. Note nominal size under comments

Level	Strut no. / Station	1 / 70 + 43	4 / 70 + 79	5 / 70 + 91	6 / 71 + 02	7 / 71 + 15	8 / 71 + 27	11 / 71 + 63	13 / 71 + 87	14 / 71 + 99
A	Temp. °F Hi / R / Lo	1-1 0000 1-2 1295	4-1 0000 4-2 1369-8	5-1 1328 5-2 0786		7-1 1510 7-2 0939	8-1 1014 8-2 1096	11-1 1320 11-2 1172		14-1 ____ 14-2 ____
B	Hi / R / Lo	1-3 0615-4 1-4 0736-5	4-3 0736 4-4 0637	5-3 0747 5-4 0804	6-3 OSC 6-4 0651-2	7-3 OSC 7-4 0344	8-3 0766 8-4 OSC	11-3 0829 11-4 0838	13-3 0000 13-4 1238	14-3 0000 14-4 1111
C	Hi / R / Lo	3-5 0931 3-6 1128	4-5 1048 4-6 1107-8	5-5 1219 5-6 0870	6-5 1221-2 6-6 OSC	7-5 OSC 7-6 1069	8-5 1017 8-6 1077-6	11-5 1093 11-6 1070	13-5 1871-2 13-6 0947	14-5 1262-1 14-6 1066
D	Hi / R / Lo	GAUGE FREQUENCIES, cps						11-7 ____ 11-8 ____	13-7 ____ 13-8 ____	14-7 ____ 14-8 ____

Date 25 Nov 68
Reader L. BOMBARDIER
Time 14:30
Weather CLOUDY
Temp (above ground):
Hi
°F R (at reading) 43°F
Lo

Comments:

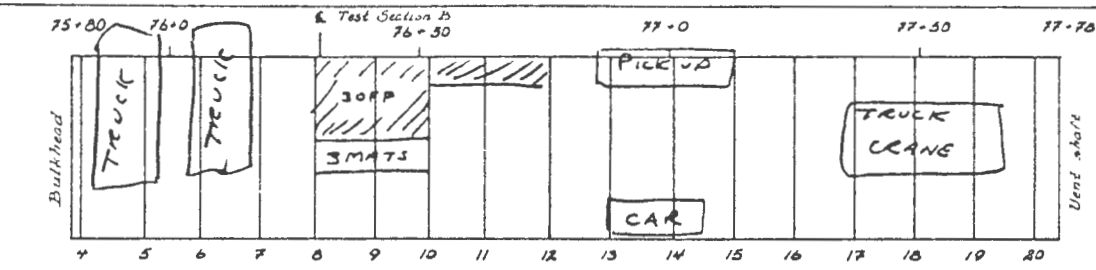

MBTA - MIT
TEST SECTION B
DAILY STRAIN GAUGE REPORT

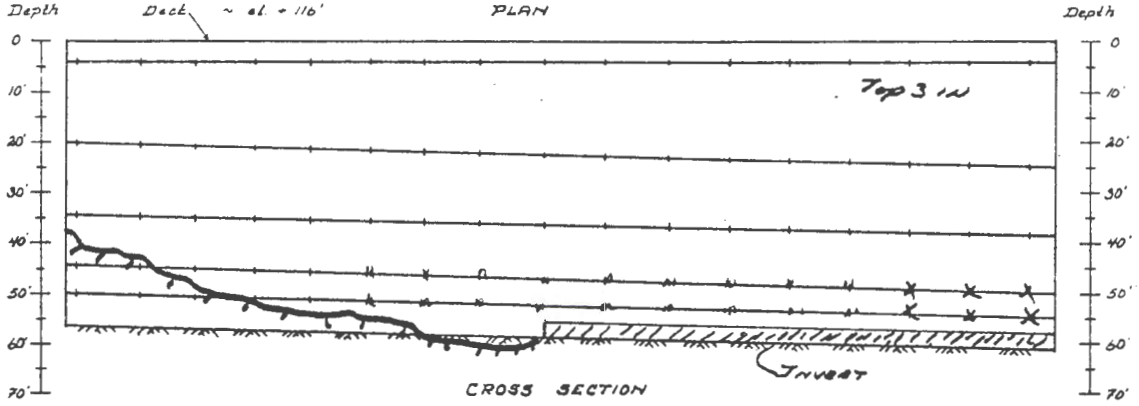

Scale
0 10' 20' 30'
1 cm = 10'

Indicate:
Depth of excavation, water level
Location of cranes, decking, surcharge loads, etc.

Circle all struts installed since date of last reading.
Note nominal size under comments.

Level	Strut: / Station:	5 / 75+95	6 / 76+07	7 / 76+18	8 / 76+29	9 / 76+41	10 / 76+53	11 / 76+64	12 / 76+77	13 / 76+88	14 / 77+01	15 / 77+13
1	Temp. °F					9-1 823-2						
	Hi	5-1 998-8			8-1 1495	9-2 1555		11-1 000			14-1 1393	
	R	5-2 972			8-2 1078	9-3 1089		11-2 000			14-2 1233	
	Lo					9-4 1394						
2	Hi	5-3 000			8-3 1436	9-5 000 9-9 1015		11-3 1217			14-3 1053	15-1 —
	R	5-4 000			8-4 1318	9-6 000 9-10 000		11-4 1268			14-4 1044-5	15-2 —
	Lo					9-7 1296-7						
						9-8 1588						
3	Hi	5-5 1279			8-5 1241-2	9-11 1299		11-5 1335			14-5 1062-3	15-3 1237
	R	5-6 1103-2			8-6 1535-6	9-12 1198		11-6 1311-2			14-6 1544-5	15-4 1296
	Lo											
4	Hi	5-7			8-7	9-13 1580		11-7 1253-2			14-7 1126	15-5 1336-7
	R	5-8			8-8	9-14 1352		11-8 1317			14-8 1083-2	15-6 1376
	Lo											
5	Hi	5-9			8-9	9-15 963-2		11-9 910			14-9 1350	15-7 1381 382 Tons
	R	5-10			8-10	9-16 1365		11-10 1397			14-10 977	15-8 1031
	Lo											

GAUGE FREQUENCIES, cps

FIGURE A-5 DAILY STRAIN GAUGE REPORT - TEST SECTION B

OPEN HYDRAULIC PIEZOMETER INSTALLATION REPORT

Project MBTA - PHASE I Instrument No. PBH4

Instrument Location TEST SECT. B - STA. 76+33 - RIGHT 85' FROM ℄ TRACK #2

Date Installed START - DEC 14 FINISH - JAN 5 By GEOMEASUREMENTS

JACK ESTABROOK & KEITH CHRISMAN Inspector E. CARDOZA & PAUL SAULNIER

Piezometer Tip GEOMEASUREMENTS TYPE - POROUS PLASTIC - HOLLOW

Leads PLASTIC TUBING (3/8" ID & 1/4" ID)

Cover Assembly Type Manhole

Elevation Top of Leads +113.76' FEB 67 +115.70' NOV 68

Comments:

1) HOLE ADVANCED BY AUGER FOR SPLIT SPOON SAMPLING & WASH BORING WITH MUD UP TO LAST 8'
2) TRIED TO WASH BELOW THE CASING WITH CLEAR WATER BUT COULD NOT CARRY UP THE STONES. WASHED 1½' BELOW CASING
3) BUMPED CASING UP 1½' TO GET FULL 3' OF SPACE UNDER THE CASING.
4) FIELD BOOK MBTA #2

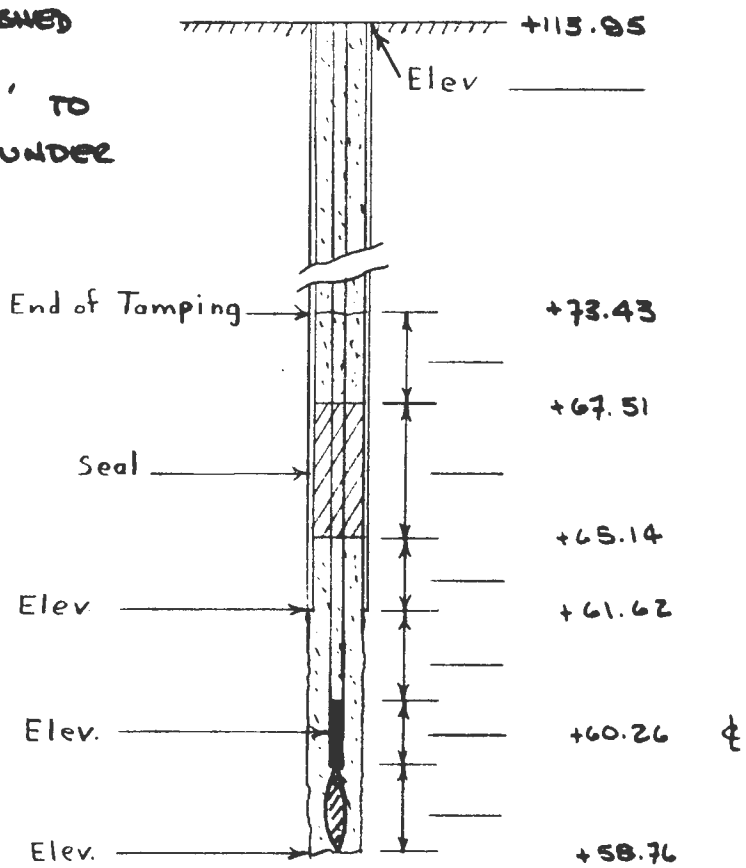

Subsoil at Tip Elev.
FIELD: LARGE (1-1½" ϕ) SHARP-EDGED STONES MIXED WITH FINE SAND & A CLAYEY SILT

FIGURE A-6 HYDRAULIC PIEZOMETER INSTALLATION REPORT

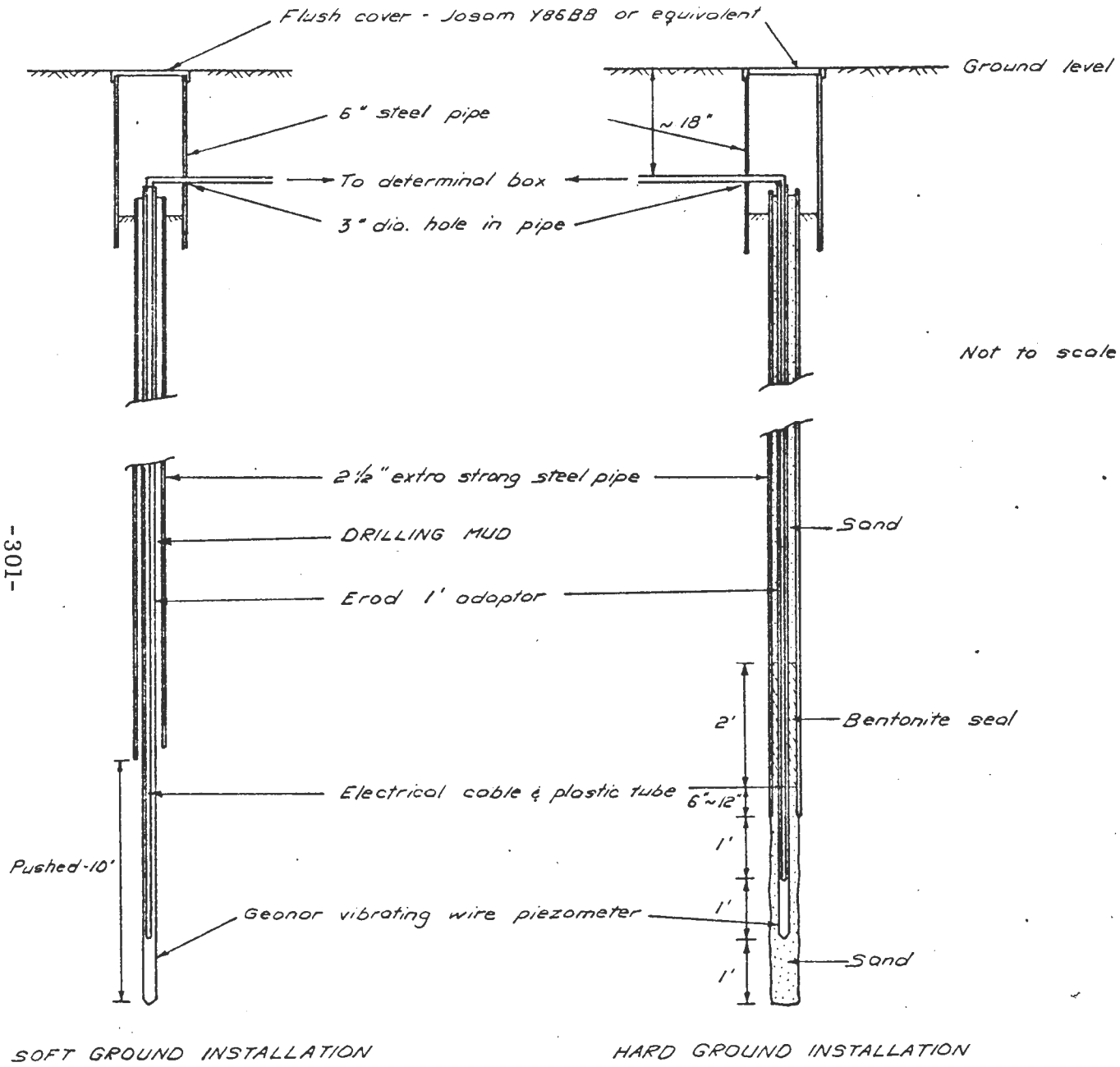

FIGURE A - 7 GEONOR VIBRATING WIRE PIEZOMETER

VIBRATING-WIRE PIEZOMETER INSTALLATION REPORT

Project [illegible] Instrument No. [illegible]

Instrument Location SECTION 15 STA 76+49.2 RIGHT 44.4 [illegible]

Date Installed 1/19/67 by [illegible]

[illegible] Inspector P. [illegible]

Vibrating-Wire Piezometer #61099 [illegible]

Leads [illegible]

Banding/Marking on Leads PBE-4 #61099

Terminal Board Connection [illegible]

Cover Assembly Type In trench of cement blocks into manhole for SIB-3

Field Book MBTA #2

Soft Ground Installation

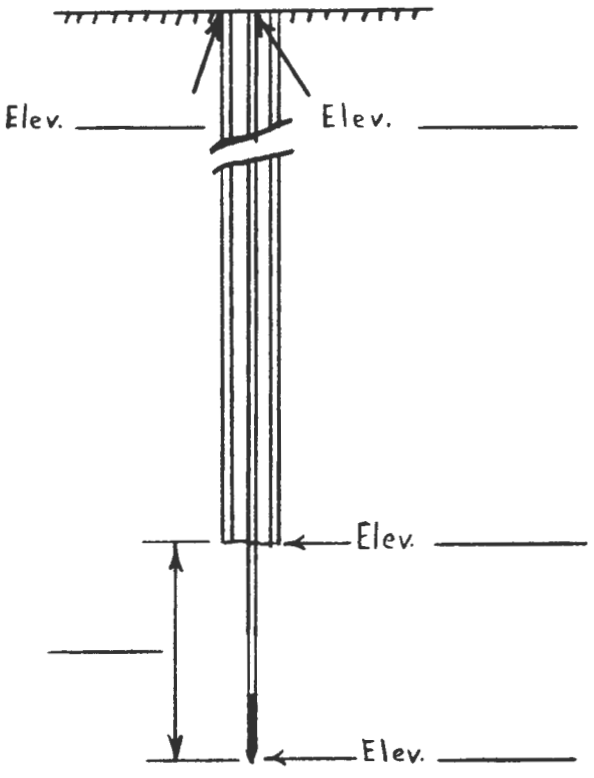

Hard Ground Installation

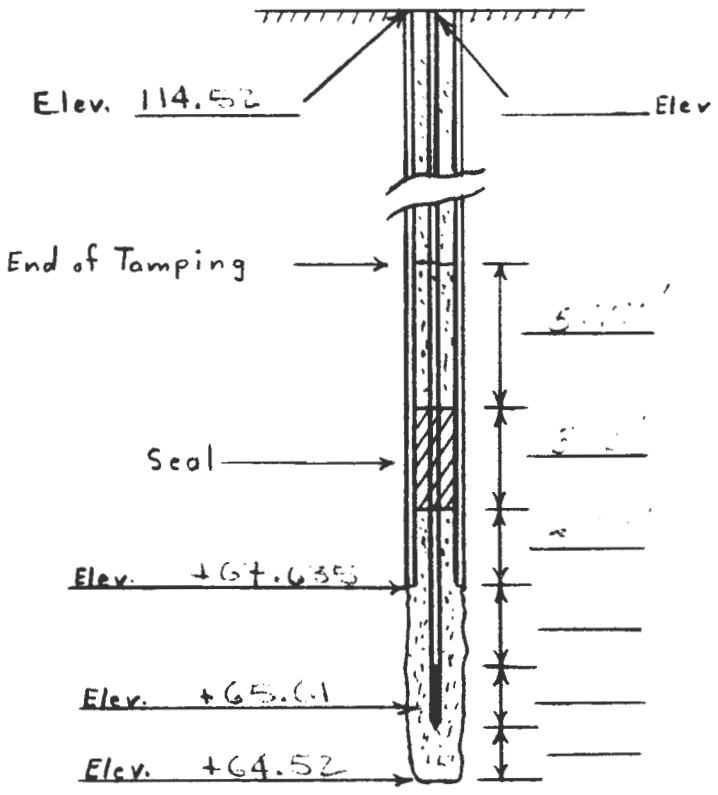

Subsoil at Tip [illegible]

See comments on reverse side:

FIGURE A-8 VIBRATING WIRE PIEZOMETER INSTALLATION REPORT

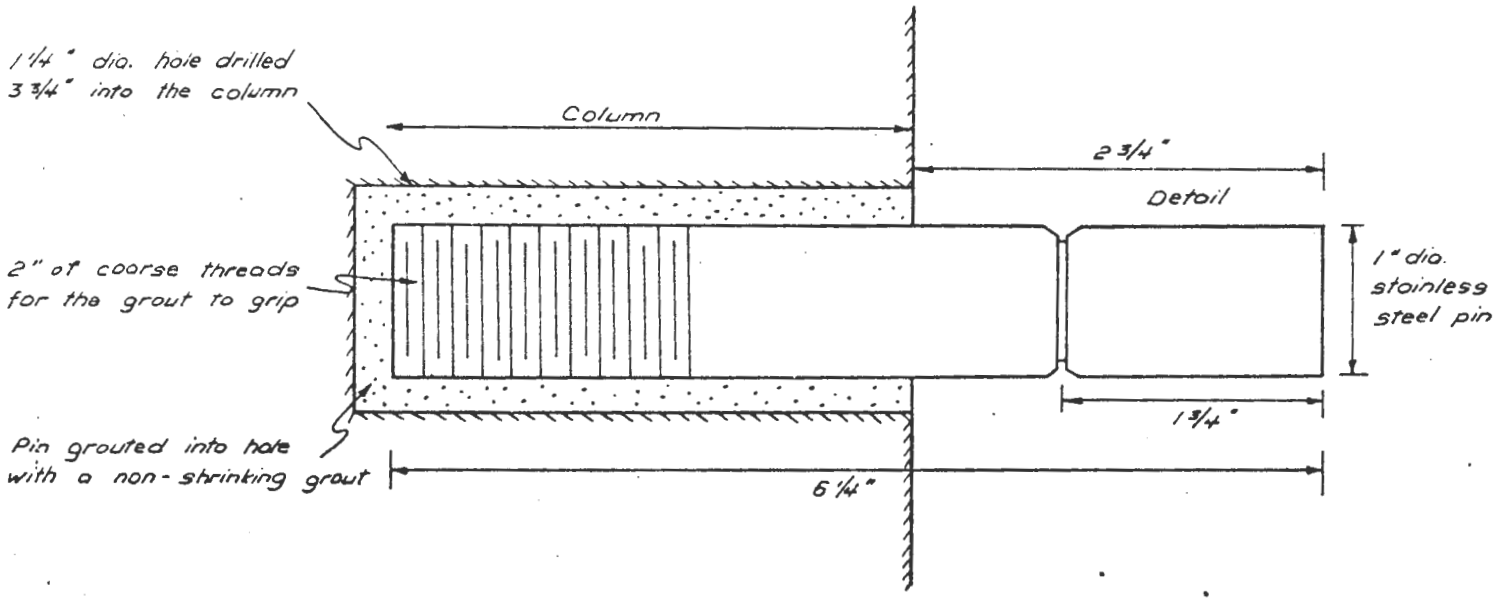

Scale : 1" = 1"

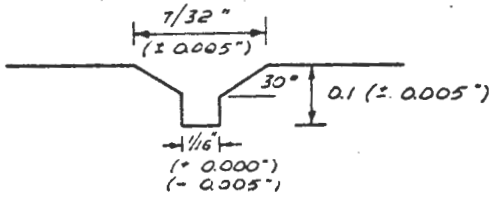

Scale : 1" = 1/4"

DETAIL OF GROOVE

FIGURE A-9 COLUMN PIN

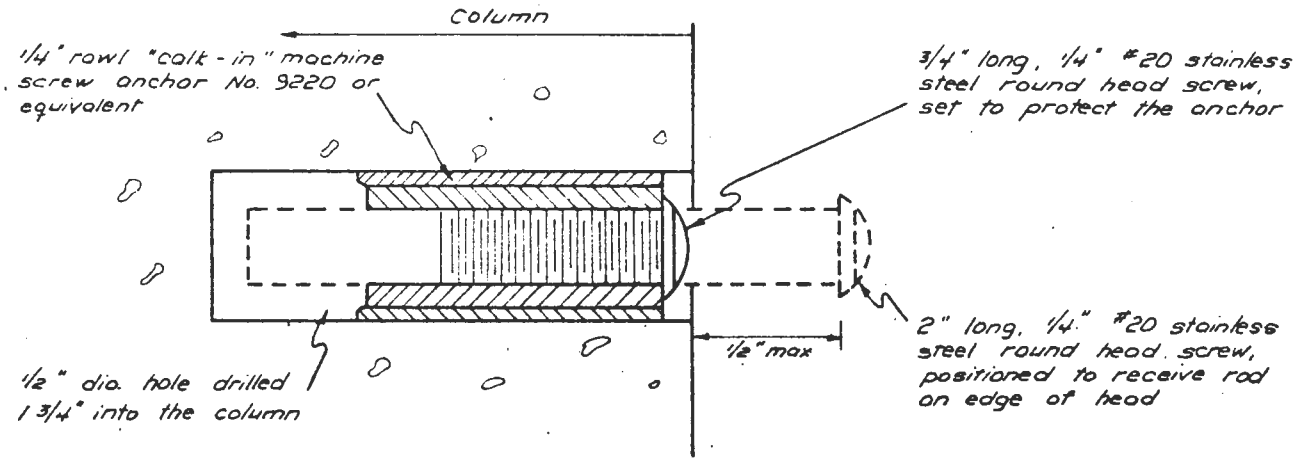

Note: When the 3/4" screw is replaced after a settlement observation, the 3/4" screw should be properly lubricated and "finger tightened" to prevent siezure

FIGURE A-10 SETTLEMENT SCREW

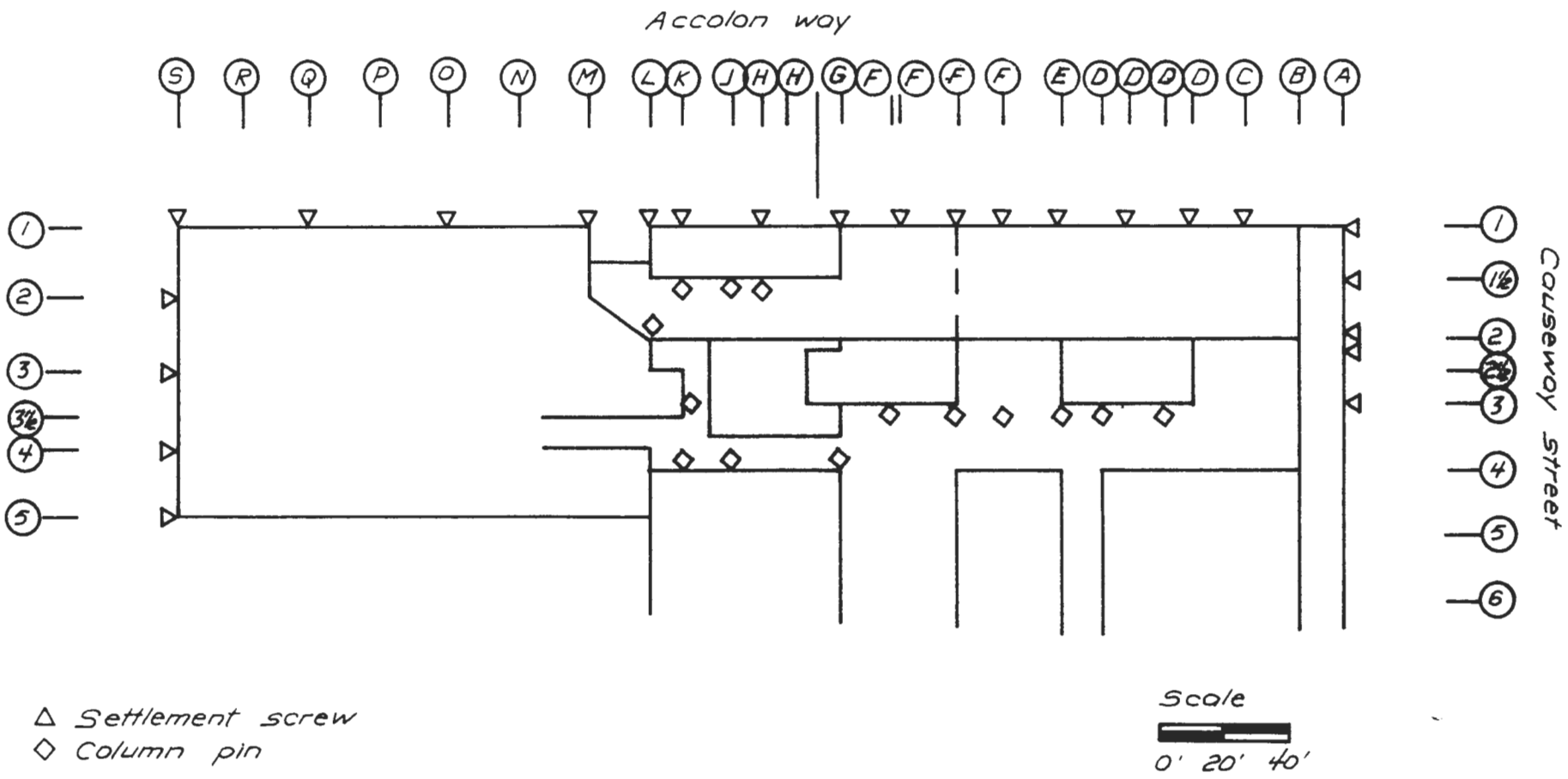

FIGURE A - 11 LOCATION OF SETTLEMENT SCREWS AND COLUMN PINS NORTH STATION

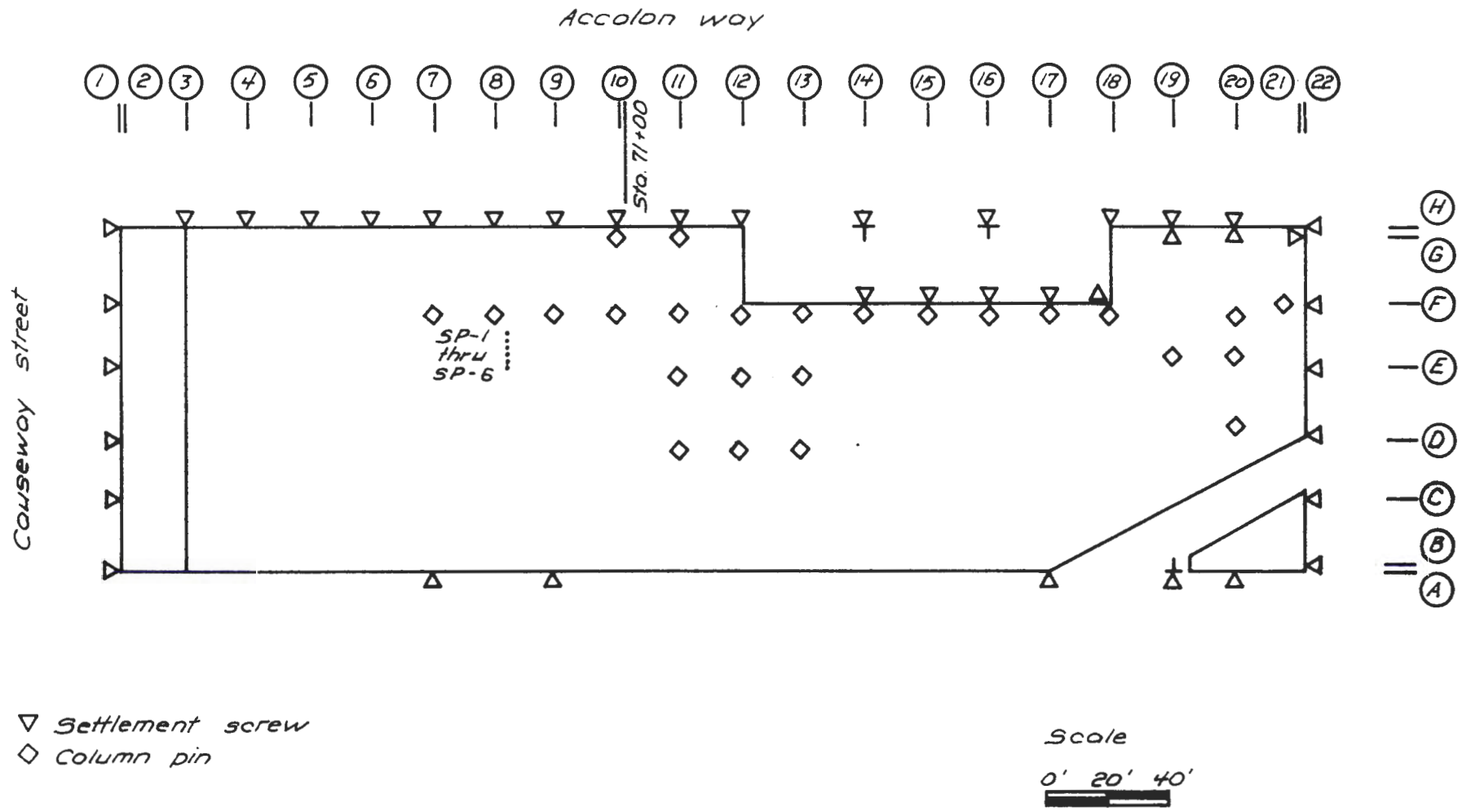

FIGURE A-12 LOCATION OF SETTLEMENT SCREWS AND COLUMN PINS ANELEX BUILDING

SETTLEMENT REFERENCE POINT RECORD

Project MBTA - Test Section 8 Sheet _____

Type of Reference Point Surface Settlement Point

Point Number SSB-2 Location In manhole over PBH-2, Sta 76+22.2 Left 14.0' from track no 2.

Date Installed 11/1 1967 by MXH & RCK

Elev. of Point + 115.074 Date Set 11/6 1967

Datum MBTA - BM-1

Comments:

FIGURE A-13 SURFACE SETTLEMENT POINT INSTALLATION REPORT

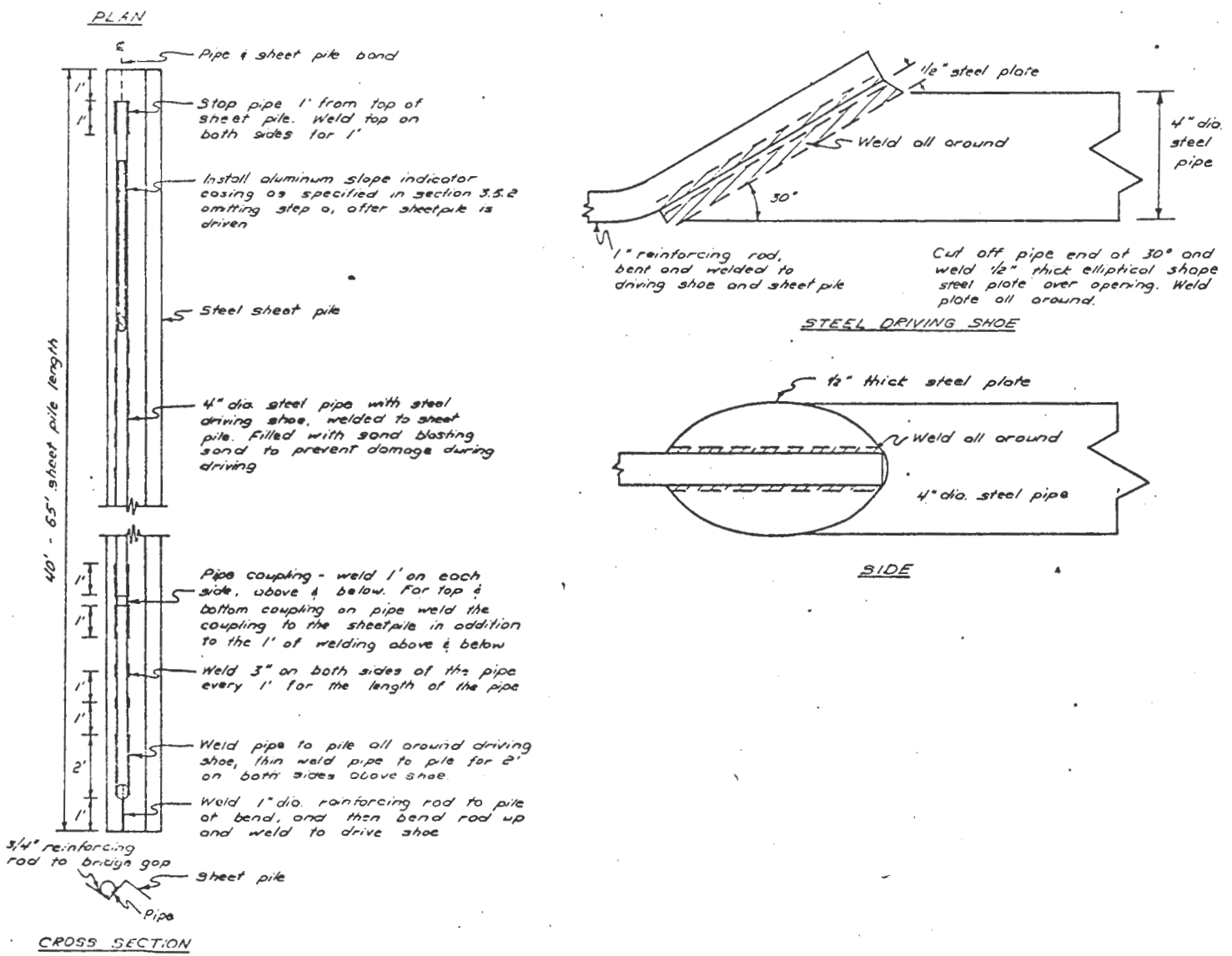

FIGURE A-14 DETAIL OF SLOPE INDICATOR INSTALLATION ON STEEL SHEET PILING

SLOPE INDICATOR WELL INSTALLATION REPORT

Project MBTA Haymarket-Charles Instrument No. SIB - 3

Date Installed 1/21 - 2/21 67 by Geomeasurements

Inspector PE Sanborn

Cover Assembly Type Manhole - extra large to [illegible] vibrating wire pie[illegible]

Slope Indicator Casing Type Aluminum telling 12"c[illegible]

Band and Seal Type 12" couplings sealed with elect[illegible]

Number of Sections of Slope Indicator Casing Used 13

Length of Sections 5'0" + 6" pr. coupling

Orientation of Grooves ⊥ + ∥ to new track line

Comments:

Installation at Sta 76+53.2' [illegible] 46.0' of ℄ track [illegible] Manhole installed 2/22 67, enlarged to 2½ by 2 inches, 3 layers deep to accommodate leads to PBE 1, 2, 3, 4, 5. [illegible] as described in field book MBTA #2

29 July 70 - WRB inspected. SI Casing gauge deep in Manhole probably unchanged since installation. Manhole to be rebuilt.

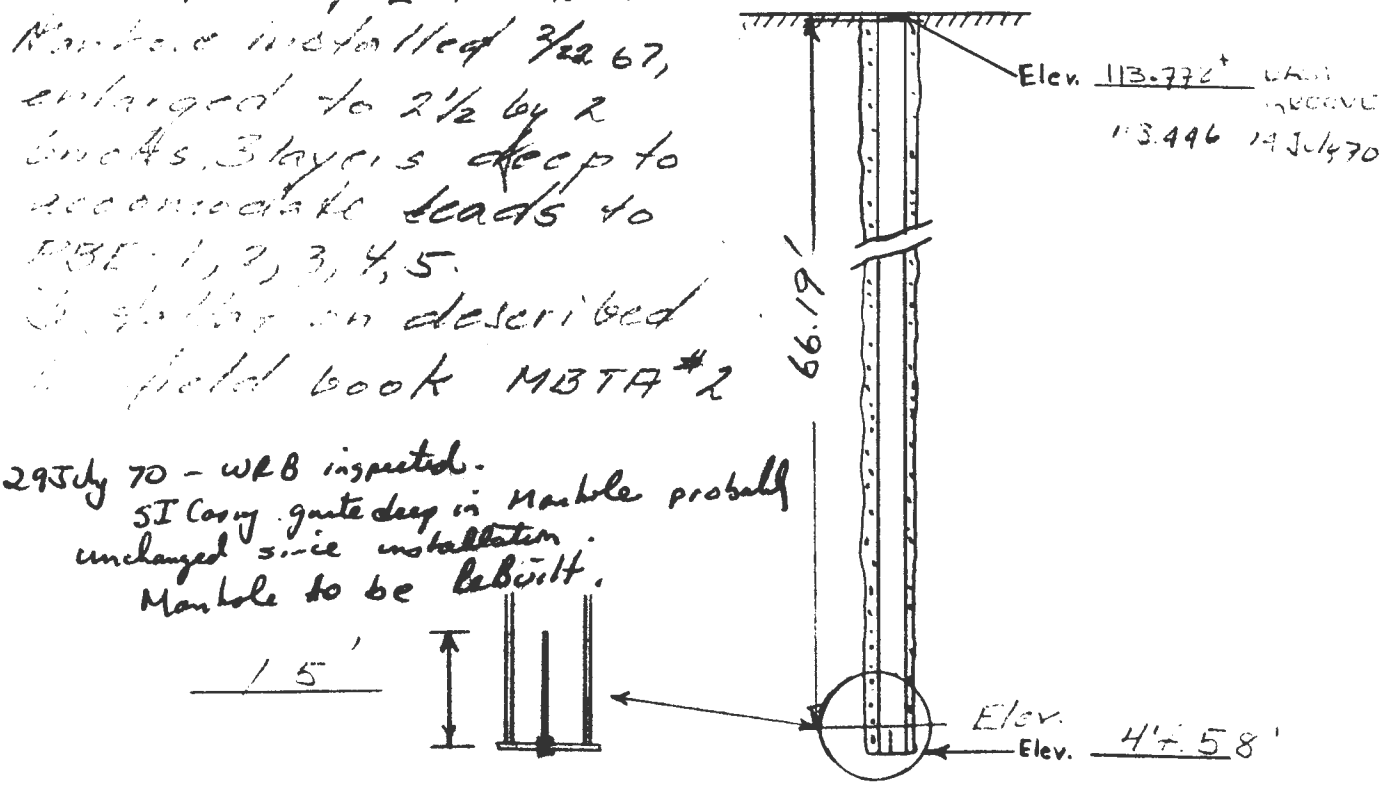

FIGURE A-15 SLOPE INDICATOR WELL INSTALLATION REPORT

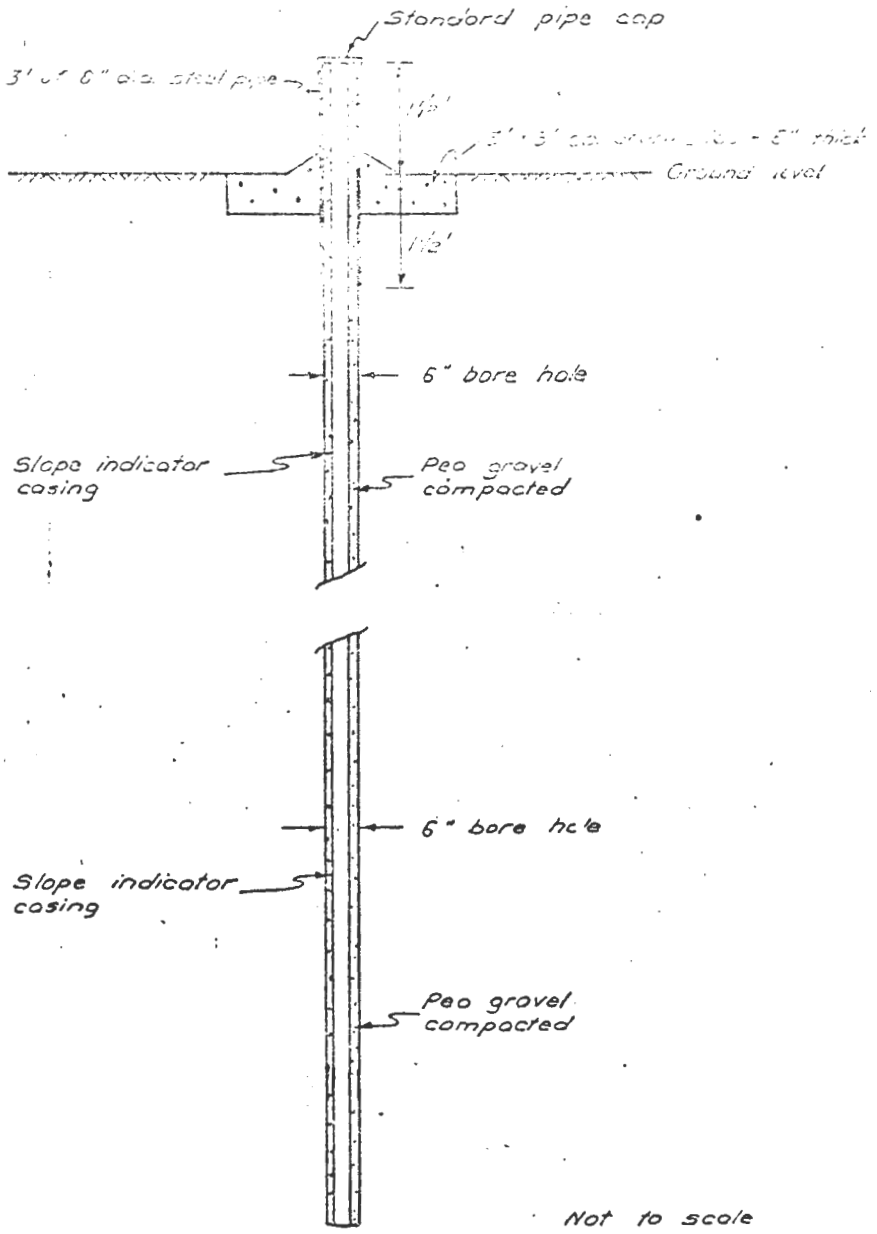

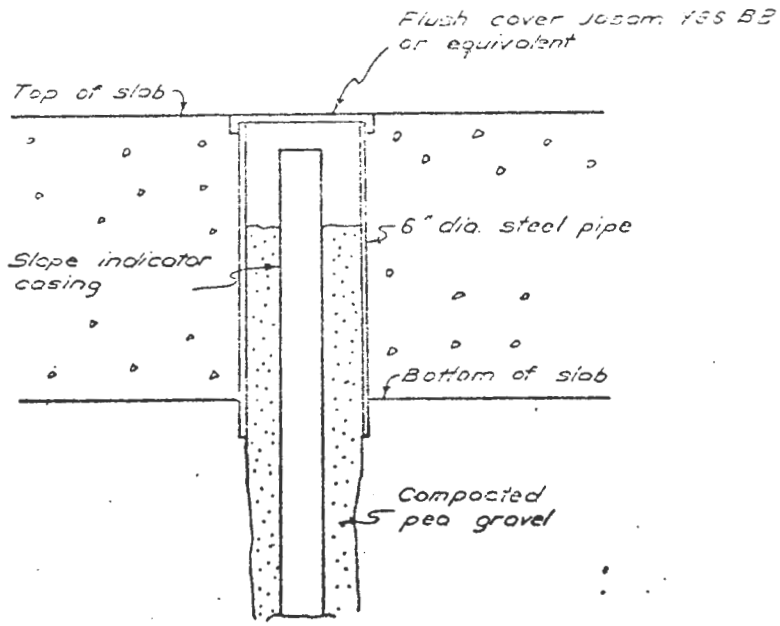

INSTALLATION THROUGH FLOOR SLAB

FIGURE A-16 SLOPE INDICATOR WELL INSTALLATION

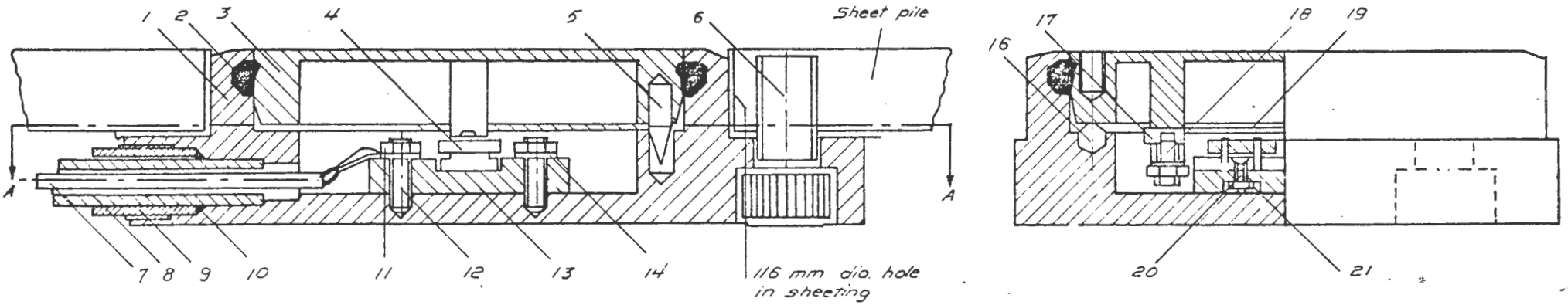

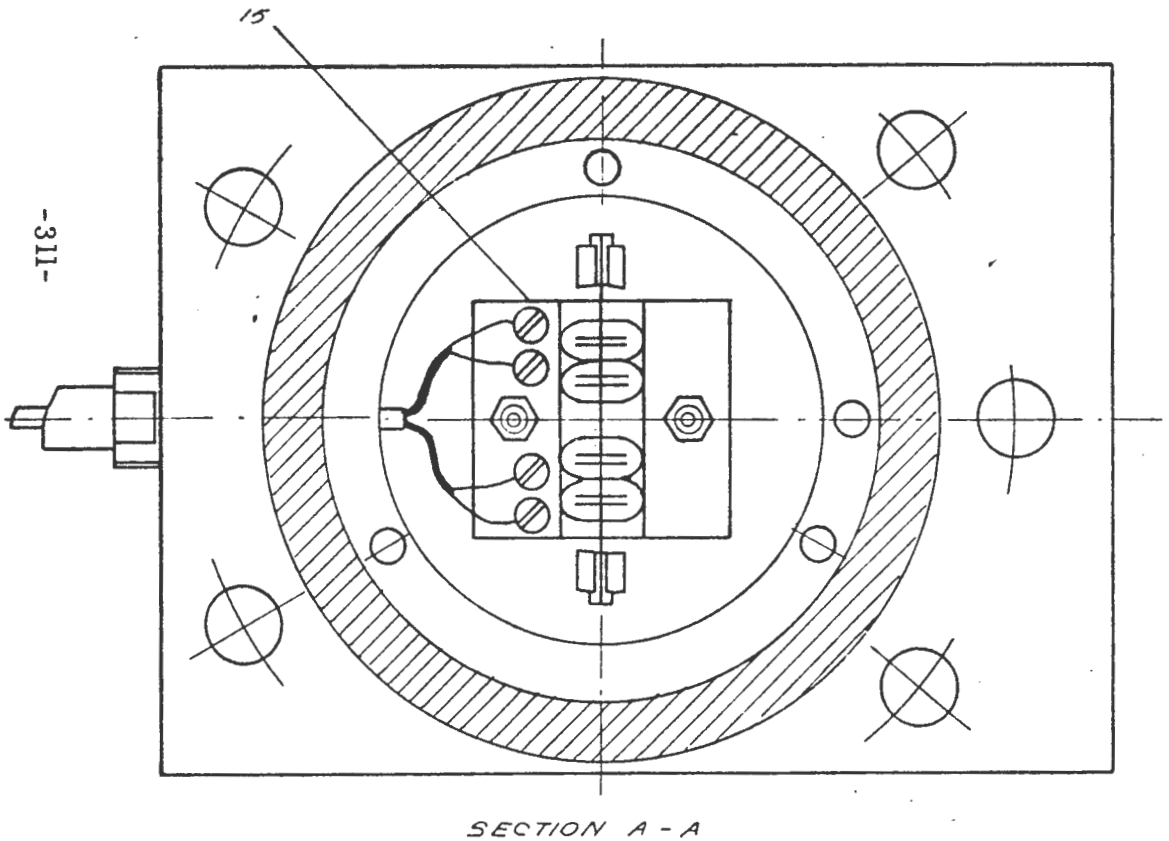

SECTION A - A

ITEM	NO.
Nut (2)	21
Bolt (2)	20
Steel wire (vibrating - wire)	19
Set screw (2)	18
Wedge pin for vibrating wire (2)	17
Steel ball	16
Terminal screw (4)	15
Lock washer (4)	14
Electromagnet holder	13
Bolt (2)	12
Nut (4)	11
O - ring	10
Lock screw	9
Copper tube	8
Electrical coble (single strond shielded)	7
Housing bolt	6
Guide pin	5
Electromagnet assembly (4)	4
Steel pressure diophrogm	3
O - ring diophrogm seal	2
Steel housing	1

FIGURE A - 17 GEONOR VIBRATING - WIRE STRESS CELL

Section I

replaced with new cell with 18-67 a [illegible] from bridge [illegible]

VIBRATING WIRE STRESS CELL INSTALLATION

Cell no.: S - 158 - Z (replaced 10-67)

Date of installation: 8/1 1967

Project: MBTA - Phase II

Location: Test Section B, Sheet 2 of 2 Sta. 76 + 00.00 East [illegible]

Depth, ft.: 8.21'

Elevation, ft.: + 107.79

Initial zero reading, cps: _____

Location of readout: Instrumentation readout [illegible]

Remarks: Cell broken, removed 10/6 1967, repaired, recalibrated and installed again on 10/9 1967. New zero reading ~1263 cps @ field temp (~ 50°F).

FIGURE A-18 VIBRATING WIRE STRESS CELL INSTALLATION REPORT

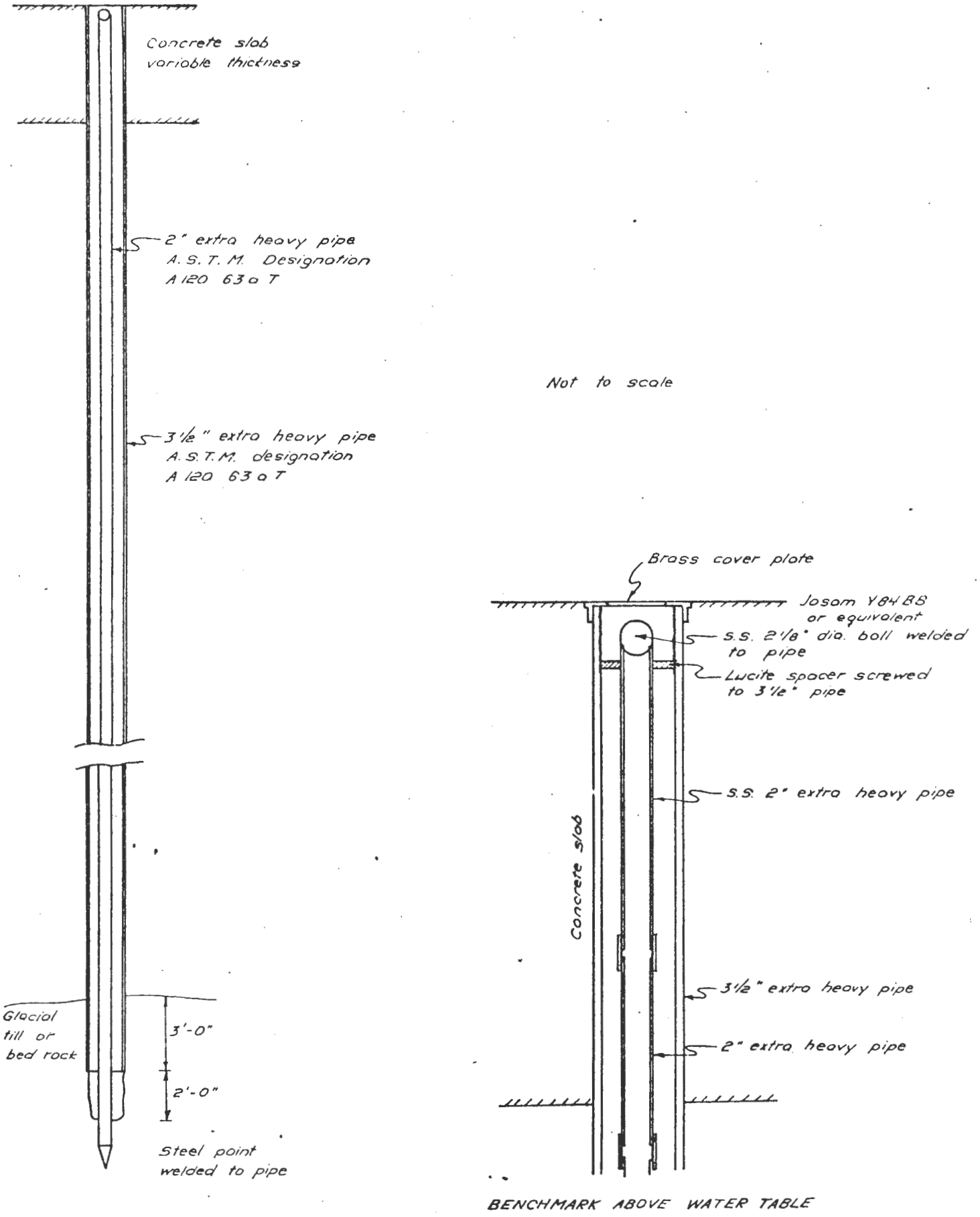

FIGURE A - 19 PEMANENT BENCHMARK

BENCH MARK INSTALLATION REPORT

Project MBTA - Extension Bench Mark No. BM-2

Bench Mark Location Inside North Station Sta 71+10

Date Installed 12/1966 - 12/1966 By Geomeasurements

_____ Inspector Field instrumentation

Cover Assembly Type _____

Bench Mark Elevation +118.528'

Datum Mag Nail N12 on column #5A North Station

Level Run Recorded

in Field Book No. MBTA #3

Date Elev. Set 2/1 1967

Comments:

Location described in record book No. MBTA #1,4

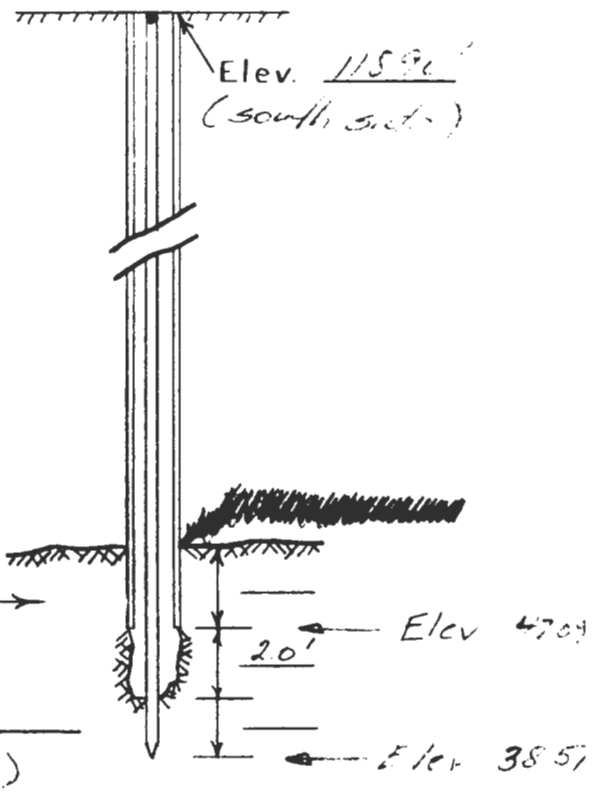

Material Field: Clayey stiff sand

_____

Blow count per inch for last 6 inches _____

Blows/350# hammer or 18" fall	Drive (1")
100	3"
100	1½"
100	1¾"
100	3/4"

FIGURE A-20 BENCHMARK INSTALLATION REPORT

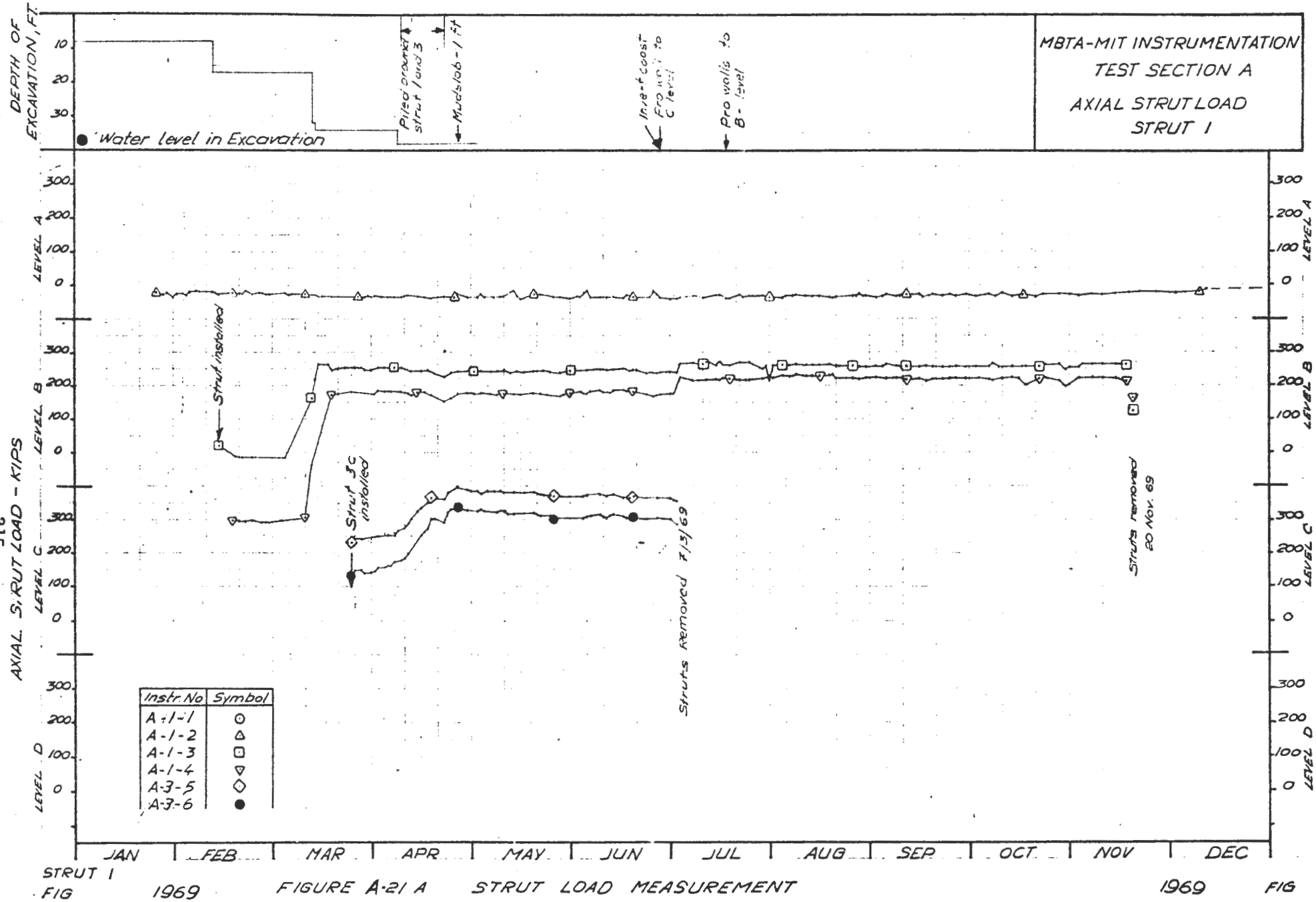
MBTA-MIT INSTRUMENTATION
TEST SECTION A
AXIAL STRUT LOAD
STRUT 1
DEPTH OF EXCAVATION, FT.
10
20
30
Water level in Excavation
Piled drained strut 1 and 3
Mud slab - 1 ft
Inst. at coast
Pro walls to
B - level
AXIAL STRUT LOAD - KIPS
LEVEL A
LEVEL B
LEVEL C
LEVEL D
300
200
100
0
Strut installed
Strut 3C installed
Struts removed 7/3/69
Struts removed 20 Nov. 69
Instr. No
Symbol
A-1-1
A-1-2
A-1-3
A-1-4
A-3-5
A-3-6
JAN
FEB
MAR
APR
MAY
JUN
JUL
AUG
SEP
OCT
NOV
DEC
STRUT 1
FIG
1969
FIGURE A-21 A STRUT LOAD MEASUREMENT
1969
FIG

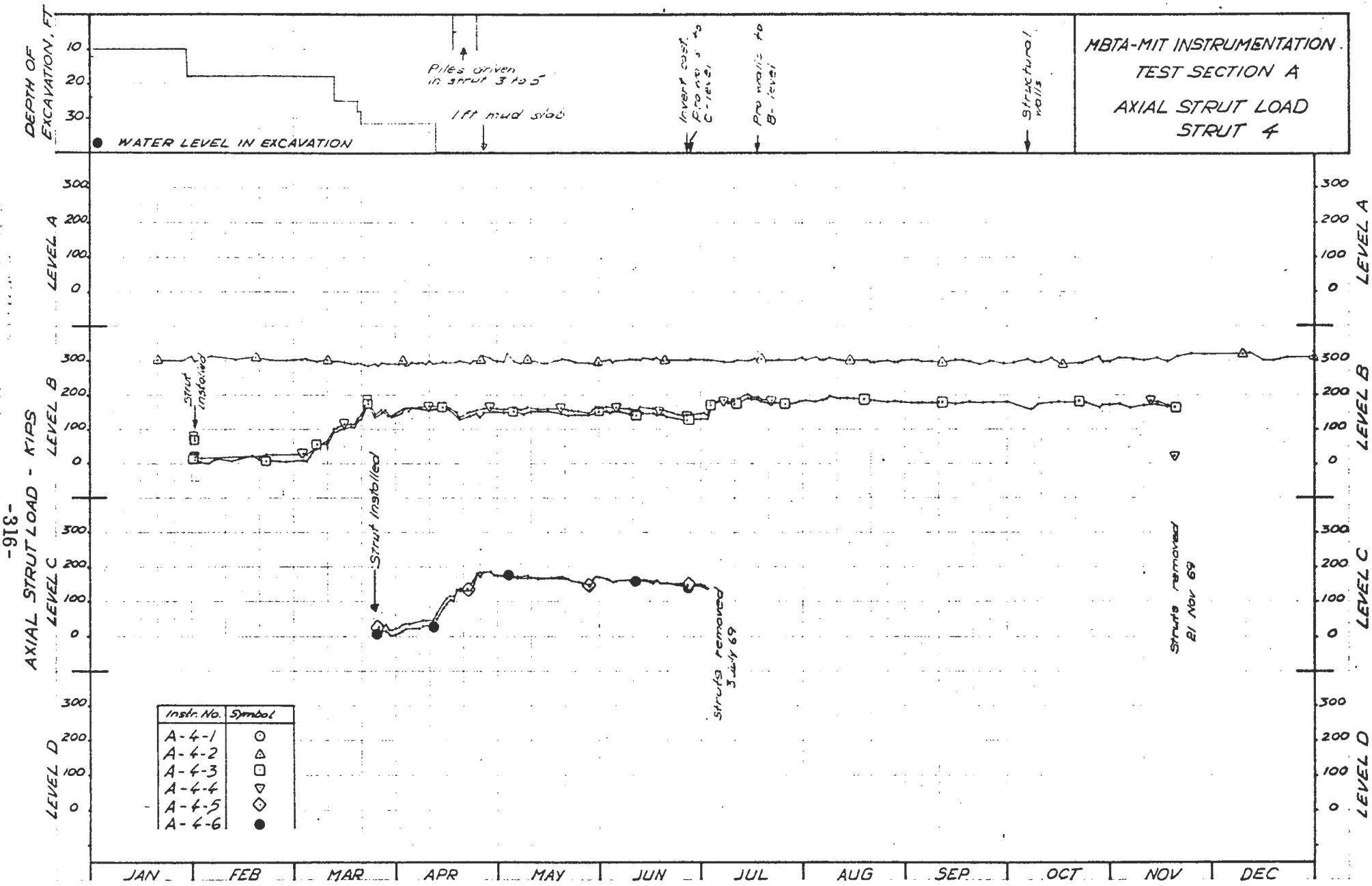

STRUT 4 FIG. 1969 FIGURE A-21B STRUT LOAD MEASUREMENT 1969 FIG.

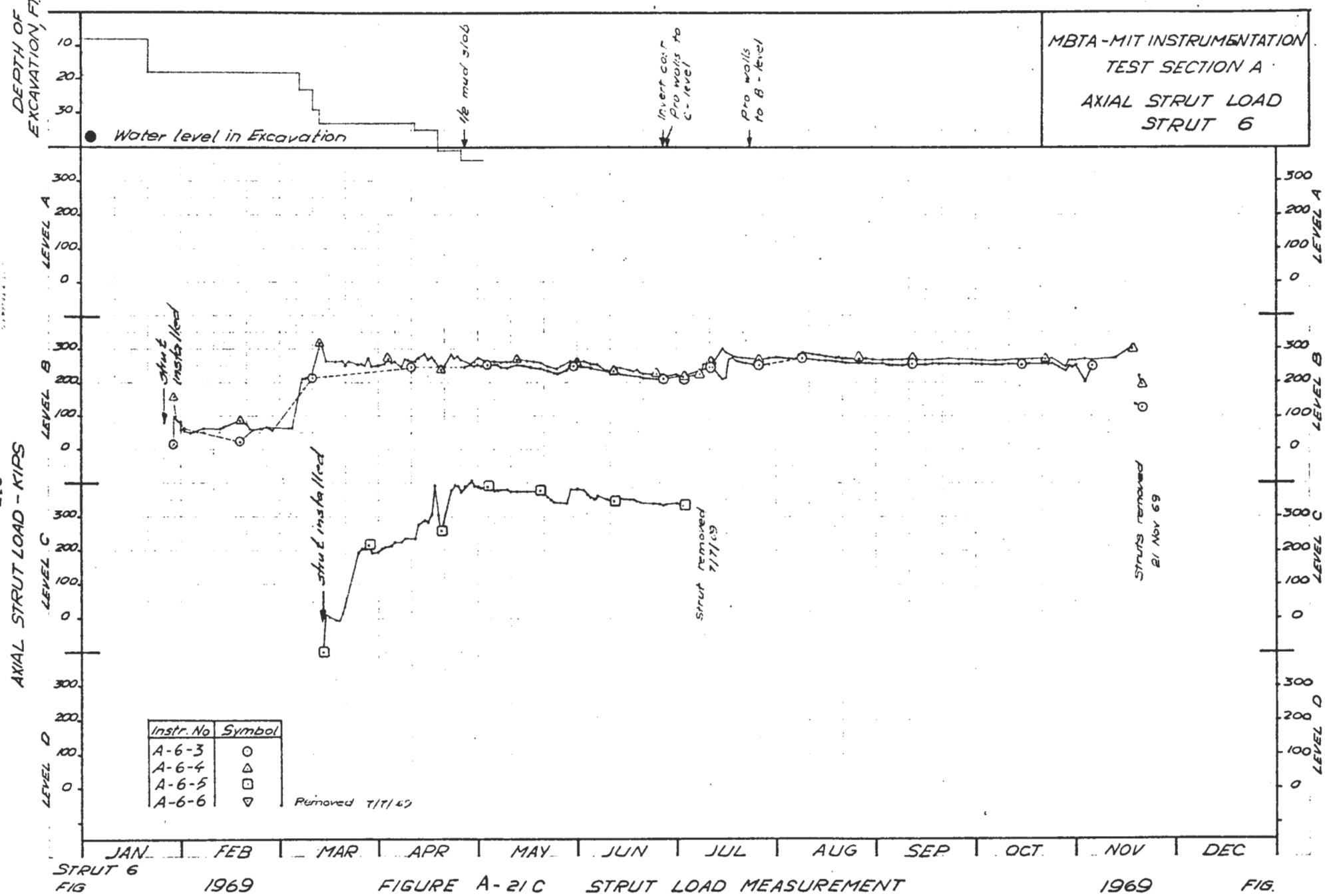

STRUT 6 FIG

FIGURE A-21C STRUT LOAD MEASUREMENT FIG.

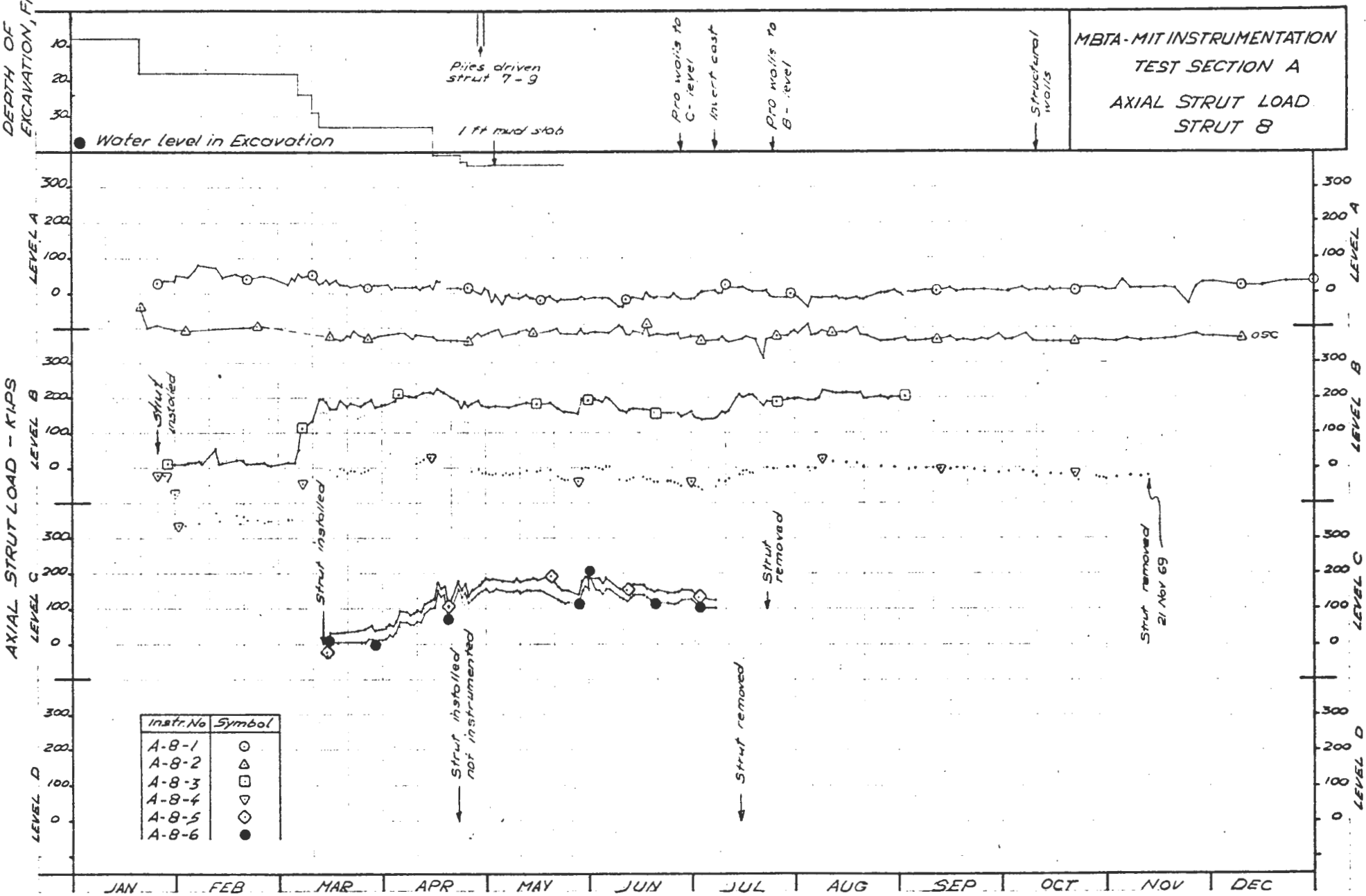

-318-

STRUT 8 FIG 1969 FIGURE A-21 D STRUT LOAD MEASUREMENT 1969 FIG.

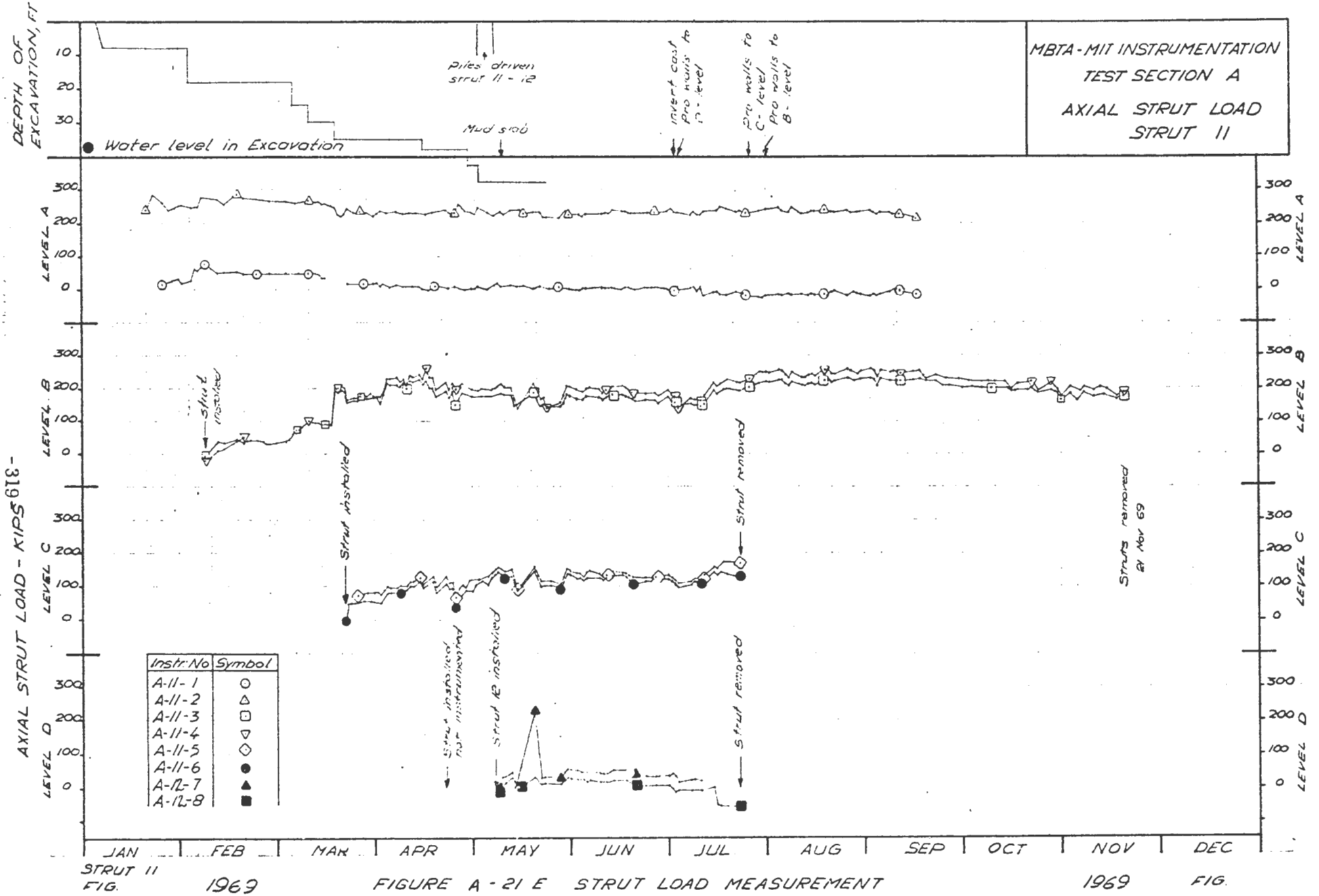

STRUT 11 FIG.

FIGURE A - 21 E STRUT LOAD MEASUREMENT

1969 FIG.

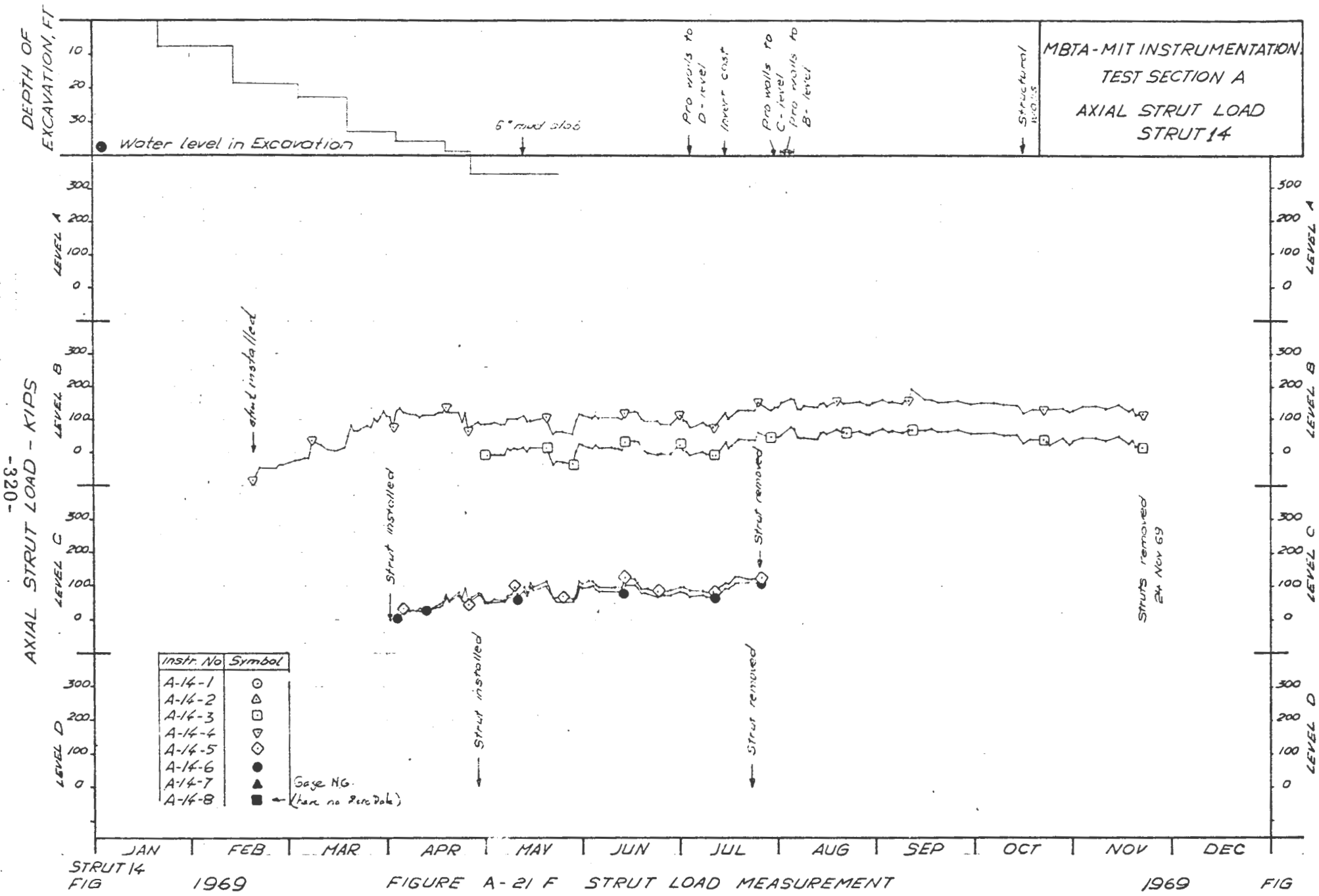

STRUT 14 FIG

FIGURE A-21 F STRUT LOAD MEASUREMENT

1969 FIG

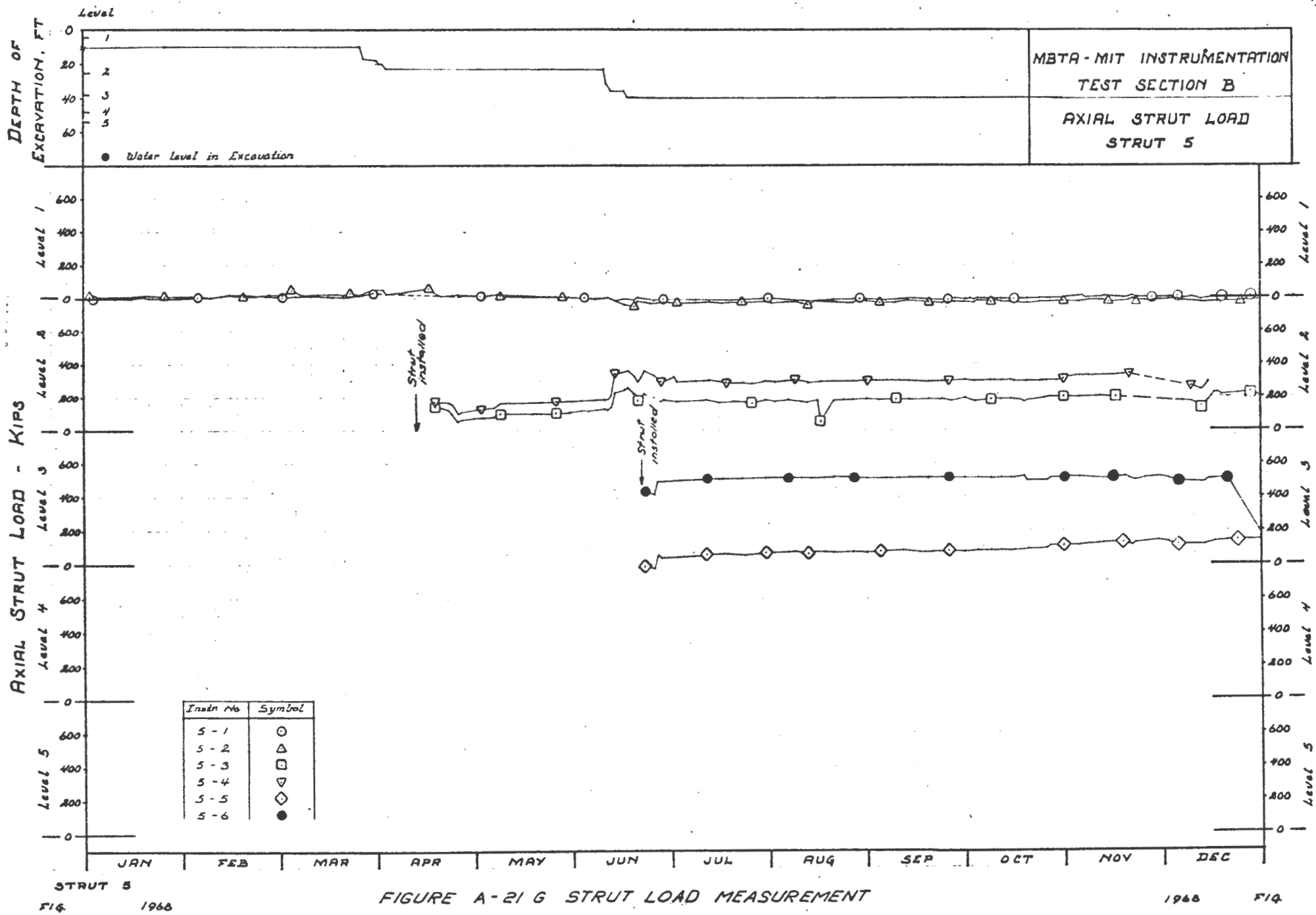

FIGURE A-21 G STRUT LOAD MEASUREMENT

FIG. 1968

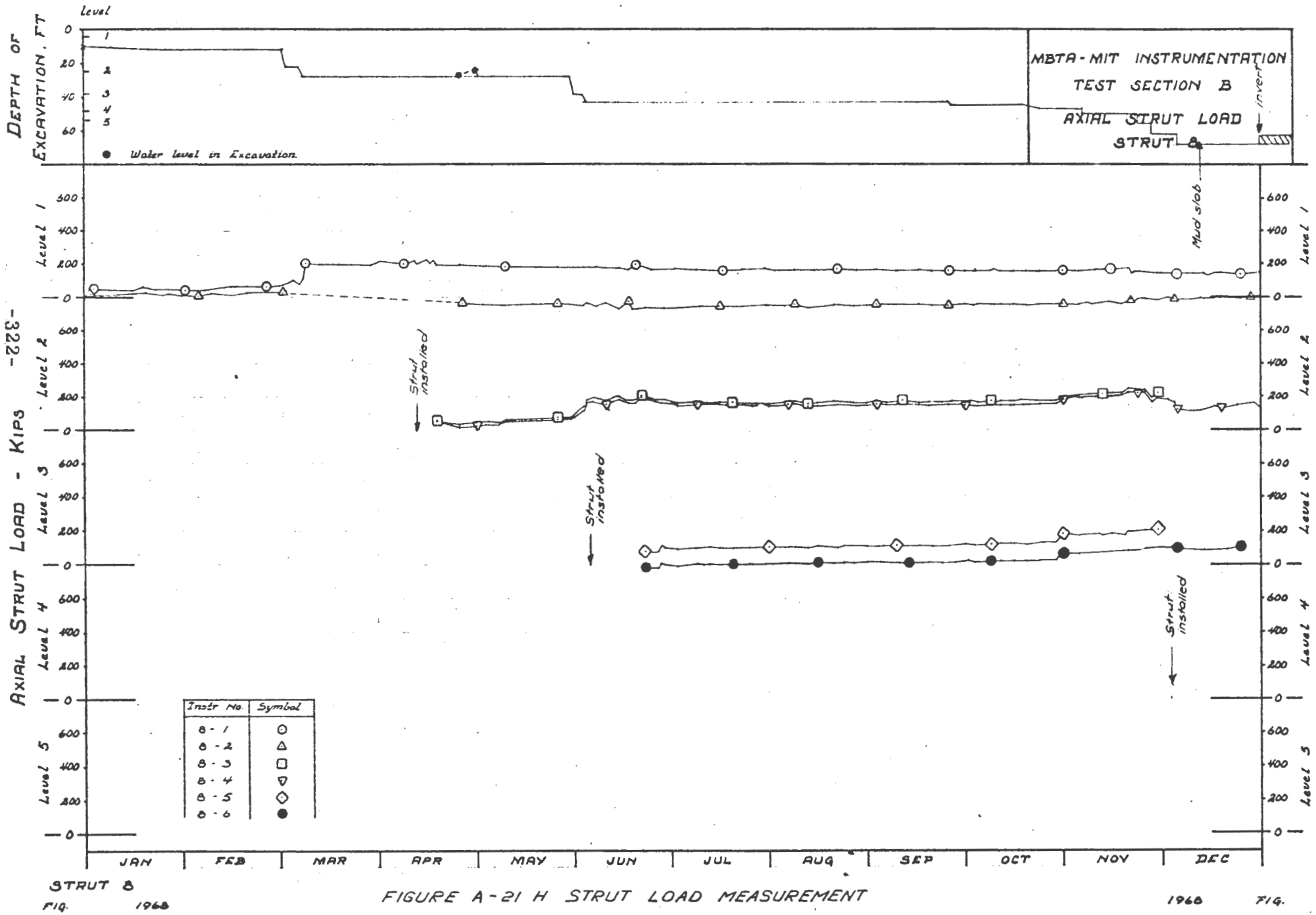

FIGURE A-21 H STRUT LOAD MEASUREMENT

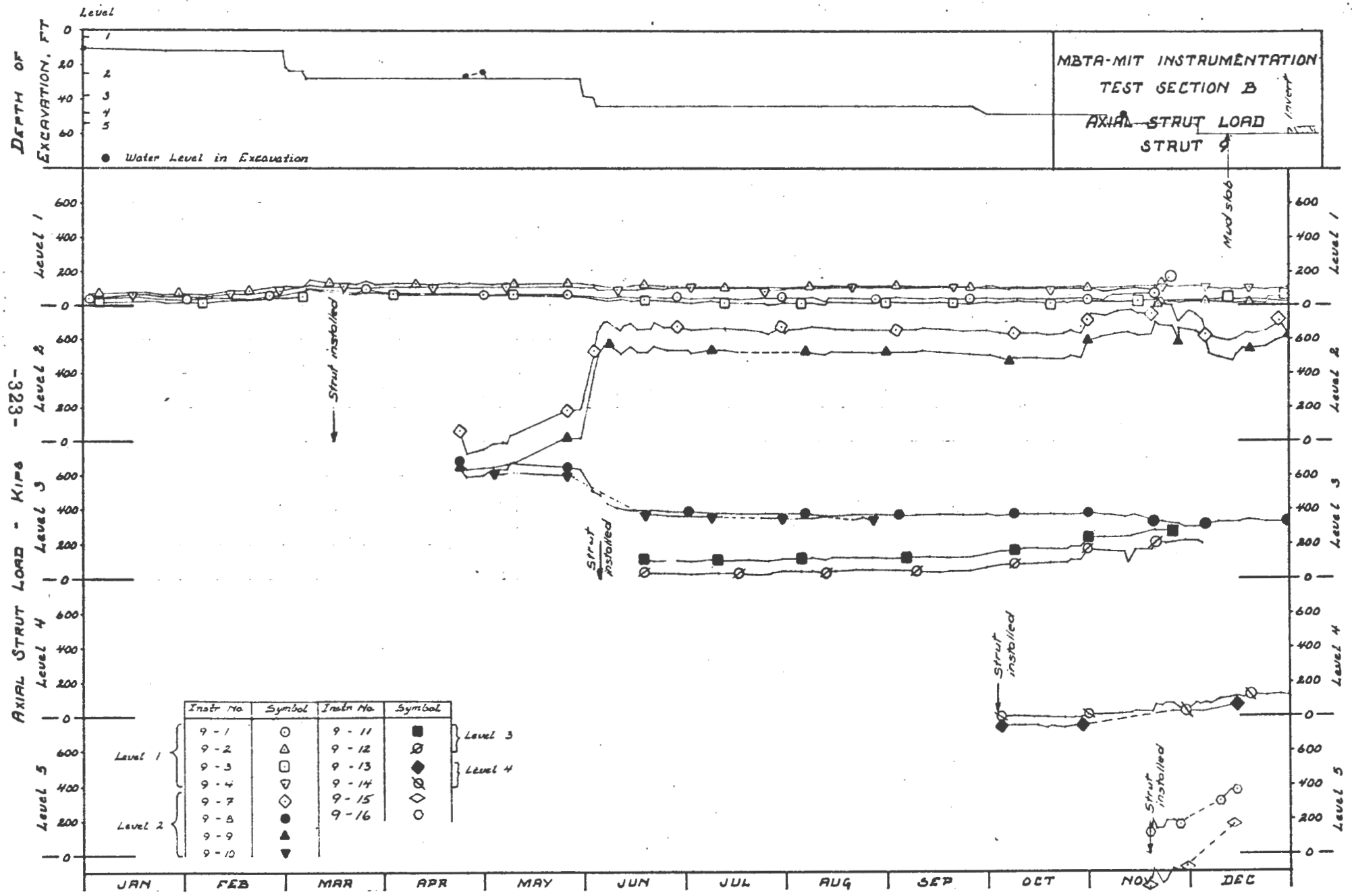

STRUT 9

FIGURE A-21 I STRUT LOAD MEASUREMENT

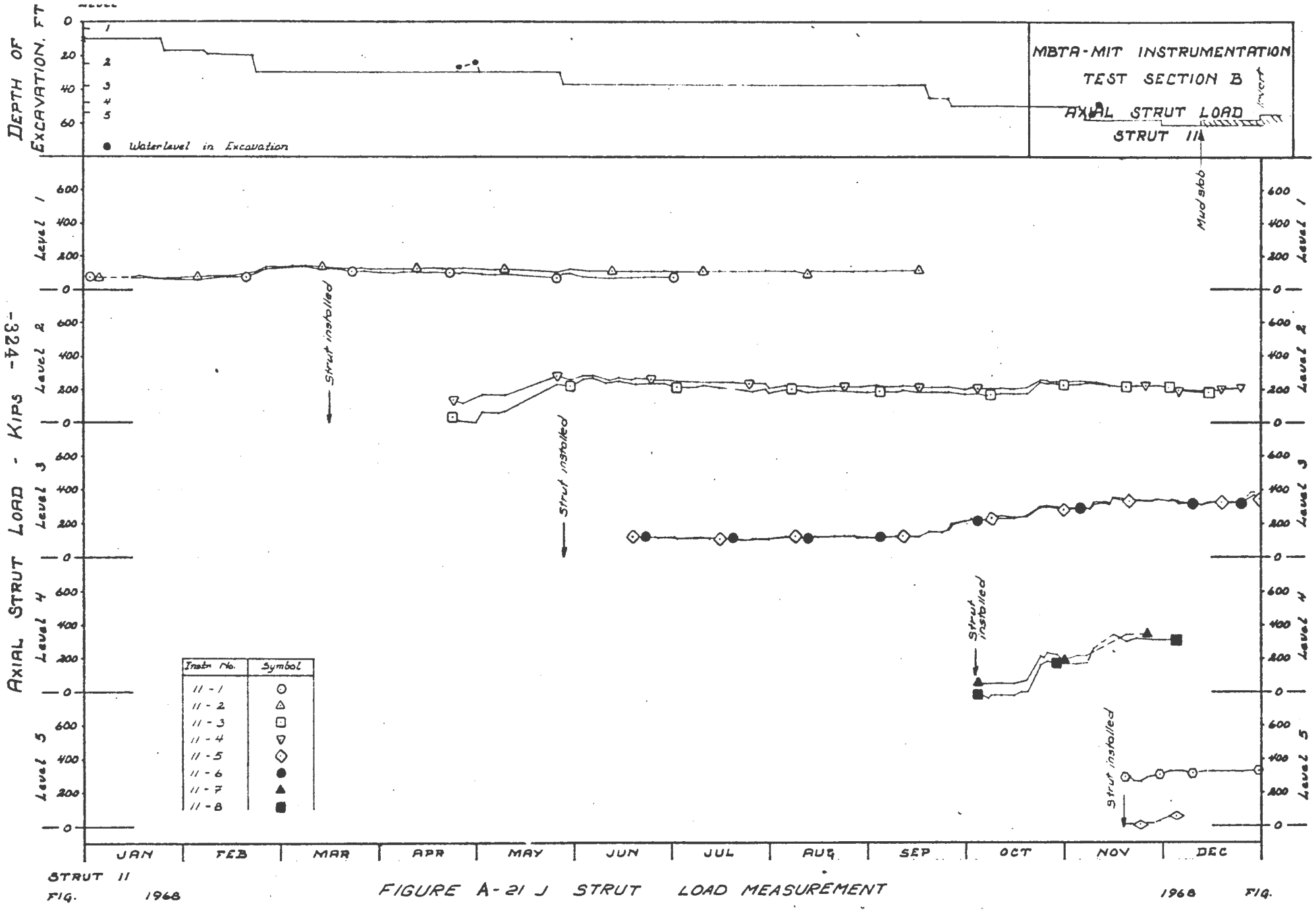

STRUT 11 FIG.

FIGURE A-21 J STRUT LOAD MEASUREMENT

1968 FIG.

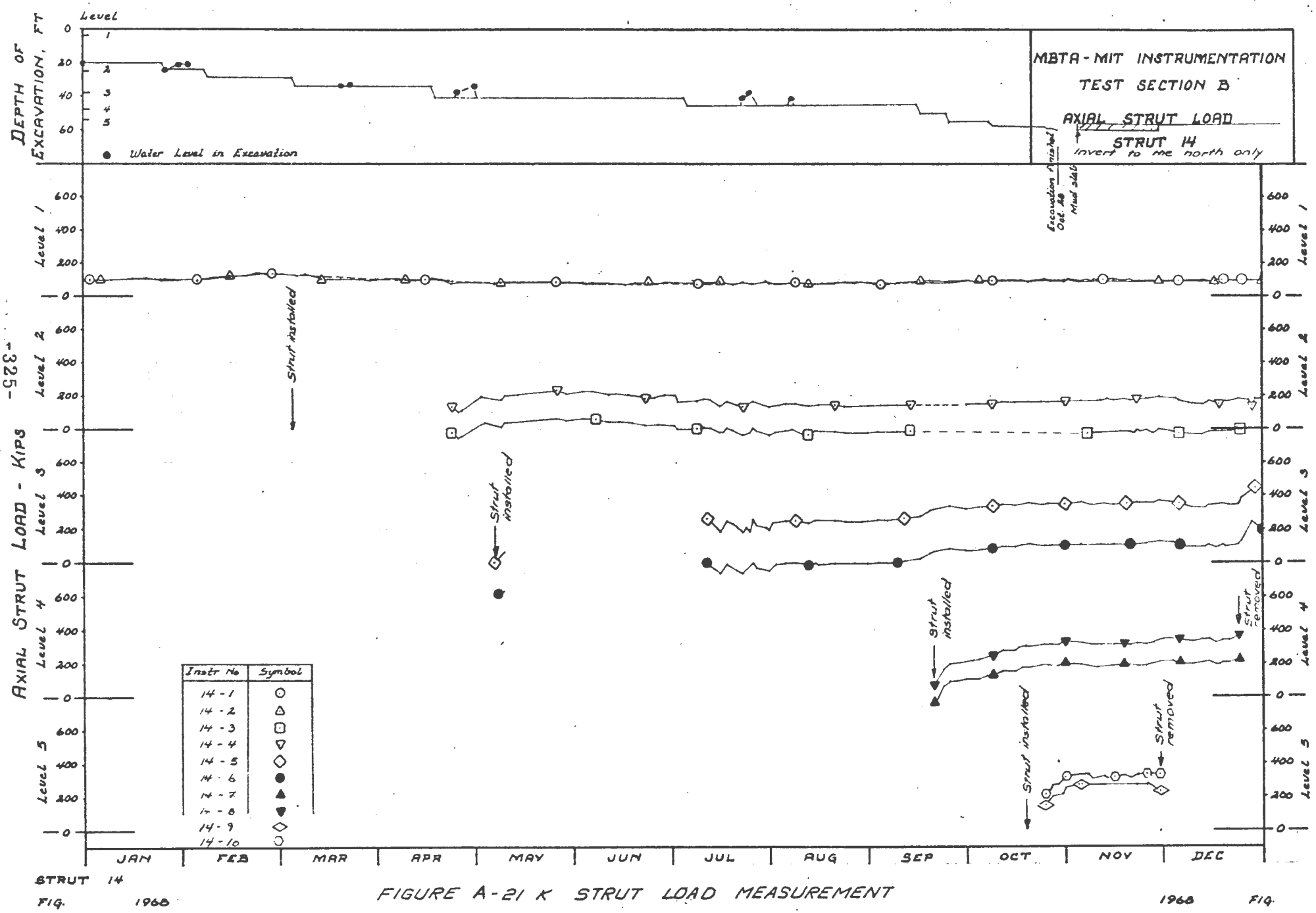

STRUT 14

FIG. 1968

FIGURE A-21 K STRUT LOAD MEASUREMENT

1968 FIG.

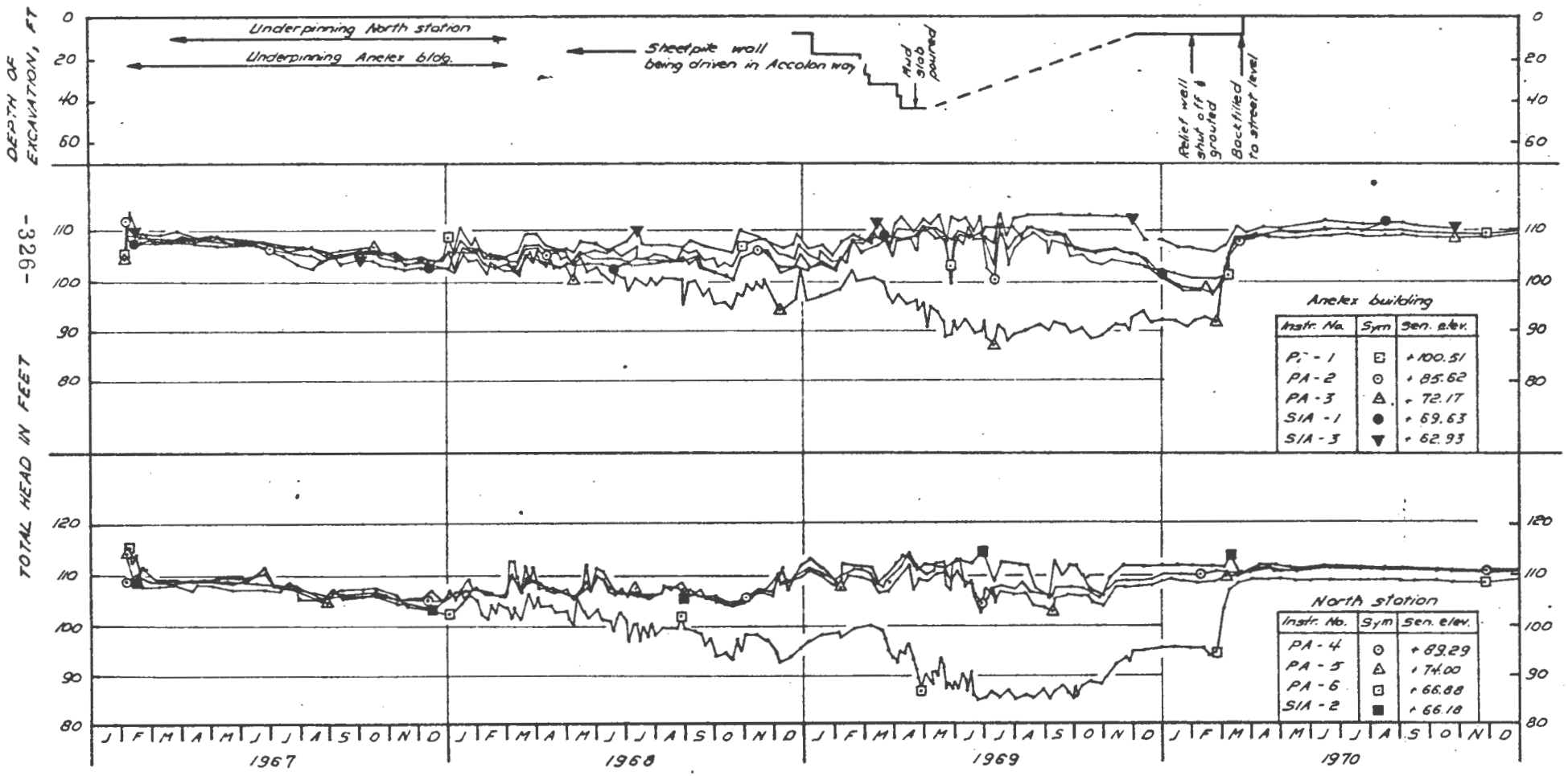

FIGURE A-22A PORE PRESSURE MEASUREMENTS - TEST SECTION A

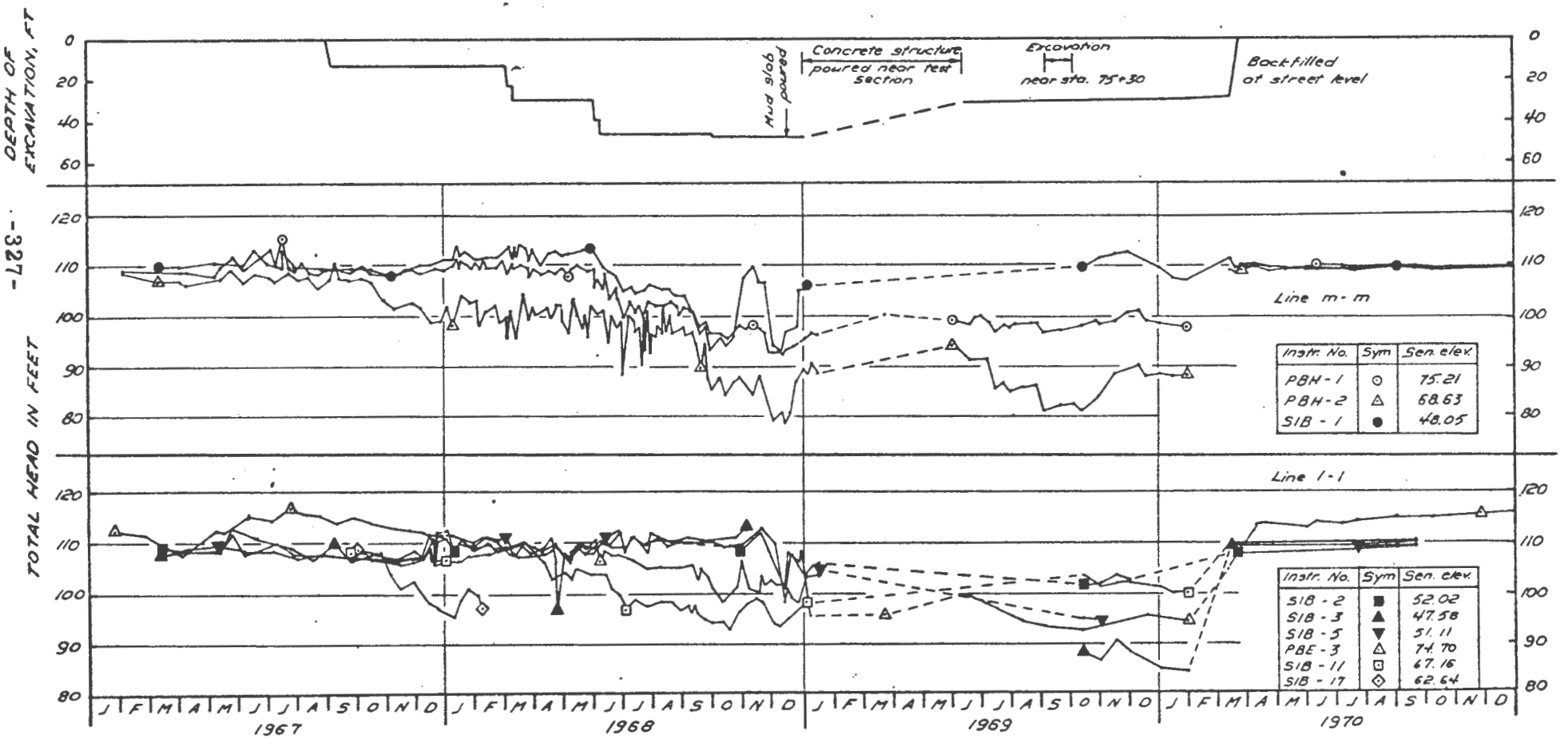

FIGURE A-22B PORE PRESSURE MEASUREMENTS TEST SECTION B

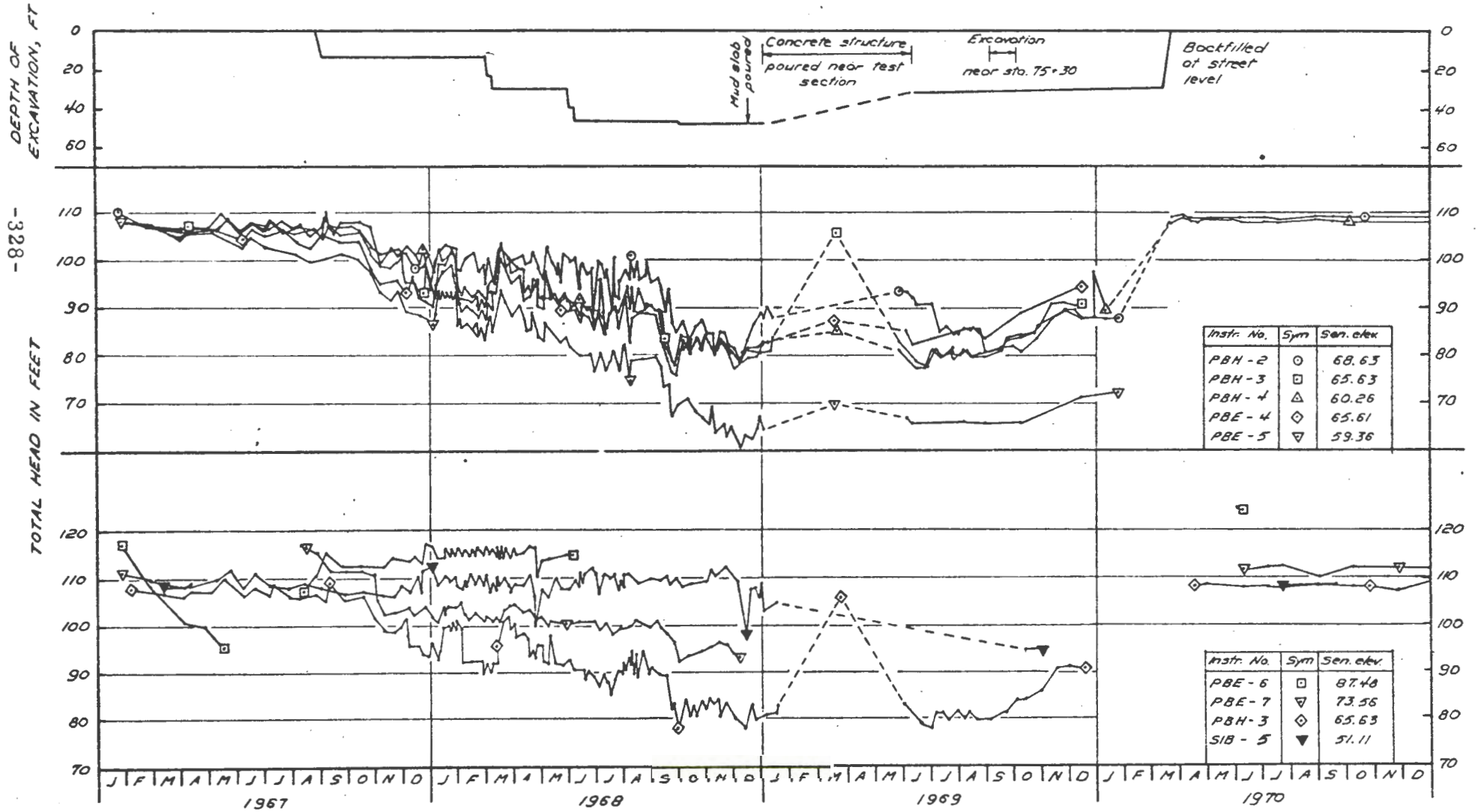

FIGURE A - 22C PORE PRESSURE MEASUREMENTS TEST SECTION B

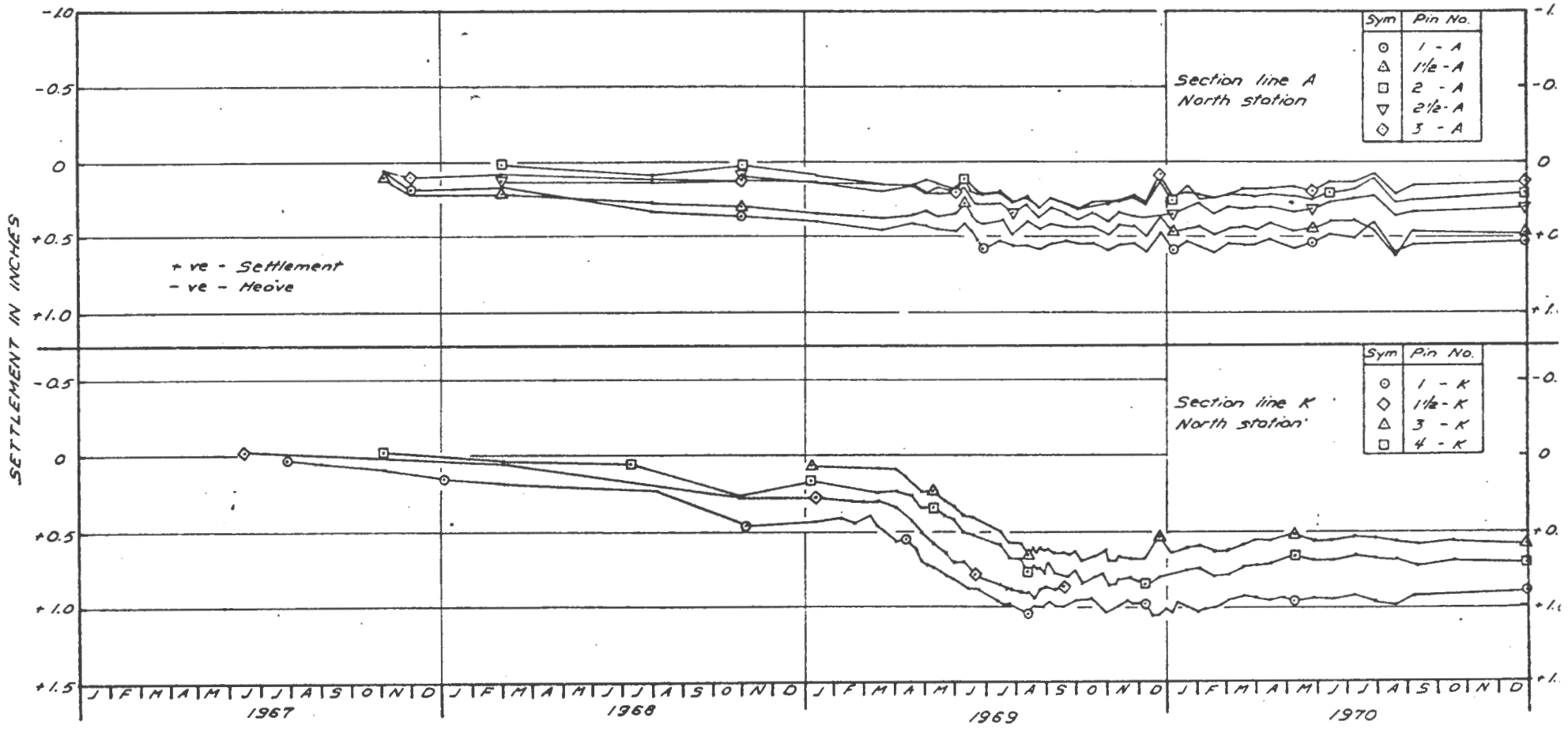

FIGURE A-23A SETTLEMENT MEASUREMENTS TEST SECTION A

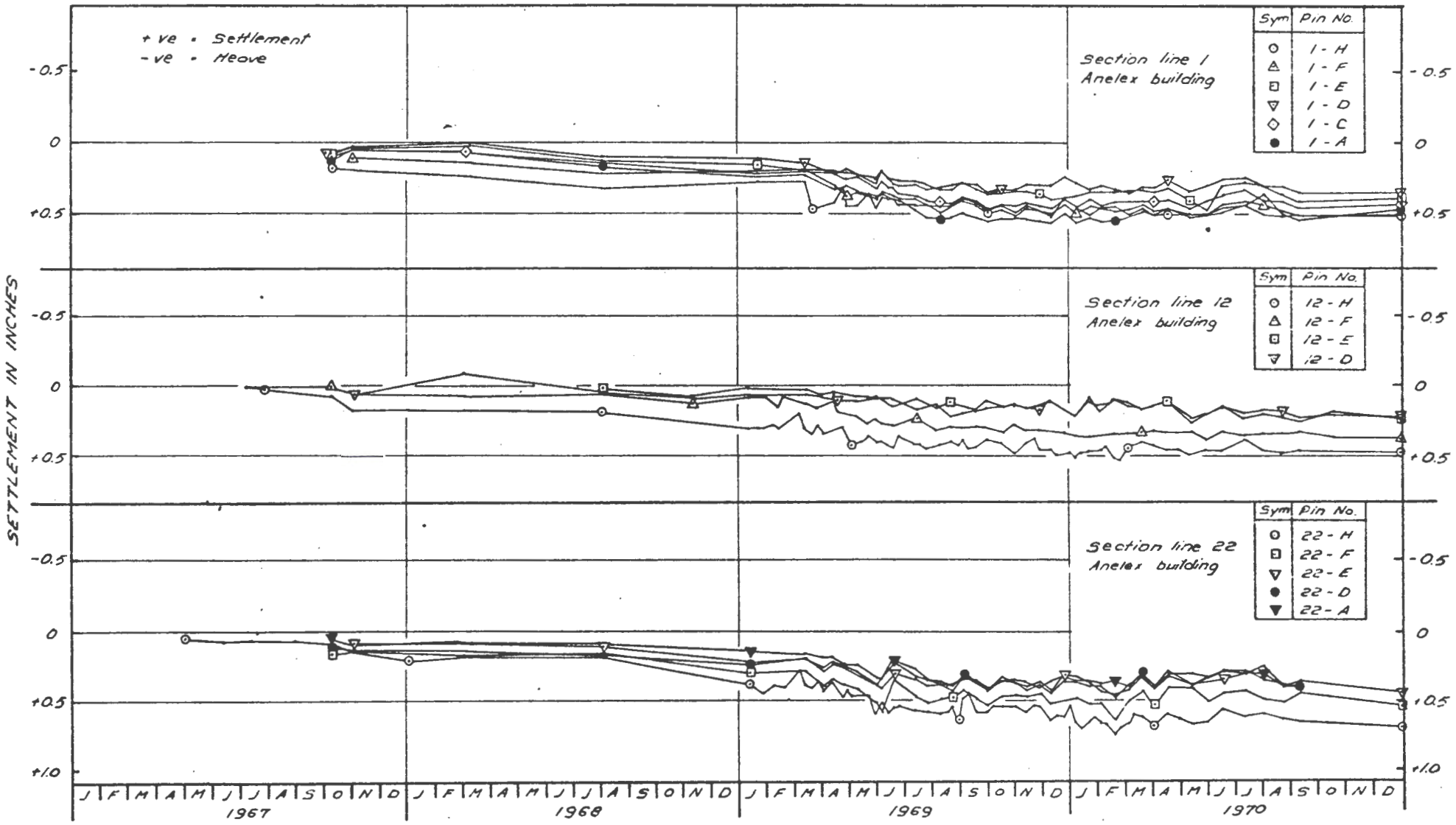

FIGURE A -23 B SETTLEMENT MEASUREMENTS TEST SECTION A

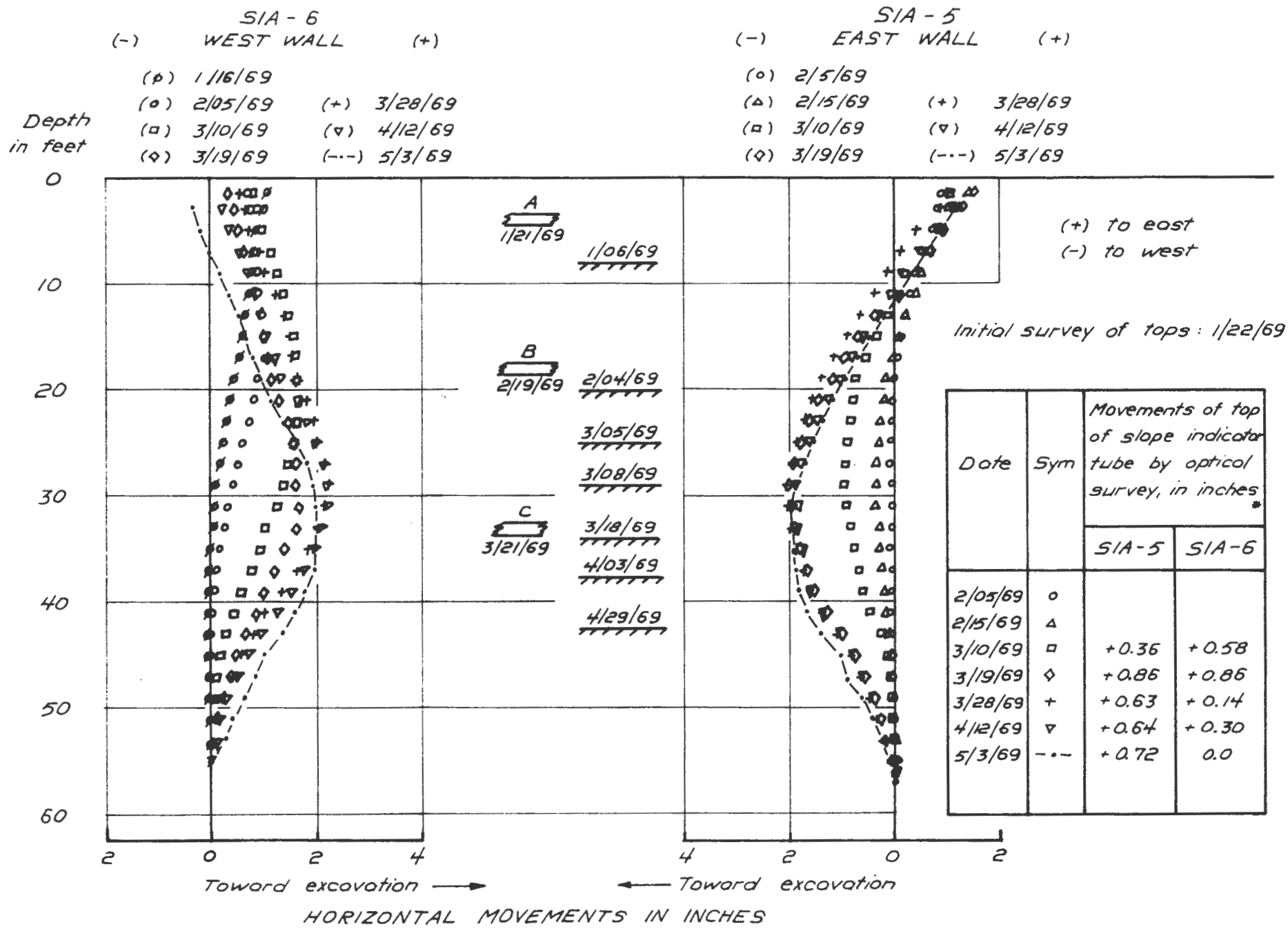

Date	Sym	Movements of top of slope indicator tube by optical survey, in inches *	
		SIA-5	SIA-6
2/05/69	o		
2/15/69	△		
3/10/69	□	+0.36	+0.58
3/19/69	◇	+0.86	+0.86
3/28/69	+	+0.63	+0.14
4/12/69	▽	+0.64	+0.30
5/3/69	-·-	+0.72	0.0

FIGURE A-24A WALL MOVEMENT MEASUREMENT TEST SECTION A

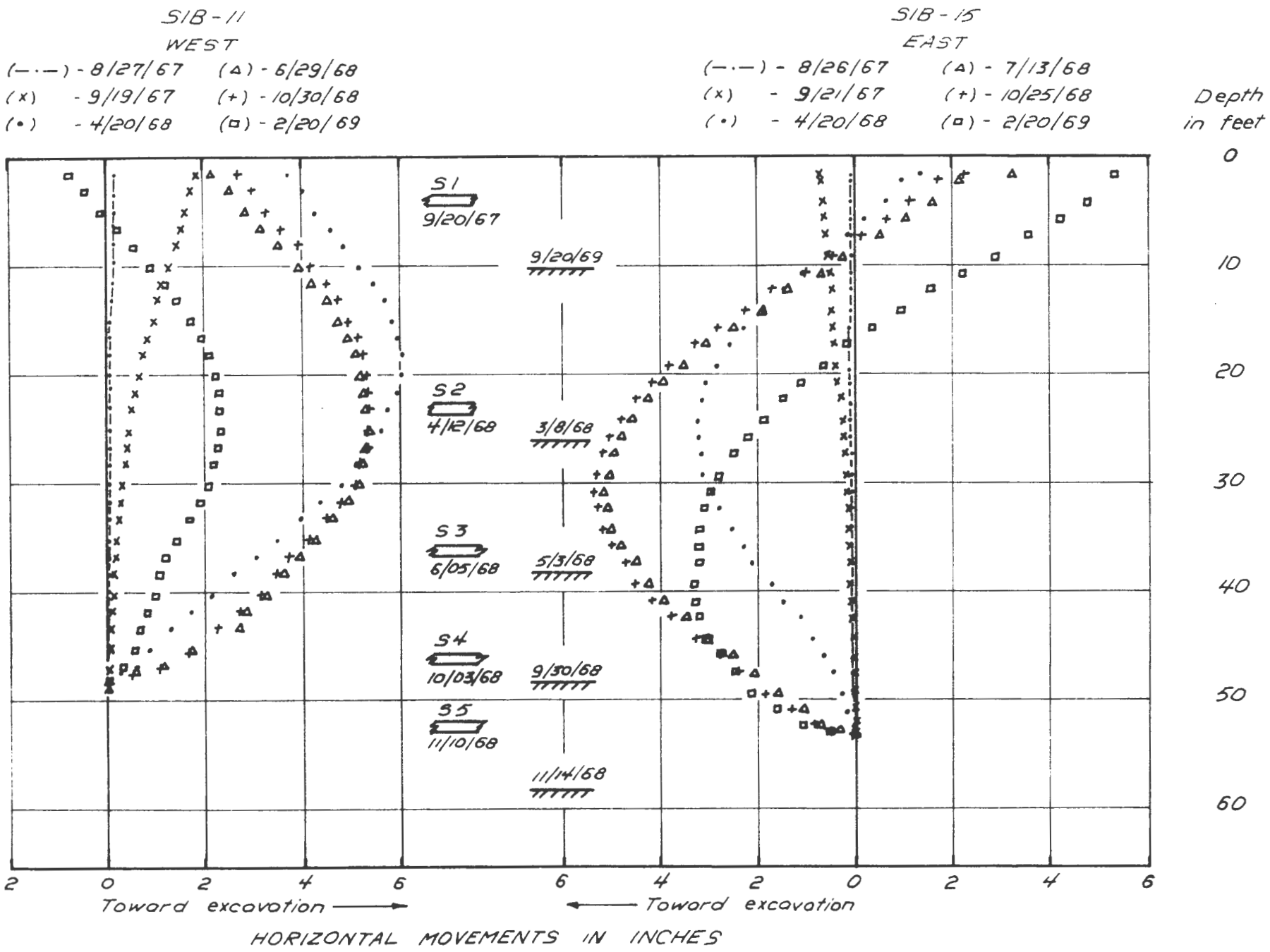

FIGURE A-24B WALL MOVEMENT MEASUREMENT TEST SECTION B

APPENDIX II-B

DATA ACQUISITION AND MANAGEMENT

LIST OF FIGURES

APPENDIX II-B

Figure No.	Title
B-1	Field Control Data Acquisition Unit
B-2	Photograph of Beaver Inclinometer System
B-3	Schematic of the Beaver Inclinometer System
B-4	Example of a "Computer Plot"

ENCLOSURE I

Beaver System Programs: User's Manual

PART II

APPENDIX IIB

DATA ACQUISITION AND MANAGEMENT

This appendix describes the system of data acquisition and management connected with the program of instrumentation of Test Sections A and B, North Station.

A. FIELD DATA ACQUISITION

Three methods were used to read the instruments installed at Test Sections A and B. These three methods are:

1. Manual Method

The instruments read manually were hydraulic piezometers, surface settlement points, column pins, settlement screws, and Wilson slope indicators. The movements of the top of the slope indicator wells were surveyed optically.

2. Method Using Field Central Data Acquisition Unit

The field central data acquisition unit is shown in Fig. B-1. This unit was installed in a small shack at the site and allowed remote reading of the vibrating wire piezometers, strain gauges and stress cells.

3. Method Using Mobile Data Acquisition Unit

Bromwell et al (1970) report the development of the Beaver Inclinometer system. This system incorporated a mobile data acquision unit. Figure B-2 shows a photograph and Fig. B-3 shows a schematic of the Beaver inclinometer system.

The Beaver inclinometer system was designed for operation in the field by one man. The mobile data acquisition unit was mounted in a vehicle. The components that must be carried from hole to hole are small and lightweight. The operator at the hole controls the entire system by means of a remote control box.

B. DATA HANDLING AND MANAGEMENT

1. Manual

When an instrument was read the reading was recorded in a field notebook or in a daily report sheet (such as Figs. D-4 and D-5). As soon as possible (usually in the same day), the field notebooks and the daily report sheets were brought back to M.I.T. The data in the field notebook was recorded in an office notebook while the daily report sheet was put in a file.

As soon as possible the data was processed and the results entered in summary plots. The updated summary plots were distributed to interested parties such as MBTA, the Contractor and the Project Supervisors at M.I.T.

2. Automated

The data collected using the Beaver Inclinometer system were stored on an IBM tape. The tape was input directly to a digital computer for processing. High-quality summary plots showing deflections as a function of depth at various times were obtained as computer output.

Figure B-4 shows an example of a computer plot of deflections. Enclosure I contains the User's Manuals for the programs used for the processing and plotting of the data.

C. FUTURE DEVELOPMENT OF DATA ACQUISITION, HANDLING AND MANAGEMENT

Techniques used to store inclinometer data have been refined and extended to include all types of field data. The goal is to have a program written for a time sharing system that will enable a user to query the data structure and make comparison plots on a typewriter console. Once the user is satisfied with this rough plot, he will be able to generate a report quality plot. English language commands and "free" input format will make the system easy to master. Presently (February 1972) these programs have been written using a batch process.

REFERENCE

Bromwell, L. G., Ryan, C. R. and Toth, W. E., "Recording Inclinometer for Measuring Soil Movement," Paper submitted to the Fourth Panamerican Conference on Soil Mechanics and Foundation Engineering, Puerto Rico, 1971.

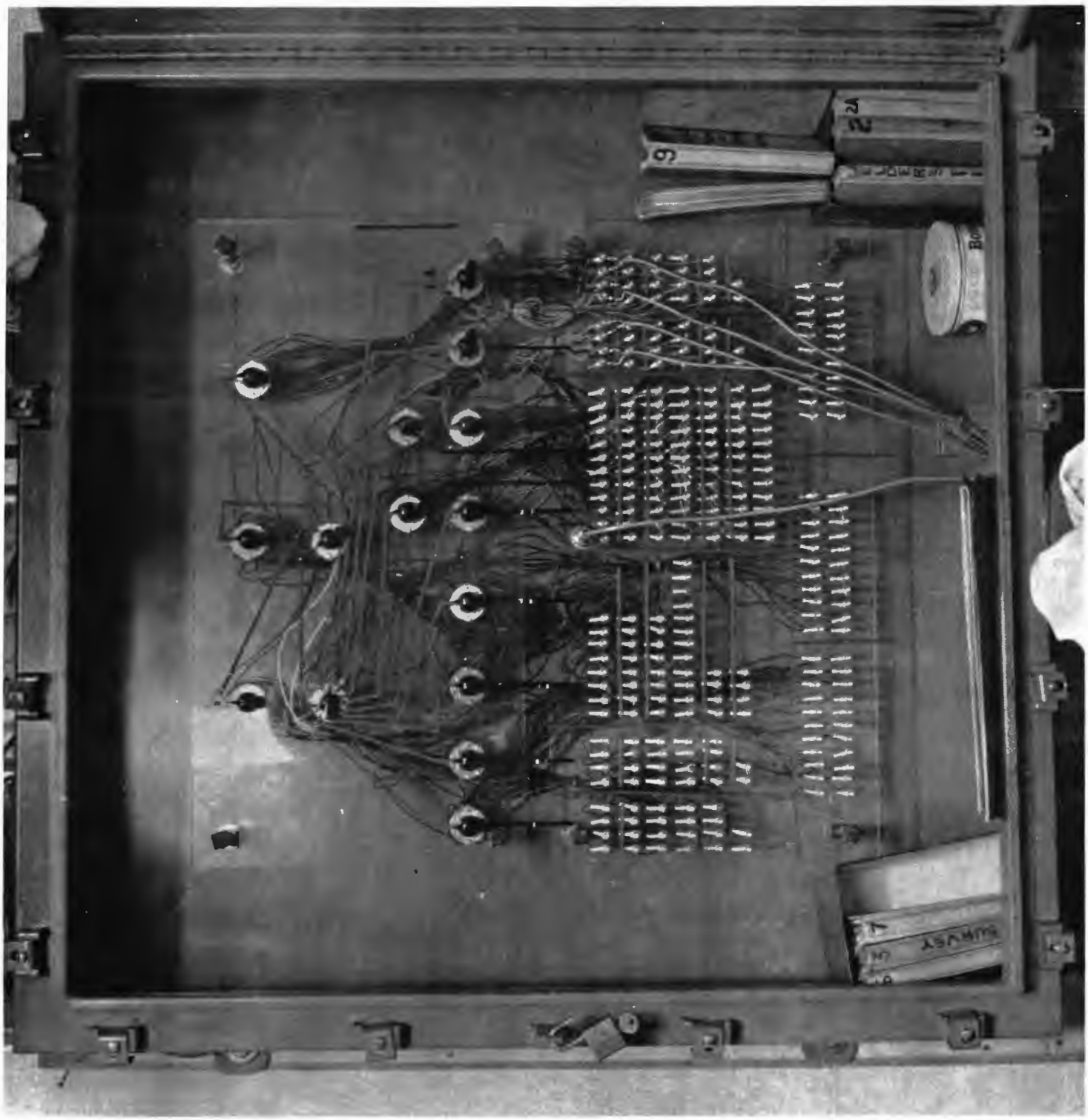

FIGURE B.1 FIELD CENTRAL DATA ACQUISITION UNIT

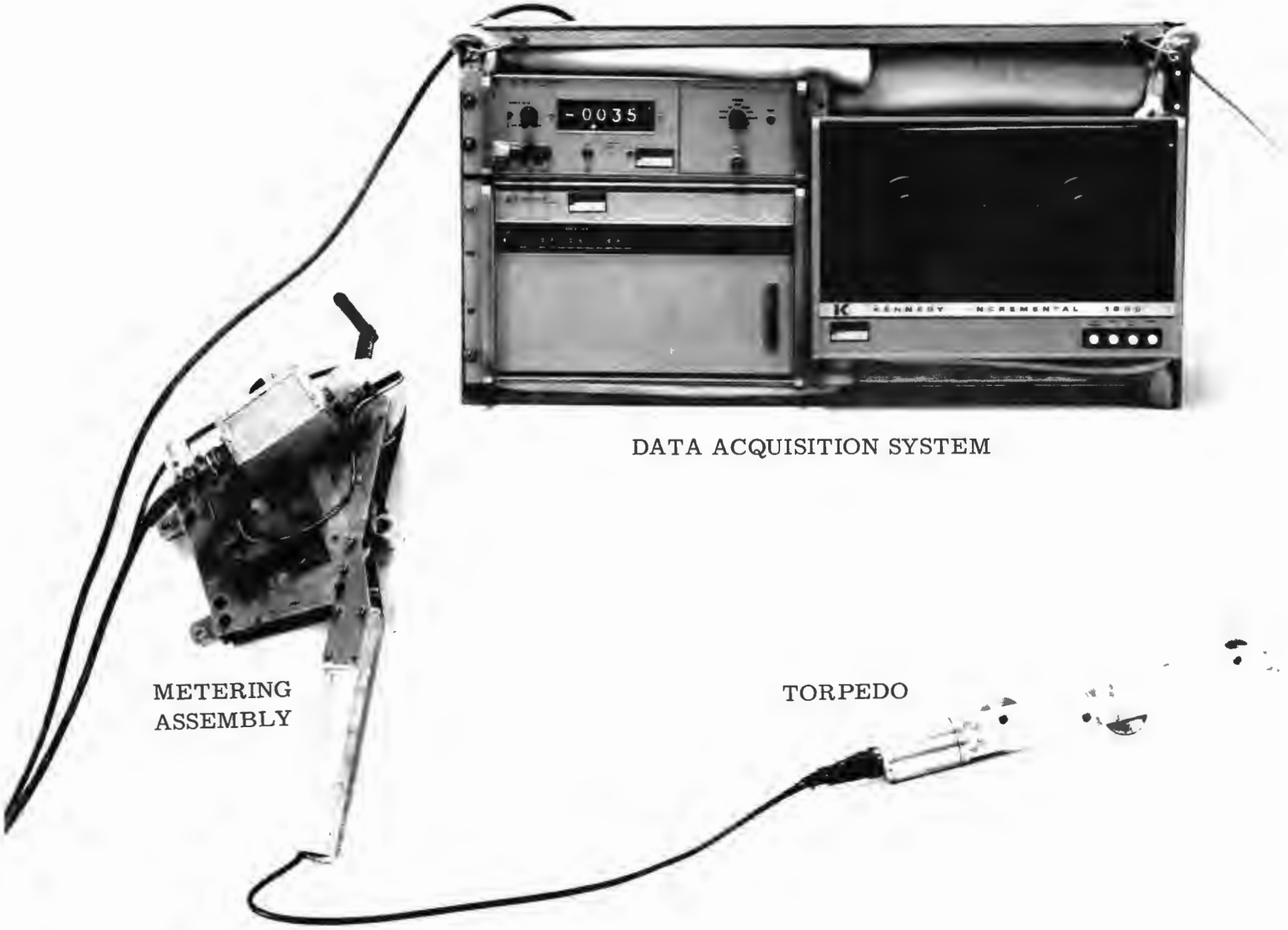

FIGURE B.2 PHOTOGRAPH OF BEAVER INCLINOMETER SYSTEM

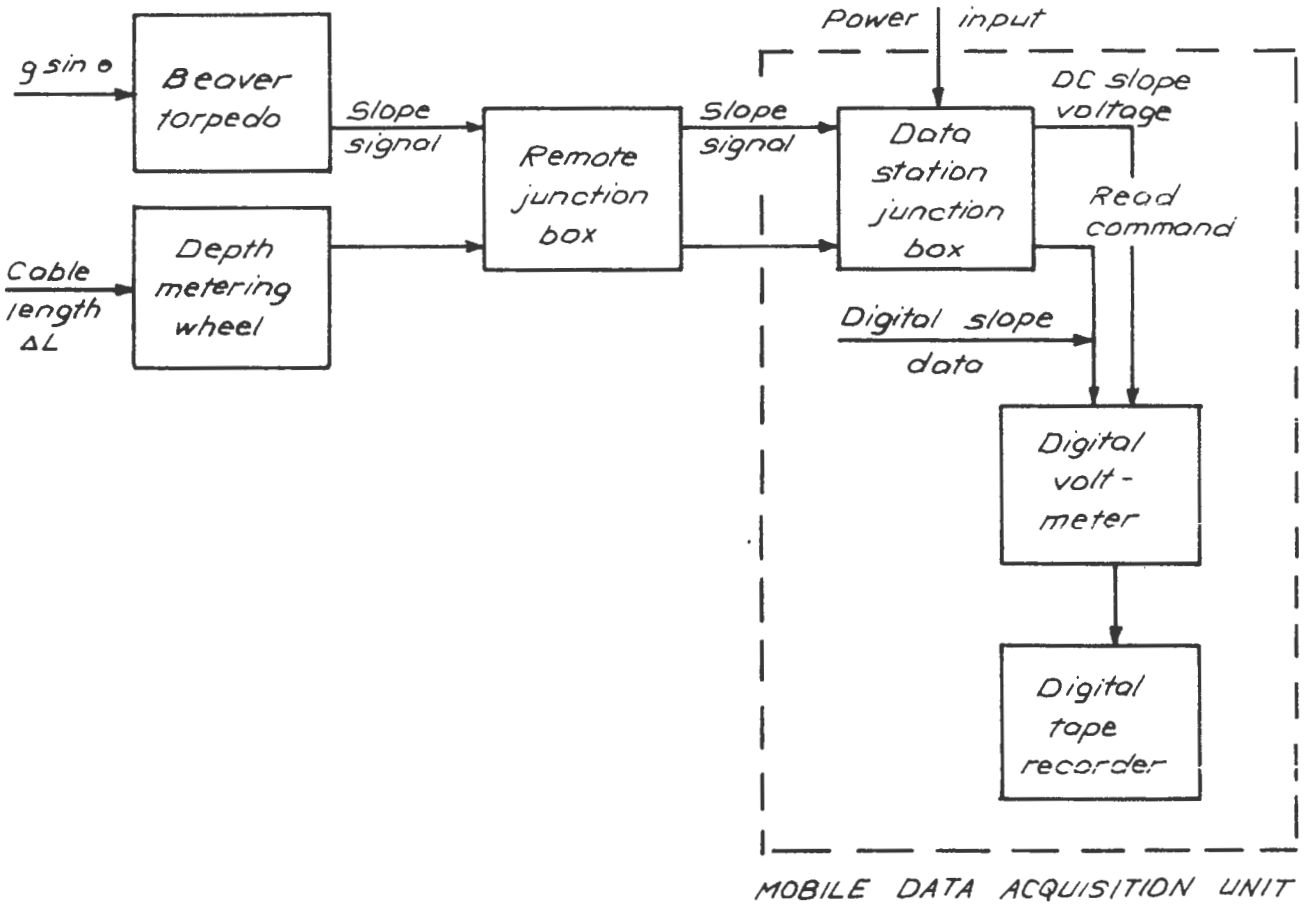

FIGURE B.3 SCHEMATIC OF THE BEAVER INCLINOMETER SYSTEM

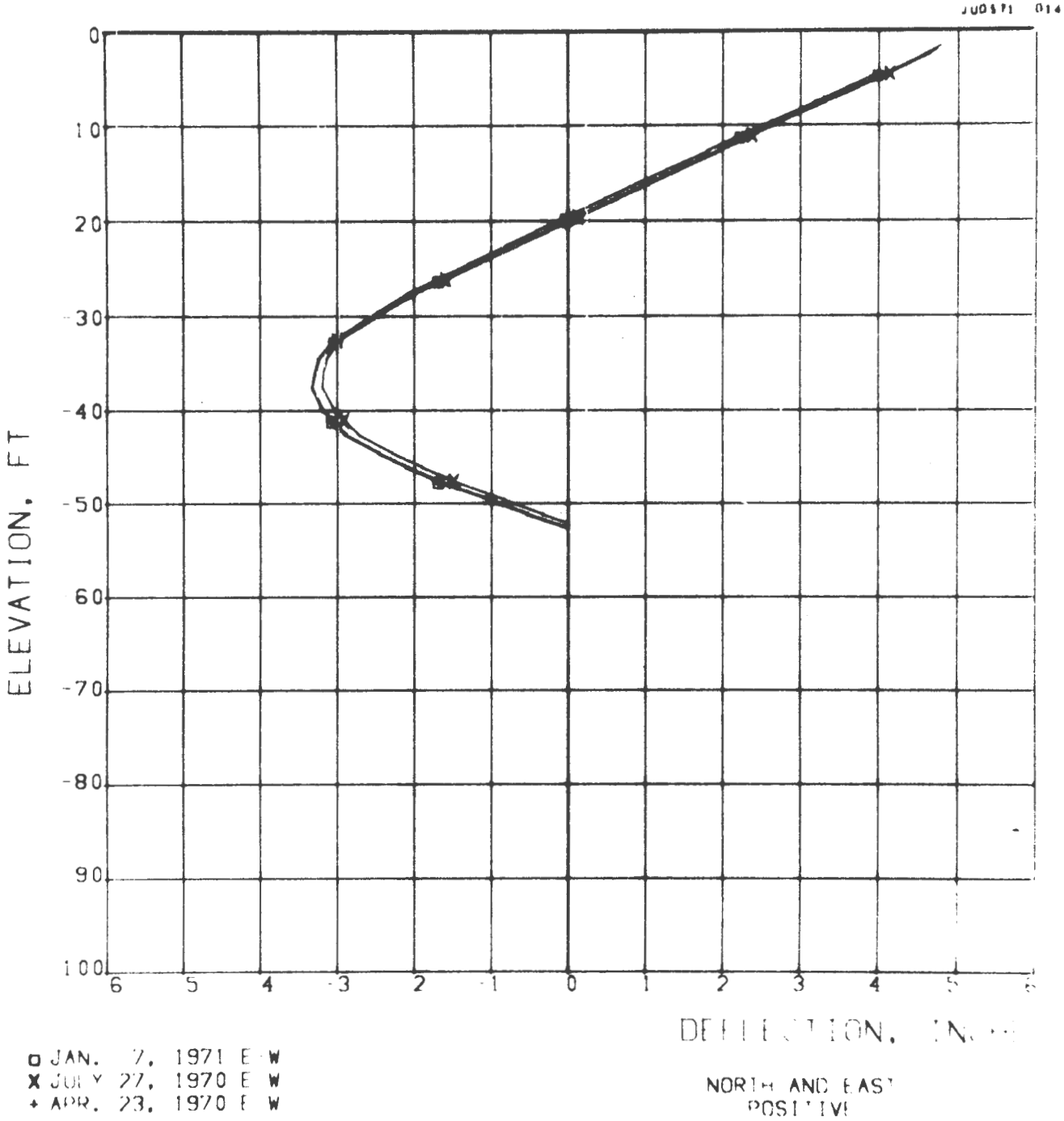

SIB-13 NORTH STATION

FIGURE B.4 EXAMPLE OF A "COMPUTER PLOT"

ENCLOSURE I

BEAVER SYSTEM PROGRAMS: USER'S MANUAL

Date: June 1971

Language: FORTRAN IV-G

Programmer: Christopher R. Ryan

Massachusetts Institute of Technology
Department of Civil Engineering
Soil Mechanics Division

INTRODUCTION

The Beaver System is a series of programs designed to eliminate tedious hand-calculation and hand-plotting of inclinometer results. Data may be read from magnetic tapes or punch cards. Computed results are filed on disk. A plotting program produces report-quality plots with a minimum of effort on the part of the engineer. Instructions for installing the system are included in the appendix.

The Beaver System software consists of four programs:

1. BEAVTAPE. Reads data from tape produced in the field. Files data on disk and outputs list of data for inspection and one card per hole with the location of the data.

2. BEAVER. Finds data and appropriate initials on disk, computes new deflections, outputs results in a list and a rough plot, and files results on disk.

3. PLOTROLL. Produces report-quality plots. Also, it will list on request the dates for which results have been filed on disk for any hole. A purge feature allows results to be deleted from the file.

4. SLPFILE. Adds results stored on cards to disk file.

The first two programs are production programs and will process every data set. The third is a control program and is only used when results are to be plotted and to monitor the contents of the files. The input and output of the four programs has been simplified as far as possible. No knowledge of computer programming is required to use any of the programs.

The present capacity of the Beaver System is 150 (200-foot) holes

where data is taken at 6 inch intervals and results computed and stored at 1 foot intervals. The number of holes is easily expandable; the number of readings per hole is expandable if necessary; the distance between readings may be increased to stay within program limits on longer holes.

This manual is designed solely as a user's guide to the Beaver system programs. It does not include information applicable to the processing of any computer run, the operation of the Computation Center or explanations of slope indicator calculations.

Hole Number and Date Codes

Due to the complexity of the existing numbering system for slope indicator installations it is necessary to assign to each hole a 3-digit code number. A list of code numbers must be kept current in the office and the field. These code numbers are used internally to reference the filing system. All output will be labeled with both the code number and the English language title of the installation. If the disk filing system is not used, code numbers are not necessary.

All four programs have date inputs. To standardize these inputs they will all be converted into 6 digit numbers according to the following convention:

First 2 digits - year
Second 2 digits - month
Third 2 digits - day

For example, the 24th of August 1970 is 700824.

PROGRAM MANUAL

BEAVTAPE II

This program translates a properly formulated tape (see manual for field tape format) into a form compatible with BEAVER input. Field mistakes are deleted, N-S-E-W runs are cut off at the top to be equal length, and the results are filed on disk. For each "run" i.e., four directions on any hole, one card is punched out giving the location of the data. This program is only applicable to the M.I.T. system, but is typical of programs needed to process paper or magnetic tapes for computer usage.

Printed output should be checked before the readings are input to BEAVER III.

Input

1. One card with the coded date punched in columns 1-6.

Output

1. List of data as entered on tape, including all "signal voltages" and field errors to be erased.
2. List of data as filed.
3. Total number of readings recorded in each direction.
4. Hole identification information, date.
5. One card (information card) per hole to be used as Input to BEAVER III.

Watch For

1. Obvious errors.

2. Gross differences in the length of runs in each axis.

3. "218" error - "Data Check." This error occurs fairly frequently. It is usually caused by dirt on the tape. It does not affect the validity of the results. More than two of these on a tape is a signal to clean the tape. (Free service, check with Tape Librarian at I. P. C.)

PROGRAM MANUAL

BEAVER

The BEAVER Program is the heart of the inclinometer system. Data is read from a disk file or from cards; initial deflections and elevations are read from another disk file or cards. Results are computed, a list of deflections and a rough plot output and the results are either punched out on cards or filed on disk.

INPUT

A. Title card 80 cc, free format

B. Information card (see Table I)

C. Installation Title card for Initial Run (if any) 40 cc, free format

D. Initial cards (if any) see format below

E. Data cards (if any) see format below.

OUTPUT

1. Input parameters
2. Bias check results
3. List of deflections
4. Extrapolated defl. on the top of the tube
5. Rough plot of deflections
6. Location of results filed on disk.

Initials

The term 'initials' used in this manual refers to the deflections measured the first time in a given installation. Since the output normally requested is the difference between later sets of data and initial sets, the initial set is stored and recalled for use in later

calculations. To enable instruments with different calibrations to be interchanged, initials are stored in terms of computed deflections rather than the readings themselves. When a later set of data is taken, absolute deflections are calculated and then movements computed by subtracting the initial deflections. When the disk file is used the first set of results will be assumed to be the initials. Deflections may be compared to later sets of data by submitting an initial deck (see format below). Results obtained before installation of the disk file may be added to the file using the program SLPFILE. If the Beaver program is used to calculate initial deflections a '1' in c.c. 40 of the Information Card indicates that a title card will follow. The title will be used to label the file and will appear on all output as well as plots generated by PLOTROLL. If the initial deflections are <u>not</u> to be filed on disk, do not insert a '1' in c.c. 40 and do not insert an installation title card.

<u>Elevations of Readings</u>

Research has shown that changing the vertical interval between readings during the life of installation will yield erroneous results. Some installations are initially read at uneven intervals to avoid couplings between sections of tubing. Field experimentation has shown that field reading time is greatly decreased if a short, regular interval is used rather than irregular intervals. One version of the Beaver Inclinometer actually reads every six inches automatically. The program has been set up to select readings that are at, or closest to, the elevations stored with the initials and disregard the rest. This feature may be bypassed when making initial runs by inputting a value of cc 33 for the information card.

For cases where couplings are to be avoided in initial runs,

input a bogus initial deck (see format below) with the elevations to be used in calculations, and indicate in c.c. 40 that the data is for an initial run and is to be filed accordingly. Note that readings are stored by elevation not depth and for the case where the top of the tube is the reference, input the negative of the depth of each reading. It is important to decide at the outset of a project whether readings are to be stored on the basis of true elevation or with respect to the top of the tube, as this cannot be easily changed.

Readings at the bottom reading point are used to calculate the deflection at the point immediately above. Therefore, the computed deflection at the lowest reading point is always zero. If the tube is silted up, or for some other reason, the torpedo cannot be lowered to the same depth as was attained on the initial run, movements below the new depth are set equal to zero. If appreciable movements have occurred below the new depth, or if the bottom is kicked out, the plotting routine PLOTROLL has a feature that allows a deflection to be input for the bottom of the tube.

Interpreting the Bias Check

The Beaver program has a feature that allows data to be screened before computations are carried out. Errors may be present in the data due to joints in the casing or key punching errors. Since readings are taken in opposite grooves the readings in, for example, the south groove should be the negative of the readings in the north groove plus a fixed constant; the addition of two readings taken at the same elevation in opposite grooves should be a constant. This constant is called the BIAS and it should be independent of the magnitude of the readings. (The subtraction of the readings is used for computing deflections.)

The Beaver program adds up all the pairs of numbers and com-

putes a median bias. All readings whose computed 'bias' falls outside a limit are then replaced by a distance-weighted average of their neighbors. A new 'average bias' can be computed now that gross errors have been deleted. All readings whose computed bias falls outside a lesser limit are then replaced in the same manner.

The program prints out the mean and average bias used in this computation. A list of readings that have been replaced is also printed out. The bias printed out should always be inspected. A bias that changes during a short period of time indicates faulty equipment. The list of readings printed out should be inspected for a continuous string of readings. If several feet of casing has readings replaced the data set should be suspect. The usual case is that only data taken in joints is replaced. If initial readings avoided the joints the data replaced will not be used anyway. A few random readings replaced will not significantly affect the results.

Format of Data Cards (2014)

If data is punched on cards the first data item should be the reading at the bottom of the tube in the north direction, the second item would be the second reading from the bottom, and so on. Directions are always input in the order NSEW. At the end of each 'direction' a 9999 should be punched; the next direction begins on a new card. If no readings are taken in a direction, punch a 9999 in the first slot on a card. There should always be four 9999 entries for every run input; the most common error is to forget or to punch the 9999 entry out of its slot.

Twenty data items are punched on each card. Four card columns are allowed for the data entry including the sign. Blanks to the right of an entry in its four card-column slot are read as zeros. Be sure

to punch entries so that the last digit falls in the rightmost card-column of the four card column slot. Decimal points are not to be punched.

Format of Initial Cards (10A4, (9F8.3)

A title card with free format precedes the data. The format of the rest of the deck is: Elev., N-S. Defl., E-W. Elev., N.S. Defl., E-W defl., etc. There are nine entries (data for three elevations) on each card. Start with the lowest elevation and proceed up the tube in sequential order. Each entry is allowed 8 card columns and must have a decimal point. After the last elevation punch a +999.0 as a marker. Remember that the data is referenced by elevation not depth; for tubes where the top is the reference point input the negative of the depth.

Table 1 Format for Information Card

cc	VARIABLE	DEFAULT	UNITS	FORMAT[1]
1-3	Hole No.			INT.
5-10	Date			INT.
11-15	Depth[2]		Feet	DEC.
16-17	File No. of Data[3]			INT.
18-21	Record No. of Data			INT.
22-30	Calibration	.000132	(4)	
31	Run No.	1		INT.
32	Reading Internal Code	(5)		INT.
33	Interval Multiplier		(6)	INT.
34	0 = Subtract Initials - find on disk 1 = Do Not Subtract Initials 2 = Subtract Initials - find on cards 3 = Punch Out Data and Calculate (initials found on disk) 9 = Punch Out Data but do not calculate			INT.
35-38	Order of Axes on Disk[8]	1234		INT.
39	0 = File Results on Disk 1 = Punch Results on Cards 2 = File and Punch	0		INT.
40	Find Initial on Disk - 0 This Run Initial Run - 1, Title Follows	0		INT.
41-50	E-W Calibration (for double axis instrument)[9]			DEC.
51-60	Top Elevation of Hole			DEC.

See notes on next page.

NOTES

(1) FORMAT

INT - INTEGER; no decimal point.

Blanks to the right of a number in a "slot" are read as zeros, e.g., 14 in cc's 1 and 2 would be read as Hole No. 140.

DEC - DECIMAL; Decimal Point is included. Entry may be punched anywhere in the "slot."

(2) Depth - this must be the depth from EL 0.0 to the bottom. In most cases El 0.0 is the top of the tube.

(3) If the File No. is 69 data will be read in from cards.

(4) The units of CALIBRATION are:

In. defl. per (number of reading units divided by two) per inch of elevation between readings.

The calibrations of commonly used instruments at M.I.T. are:

Beaver	1G Donner Accelerometer	.000132
Wilson	Slope Indicator	.0005
Beaver	Schaevitz Accelerometer	.0002
DIGITILT	0.5G with voltage divided	North South -0.000139 East West +0.000135

(5) Reading Interval Code

0 6"

1 1'

2 2'

9 readings taken at the same elevations as the initials and only at those elevations.

(6) n;

For example, if the Reading Interval is 6 in. and n = 2, computations will be performed every foot. If n = 0 or blank the

readings closest to the elevation of each initial reading will be used.

(7) If the axes were not read in N-S-E-W order in the field this parameter may change them. For example, if field readings were taken in the order S-E-W-N, input 2341.

FOR MOST RUNS NO INFORMATION WILL BE ADDED TO THE CARD PUNCHED OUT BY BEAVTAPE II.

PROGRAM MANUAL

PLOTROLL

PLOTROLL is the plotting and control program for the Beaver system. SC4020 plots of results in the disk files may be obtained, the contents of the files listed, and members of the files may be purged.

There are five types of control cards, named: STOP, LIST, PURGE, FIXUP and PLOT; each control card has data cards (described below) associated with it. There are no restrictions on the order or number of control cards. Error statements will be printed if mistakes are made. Printed output enables the user to review the program's action.

DEFINITION OF PLOTROLL COMMANDS

STOP

This card follows every data set and is immediately followed by a /* card.

Input

A. STOP cc. 1-4.

LIST

Listing enables the user to find out what dates are on file for a hole. A list of dates will automatically be made if a date not on file for a given hole is specified on a PLOT or PURGE card.

Input

A. LIST cc. 1-4

B. Hole No. (1) cc. 1-3
   Hole No. (2) cc. 5-7

If Hole No. (2) is blank the dates on file for Hole No. (1) are listed. If Hole No. (2) is greater than Hole No. (1) the listing will be repeated for all holes within the range specified by the two hole numbers.

PURGE

Purging enables the user to eliminate erroneous results from the file. If this is not done the plotting routine will not be able to find corrected versions with the same date and run number.

Input

A. PURGE cc 1-5 or PURGE cc 1-4

B. Hole No. cc-1-3
Date cc 5-10
Run No. cc 12 (Default $ 1).

FIXUP

The Fixup command frees space occupied by "purged" dates. It also orders a file by date.

Input

A. FIXUP cc 1-5

B. Hole No. (1) cc 1-5
Hole No. (2) cc 5-7

If Hole No. (2) is not blank and greater than Hole No. (1) the operation will be carried out over the specified range.

PLOT

This command is used to generate report-quality plots of inclinometer results. The grid specification card generates a grid and the line specification card plots data.

A. GRID SPECIFICATIONS (one card per plot)

cc	Variable	Default	Units	Format
1-4	PLOT			ALPHA

6-10	X-scale width	6.	inches	DEC.
11-15	Y-scale height	100.	feet	DEC.
16-20	X-scale center	0.	inches	DEC.
21-25	Y-scale top	0.	feet	DEC.
26-30	Thesis margins*	0.		DEC.
41-80	Title (optional)**			ALPHA

* If thesis margins input is not 0. a five inch wide plot will be produced instead of the standard six inches.

** If no title is input the title of the hole will be retrieved from disk.

B. LINE SPECIFICATION (one card per line to be plotted - maximum is 6.)

cc.	Variable	Default	Units	Format
5-10	Date			INT.
12	Direction	(1 = North, 2 = East)		INT.
14	Run No.	1		INT.
16-25	Bottom Defl.	0.	Inches	DEC.
41-80	Legend (optional)			ALPHA

If no legend is input the date, direction and run number will be used for the legend. The bottom deflection entry allows for 'toe kickout' or 'optical corrections' to be input.

NOTE: If lines from more than one hole are to be plotted on the same grid, the "automatic" title and legends will be confusing; a title and legend should be input for this case.

Choice of Scales

Any grid limits may be chosen but a better looking plot will be produced by following the following conventions:

Y scale width $\leq$	1000 ft.	limits integer multiples of 10
Y scale width $>$	100 ft.	limits integer multiples of 20
X scale width $\leq$	9 in.	limits and center multiples of 1
X scale width $>$	9 in.	limits and center multiples of 2

Grids may be pasted together checkerboard fashion to allow larger scales by specifying the same plot twice but with two different vertical intervals. For example, a large-scale plot of a 180 ft. hole could be obtained by specifying one grid to cover from 0 to -100 ft. and the other from -100 to -200 ft. Note that horizontal and vertical scale widths must be equal.

PROGRAM MANUAL

SLPFILE

SLPFILE is a utility program; its sole function is to transfer results that have been stored on cards to a disk file.

Input

A. Control Card

cc	Entry	Default
1-3	Coded Hole No.	
5-10	Coded date	
12	Direction 0 = Both 1 = N.S. 2 = E.W.	0
14	Initial Run? 0 = No 1 = Yes	0
16	Run Number	
21-60	Installation Title (only if cc 14 = 1)	

B. Initial deck or output of Beaver program including Title Card.